Proceedings of
the 25th Workshop on General Relativity and Gravitation in Japan

7 — 11 December 2015

Yukawa Institute for Theoretical Physics, Kyoto University
Kyoto, Japan

Volume 2

Oral Presentations: Second Day

Contents

Oral Presentations: Second Day

Tuesday 8 December

Plenary Session 3 [Chair: Takashi Nakamura]

9:30 Robert M. Wald (U. of Chicago) [Invited]
"Dynamic and Thermodynamic Stability of Black Holes and Black Branes"
[JGRG25(2015)I04]

10:30 Short poster talks (2/3)

10:45-11:00 Caffee break

Parallel Session 2a [Chair: Yasusada Nambu]

11:00 Kazuharu Bamba (Fukushima U.)
"Inflationary cosmology in fluid description"
[JGRG25(2015)2a1]

11:15 Hiroyuki Kitamoto (Kyoto U.)
"Stochastic Dynamics of Infrared Fluctuations in Accelerating Universe"
[JGRG25(2015)2a2]

11:30 Xian Gao (TiTech)
"Disformal transformation & cosmological perturbations of spatially covariant theories of gravity"
[JGRG25(2015)2a3]

11:45 Yi-Peng Wu (IoP, AS)
"Tracking dark energy with nonmininal coupling to gravity"
[JGRG25(2015)2a4]

12:00 Fumika Suzuki (UBC & IMS)
"Real & false loss of coherence in weak gravity"
[JGRG25(2015)2a5]

12:15 Yota Watanabe (Kavli IPMU)
"Derivative-dependent metric transformation and physical degrees of freedom"
[JGRG25(2015)2a6]

Parallel Session 2b [Chair: Masaru Shibata]

11:00 Kenta Kiuchi (YITP)
"Black hole-magnetize neutron star merger : Mass ejection and short gamma-ray burst"
[JGRG25(2015)2b1]

11:15 Kentaro Takami (KCCT)
"Rotational Properties of Hypermassive Neutron Stars from Binary Mergers"
[JGRG25(2015)2b2]

11:30 Ryuichi Fujita (IST)
"Arbitrarily eccentric orbits around a black hole"
[*]

11:45 Koutarou Kyutoku (iTHES, RIKEN)
"Reducing orbital eccentricity in initial data of black hole-neutron star binaries in the puncture framework"
[JGRG25(2015)2b4]

12:00 Kyohei Kawaguchi (YITP)
"Gravitational waves from precessing black hole-neutron star mergers"
[JGRG25(2015)2b5]

12:15 Tomoya Kinugawa (Kyoto U.)
"The detection rate of Inspiral and QNMs of Pop III BH-BHs which can confirm or refute the GR in the strong gravity region"
[JGRG25(2015)2b6]

12:30-14:30 Lunch & poster view

Parallel Session 3a [Chair: Masahide Yamaguchi]

14:00 Chulmoon Yoo (Nagoya U.)
"Gravitational Collapse of a Collisionless Particle System in an Expanding Universe"
[JGRG25(2015)3a1]

14:15 Guillem Domènech Fuertes (YITP)
"Stationary bubbles and their tunneling channels toward trivial geometry"
[JGRG25(2015)3a2]

14:30 Mitsuhiro Fukushima (Waseda U.)
"Gravitational Baryogenesis after Anisotropic Inflation"
[JGRG25(2015)3a3]

14:45 Takahiro Hayashinaka (RESCEU)
"Fermionic Schwinger current in 4-d de Sitter spacetime"
[JGRG25(2015)3a4]

15:00 Asuka Ito (Kobe U.)
"Designing Anisotropic Inflation with Form Fields"
[JGRG25(2015)3a5]

15:15 Naritaka Oshita (RESCEU)
"Black holes as seeds of baby universe"
[JGRG25(2015)3a6]

Parallel Session 3b [Chair: Ken-ichi Nakao]

14:00 Sachiko Kuroyanagi (Nagoya U.)
“Probing properties of cosmic strings through Pulsar Timing Arrays”
[JGRG25(2015)3b1]

14:15 Chunshan Lin (YITP)
“Resonant Primordial Gravitational Waves Amplification”
[JGRG25(2015)3b2]

14:30 Ryo Namba (Kavli IPMU)
“Scale-dependent gravitational waves from a rolling axion”
[JGRG25(2015)3b3]

14:45 Hirotaka Yoshino (KEK)
“Axion Bosenova and Gravitational Waves”
[JGRG25(2015)3b4]

15:00 Ippei Obata (Kyoto U.)
“Primordial Chiral Gravitational Waves from a Non-Abelian Gauge Field”
[JGRG25(2015)3b5]

15:15 Peng Zhao (UCAS)
“The quasi-normal modes of charged scalar fields in Kerr-Newman black hole and its geometric interpretation”
[JGRG25(2015)3b6]

15:30-16:30 Group photo, coffee break, & poster view

Plenary Session 4 [Chair: Hisaaki Shinkai]

16:30 Eiichi Hirose (U. of Tokyo)
“Status of the KAGRA detector”
[JGRG25(2015)I05]

17:15 Ken-ichi Oohara (Niigata U.)
“KAGRA Data Analysis and Data Management”
[JGRG25(2015)I06]

“Dynamic and Thermodynamic Stability of Black Holes and Black Branes”

by Robert M. Wald (invited)

[JGRG25(2015)I04]

Dynamic and Thermodynamic Stability of Black Holes and Black Branes

Robert M. Wald

with Stefan Hollands

arXiv:1201.0463

Commun. Math. Phys. **321**, 629 (2013)

(see also K. Prabhu and R.M. Wald, Commun. Math. Phys. **340**, 253 (2015); arXiv:1501.02522)

Stability of Black Holes and Black Branes

Black holes in general relativity in 4-dimensional spacetimes are believed to be the end products of gravitational collapse. Kerr black holes are the unique stationary black hole solutions in 4-dimensions. It is considerable physical and astrophysical importance to determine if Kerr black holes are stable.

Black holes in higher dimensional spacetimes are interesting playgrounds for various ideas in general relativity and in string theory. A wide variety of black hole solutions occur in higher dimensions, and it is of interest to determine their stability. It is also of interest to consider the stability of "black brane" solutions, which in vacuum general relativity with vanishing cosmological constant are simply $(D+p)$-dimensional spacetimes with metric of the form

$$d\tilde{s}^2_{D+p} = ds^2_D + \sum_{i=1}^{p} dz_i^2 \,,$$

where ds^2_D is a black hole metric.

In this work, we will define a quantity, $\mathcal{E}$, called the *canonical energy*, for a perturbation γ_{ab} of a black hole or black brane and show that positivity of $\mathcal{E}$ is necessary and sufficient for linear stability to axisymmetric perturbations in the following senses: (i) If $\mathcal{E}$ is non-negative for all perturbations, then one has mode

stability, i.e., there do not exist exponentially growing perturbations. (ii) If $\mathcal{E}$ can be made negative for a perturbation γ_{ab}, then γ_{ab} cannot approach a stationary perturbation at late times; furthermore, if γ_{ab} is of the form $\pounds_t \gamma'_{ab}$, then γ_{ab} must grow exponentially with time.

These results are much weaker than one would like to prove, and our techniques, by themselves, are probably not capable of establishing much stronger results. Thus, our work is intended as a supplement to techniques presently being applied to Kerr stability, not as an improvement/replacement of them. Aside from its general applicability, the main strength of the work is that we can also show that positivity of $\mathcal{E}$ is equivalent to thermodynamic stability and is also equivalent to the satisfaction of a local Penrose inequality. This also will allow us to give an extremely simple sufficient criterion for the instability of black branes.

We restrict consideration here to asymptotically flat black holes in vacuum general relativity in D-spacetime dimensions, as well as the corresponding black branes. However, our techniques and many of our results generalize straightforwardly to include matter fields and other asymptotic conditions.

Thermodynamic Stability

Consider a *finite* system with a large number of degrees of freedom, with a time translation invariant dynamics. The energy, E, and some finite number of other "state parameters" X_i will be conserved under dynamical evolution but we assume that the remaining degrees of freedom will be "effectively ergodic." The entropy, S, of any state is the logarithm of the number of states that "macroscopically look like" the given state. By definition, a thermal equilibrium state is an extremum of S at fixed (E, X_i). For thermal equilibrium states, the entropy, S, may be viewed as a function of the state parameters, $S = S(E, X_i)$. Perturbations of thermal equilibrium states satisfy the first law of thermodynamics,

$$\delta E = T\delta S + \sum_i Y_i \delta X_i \,,$$

where $Y_i = (\partial E/\partial X_i)_S$. Note that this relation holds even if the perturbations are not to other thermal equilibrium states.

A thermal equilibrium state will be locally *thermodynamically stable* if S is a local maximum at fixed (E, X_i), i.e., if $\delta^2 S < 0$ for all variations that keep (E, X_i) fixed to first and second order. In view of the first law (and assuming $T > 0$), this is equivalent the condition

$$\delta^2 E - T\delta^2 S - \sum_i Y_i \delta^2 X_i > 0$$

for all variations for which (E, X_i) are kept fixed only to first order.

Now consider a homogeneous (and hence infinite) system, whose thermodynamic states are characterized by (E, X_i), where these quantities now denote the amount of energy and other state parameters "per unit volume" (so these quantities are now assumed to be "extensive"). The condition for thermodynamic stability remains the same, but now there is no need to require that (E, X_i) be fixed to first order because energy and other extensive variables can be "borrowed" from one part of the system and given to another. Thus, for the system to be thermodynamically unstable, the above equation must hold for any first order variation. In particular, the system will be thermodynamically unstable if the Hessian matrix

$$\mathbf{H}_S = \begin{pmatrix} \frac{\partial^2 S}{\partial E^2} & \frac{\partial^2 S}{\partial X_i \partial E} \\ \frac{\partial^2 S}{\partial E \partial X_i} & \frac{\partial^2 S}{\partial X_i \partial X_j} \end{pmatrix} .$$

admit a positive eigenvalue. If this happens, then one can increase total entropy by exchanging E and/or X_i between different parts of the system. For the case of E, this corresponds to having a negative heat capacity. In particular, a homogeneous system with a negative heat capacity must be thermodynamically unstable, but this need not be the case for a finite system.

Stability of Black Holes and Black Branes

Black holes and black branes are thermodynamic systems, with

$$\begin{aligned} E &\leftrightarrow M \\ S &\leftrightarrow \frac{A}{4} \\ X_i &\leftrightarrow J_i, Q_i \end{aligned}$$

Thus, in the vacuum case ($Q_i = 0$), the analog of the criterion for thermodynamic stablity of a black hole (i.e., a finite system) is that for all perturbations for which $\delta M = \delta J_i = 0$, we have

$$\delta^2 M - \frac{\kappa}{8\pi}\delta^2 A - \sum_i \Omega_i \delta^2 J_i > 0\,.$$

We will show that this criterion is equivalent to positivity of canonical energy, $\mathcal{E}$, and thus, for axisymmetric perturbations, is necessary and sufficient for dynamical stability of a black hole.

On the other hand, black branes are homogeneous systems, so a sufficient condition for instability of a black brane is that the Hessian matrix

$$\mathbf{H}_A = \begin{pmatrix} \frac{\partial^2 A}{\partial M^2} & \frac{\partial^2 A}{\partial J_i \partial M} \\ \frac{\partial^2 A}{\partial M \partial J_i} & \frac{\partial^2 A}{\partial J_i \partial J_j} \end{pmatrix} .$$

admits a positive eigenvalue. It was conjectured by Gubser and Mitra that this condition is sufficient for black brane instability. We will prove the Gubser-Mitra conjecture.

As an application, the Schwarzschild black hole has negative heat capacity namely ($A = 16\pi M^2$, so $\partial^2 A/\partial M^2 > 0$). This does not imply that the Schwarzschild black hole is dynamically unstable (and, indeed, it is well known to be stable). However, this calculation does imply that the Schwarzschild black string is unstable!

Local Penrose Inequality

Suppose one has a family of stationary, axisymmetric black holes parametrized by M and angular momenta $J_1, \ldots, J_N$. Consider a one-parameter family $g_{ab}(\lambda)$ of axisymmetric spacetimes, with $g_{ab}(0)$ being a member of this family with surface gravity $\kappa > 0$. Consider initial data on a hypersurface Σ passing through the bifurcation surface B. By the linearized Raychauduri equation, to first order in λ, the event horizon coincides with the apparent horizon on Σ. They need not coincide to second order in λ, but since B is an extremal surface in the background spacetime, their areas must agree to second order. Let $\mathcal{A}$ denotes the area of the apparent horizon of

the perturbed spacetime, $\bar{A}$ denotes the the event horizon area of the stationary black hole with the same mass and angular momentum as the perturbed spacetime. Suppose that to second order, we have

$$\delta^2 \mathcal{A} > \delta^2 \bar{A}$$

Since (i) the area of the event horizon can only increase with time (by cosmic censorship), (ii) the final mass of the black hole cannot be larger than the initial total mass (by positivity of Bondi flux), (iii) its final angular momenta must equal the initial angular momenta (by axisymmetry), and (iv) $\bar{A}(M, J_1, \ldots, J_N$ is an increasing function of M at fixed J_i (by the first law of black hole mechanics with $\kappa > 0$), it follows that there would be a contradiction if the perturbed black hole solution were to settle down to a stationary black hole in the family. This implies that satisfaction of this inequality implies instablity—although it does not imply stability if $\delta^2 \mathcal{A} \leq \delta^2 \bar{A}$ always holds.

Our fundamental stability criterion $\mathcal{E} \geq 0$ implies that satisfaction of $\delta^2 \mathcal{A} \leq \delta^2 \bar{A}$ is necessary and sufficient for black hole stability with respect to axisymmetric perturbations.

Variational Formulas

Lagrangian for vacuum general relativity:

$$L_{a_1 \dots a_D} = \frac{1}{16\pi} R \, \epsilon_{a_1 \dots a_D} \, .$$

First variation:

$$\delta L = E \cdot \delta g + d\theta \, ,$$

with

$$\theta_{a_1 \dots a_{d-1}} = \frac{1}{16\pi} g^{ac} g^{bd} (\nabla_d \delta g_{bc} - \nabla_c \delta g_{bd}) \epsilon_{c a_1 \dots a_{d-1}} \, .$$

Symplectic current ($(D-1)$-form):

$$\omega(g; \delta_1 g, \delta_2 g) = \delta_1 \theta(g; \delta_2 g) - \delta_2 \theta(g; \delta_1 g) \, .$$

Symplectic form:

$$
\begin{aligned}
W_\Sigma(g;\delta_1 g,\delta_2 g) &\equiv \int_\Sigma \omega(g;\delta_1 g,\delta_2 g) \\
&= -\frac{1}{32\pi}\int_\Sigma (\delta_1 h_{ab}\delta_2 p^{ab} - \delta_2 h_{ab}\delta_1 p^{ab}),
\end{aligned}
$$

with

$$p^{ab} \equiv h^{1/2}(K^{ab} - h^{ab}K).$$

Noether current:

$$
\begin{aligned}
\mathcal{J}_X &\equiv \theta(g,\pounds_X g) - X\cdot L \\
&= X\cdot C + dQ_X .
\end{aligned}
$$

Fundamental variational identity:

$$
\begin{aligned}
\omega(g;\delta g,\pounds_X g) &= X\cdot[E(g)\cdot\delta g] + X\cdot\delta C \\
&\quad + d\left[\delta Q_X(g) - X\cdot\theta(g;\delta g)\right]
\end{aligned}
$$

Hamilton's equations of motion: H_X is said a Hamiltonian for the dynamics generated by X iff the equations of motion for g are equivalent to the relation

$$\delta H_X = \int_\Sigma \omega(g;\delta g,\pounds_X g)$$

holding for all perturbations, δg of g.

ADM conserved quantities:

$$\delta H_X = \int_\infty \left[\delta Q_X(g) - X\cdot\theta(g;\delta g)\right]$$

For a stationary black hole, choose X to be the horizon Killing field

$$K^a = t^a + \sum \Omega_i \phi_i^a$$

Integration of the fundamental identity yields the first law of black hole mechanics:

$$0 = \delta M - \sum_i \Omega_i \delta J_i - \frac{\kappa}{8\pi} \delta A \, .$$

Horizon Gauge Conditions

Consider stationary black holes with surface gravity $\kappa > 0$, so the event horizon is of "bifurcate type," with bifurcation surface B. Consider an arbitrary perturbation $\gamma = \delta g$. Gauge condition that ensures that the location of the horizon does not change to first order:

$$\delta \vartheta |_B = 0 \, .$$

Additional gauge condition that we impose:

$$\delta \epsilon |_B = \frac{\delta A}{A} \epsilon \, .$$

Canonical Energy

Define the *canonical energy* of a perturbation $\gamma = \delta g$ by

$$\mathcal{E} \equiv W_\Sigma \left(g; \gamma, \pounds_t \gamma\right)$$

The second variation of our fundamental identity then yields (for axisymmetric perturbations)

$$\mathcal{E} = \delta^2 M - \sum_i \Omega_i \delta^2 J_i - \frac{\kappa}{8\pi} \delta^2 A \,.$$

More generally, can view the canonical energy as a bilinear form $\mathcal{E}(\gamma_1, \gamma_2) = W_\Sigma(g; \gamma_1, \pounds_t \gamma_2)$ on perturbations. $\mathcal{E}$ can be shown to satisfy the following properties:

- $\mathcal{E}$ is conserved, i.e., it takes the same value if evaluated on another Cauchy surface Σ' extending from infinity to B.
- $\mathcal{E}$ is symmetric, $\mathcal{E}(\gamma_1, \gamma_2) = \mathcal{E}(\gamma_2, \gamma_1)$
- When restricted to perturbations for which $\delta A = 0$ and $\delta P_i = 0$ (where P_i is the ADM linear momentum), $\mathcal{E}$ is gauge invariant.
- When restricted to the subspace, $\mathcal{V}$, of perturbations for which $\delta M = \delta J_i = \delta P_i = 0$ (and hence, by the first law of black hole mechanics $\delta A = 0$), we have $\mathcal{E}(\gamma', \gamma) = 0$ for all $\gamma' \in \mathcal{V}$ if and only if γ is a perturbation towards another stationary and

axisymmetric black hole.

Thus, if we restrict to perturbations in the subspace, $\mathcal{V}'$, of perturbations in $\mathcal{V}$ modulo perturbations towards other stationary black holes, then $\mathcal{E}$ is a non-degenerate quadratic form. Consequently, on $\mathcal{V}'$, either (a) $\mathcal{E}$ is positive definite or (b) there is a $\psi \in \mathcal{V}'$ such that $\mathcal{E}(\psi) < 0$. If (a) holds, we have mode stability.

Flux Formulas

Let δN_{ab} denote the perturbed Bondi news tensor at null infinity, $\mathcal{I}^+$, and let $\delta\sigma_{ab}$ denote the perturbed shear on the horizon, $\mathcal{H}$. If the perturbed black hole were to "settle down" to another stationary black hole at late times, then $\delta N_{ab} \to 0$ and $\delta\sigma_{ab} \to 0$ at late times. We show that—for axisymmetric perturbations—the change in canonical energy would then be given by

$$\Delta\mathcal{E} = -\frac{1}{16\pi}\int_{\mathcal{I}} \delta\tilde{N}_{cd}\delta\tilde{N}^{cd} - \frac{1}{4\pi}\int_{\mathcal{H}} (K^a\nabla_a u)\ \delta\sigma_{cd}\delta\sigma^{cd} \ \leq 0\,.$$

Thus, $\mathcal{E}$ can only decrease. Therefore if one has a perturbation $\psi \in \mathcal{V}'$ such that $\mathcal{E}(\psi) < 0$, then ψ cannot "settle down" to a stationary solution at late times because $\mathcal{E} = 0$ for stationary perturbations with $\delta M = \delta J_i = \delta P_i = 0$. Thus, in case (b) we have instability in the sense that the perturbation cannot asymptotically approach a stationary perturbation.

Instability of Black Branes

Theorem: Suppose a family of black holes parametrized by (M, J_i) is such that at (M_0, J_{0A}) there exists a perturbation within the black hole family for which $\mathcal{E} < 0$. Then, for any black brane corresponding to (M_0, J_{0A}) one can find a sufficiently long wavelength perturbation for which $\tilde{\mathcal{E}} < 0$ and $\delta\tilde{M} = \delta\tilde{J}_A = \delta\tilde{P}_i = \delta\tilde{A} = \delta\tilde{T}_i = 0$.

This result is proven by modifying the initial data for the perturbation to another black hole with $\mathcal{E} < 0$ by multiplying it by $\exp(ikz)$ and then re-adjusting it so that the modified data satisfies the constraints. The new data will automatically satisfy

$\delta\tilde{M} = \delta\tilde{J}_A = \delta\tilde{P}_i = \delta\tilde{A} = \delta\tilde{T}_i = 0$ because of the $\exp(ikz)$ factor. For sufficiently small k, it can be shown to satisfy $\tilde{\mathcal{E}} < 0$.

Equivalence to Local Penrose Inequality

Let $\bar{g}_{ab}(M, J_i)$ be a family of stationary, axisymmetric, and asymptotically flat black hole metrics on M. Let $g_{ab}(\lambda)$ be a one-parameter family of axisymmetric metrics such that $g_{ab}(0) = \bar{g}_{ab}(M_0, J_{0A})$. Let $M(\lambda), J_i(\lambda)$ denote the mass and angular momenta of $g_{ab}(\lambda)$ and let $\mathcal{A}(\lambda)$ denote the area of its apparent horizon. Let $\bar{g}_{ab}(\lambda) = \bar{g}_{ab}(M(\lambda), J_i(\lambda))$ denote the one-parameter family of stationary black holes with the same mass and angular momenta as $g_{ab}(\lambda)$.

Theorem: There exists a one-parameter family $g_{ab}(\lambda)$ for which

$$\mathcal{A}(\lambda) > \bar{A}(\lambda)$$

to second order in λ if and only if there exists a perturbation γ'_{ab} of $\bar{g}_{ab}(M_0, J_{0A})$ with $\delta M = \delta J_i = \delta P_i = 0$ such that $\mathcal{E}(\gamma') < 0$.

Proof: The first law of black hole mechanics implies $\mathcal{A}(\lambda) = \bar{\mathcal{A}}(\lambda)$ to first order in λ, so what counts are the second order variations. Since the families have the same mass and angular momenta, we have

$$
\begin{aligned}
\frac{\kappa}{8\pi}\left[\frac{d^2 A}{d\lambda^2}(0) - \frac{d^2 \bar{A}}{d\lambda^2}(0)\right] &= \mathcal{E}(\bar{\gamma}, \bar{\gamma}) - \mathcal{E}(\gamma, \gamma) \\
&= -\mathcal{E}(\gamma', \gamma') + 2\mathcal{E}(\gamma', \bar{\gamma}) \\
&= -\mathcal{E}(\gamma', \gamma')
\end{aligned}
$$

where $\gamma' = \bar{\gamma} - \gamma$.

Are We Done with Linear Stability Theory for Black Holes?

Not quite:

- The formula for $\mathcal{E}$ is rather complicated, and the linearized initial data must satisfy the linearized constraints, so its not that easy to determine positivity of $\mathcal{E}$.
- There is a long way to go from positivity of $\mathcal{E}$ and (true) linear stability and instability.
- Only axisymmetric perturbations are treated.

And, of course, only linear stability is being analyzed.

$$
\begin{aligned}
\mathcal{E} \;=\; & \int_\Sigma N\Bigg(h^{\frac{1}{2}}\Bigg\{ \frac{1}{2}\ R_{ab}(h) q_c{}^c q^{ab} - 2\ R_{ac}(h) q^{ab} q_b{}^c \\
& -\frac{1}{2}\ q^{ac} D_a D_c q_d{}^d - \frac{1}{2}\ q^{ac} D^b D_b q_{ac} + q^{ac} D^b D_a q_{cb} \\
& -\frac{3}{2}\ D_a(q^{bc} D^a q_{bc}) - \frac{3}{2}\ D_a(q^{ab} D_b q_c{}^c) + \frac{1}{2}\ D_a(q_d{}^d D^a q_c{}^c) \\
& +2\ D_a(q^a{}_c D_b q^{cb}) + D_a(q^b{}_c D_b q^{ac}) - \frac{1}{2}\ D^a(q_c{}^c D^b q_{ab}) \Bigg\} \\
& +h^{-\frac{1}{2}}\Bigg\{ 2\ p_{ab} p^{ab} + \frac{1}{2}\ \pi_{ab}\pi^{ab}(q_a{}^a)^2 - \pi_{ab} p^{ab} q_c{}^c \\
& -3\ \pi^a{}_b \pi^{bc} q_d{}^d q_{ac} - \frac{2}{D-2}\ (p_a{}^a)^2 + \frac{3}{D-2}\ \pi_c{}^c p_b{}^b q_a{}^a \\
& +\frac{3}{D-2}\ \pi_d{}^d \pi^{ab} q_c{}^c q_{ab} + 8\ \pi^c{}_b q_{ac} p^{ab} + \pi_{cd}\pi^{cd} q_{ab} q^{ab}
\end{aligned}
$$

$$
\begin{aligned}
& +2\ \pi^{ab}\pi^{dc} q_{ac} q_{bd} - \frac{1}{D-2}\ (\pi_c{}^c)^2 q_{ab} q^{ab} \\
& -\frac{1}{2(D-2)}\ (\pi_b{}^b)^2 (q_a{}^a)^2 - \frac{4}{D-2}\ \pi_c{}^c p^{ab} q_{ab} \\
& -\frac{2}{D-2}\ (\pi^{ab} q_{ab})^2 - \frac{4}{D-2}\ \pi_{ab} p_c{}^c q^{ab} \Bigg\}\Bigg) \\
& -\int_\Sigma N^a\Bigg(-2\ p^{bc} D_a q_{bc} + 4\ p^{cb} D_b q_{ac} + 2\ q_{ac} D_b p^{cb} \\
& -2\ \pi^{cb} q_{ad} D_b q_c{}^d + \pi^{cb} q_{ad} D^d q_{cb} \Bigg) \\
& +\kappa \int_B s^{\frac{1}{2}} \Bigg(\delta s_{ab} \delta s^{ab} - \frac{1}{2}\ \delta s_a{}^a \delta s_b{}^b \Bigg)
\end{aligned}
$$

Further Developments

One can naturally break-up the canonical energy into a *kinetic energy* (arising from the part of the perturbation that is odd under "$(t-\phi)$-reflection") and a *potential energy* (arising from the part of the perturbation that is even under "$(t-\phi)$-reflection"). Prabhu and I have proven that the kinetic energy is always positive (for any perturbation of any black hole or black brane). We were then able to prove that if the potential energy is negative for a perturbation of the form $\pounds_t \gamma'_{ab}$, then this perturbation must grow exponentially in time.

One can straightforwardly generalize our results to black holes with a negative cosmological constant in

asymptotically AdS spacetimes. In this case, there is only one boundary through which there can be a canonical energy flux, so there is no need to restrict to axisymmetric perturbations. Green, Hollands, Ishibashi and I have proven that, in this context, all black holes that possess an ergoregion (i.e., a region where the horizon KVF becomes spacelike) are unstable.

Main Conclusion

Dynamical stability of a black hole is equivalent to its thermodynamic stability with respect to axisymmetric perturbations.

Thus, the remarkable relationship between the laws of black hole physics and the laws of thermodynamics extends to dynamical stability.

"Inflationary cosmology in fluid description"

by Kazuharu Bamba

[JGRG25(2015)2a1]

Inflationary cosmology in fluid description

JGRG25
The 25th Workshop on General Relativity and Gravitation in Japan
Yukawa Institute for Theoretical Physics
Kyoto University

8th December, 2015

Fukushima University

Presenter: **Kazuharu Bamba (*Fukushima University*)**

References

[1] arXiv:1508.05451 [gr-qc]

Collabolator: **Sergei D. Odintsov (*ICE/CSIC-IEEC and ICREA*)**

[2] Phys. Rev. D 90, 124061 (2014) [arXiv:1410.3993 [hep-th]]

Collabolators:

Shin'ichi Nojiri (*Dep. of Phys./KMI, Nagoya University*)

Sergei D. Odintsov (*ICE/CSIC-IEEC and ICREA*)

Diego Sáez-Gómez (*Cape Town University*)

Planck 2015 results

[Ade *et al.* [Planck Collaboration], arXiv:1502.02114]

(1) Spectral index of power spectrum of the curvature perturbations

$$n_s = 0.968 \pm 0.006 \quad (68\% \text{ CL})$$

(2) Tensor-to-scalar ratio

$$r < 0.11 \, (95\% \text{ CL})$$

Keck Array and BICEP2 constraints

$$r_{0.05} < 0.09 \; (0.07) \quad (95\% \text{ CL})$$

(Combined results with the Planck analysis)

[Ade *et al.* [Keck Array and BICEP2 Collaborations], arXiv:1510.09217]

Planck 2015 results (2)

[Ade *et al.* [Planck Collaboration], arXiv:1502.02114]

(3) Running of the spectral index n_{S}

$$\alpha_{\mathrm{S}} \equiv \frac{dn_{\mathrm{s}}}{d \ln k} = -0.003 \pm 0.007 \quad (68\% \text{ CL})$$

Motivations and Purposes

INFLATION　　DARK ENERGY

(1) Scalar field theories

Chaotic inflation

[Linde, Phys. Lett. B 108, 389 (1982)]

X-matter, Quintessence

[Chiba, Sugiyama and Nakamura, Mon. Not. Roy. Astron. Soc. 289, L5 (1997)]

[Caldwell, Dave and Steinhardt, Phys. Rev. Lett. 80, 1582 (1998)]

(2) Modifications of gravity

R^2 (Starobinsky) inflation

[Starobinsky, Phys. Lett. B 91, 99 (1980)]

$F(R)$ gravity

[Capozziello, Cardone, Carloni and Troisi, Int. J. Mod. Phys. D 12, 1969 (2003)]

[Carroll, Duvvuri, Trodden and Turner, Phys. Rev. D 70, 043528 (2004)]

[Nojiri and Odintsov, Phys. Rev. D 68, 123512 (2003)]

5

Motivations and Purposes (2)

INFLATION　　DARK ENERGY

(3) Fluid models

THIS WROK

Cf. [Barrow and Mimoso, Phys. Rev. D 50, 3746 (1994)]

[Barrow and Ganguly, arXiv:1510.01095]

[Paliathanasis, Tsamparlis, Basilakos and Barrow, arXiv:1511.00439]

Chaplygin gas

[Kamenshchik, Moschella and Pasquier, Phys. Lett. B 511, 265 (2001)]

Viscous fluid

[Brevik, Obukhov and Timoshkin, Astrophys. Space Sci. 355, 399 (2015)]

We explore fluid models to explain inflation.

6

R^2 (Starobinsky) inflation

Action: $$S = \int d^4x\sqrt{-g}\,\frac{1}{2\kappa^2}\left(R\underline{+\beta R^2}\right)$$

g : Determinant of the metric $g_{\mu\nu}$ $\qquad \kappa^2 \equiv 8\pi G_{\mathrm{N}}$

R : Scalar curvature, β : Constant , G_{N} : Gravitatioanl constant

- $N = 60 \longrightarrow n_{\mathrm{s}} = 0.967, \quad r = 3.33 \times 10^{-3}$

  $\alpha_{\mathrm{s}} = -5.56 \times 10^{-4}$

N : Number of e-folds during inflation

Cf. [Hinshaw *et al.*, Astrophys. J. Suppl. 208, 19 (2013)]

Inflationary models with $n_{\mathrm{s}} - 1 = -\frac{2}{N}$

- **R^2 (Starobinsky) inflation**

  [Starobinsky, Phys. Lett. B 91, 99 (1980)]

- **Chaotic inflation** [Linde, Phys. Lett. B 108, 389 (1982)]

- **Higgs inflation with its non-minimal coupling**

  [Salopek, Bond and Bardeen, Phys. Rev. D 40, 1753 (1989)]

  [Bezrukov and Shaposhnikov, Phys. Lett. B 659, 703 (2008)]

- **α-attractor** [Kallosh and Linde, JCAP 1307, 002 (2013); Phys. Rev. D 91, 083528 (2015); arXiv:1503.06785 [hep-th]]

Subjects

- **From the spectral index of $n_{\mathrm{s}} - 1 = -\frac{2}{N}$, the inflaton potential V of a scalar field theory has been reconstructed.**

[Chiba, PTEP 2015, 073E02 (2015)]

By applying this procedure to fluids, we reconstruct fluid models.

Assumption

- **We suppose that the representation of inflation in fluid models can be equivalent to that of the so-called slow-roll inflation driven by inflaton potential in scalar field theories.**

Under this assumption, even in the fluid description, it is considered that the three observables$(n_{\mathrm{s}}, r, \alpha_{\mathrm{s}})$ of the inflationary universe can be defined.

Flat Friedmann-Lemaitre-Robertson-Walker (FLRW) space-time

$$ds^2 = -dt^2 + a^2(t) \sum_{i=1,2,3} \left(dx^i\right)^2$$

$a(t)$: Scale factor

$H = \dot{a}/a$: Hubble parameter

* The dot shows the time derivative.

II. Fluid descriptions

Gravitational field equations

$$\frac{3}{\kappa^2}(H(N))^2 = \rho \,, \qquad -\frac{2}{\kappa^2} H(N) H'(N) = \rho + P$$

* The prime denotes the derivative with respect to *N*.

Equation of state (EoS)

$$P(N) = -\rho(N) \underline{+ f(\rho)}$$

ρ, P : Energy density and pressure of a fluid

$f(\rho)$: Arbitrary function of ρ

Conservation law

$$0 = \rho'(N) + 3\left(\rho(N) + P(N)\right)$$

III. Reconstruction of EoS of the fluid from the spectral index

Canonical scalar field theory

Action

$$S = \int d^4x \sqrt{-g} \left(\frac{R}{2\kappa^2} - \frac{1}{2}\partial_\mu \phi \partial^\mu \phi - V(\phi) \right)$$

ϕ : **Inflaton**

$V(\phi)$: **Inflaton potential**

Reconstruction method

For scalar field theories with the potential $V(N)$,

$$n_{\mathrm{s}} - 1 = \frac{d}{dN}\left[\ln \left(\frac{1}{V^2(N)} \frac{dV(N)}{dN} \right) \right]$$

$$r = \frac{8}{V(N)} \frac{dV(N)}{dN} \,, \quad \alpha_{\mathrm{s}} = -\frac{d^2}{dN^2}\left[\ln \left(\frac{1}{V^2(N)} \frac{dV(N)}{dN} \right) \right]$$

[Chiba, PTEP 2015, 073E02 (2015)]

- $H = H(N)$
- **Gravitational field equations**

⇨ **We reconstruct the EoS of fluids.**

EoS of the fluid

$$P = -\rho + \boxed{A\rho^{\beta} + \underline{\zeta(H)}}$$

$$\zeta(H) = \bar{\zeta} H^{\gamma}$$

$A, \beta, \gamma, \bar{\zeta}$
: Constants

$f(\rho)$

$$\Rightarrow f(\rho) = A\rho^{\beta} + \zeta(H(\rho)) = A\rho^{\beta} + \bar{\zeta}\left(\frac{\kappa}{\sqrt{3}}\right)^{\gamma} \rho^{\gamma/2}$$

Friedmann equation

Inflationary models with $n_{\mathrm{s}} - 1 = -\frac{2}{N}$ (2)

$$\Rightarrow V(N) = \frac{1}{(C_1/N) + C_2}$$

$C_1(>0), C_2$: Constants

$$r = \frac{8}{N\left[1 + (C_2/C_1)\,N\right]}, \qquad \alpha_{\mathrm{s}} = -\frac{2}{N^2}$$

[Chiba, PTEP 2015, 073E02 (2015)]

Suppose $\left(3/\kappa^2\right)\left(H(N)\right)^2 = \rho(N) \approx V(N)$,

$$\longrightarrow N \approx \frac{C_1 \rho}{1 - C_2 \rho}, \qquad H(N) \approx \kappa \sqrt{\frac{1}{3\left[(C_1/N) + C_2\right]}}$$

$(C_1/N) + C_2 > 0$

Inflationary models with $n_s - 1 = -\frac{2}{N}$ (3)

Equation of state

$$P = -\rho - \frac{2}{\kappa^2} H(N) H'(N) \approx -\rho - \underline{\frac{3C_1}{N^2 \kappa^4} H^4}$$

$f(\rho)$

$$\Rightarrow \quad \underline{f(\rho) \approx -\frac{1}{3C_1}\left(1 - 2C_2\rho + C_2^2\rho^2\right)}$$

By comparing with this expression, we can obtain the EoS of fluids.

Reconstructed fluid models

Model (a) ($|C_2\rho| \gg 1$)

$$P = -\rho + \left(\frac{2C_2}{3C_1}\right)\rho - \left(\frac{3C_2^2}{C_1\kappa^4}\right) H^4$$

Model (b) ($|C_2\rho| \gg 1$)

$$P = -\rho - \left(\frac{C_2^2}{3C_1}\right)\rho^2 + \left(\frac{2C_2}{C_1\kappa^2}\right) H^2$$

Model (c) ($|C_2\rho| \ll 1$)

$$P = -\rho - \left(\frac{1}{3C_1}\right) + \left(\frac{2C_2}{C_1\kappa^2}\right) H^2$$

Model (d) ($|C_2\rho| \ll 1$)

$$P = -\rho + \left(\frac{2C_2}{3C_1}\right)\rho - \left(\frac{1}{3C_1}\right)$$

Observables $(n_{\mathrm{s}}, r, \alpha_{\mathrm{s}})$ of the inflationary universe

(1) $n_{\mathrm{s}} - 1 = -\dfrac{2}{N}$ $\Rightarrow$ $N = 60 \longrightarrow n_{\mathrm{s}} = 0.967$

(2) $r = \dfrac{8}{N\left[1 + \left(C_2/C_1\right) N\right]}$

Models (a), (b)
Models (c), (d) with $C_2 < 0$ $\Rightarrow$ $N \gtrsim 73\,, \quad r < 0.11$

Models (c), (d) with $C_2 > 0$ $\Rightarrow$ $N \gtrsim 60\,, \quad r < 0.11$

(3) $\alpha_{\mathrm{s}} = -\dfrac{2}{N^2}$ $\Rightarrow$ $N = 60 \longrightarrow \alpha_{\mathrm{s}} = -5.56 \times 10^{-4}$

IV. Graceful exit from inflation

Perturbation of the de Sitter solution

$$H = H_{\mathrm{inf}} + \underline{H_{\mathrm{inf}} \delta(t)}$$

$|\delta(t)| \ll 1$

$H_{\mathrm{inf}} (> 0)$

: Hubble parameter at the inflationary stage

Gravitational field equation

$$\longrightarrow \ddot{H} - \frac{\kappa^4}{2} \left[\beta A^2 \left(\frac{3}{\kappa^2} \right)^{2\beta} H^{4\beta-1} + \left(\beta + \frac{\gamma}{2} \right) A \bar{\zeta} \left(\frac{3}{\kappa^2} \right)^{\beta} H^{2\beta+\gamma-1} + \frac{\gamma}{2} \bar{\zeta}^2 H^{2\gamma-1} \right] = 0$$

Instability of the de Sitter solutions

Perturbation: $\delta(t) = \exp(\lambda t)$

$$\Rightarrow \quad \lambda^2 - \frac{1}{2}\frac{\kappa^4}{H_{\rm inf}^2}\mathcal{Q} = 0 \qquad \lambda \text{ : Constant}$$

$$\mathcal{Q} \equiv \beta\left(4\beta - 1\right) A^2 \left(\frac{3}{\kappa^2}\right)^{2\beta} H_{\rm inf}^{4\beta}$$

$$+ \left(\beta + \frac{\gamma}{2}\right)\left(2\beta + \gamma - 1\right) A\bar{\zeta}\left(\frac{3}{\kappa^2}\right)^{\beta} H_{\rm inf}^{2\beta+\gamma} + \frac{\gamma}{2}\left(2\gamma - 1\right)\bar{\zeta}^2 H_{\rm inf}^{2\gamma}$$

$\longrightarrow$ **Solution:** $\lambda = \lambda_{\pm} \equiv \pm\dfrac{1}{\sqrt{2}}\dfrac{\kappa^2}{H_{\rm inf}}\sqrt{\mathcal{Q}}$

21

Instability of the de Sitter solutions (2)

$\Rightarrow$ **It is possible to exist a positive solution.**

$$\lambda = \lambda_{+} > 0$$

$\longrightarrow$ **The de Sitter solution can be unstable.**

$\Downarrow$

The universe can gracefully exit from inflation.

Conditions for the existence of $\lambda = \lambda_+ > 0$

$$\longrightarrow \quad \mathcal{Q} > 0$$

Model (a): **No condition**

Model (b): **No condition**

Model (c): $C_2 < 0$ **or** $C_2 > \frac{1}{36}\left(\frac{\kappa}{H_{\mathrm{inf}}}\right)^2$

Model (d): $C_2 < 0$ **or** $C_2 > \frac{1}{18}\left(\frac{\kappa}{H_{\mathrm{inf}}}\right)^2$

V. Singular inflation

[Barrow and Graham, Phys. Rev. D 91, 083513 (2015)]

[Nojiri, Odintsov and Oikonomou, Phys. Lett. B 747, 310 (2015)]

Hubble parameter and scale factor

$$H = H_{\mathrm{inf}} + \bar{H}\left(t_{\mathrm{s}} - t\right)^q , \qquad q > 1$$

$$a = \bar{a} \exp\left[H_{\mathrm{inf}} t - \frac{\bar{H}}{q+1}\left(t_{\mathrm{s}} - t\right)^{q+1}\right]$$

$\bar{H},\ \bar{a},\ q$: Constants

Gravitational field equations

$$\rho = \frac{3H^2}{\kappa^2} , \qquad P = -\frac{2\dot{H} + 3H^2}{\kappa^2}$$

Singular inflation (2)

When $t \to t_s$, all of a, ρ, and P become finite values, but higher derivatives of H diverge.

$\longrightarrow$ **Type IV singularity appears at $t = t_s$.**

[Nojiri, Odintsov and Tsujikawa, Phys. Rev. D 71, 063004 (2005)]

Equation of state

$$P = -\rho + f(\rho)\,, \quad f(\rho) = \frac{2q\bar{H}^{1/q}}{\kappa^2}\left(\kappa\sqrt{\frac{\rho}{3}} - H_{\mathrm{inf}}\right)^{(q-1)/q}$$

EoS of viscous fluid models

For $H_{\mathrm{inf}}/\sqrt{\kappa^2\rho/3} = H_{\mathrm{inf}}/H \ll 1$ **,**

$$f(\rho) \approx \frac{2}{3^{(q-1)/(2q)}}\frac{\bar{H}^{1/q}}{\kappa^{(q+1)/q}} \times \left[\rho^{(q-1)/(2q)} - \frac{\sqrt{3}\,(q-1)}{q}\frac{H_{\mathrm{inf}}}{\kappa}\rho^{-1/(2q)}\right]$$

Linear combination of two kinds of power of ρ

A kind of the reconstructed fluid models

We have taken the first order quantity of $\left(H_{\mathrm{inf}}/\sqrt{(\kappa^2\rho)/3}\right)$.

VI. Conclusions

- **We have explicitly reconstructed the EoS of fluids from the spectral index**
  $n_{\mathrm{s}} - 1 = -2/N$ **.**

- **We have shown that the spectral index n_{s} , the tensor-to-scalar ratio r , and the running α_{s} of the spectral index can be consistent with the recent Planck results.**

- **We have demonstrated that the universe can gracefully exit from inflation.**

Discussions

- **The existence of an unstable de Sitter solution is only the necessary conditions for inflationary cosmology based on fundamental physics, in which the reheating stage occurs after the end of inflation.**

- **The fluid models reconstructed in this work are phenomenological one.**

$\longrightarrow$ **It is important to obtain some clues to connect such phenomenological models to basic physics in the future works.**

Backup slides

Cosmological perturbation theory

Perturbed Einstein equation

$\longrightarrow$ **Metric perturbation = Matter density perturbation**

(1) Scalar mode (Curvature perturbation)

Temperature perturbation of the cosmic microwave background (CMB) radiation: $\frac{\delta T}{T} \simeq 10^{-5}$

(2) Vector mode

T : Temperature

(3) Tensor mode (Primordial gravitational wave)

Comparison with observations

- **Spectrum of scalar and tensor perturbations**

$$\mathcal{P}_{\mathcal{R}}(k) = A_{\mathrm{s}} \left(\frac{k}{k_*} \right)^{n_{\mathrm{s}}-1}$$

$A_{\mathrm{s\,(t)}}$: Scalar (tensor) amplitude

$$\mathcal{P}_{\mathrm{t}}(k) = A_{\mathrm{t}} \left(\frac{k}{k_*} \right)^{n_{\mathrm{t}}}$$

$n_{\mathrm{S\,(t)}}$: **Scalar** (tensor) **spectral index**

k : Wave number, $k_* = 0.05\ \mathrm{Mpc}^{-1}$

- **Tensor-to-scalar ratio** $r = \dfrac{\mathcal{P}_{\mathrm{t}}(k_*)}{\mathcal{P}_{\mathcal{R}}(k_*)}$

[Ade *et al.* [Planck Collaboration], arXiv:1502.02114]

31

Constraints on the inflationary models from the observations

⇨ **The observables (n_{S}, r) can mainly be used to constrain the inflationary models.**

(n_s, r) Contours [Planck 2015]

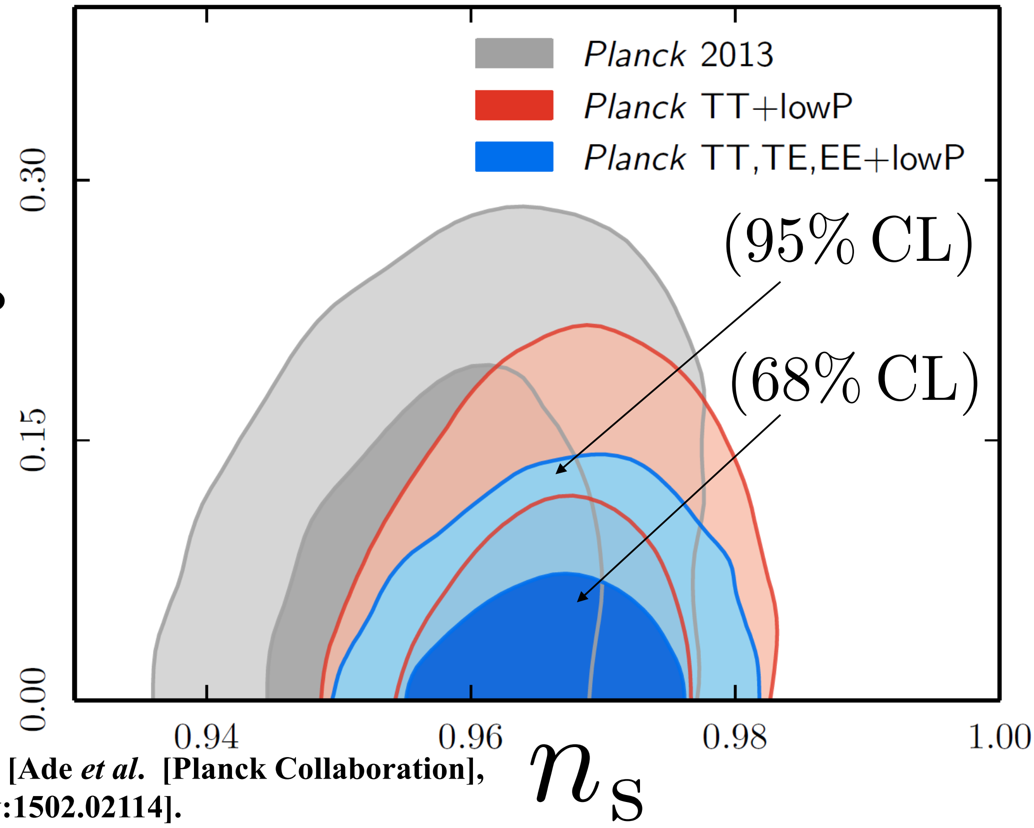

From [Ade *et al.* [Planck Collaboration], arXiv:1502.02114].

33

Constraints on inflationary models

$r_{0.002}$ $(k = 0.002\ \mathrm{Mpc}^{-1})$ R^2 **Inflation**

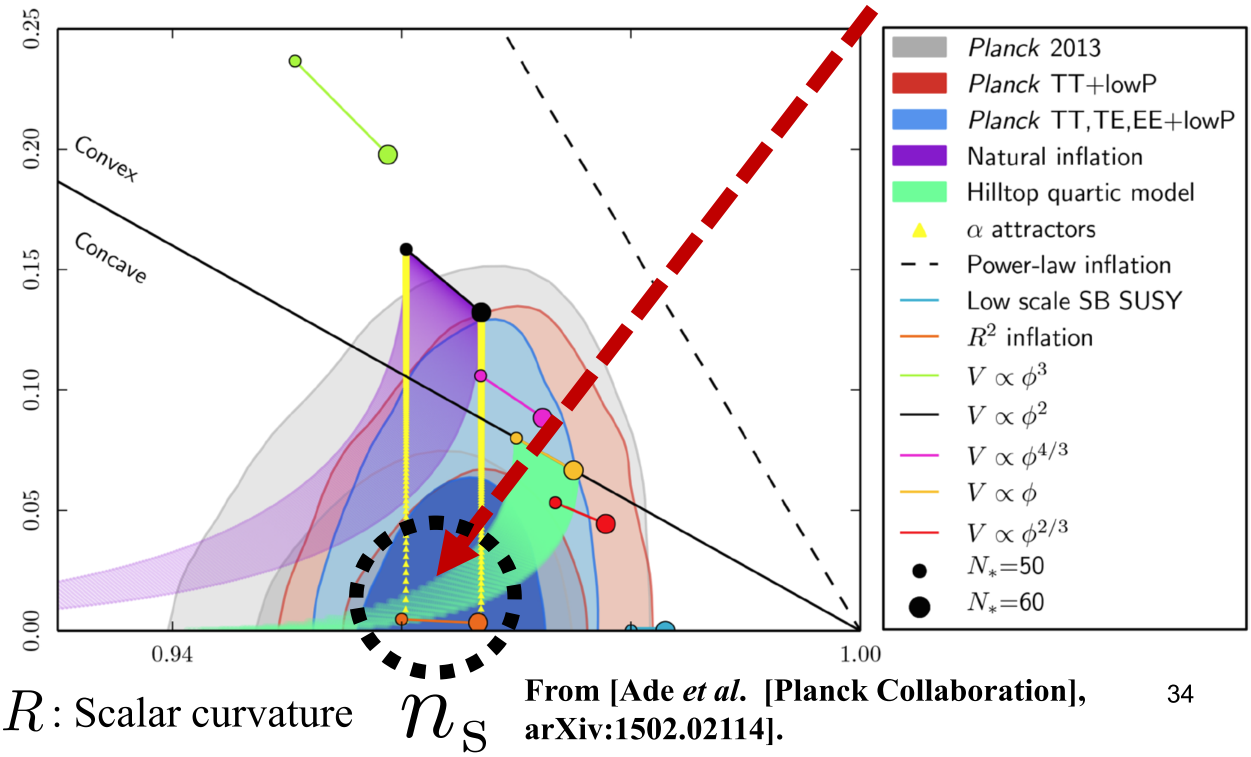

R : Scalar curvature

From [Ade *et al.* [Planck Collaboration], arXiv:1502.02114].

34

Running α_{s} of the spectral index n_{s}

From [Ade *et al.* [Planck Collaboration], arXiv:1502.02114].

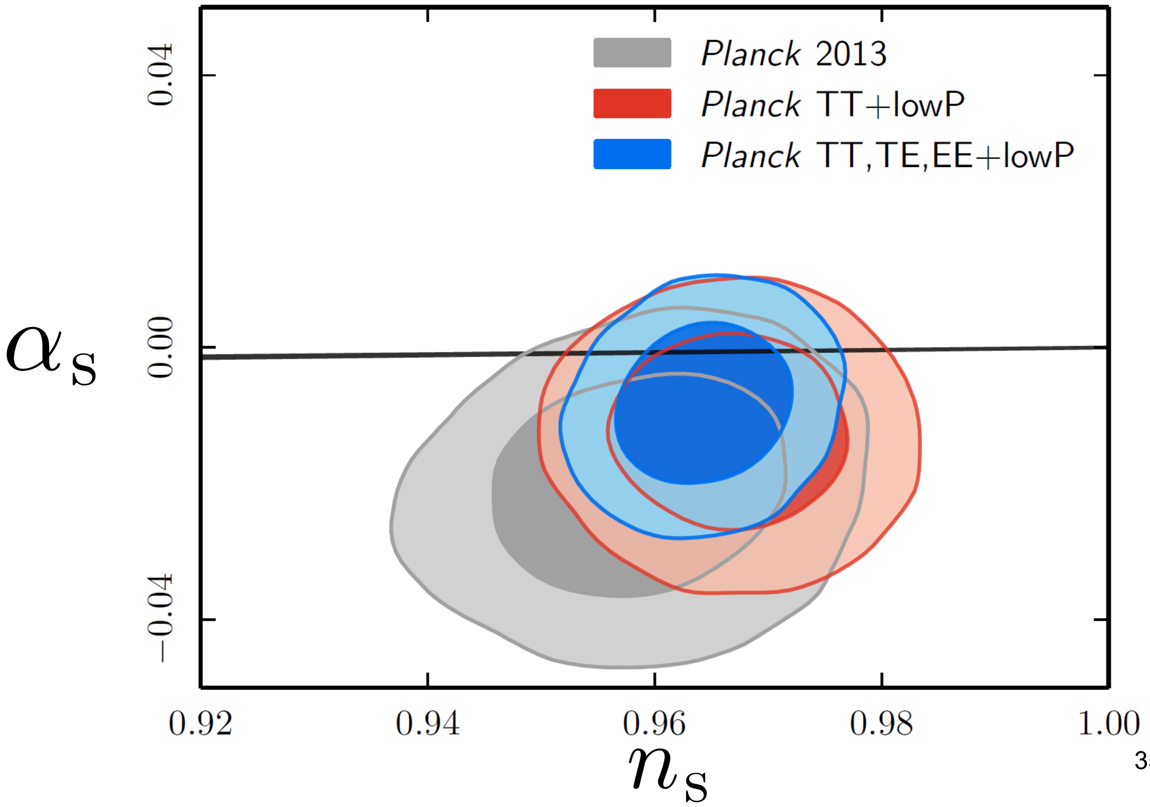

35

R^2 (Starobinsky) inflation

$$F(R) = R + \underline{\beta_{\mathrm{s}} \kappa^2 R^2}$$

β_{s} : Constant

[Starobinsky, Phys. Lett. B 91, 99 (1980)]

Potential in the Einstein frame

φ : Scalar field

$$V(\varphi) = [1/(8\beta_{\mathrm{s}}\kappa^2)]\left(1 - \exp\left(-\sqrt{2/3}\kappa\varphi\right)\right)^2$$

$$n_{\mathrm{s}} \simeq 1 - \frac{2}{N}, \quad r = \frac{12}{N^2}, \quad \alpha_{\mathrm{s}} = -\frac{2}{N^2}$$

- $N = 50 \longrightarrow$ $n_{\mathrm{s}} = 0.960, \quad r = 4.80 \times 10^{-3}$
  $\alpha_{\mathrm{s}} = -8.00 \times 10^{-5}$
- $N = 60 \longrightarrow$ $n_{\mathrm{s}} = 0.967, \quad r = 3.33 \times 10^{-3}$
  $\alpha_{\mathrm{s}} = -5.56 \times 10^{-4}$

36

Cf. [Hinshaw *et al.*, Astrophys. J. Suppl. 208, 19 (2013)]

Models (a) and (b)

- $\underline{|C_2\rho| \gg 1}$ $\longrightarrow$ $f(\rho) \approx \frac{2C_2}{3C_1}\rho - \frac{C_2^2}{3C_1}\rho^2$
- $C_2 < 0$ $\longrightarrow$ $(-C_2)/C_1 \approx 1/N \ll 1$

$$\Rightarrow \quad w = \frac{P}{\rho} \approx -1 + \frac{1}{3N}(-2 - C_2\rho)$$

If $|C_2\rho| = \mathcal{O}(10)$ **and** $N \gtrsim 60$ **,**

$w \approx -1$ $\Rightarrow$ **(Quasi-)de Sitter inflation can occur.**

Models (c) and (d)

- $\underline{|C_2\rho| \ll 1}$ $\longrightarrow$ $f(\rho) \approx -\frac{1}{3C_1} + \frac{2C_2}{3C_1}\rho$
- $C_1\rho \approx N \gg 1$ $\longrightarrow$ $|C_2|/C_1 \ll 1$

$$\Rightarrow \quad w = \frac{P}{\rho} \approx -1 + \frac{1}{3}\left(-\frac{1}{N} + 2\frac{C_2}{C_1}\right)$$

$$\longrightarrow \quad w \approx -1$$

$\Downarrow$

(Quasi-)de Sitter inflation can be realized.

Viscous fluid models and inflation

$$P = -\rho + f(\rho) = -\rho + A\rho^{\beta} + \bar{\zeta}\left(\frac{\kappa}{\sqrt{3}}\right)^{\gamma}\rho^{\gamma/2}$$

Case 1: $|C_2\rho| \gg 1$ $\quad (-C_2)/C_1 \approx 1/N \ll 1$

$C_2 < 0$

$$f(\rho) \approx \frac{2C_2}{3C_1}\rho - \frac{C_2^2}{3C_1}\rho^2$$

$$a(t) = a_{\mathrm{i}} \exp\left[H_{\mathrm{inf}}(t - t_{\mathrm{i}})\right]$$

$$w = \frac{P}{\rho} \approx -1 - \frac{2}{3}\left(-\frac{C_2}{C_1}\right) + \frac{1}{3}\left(-\frac{C_2}{C_1}\right)(-C_2\rho) \approx -1 + \frac{1}{3N}(-2 - C_2\rho)$$

39

Viscous fluid models and inflation

Case 2: $|C_2\rho| \ll 1$ $\quad C_1\rho \approx N \gg 1$

$$f(\rho) \approx -\frac{1}{3C_1} + \frac{2C_2}{3C_1}\rho$$

$|C_2|/C_1 \ll 1$

$$w = \frac{P}{\rho} \approx -1 - \frac{1}{3}\frac{1}{C_1\rho} + \frac{2}{3}\left(\frac{C_2}{C_1}\right) \approx -1 + \frac{1}{3}\left(-\frac{1}{N} + 2\frac{C_2}{C_1}\right)$$

$C_2 > 0$ $\quad C_2 = (2/3)\,C_1$

$\bar{\zeta} = 4/\left(3\kappa^2\right)$ $\quad A = 4/9$

Case	Model	A	$\bar{\zeta}$	β	γ
(i)	(a)	$2C_2/\left(3C_1\right)$	$-3C_2^2/\left(C_1\kappa^4\right)$	1	4
(i)	(b)	$-C_2^2/\left(3C_1\right)$	$2C_2/\left(C_1\kappa^2\right)$	2	2
(ii)	(c)	$-1/\left(3C_1\right)$	$2C_2/\left(C_1\kappa^2\right)$	0	2
(ii)	(d)	$2C_2/\left(3C_1\right)$	$-1/\left(3C_1\right)$	1	0

Model	EoS
(a)	$P=-\rho+\left[2C_2/\left(3C_1\right)\right]\rho-\left[3C_2^2/\left(C_1\kappa^4\right)\right]H^4$
(b)	$P=-\rho-\left[C_2^2/\left(3C_1\right)\right]\rho^2+\left[2C_2/\left(C_1\kappa^2\right)\right]H^2$
(c)	$P=-\rho-\left[1/\left(3C_1\right)\right]+\left[2C_2/\left(C_1\kappa^2\right)\right]H^2$
(d)	$P=-\rho+\left[2C_2/\left(3C_1\right)\right]\rho-\left[1/\left(3C_1\right)\right]$

Description of a perfect fluid

- **Second gravitational equation**
- **Conversation law**

$$\Rightarrow \quad \frac{2}{\kappa^2}\left(H(N)\right)^2\left[\left(\frac{H'(N)}{H(N)}\right)^2+\frac{H''(N)}{H(N)}\right]=3f'(\rho)f(\rho)$$

$$f'(\rho)\equiv df(\rho)/d\rho$$

It is possible to express $H(N)$ and its derivatives with respect to N only with $\rho(N)$ and $f(\rho(N))$.

Description of a perfect fluid (2)

The slow-roll parameters can be described in terms of $H(N)$ and its derivatives with respect to N .

$$\Downarrow$$

The observables of the inflationary models $(n_{\mathrm{S}}, r, \alpha_{\mathrm{S}})$ can be represented with $\rho(N)$ and $f(\rho(N))$.

Observables of the inflationary models

- **For** $\left|f(\rho)/\rho(N)\right| \ll 1$ **,**

$$\longrightarrow \quad n_{\mathrm{s}} \approx 1 - 6\frac{f(\rho)}{\rho(N)}\,, \qquad r \approx 24\frac{f(\rho)}{\rho(N)}$$

$$\alpha_{\mathrm{s}} \approx -9\left(\frac{f(\rho)}{\rho(N)}\right)^2$$

- **If** $f(\rho)/\rho(N) = 4.35 \times 10^{-3}$ **,**

$$(n_{\mathrm{s}}, r, \alpha_{\mathrm{s}}) = (0.974, 0.104, -1.70 \times 10^{-4})$$

Viscous fluid models

$$\frac{f(\rho)}{\rho} = A\rho_{\mathrm{c}}^{\beta-1}\left(\frac{\rho}{\rho_{\mathrm{c}}}\right)^{\beta-1} + \bar{\zeta}\left(\frac{\kappa}{\sqrt{3}}\right)^{\gamma}\rho_{\mathrm{c}}^{\gamma/2-1}\left(\frac{\rho}{\rho_{\mathrm{c}}}\right)^{\gamma/2-1}$$

$$= A\rho_{\mathrm{c}}^{\beta-1}\left(\frac{H_{\mathrm{inf}}}{H_0}\right)^{2(\beta-1)} + \bar{\zeta}\left(\frac{\kappa}{\sqrt{3}}\right)^{\gamma}\rho_{\mathrm{c}}^{\gamma/2-1}\left(\frac{H_{\mathrm{inf}}}{H_0}\right)^{\gamma-2}$$

H_{inf} : Hubble parameter at the inflationary stage

$\rho_{\mathrm{c}} \equiv 3H_0^2/\kappa^2 = 8.10 \times 10^{-47}\,\mathrm{GeV}^4$

: Critical density

$H_0 = 100h\,\mathrm{km\,sec^{-1}\,Mpc^{-1}} = 2.13h \times 10^{-42}\mathrm{GeV}$

: Current Hubble parameter $\quad h = 0.678$

Viscous fluid models (2)

For simplicity, if $\gamma = 2\beta$ **,**

$$\frac{f(\rho)}{\rho} = J \left(\frac{H_{\mathrm{inf}}}{H_0} \right)^{2(\beta-1)}, \quad J \equiv \left[A + \bar{\zeta} \left(\frac{\kappa}{\sqrt{3}} \right)^{2\beta} \right] \rho_{\mathrm{c}}^{\beta-1}$$

- $\beta = 1$, $J = 4.35 \times 10^{-3}$
- $\beta = 2$, $(H_{\mathrm{inf}}, J) = (1.0 \times 10^{10}\,\mathrm{GeV}, 9.10 \times 10^{-107})$
  $(1.0 \times 10^{5}\,\mathrm{GeV}, 9.10 \times 10^{-97})$

$\Longrightarrow$ $f(\rho)/\rho(N) = 4.35 \times 10^{-3}$

$\longrightarrow$ **The Planck results can be realized.**

EoS of viscous fluid models (2)

$$\frac{f(\rho)}{\rho} \approx \frac{2q}{3} \bar{H}^{1/q} \left(\frac{\kappa^2 \rho}{3} \right)^{-(q+1)/(2q)} \left[1 - \frac{(q-1)}{q} \frac{H_{\mathrm{inf}}}{\sqrt{\kappa^2 \rho / 3}} \right]$$

$$= \frac{2q}{3} \left(\frac{\bar{H}}{H^{q+1}} \right)^{1/q} \left[1 - \frac{(q-1)}{q} \frac{H_{\mathrm{inf}}}{H} \right]$$

$$\bar{H}/H^{q+1} \ll 1 \quad \Longrightarrow \quad f(\rho)/\rho \ll 1$$

Cf. [Nojiri, Odintsov, Oikonomou and Saridakis, arXiv:1503.08443 [gr-qc]]
[Odintsov and Oikonomou, arXiv:1507.05273 [gr-qc]]

“Stochastic Dynamics of Infrared Fluctuations in Accelerating Universe”

by Hiroyuki Kitamoto

[JGRG25(2015)2a2]

Stochastic Dynamics of Infrared Fluctuations in Accelerating Universe

Hiroyuki Kitamoto (Kyoto Univ.)
with Gihyuk Cho, Cook Hyun Kim (SNU)

Based on arXiv: 1508.07877

Introduction

- In the presence of massless and minimally coupled scalar fields in accelerating universes, quantum fluctuations at super-horizon scales make vacuum expectation values of field operators growing with time

  (Infrared effects)

- From a semiclassical view point, it was proposed that such infrared effects are well-described by a Langevin equation

  ’94 J. Yokoyama, A. A. Starobinsky

- In de Sitter space, the stochastic approach has been proved to be equivalent to the leading power resummation of the growing time dependences

  ’05 N. C. Tsamis, R. P. Woodard

- We extend these investigations in a general accelerating universe

Free scalar field in Accelerating universe

'03 N. C. Tsamis, R. P. Woodard

$$ds^2 = -dt^2 + a^2(t)d\mathbf{x}^2$$

$$H \equiv \frac{\dot{a}}{a} > 0 : \text{ expanding era} \qquad \dot{} \equiv \partial_t$$

$$0 \leq \epsilon \equiv \frac{-\dot{H}}{H^2} < 1 : \text{ acceleration}$$

massless, minimally coupled

$$S_2 = -\frac{1}{2}\int \sqrt{-g}d^4x \, [g^{\mu\nu}\partial_\mu\varphi\partial_\nu\varphi \; \cancel{+m^2\varphi^2 + \xi R\varphi^2}]$$

$$\varphi_0(x) = \int \frac{d^3p}{(2\pi)^3} \, [a_{\mathbf{p}}\phi_{\mathbf{p}}(x) + a^\dagger_{\mathbf{p}}\phi^*_{\mathbf{p}}(x)]$$

At $P \equiv p/a \ll H,$

$$\phi_{\mathbf{p}}(x) \simeq -i\underbrace{\frac{2^{\nu_*-1}\Gamma(\nu_*)}{\sqrt{\pi}} \frac{\{(1-\epsilon_*)H_* a_*^{\epsilon_*}\}^{\frac{1}{1-\epsilon_*}}}{p^{\nu_*}}}_{\text{freezing}} e^{+i\mathbf{p}\cdot\mathbf{x}}$$

$$\nu = \frac{3}{2} + \frac{\epsilon}{1-\epsilon}$$

$*$: horizon crossing

Free propagator

Propagator acquires a growing time dependence through the increase of d. o. f. at super-horizon scales

Accelerating universe:

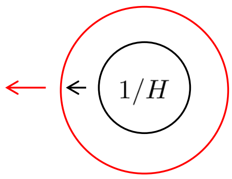

size of universe: a/p_0

$$\langle\varphi_0^2(x)\rangle \simeq \int_{p<Ha} \frac{d^3p}{(2\pi)^3} \frac{2^{2\nu_*-2}\Gamma^2(\nu_*)}{\pi} \frac{\{(1-\epsilon_*)H_* a_*^{\epsilon_*}\}^{\frac{2}{1-\epsilon_*}}}{p^{2\nu_*}} \qquad \nu \geq 3/2$$

$$= \int_{p_0}^{Ha} dp \, \frac{2^{2\nu_*-3}\Gamma^2(\nu_*)}{\pi^3} \frac{\{(1-\epsilon_*)H_* a_*^{\epsilon_*}\}^{\frac{2}{1-\epsilon_*}}}{p^{2\nu_*-2}} \qquad p_{\min} \text{ is fixed}$$

Changing variables: $p = H'a' \Rightarrow dp = \underline{(1-\epsilon')}pH'dt',$

$$\langle\varphi_0^2(x)\rangle = \int_{t_0}^{t} dt' \, \underbrace{(1-\epsilon')}_{>0} \times \frac{(2-2\epsilon')^{2\nu'-3}\Gamma^2(\nu')}{\pi^3}(1-\epsilon')^2 H'^3$$

$$\rightarrow \frac{H^3}{4\pi^2}(t-t_0) = \frac{H^2}{4\pi^2}\log(a/a_0) \text{ at dS limit}$$

In interacting field theories

With each increase of # of vertices, additional propagators appear

$$\begin{cases} \text{one of them is } G^R(x,x') = \theta(t-t')[\varphi_0(x), \varphi_0(x')] \\ \text{the others are } \langle \varphi_0(x)\varphi_0(x')\rangle \text{ and } \langle \varphi_0(x')\varphi_0(x)\rangle \end{cases} \quad \text{Causality}$$

- Secular growths of the Wightman functions originate in

$$\varphi_0(x) \simeq \int \frac{d^3p}{(2\pi)^3}\,\theta(Ha-p)\big[-i\underbrace{\frac{2^{\nu_*-1}\Gamma(\nu_*)}{\sqrt{\pi}}\frac{\{(1-\epsilon_*)H_* a_*^{\epsilon_*}\}^{\frac{1}{1-\epsilon_*}}}{p^{\nu_*}}}_{\text{const.}} e^{+i\mathbf{p}\cdot\mathbf{x}} a_{\mathbf{p}} + (\text{h.c.})\big]$$

- Each vertex integral induces a secular growth

$$\int \sqrt{-g'}d^4x'\; G^R(x,x') \simeq -i\underline{\int^t dt'}\;\Big(a'^3 \int_{t'}^{\infty} dt''\; a''^{-3}\Big)$$

$$\to \frac{-i}{3H^2}\int^a d(\log a') \text{ at dS limit}$$

Leading IR effects

For example $V = \frac{\lambda}{4!}\varphi^4$, with each increase in the loop level, quantum corrections are multiplied by up to the factor:

$$\lambda\Big[\underbrace{\int^t dt'\;\Big(a'^3\int_{t'}^{\infty} dt'''\; a'''^{-3}\Big)}_{\int \sqrt{-g'}d^4x'\; G^R(x,x')} \times \underbrace{\int^{t'} dt''\; \frac{(2-2\epsilon'')^{2\nu''-3}\Gamma^2(\nu'')}{\pi^3}(1-\epsilon'')^3 H''^3}_{\text{Wightman function}}\Big]$$

$$\to \lambda[\;\log^2(a/a_0)\;] \text{ at dS limit}$$

Even if $\lambda \ll 1$, the perturbation theory is eventually broken after an enough time: $\lambda[\;\cdots\;] \sim 1$ passed

$$\Downarrow$$

Resummation formula for the leading powers of the growing time dependence is necessary to evaluate them nonperturbatively

Resummation formula

Yang-Feldman formalism is reduced to the Langevin eq.
up to the leading IR effects

$$\varphi(x) = \varphi_0(x) - i\int \sqrt{-g'}d^4x'\ G^R(x,x')\frac{\partial}{\partial\varphi}V(\varphi(x'))$$

Up to the leading IR effects

$$\varphi_0(x) \simeq \bar{\varphi}_0(x) = \int \frac{d^3p}{(2\pi)^3}\ \theta(Ha-p)\big[\underline{(\text{const. spectrum})}\big]$$

$$\int \sqrt{-g'}d^4x\ G^R(x,x') \simeq -i\int^t dt'\ \left(a'^3\int_{t'}^{\infty} dt''\ a''^{-3}\right)$$

Langevin eq.: $$\dot{\varphi}(x) = \dot{\bar{\varphi}}_0(x) - \underline{\left(a^3\int_t^{\infty} dt'\ a'^{-3}\right)}\frac{\partial}{\partial\varphi}V(\varphi(x))$$

$\to 1/3H$ at dS limit

$$\langle\dot{\bar{\varphi}}_0(t,\mathbf{x})\dot{\bar{\varphi}}_0(t',\mathbf{x})\rangle = \frac{(2-2\epsilon)^{2\nu-3}\Gamma^2(\nu)}{\pi^3}\big\{(1-\epsilon)H\big\}^3\underline{\delta(t-t')}$$

White noise

Fokker-Planck equation

Langevin eq. is translated to the equation of the probability density ρ:

$$\dot{\rho}(t,\phi) = \frac{AH^3}{2}\frac{\partial^2}{\partial\phi^2}\rho(t,\phi) + \left(a^3\int_t^{\infty} dt'\ a'^{-3}\right)\frac{\partial}{\partial\phi}\Big(\rho(t,\phi)\frac{\partial}{\partial\phi}V(\phi)\Big)$$

$$A = \frac{(2-2\epsilon)^{2\nu-3}\Gamma^2(\nu)}{\pi^3}(1-\epsilon)^3 > 0$$

$$\langle F(\varphi(x))\rangle = \int_{-\infty}^{\infty} d\phi\ \rho(t,\phi)F(\phi), \qquad F\text{: arbitrary function}$$

If the variations of H, ϵ are negligible during the IR effects grow, eventually,

$$\rho(t,\phi) \to N^{-1}\exp\Big(-\frac{2}{AH^3}\left(a^3\int_t^{\infty} dt'\ a'^{-3}\right)V(\phi)\Big)$$

e.g. $V = \frac{\lambda}{4!}\varphi^4$, $$\langle V(\varphi(x))\rangle \to \underline{\frac{AH^3}{8}\left(a^3\int_t^{\infty} dt'\ a'^{-3}\right)^{-1}}$$

Not suppressed by $\lambda \ll 1$

Naive semiclassical description

$$\left(\frac{\partial^2}{\partial t^2}+3H\frac{\partial}{\partial t}-\frac{1}{a^2}\frac{\partial^2}{\partial \mathbf{x}^2}\right)\varphi(x)=-\frac{\partial}{\partial\varphi}V(\varphi(x))$$

Extracting IR dynamics: $\varphi=\bar{\varphi}+\varphi_{\rm UV}$

Neglecting ∂_t^2, $\partial_{\mathbf{x}}^2$

Identifying $\varphi_{\rm UV}$ as a source of $\bar{\varphi}$

$$3H\frac{\partial}{\partial t}\{\bar{\varphi}(x)+\varphi_{\rm UV}(x)\}=-\frac{\partial}{\partial\bar{\varphi}}V(\bar{\varphi}(x))$$

$$\varphi_{\rm UV}(x)=\int\frac{d^3p}{(2\pi)^3}\,\theta(p-Ha)\big[(\text{const. spectrum})\big]$$

Since $\dot{\varphi}_{\rm UV}=-\dot{\varphi}_0$,

$$\dot{\bar{\varphi}}(x)=\dot{\bar{\varphi}}_0(x)-\underline{\frac{1}{3H}}\frac{\partial}{\partial\bar{\varphi}}V(\bar{\varphi}(x))$$

Inconsistent with Resummation formula except in dS space

Improved semiclassical description

For a general choice of time coordinate: $dT=\mathcal{H}dt$,

$$\frac{\partial}{\partial t^2}+3H\frac{\partial}{\partial t}=\mathcal{H}^2\left(\frac{\partial^2}{\partial T^2}+\frac{\dot{\mathcal{H}}+3H\mathcal{H}}{\mathcal{H}^2}\frac{\partial}{\partial T}\right)$$

To compare $\frac{\partial}{\partial T}\varphi$ with $\frac{\partial^2}{\partial T^2}\varphi$ directly, we choose T as its friction coefficient is constant

$$\frac{\dot{\mathcal{H}}+3H\mathcal{H}}{\mathcal{H}^2}=\mu_0\,:\,\text{const.}$$

$$\rightarrow\qquad \mathcal{H}=\frac{1}{\mu_0}\left(a^3\int_t^\infty dt'\ a'^{-3}\right)^{-1}$$

Neglecting ∂_T^2, $\partial_{\mathbf{x}}^2$ rather than ∂_t^2, $\partial_{\mathbf{x}}^2$,

$$\mu_0\mathcal{H}^2\frac{\partial}{\partial T}\{\bar{\varphi}(x)+\varphi_{\rm UV}(x)\}=\underline{\left(a^3\int_t^\infty dt'\ a'^{-3}\right)^{-1}}\frac{\partial}{\partial t}\{\bar{\varphi}(x)+\varphi_{\rm UV}(x)\}$$

Consistent with Resummation formula

Summary

- In accelerating universes, the increase of d. o. f. at super-horizon scales makes vevs of field operators growing with time through the propagator of a massless and minimally coupled scalar field
- In order to evaluate the IR effects nonperturbatively, we extended the resummation formula of the leading IR effects in a general accelerating universe
- The resulting equation is given by a Langevin eq. with a white noise, and the coefficient of each term is modified by the slow-roll parameter
- We can derive the same stochastic equation also by the semiclassical description of the scalar field, as far as we choose the time coordinate as its friction coefficient is constant

“Disformal transformation & cosmological perturbations of spatially covariant theories of gravity”

by Xian Gao

[JGRG25(2015)2a3]

Disformal transformation & cosmological perturbations of spatially covariant theories of gravity

Xian Gao (高 顯)
Tokyo Institute of Technology

2015-12-08
JGRG'25, Kyoto University

Based on:
- ***XG,*** *Phys.Rev. D* ***90*** *(2014) 081501(R), [arXiv: 1406.0822]*
- ***X.G****, Phys.Rev. D* ***90*** *(2014) 104033, [arXiv: 1409.6708]*
- *T. Fujita,* ***XG****, J. Yokoyama, [arXiv: 1511.04324]*

k-essence, Horndeski and beyond

1915 ● GR $$\mathcal{L} = \frac{1}{16\pi G} R$$

k-essence, Horndeski and beyond

1915 GR $\qquad \mathcal{L} = \frac{1}{16\pi G} R$

1961 Brans-Dicke $\qquad \mathcal{L} = \phi\, R - \frac{\omega}{\phi}(\partial\phi)^2$

[Brans & Dicke, Phys.Rev. 124 (1961) 925-935]

k-essence, Horndeski and beyond

1915 GR $\qquad \mathcal{L} = \frac{1}{16\pi G} R$

1961 Brans-Dicke $\qquad \mathcal{L} = \phi\, R - \frac{\omega}{\phi}(\partial\phi)^2$

[Brans & Dicke, Phys.Rev. 124 (1961) 925-935]

1999 *k*-essence $\qquad \mathcal{L} = g(\phi)\, R + F(\phi, \partial\phi)$

[Armendariz-Picon, Damour & Mukhanov, 792 Phys. Lett. B 458, 209 (1999)]

k-essence, Horndeski and beyond

1915 GR $\mathcal{L} = \frac{1}{16\pi G} R$

1961 Brans-Dicke $\mathcal{L} = \phi\, R - \frac{\omega}{\phi}(\partial\phi)^2$

[Brans & Dicke, Phys.Rev. 124 (1961) 925-935]

1999 *k*-essence $\mathcal{L} = g(\phi)\, R + F(\phi, \partial\phi)$

[Armendariz-Picon, Damour & Mukhanov, 792 Phys. Lett. B 458, 209 (1999)]

k-essence:

- The most general theory for a scalar field coupled to gravity, of which the Lagrangian involves up to the first derivative of the scalar field.

k-essence, Horndeski and beyond

1915 GR $\mathcal{L} = \frac{1}{16\pi G} R$

1961 Brans-Dicke $\mathcal{L} = \phi\, R - \frac{\omega}{\phi}(\partial\phi)^2$

[Brans & Dicke, Phys.Rev. 124 (1961) 925-935]

1999 *k*-essence $\mathcal{L} = g(\phi)\, R + F(\phi, \partial\phi)$

[Armendariz-Picon, Damour & Mukhanov, 792 Phys. Lett. B 458, 209 (1999)]

Beyond *k*-essence?

Introducing second derivatives?

k-essence, Horndeski and beyond

1915 GR $\mathcal{L} = \frac{1}{16\pi G} R$

1961 **Brans-Dicke** $\mathcal{L} = \phi\, R - \frac{\omega}{\phi}(\partial\phi)^2$

[Brans & Dicke, Phys.Rev. 124 (1961) 925-935]

1999 ***k*-essence** $\mathcal{L} = g(\phi)\, R + F(\phi, \partial\phi)$

[Armendariz-Picon, Damour & Mukhanov, 792 Phys. Lett. B 458, 209 (1999)]

Beyond *k*-essence?

Introducing second derivatives?

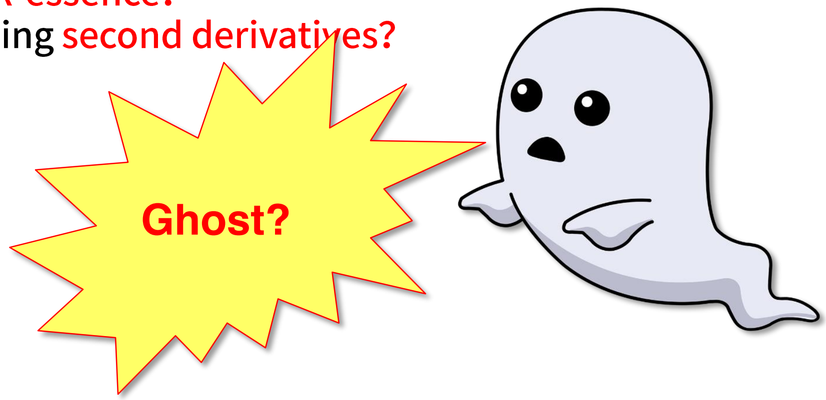

k-essence, Horndeski and beyond

1915 GR $\mathcal{L} = \frac{1}{16\pi G} R$

1961 **Brans-Dicke** $\mathcal{L} = \phi\, R - \frac{\omega}{\phi}(\partial\phi)^2$

[Brans & Dicke, Phys.Rev. 124 (1961) 925-935]

1999 ***k*-essence** $\mathcal{L} = g(\phi)\, R + F(\phi, \partial\phi)$

[Armendariz-Picon, Damour & Mukhanov, 792 Phys. Lett. B 458, 209 (1999)]

2011 **Generalized galileon**

[Deffayet, X. Gao, Steer & Zahariade Phys.Rev. D 84 (2011) 064039]

In *D*=4:

$$\begin{aligned}\mathcal{L} = {} & G_0(\phi, X) + G_1(\phi, X)\Box\phi \\ & + G_2(\phi, X)\, R + \frac{\partial G_2}{\partial X}\left[(\Box\phi)^2 - (\nabla_\mu\nabla_\nu\phi)^2\right] \\ & + G_3(\phi, X)\, G^{\mu\nu}\nabla_\mu\nabla_\nu\phi \\ & - \frac{1}{6}\frac{\partial G_3}{\partial X}\left[(\Box\phi)^3 - 3\Box\phi(\nabla_\mu\nabla_\nu\phi)^2 + 2(\nabla_\mu\nabla_\nu\phi)^3\right]\end{aligned}$$

with $X \equiv -\frac{1}{2}(\partial\phi)^2$

k-essence, Horndeski and beyond

1915 GR $\mathcal{L} = \frac{1}{16\pi G} R$

1961 Brans-Dicke $\mathcal{L} = \phi R - \frac{\omega}{\phi}(\partial\phi)^2$

[Brans & Dicke, Phys.Rev. 124 (1961) 925-935]

1999 *k*-essence $\mathcal{L} = g(\phi)\, R + F(\phi, \partial\phi)$

[Armendariz-Picon, Damour & Mukhanov, 792 Phys. Lett. B 458, 209 (1999)]

2011 Generalized galileon

[Deffayet, X. Gao, Steer & Zahariade ***Phys.Rev.*** *D 84 (2011) 064039]*

In *D*=4:

$$\mathcal{L} = G_0(\phi, X) + G_1(\phi, X)\Box\phi + G_2(\phi, X)\, R + \frac{\partial G_2}{\partial X}\left[(\Box\phi)^2 - (\nabla_\mu\nabla_\nu\phi)^2\right]$$

***Generalized galileon/Horndeski theory*:**

- The most general theory for a scalar field coupled to gravity, of which the Lagrangian/EoMs involve up to the second derivatives of the scalar field and the metric.
- Propagates 1 scalar + 2 tensor dofs.

k-essence, Horndeski and beyond

1915 GR $\mathcal{L} = \frac{1}{16\pi G} R$

1961 Brans-Dicke $\mathcal{L} = \phi R - \frac{\omega}{\phi}(\partial\phi)^2$

[Brans & Dicke, Phys.Rev. 124 (1961) 925-935]

1999 *k*-essence $\mathcal{L} = g(\phi)\, R + F(\phi, \partial\phi)$

[Armendariz-Picon, Damour & Mukhanov, 792 Phys. Lett. B 458, 209 (1999)]

2011 Generalized galileon

[Deffayet, X. Gao, Steer & Zahariade ***Phys.Rev.*** *D 84 (2011) 064039]*

In *D*=4:

$$\begin{aligned}\mathcal{L} = {} & G_0(\phi, X) + G_1(\phi, X)\Box\phi \\ & + G_2(\phi, X)\, R + \frac{\partial G_2}{\partial X}\left[(\Box\phi)^2 - (\nabla_\mu\nabla_\nu\phi)^2\right] \\ & + G_3(\phi, X)\, G^{\mu\nu}\nabla_\mu\nabla_\nu\phi \\ & - \frac{1}{6}\frac{\partial G_3}{\partial X}\left[(\Box\phi)^3 - 3\Box\phi(\nabla_\mu\nabla_\nu\phi)^2 + 2(\nabla_\mu\nabla_\nu\phi)^3\right]\end{aligned}$$

Even beyond galileon/Horndeski theory?

- Higher derivatives of the scalar field and the metric.
- Propagates 1 scalar + 2 tensor dofs.

k-essence, Horndeski and beyond

1915 GR $\mathcal{L} = \frac{1}{16\pi G} R$

1961 Brans-Dicke $\mathcal{L} = \phi R - \frac{\omega}{\phi}(\partial\phi)^2$

[Brans & Dicke, Phys.Rev. 124 (1961) 925-935]

1999 *k*-essence $\mathcal{L} = g(\phi) R + F(\phi, \partial\phi)$

[Armendariz-Picon, Damour & Mukhanov, 792 Phys. Lett. B 458, 209 (1999)]

2011 Generalized galileon

*[Deffayet, X. Gao, Steer & Zahariade **Phys.Rev.** D 84 (2011) 064039]*

In *D*=4:

$\mathcal{L} = G_0(\phi, X)$

$+G_2(\phi,$ … $(\nabla_\mu\nabla_\nu\phi)^2]$

$+G_3(\phi,$ …

$-\frac{1}{6}\frac{\partial G_3}{\partial X}[$ … $)^2 + 2(\nabla_\mu\nabla_\nu\phi)^3]$

*Even **beyond galileon/Horndeski** theory?*

- Higher derivatives of the scalar field and the metric.
- Propagates 1 scalar + 2 tensor dofs.

k-essence, Horndeski and beyond

1915 GR $\mathcal{L} = \frac{1}{16\pi G} R$

1961 Brans-Dicke $\mathcal{L} = \phi R - \frac{\omega}{\phi}(\partial\phi)^2$

[Brans & Dicke, Phys.Rev. 124 (1961) 925-935]

1999 *k*-essence $\mathcal{L} = g(\phi) R + F(\phi, \partial\phi)$

[Armendariz-Picon, Damour & Mukhanov, 792 Phys. Lett. B 458, 209 (1999)]

2011 Generalized galileon

*[Deffayet, X. Gao, Steer & Zahariade **Phys.Rev.** D 84 (2011) 064039]*

In *D*=4:

$\mathcal{L} = G_0(\phi, X)$

$+G_2(\phi,$ … $(\nabla_\mu\nabla_\nu\phi)^2]$

$+G_3(\phi,$ …

$-\frac{1}{6}\frac{\partial G_3}{\partial X}[$ … $)^2 + 2(\nabla_\mu\nabla_\nu\phi)^3]$

We need some alternative approach.

Spatially covariant theories of gravity

Spatially covariant theories of gravity

Key question：how to introduce a scalar degree of freedom?

Spatially covariant theories of gravity

Key question：how to introduce a scalar degree of freedom?

Reduction of symmetries → Extra mode(s)

Spatially covariant theories of gravity

Key question：how to introduce a scalar degree of freedom?

Reduction of symmetries → Extra mode(s)

A purely metric theory, respecting only spatial symmetries → 2 tensor + 1 scalar

Foliation of spacetime

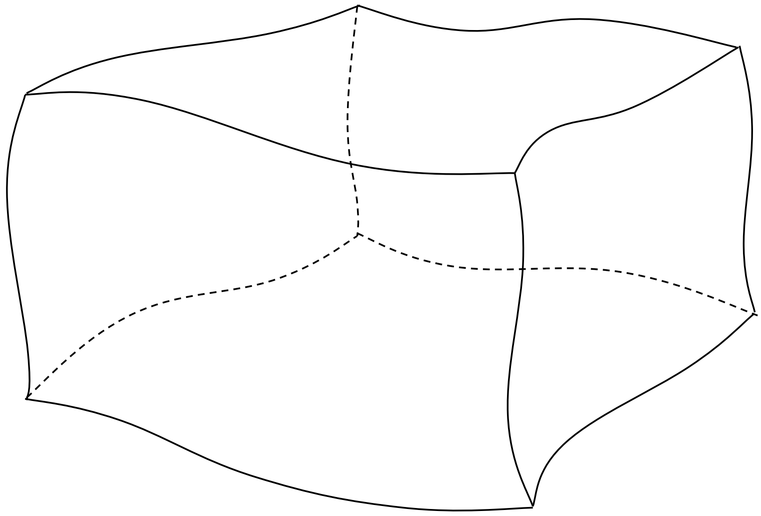

Spacetime covariant

4-D quantities
$(g_{\mu\nu}, R_{\mu\nu\rho\sigma}, \nabla_\mu)$

Foliation of spacetime

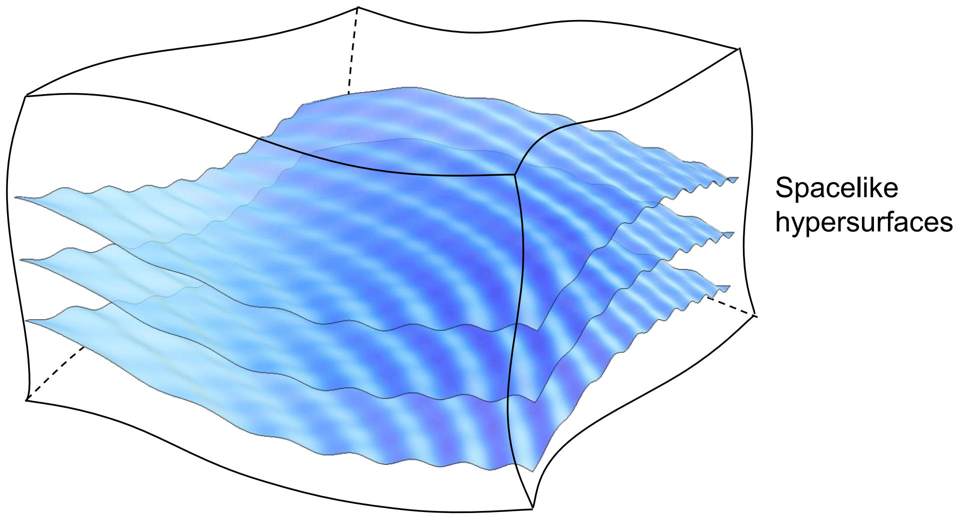

Spacetime covariant

4-D quantities
$(g_{\mu\nu}, R_{\mu\nu\rho\sigma}, \nabla_\mu)$

Foliation of spacetime

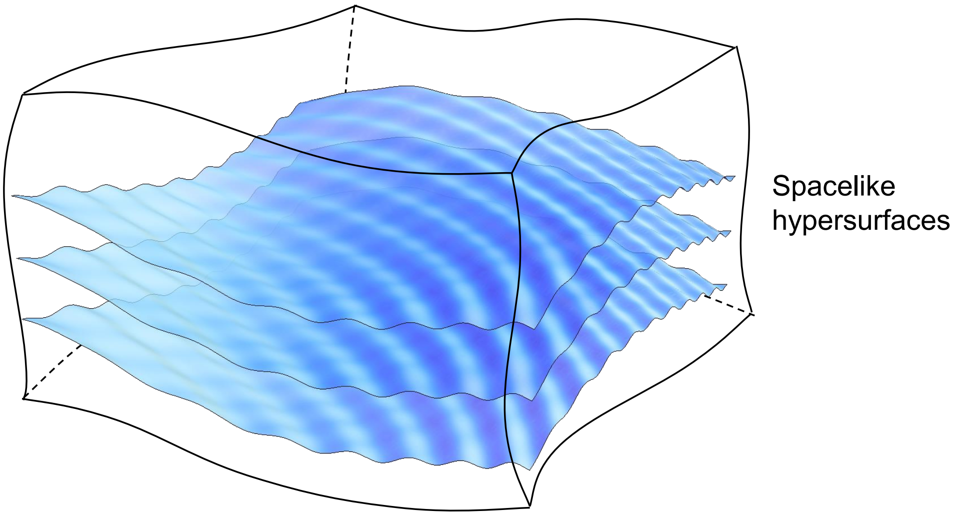

Spacetime covariant

4-D quantities

$(g_{\mu\nu}, R_{\mu\nu\rho\sigma}, \nabla_\mu)$

$\Rightarrow$

Spatially covariant

3-D quantities

$(t, N, h_{ij}, R_{ij}, \nabla_i) \quad K_{ij}$

Examples of spatially covariant theories

2004 **Ghost condensation**

[Arkani-Hamed, Cheng, Luty & Mukohyama, JHEP 0803, 014 (2008)]

2007 **Effective field theory of inflation**

[Cheung, Creminelli, Fitzpatrick, Kaplan & Senatore, JHEP 0803, 014 (2008)]

Examples of spatially covariant theories

2004 **Ghost condensation**
[Arkani-Hamed, Cheng, Luty & Mukohyama, JHEP 0803, 014 (2008)]

2007 **Effective field theory of inflation**
[Cheung, Creminelli, Fitzpatrick, Kaplan & Senatore, JHEP 0803, 014 (2008)]

2009 **Hořava gravity**
[Horava, Phys.Rev. D79 (2009) 084008]

Examples of spatially covariant theories

2004 **Ghost condensation**
[Arkani-Hamed, Cheng, Luty & Mukohyama, JHEP 0803, 014 (2008)]

2007 **Effective field theory of inflation**
[Cheung, Creminelli, Fitzpatrick, Kaplan & Senatore, JHEP 0803, 014 (2008)]

2009 **Hořava gravity**
[Horava, Phys.Rev. D79 (2009) 084008]

2014 **GLPV theory**
[Gleyzes, Langlois, Piazza & Vernizzi, Phys.Rev.Lett. 114 (2015) 21, 211101]

Examples of spatially covariant theories

2004 **Ghost condensation**
[Arkani-Hamed, Cheng, Luty & Mukohyama, JHEP 0803, 014 (2008)]

2007 **Effective field theory of inflation**
[Cheung, Creminelli, Fitzpatrick, Kaplan & Senatore, JHEP 0803, 014 (2008)]

2014 **GLPV theory**
[Gleyzes, Langlois, Piazza & Vernizzi, Phys.Rev.Lett. 114 (2015) 21, 211101]

2009 **Hořava gravity**
[Horava, Phys.Rev. D79 (2009) 084008]

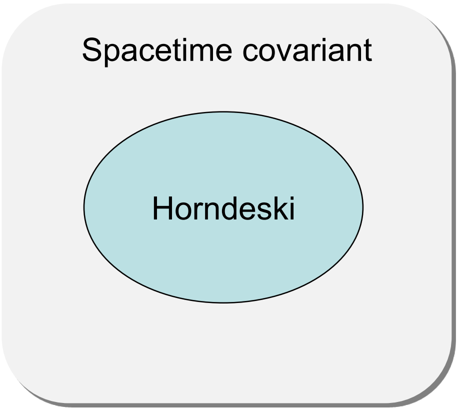

Examples of spatially covariant theories

2004 **Ghost condensation**
[Arkani-Hamed, Cheng, Luty & Mukohyama, JHEP 0803, 014 (2008)]

2007 **Effective field theory of inflation**
[Cheung, Creminelli, Fitzpatrick, Kaplan & Senatore, JHEP 0803, 014 (2008)]

2014 **GLPV theory**
[Gleyzes, Langlois, Piazza & Vernizzi, Phys.Rev.Lett. 114 (2015) 21, 211101]

2009 **Hořava gravity**
[Horava, Phys.Rev. D79 (2009) 084008]

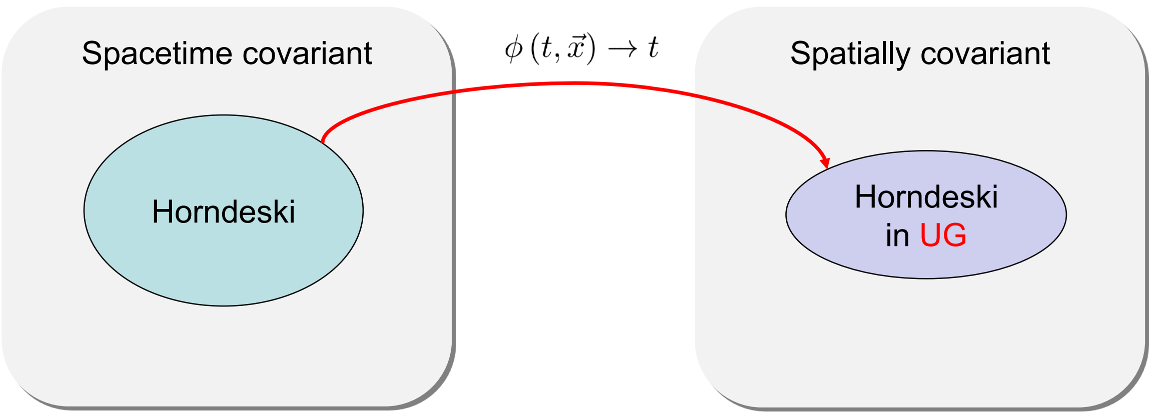

Examples of spatially covariant theories

2004 **Ghost condensation**
[Arkani-Hamed, Cheng, Luty & Mukohyama, JHEP 0803, 014 (2008)]

2007 **Effective field theory of inflation**
[Cheung, Creminelli, Fitzpatrick, Kaplan & Senatore, JHEP 0803, 014 (2008)]

2014 **GLPV theory**
[Gleyzes, Langlois, Piazza & Vernizzi, Phys.Rev.Lett. 114 (2015) 21, 211101]

2009 **Hořava gravity**
[Horava, Phys.Rev. D79 (2009) 084008]

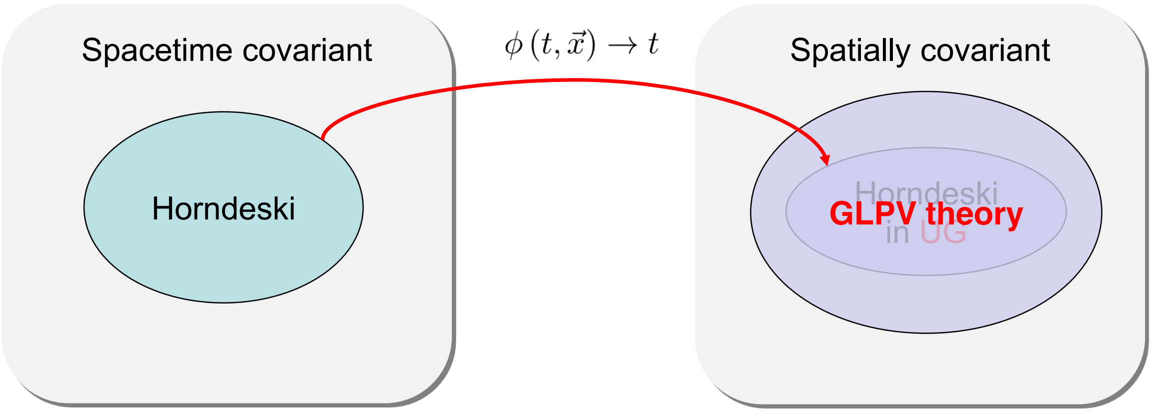

Examples of spatially covariant theories

2004 **Ghost condensation**
[Arkani-Hamed, Cheng, Luty & Mukohyama, JHEP 0803, 014 (2008)]

2007 **Effective field theory of inflation**
[Cheung, Creminelli, Fitzpatrick, Kaplan & Senatore, JHEP 0803, 014 (2008)]

2014 **GLPV theory**
[Gleyzes, Langlois, Piazza & Vernizzi, Phys.Rev.Lett. 114 (2015) 21, 211101]

2009 **Hořava gravity**
[Horava, Phys.Rev. D79 (2009) 084008]

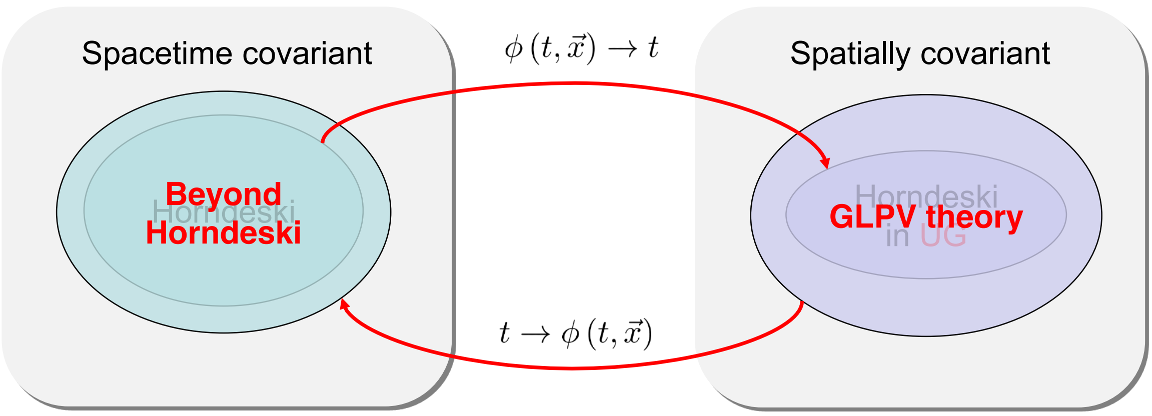

Spatially covariant theories of gravity

2004 Ghost condensation
[Arkani-Hamed, Cheng, Luty & Mukohyama, JHEP 0803, 014 (2008)]

2007 Effective field theory of inflation
[Cheung, Creminelli, Fitzpatrick, Kaplan & Senatore, JHEP 0803, 014 (2008)]

2009 Hořava gravity
[Horava, Phys.Rev. D79 (2009) 084008]

2014 GLPV theory
[Gleyzes, Langlois, Piazza & Vernizzi, Phys.Rev.Lett. 114 (2015) 21, 211101]

2014 Spatially covariant gravity
*[X. Gao, **Phys.Rev. D** 90 (2014) 081501 (**Rapid Communication**)]*

$$S=\int \mathrm{d}t\mathrm{d}^3x\, N\sqrt{h}\,\mathcal{L}(t,N,h_{ij},R_{ij},K_{ij},\mathrm{D}_i)$$

A unifying framework for scalar-tensor theories

1915 GR

1961 Brans-Dicke

1999 *k*-essence

2011 Galileon/Horndeski
*[Deffayet, **X. Gao**, Steer & Zahariade **Phys.Rev. D** 84 (2011) 064039]*

A unifying framework for scalar-tensor theories

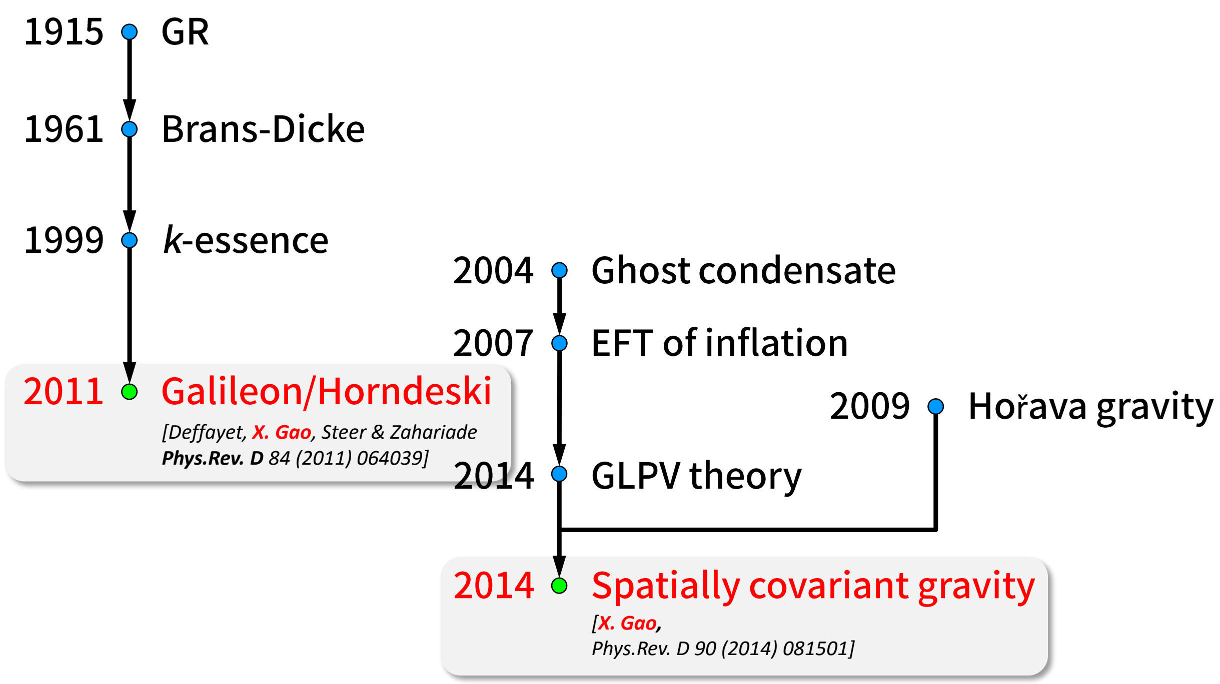

A unifying framework for scalar-tensor theories

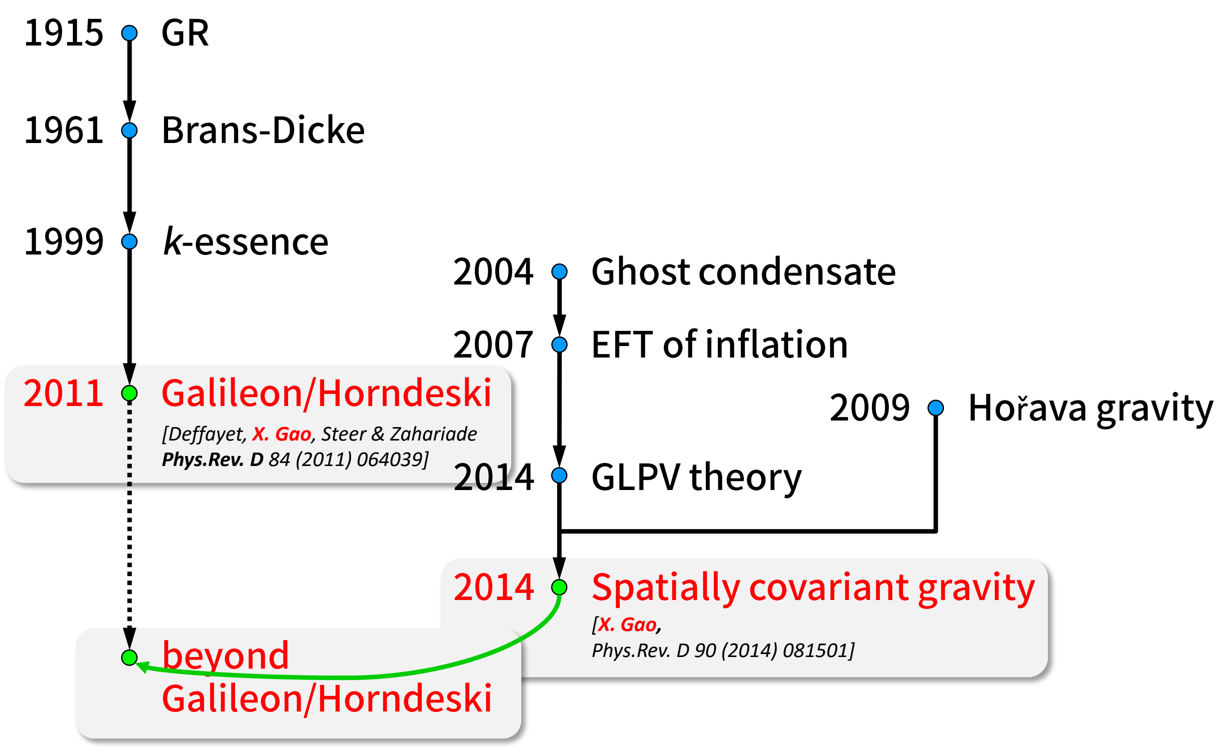

Disformal transformation

Disformal transformation

- Disformal transformation: *[Bekenstein, Phys. Rev. D48 (1993) 3641–3647]*

$$g_{\mu\nu} \to \hat{g}_{\mu\nu} = \Omega^2(\phi)\, g_{\mu\nu} + \Gamma(\phi, X)\, \partial_\mu\phi\partial_\nu\phi$$

In terms of ADM variables:

$$\hat{N} = \Phi(t, N)N, \qquad \hat{N}_i = \Omega^2(t)N_i, \qquad \hat{h}_{ij} = \Omega^2(t)h_{ij}$$

$$\Phi^2(t, N) = \Omega^2(t) - \frac{1}{N^2}\Gamma(t, N)\,(\partial_t\phi)^2$$

Disformal transformation

- Disformal transformation: *[Bekenstein, Phys. Rev. D48 (1993) 3641–3647]*

$$g_{\mu\nu} \to \hat{g}_{\mu\nu} = \Omega^2(\phi)\, g_{\mu\nu} + \Gamma(\phi, X)\, \partial_\mu\phi\partial_\nu\phi$$

In terms of ADM variables:

$$\hat{N} = \Phi(t, N)N, \qquad \hat{N}_i = \Omega^2(t)N_i, \qquad \hat{h}_{ij} = \Omega^2(t)h_{ij}$$

$$\Phi^2(t, N) = \Omega^2(t) - \frac{1}{N^2}\Gamma(t, N)\,(\partial_t\phi)^2$$

- Relation between “Horndeski / GLPV / SCG” under disformal transformation:

Disformal transformation

- Disformal transformation: *[Bekenstein, Phys. Rev. D48 (1993) 3641–3647]*

$$g_{\mu\nu} \to \hat{g}_{\mu\nu} = \Omega^2(\phi)\, g_{\mu\nu} + \Gamma(\phi, X)\, \partial_\mu\phi\partial_\nu\phi$$

In terms of ADM variables:

$$\hat{N} = \Phi(t, N)N, \qquad \hat{N}_i = \Omega^2(t)N_i, \qquad \hat{h}_{ij} = \Omega^2(t)h_{ij}$$

$$\Phi^2(t, N) = \Omega^2(t) - \frac{1}{N^2}\Gamma(t, N)\,(\partial_t\phi)^2$$

- Relation between “Horndeski / GLPV / SCG” under disformal transformation:

$$\Gamma = \Gamma(\phi)$$

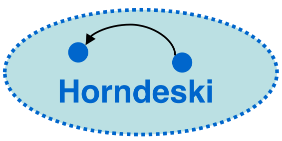

Disformal transformation

- Disformal transformation: *[Bekenstein, Phys. Rev. D48 (1993) 3641–3647]*

$$g_{\mu\nu} \to \hat{g}_{\mu\nu} = \Omega^2(\phi)\, g_{\mu\nu} + \Gamma(\phi, X)\, \partial_\mu\phi\partial_\nu\phi$$

In terms of ADM variables:

$$\hat{N} = \Phi(t,N)N, \qquad \hat{N}_i = \Omega^2(t)N_i, \qquad \hat{h}_{ij} = \Omega^2(t)h_{ij}$$

$$\Phi^2(t,N) = \Omega^2(t) - \frac{1}{N^2}\Gamma(t,N)\,(\partial_t\phi)^2$$

- Relation between "Horndeski / GLPV / SCG" under disformal transformation:

$\Gamma = \Gamma(\phi)$

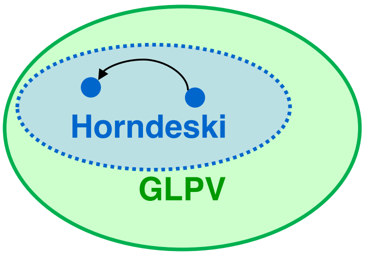

Disformal transformation

- Disformal transformation: *[Bekenstein, Phys. Rev. D48 (1993) 3641–3647]*

$$g_{\mu\nu} \to \hat{g}_{\mu\nu} = \Omega^2(\phi)\, g_{\mu\nu} + \Gamma(\phi, X)\, \partial_\mu\phi\partial_\nu\phi$$

In terms of ADM variables:

$$\hat{N} = \Phi(t,N)N, \qquad \hat{N}_i = \Omega^2(t)N_i, \qquad \hat{h}_{ij} = \Omega^2(t)h_{ij}$$

$$\Phi^2(t,N) = \Omega^2(t) - \frac{1}{N^2}\Gamma(t,N)\,(\partial_t\phi)^2$$

- Relation between "Horndeski / GLPV / SCG" under disformal transformation:

$\Gamma = \Gamma(\phi)$

$\Gamma = \Gamma(\phi, X)$

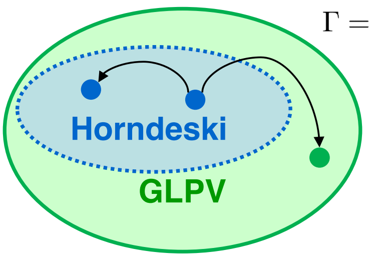

Disformal transformation

- Disformal transformation: [Bekenstein, Phys. Rev. D48 (1993) 3641–3647]

$$g_{\mu\nu} \to \hat{g}_{\mu\nu} = \Omega^2(\phi)\, g_{\mu\nu} + \Gamma(\phi, X)\, \partial_\mu\phi\partial_\nu\phi$$

In terms of ADM variables:

$$\hat{N} = \Phi(t,N)N, \qquad \hat{N}_i = \Omega^2(t)N_i, \qquad \hat{h}_{ij} = \Omega^2(t)h_{ij}$$

$$\Phi^2(t,N) = \Omega^2(t) - \frac{1}{N^2}\Gamma(t,N)\,(\partial_t\phi)^2$$

- Relation between "Horndeski / GLPV / SCG" under disformal transformation:

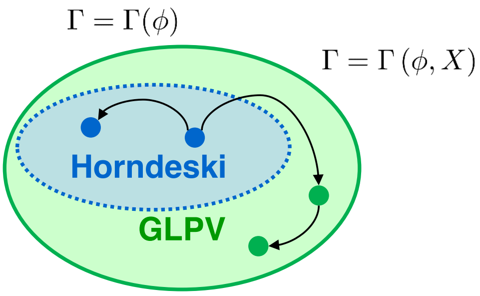

Disformal transformation

- Disformal transformation: [Bekenstein, Phys. Rev. D48 (1993) 3641–3647]

$$g_{\mu\nu} \to \hat{g}_{\mu\nu} = \Omega^2(\phi)\, g_{\mu\nu} + \Gamma(\phi, X)\, \partial_\mu\phi\partial_\nu\phi$$

In terms of ADM variables:

$$\hat{N} = \Phi(t,N)N, \qquad \hat{N}_i = \Omega^2(t)N_i, \qquad \hat{h}_{ij} = \Omega^2(t)h_{ij}$$

$$\Phi^2(t,N) = \Omega^2(t) - \frac{1}{N^2}\Gamma(t,N)\,(\partial_t\phi)^2$$

- Relation between "Horndeski / GLPV / SCG" under disformal transformation:

*T. Fujita, **X. Gao**, J. Yokoyama, [arXiv: 1511.04324]*

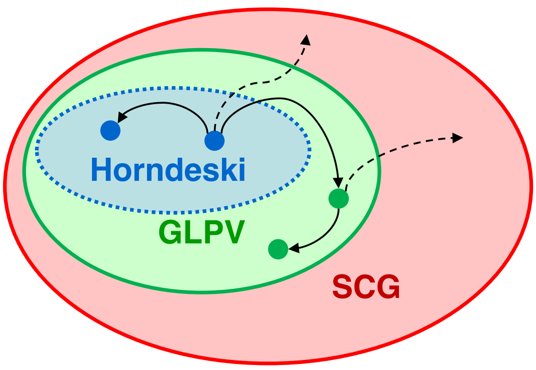

Disformal transformation

- Disformal transformation: *[Bekenstein, Phys. Rev. D48 (1993) 3641–3647]*

$$g_{\mu\nu} \to \hat{g}_{\mu\nu} = \Omega^2(\phi)\, g_{\mu\nu} + \Gamma(\phi, X)\, \partial_\mu\phi\partial_\nu\phi$$

In terms of ADM variables:

$$\hat{N} = \Phi(t,N)N, \qquad \hat{N}_i = \Omega^2(t)N_i, \qquad \hat{h}_{ij} = \Omega^2(t)h_{ij}$$

$$\Phi^2(t,N) = \Omega^2(t) - \frac{1}{N^2}\Gamma(t,N)\,(\partial_t\phi)^2$$

- Relation between "Horndeski / GLPV / SCG" under disformal transformation:

*T. Fujita, **X. Gao**, J. Yokoyama, [arXiv: 1511.04324]*

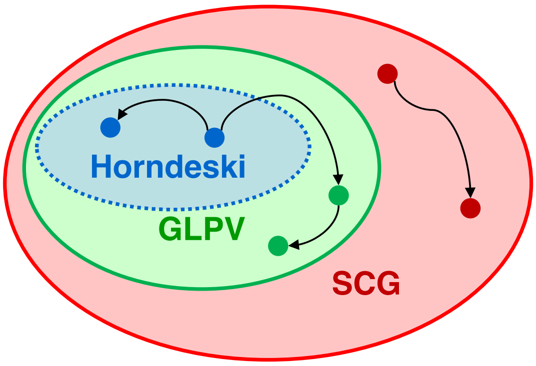

Disformal transformation

- Disformal transformation: *[Bekenstein, Phys. Rev. D48 (1993) 3641–3647]*

$$g_{\mu\nu} \to \hat{g}_{\mu\nu} = \Omega^2(\phi)\, g_{\mu\nu} + \Gamma(\phi, X)\, \partial_\mu\phi\partial_\nu\phi$$

In terms of ADM variables:

$$\hat{N} = \Phi(t,N)N, \qquad \hat{N}_i = \Omega^2(t)N_i, \qquad \hat{h}_{ij} = \Omega^2(t)h_{ij}$$

$$\Phi^2(t,N) = \Omega^2(t) - \frac{1}{N^2}\Gamma(t,N)\,(\partial_t\phi)^2$$

- Relation between "Horndeski / GLPV / SCG" under disformal transformation:

*T. Fujita, **X. Gao**, J. Yokoyama, [arXiv: 1511.04324]*

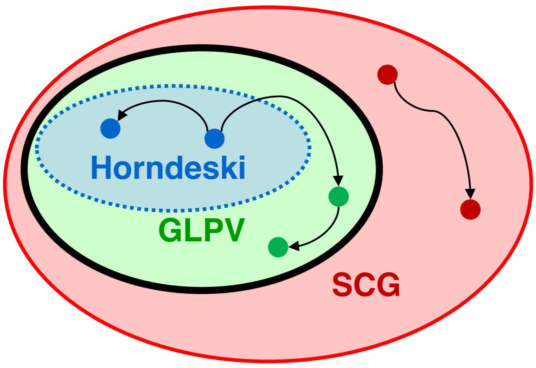

"GLPV theory" is the first connected subset that is mapped to itself in the space of Spatially Covariant Gravity theories.

Gravitational waves and Einstein frames

Gravitational waves and Einstein frames

- Under the disformal transformation

$$\hat{N} = \Phi(t, N)N, \qquad \hat{N}_i = \Omega^2(t)N_i, \qquad \hat{h}_{ij} = \Omega^2(t)h_{ij}$$

the tensor perturbations (defined as $h_{ij} = a^2 e^{\gamma_{ij}}$) are invariant:

$$\gamma_{ij} = \hat{\gamma}_{ij}, \qquad \mathcal{P}_\gamma = \hat{\mathcal{P}}_{\hat{\gamma}}$$

- A general power spectrum

$$\mathcal{P}_\gamma^{\rm gen} = \mathcal{P}_{\gamma(0)}^{\rm gen} \left(\frac{k}{k_*}\right)^{n_\gamma^{\rm gen}} (1 + \mathcal{E}^{\rm gen})$$

- Gravitational waves in GR:

$$\hat{\mathcal{P}}_\gamma^{\rm GR}(k) = \frac{2\hat{H}^2(k_*)}{\pi^2 M_{\rm Pl}^2} \left(\frac{k}{k_*}\right)^{\hat{n}_\gamma^{\rm GR}} [1 + \mathcal{E}^{\rm GR}(\hat{\epsilon}_H)],$$

$$\hat{n}_\gamma^{\rm GR} = -\frac{2\hat{\epsilon}_H}{1 - \hat{\epsilon}_H},$$

$$\mathcal{E}^{\rm GR}(\hat{\epsilon}_H) = \pi^{-1} 2^{\frac{2}{1-\hat{\epsilon}_H}} (1 - \hat{\epsilon}_H)^2 \Gamma^2 \left(\frac{3 - \hat{\epsilon}_H}{2(1 - \hat{\epsilon}_H)}\right) - 1,$$

[E. D. Stewart and D. H. Lyth, Phys. Lett. B302 (1993) 171–175]

Gravitational waves and Einstein frames

- Ansatz for disformal transformation:

$$\Omega(t) = \Omega_* \left(\frac{a}{a_*}\right)^{\epsilon_\Omega}, \qquad \bar{\Phi}(t) = \bar{\Phi}_* \left(\frac{a}{a_*}\right)^{\epsilon_{\bar{\Phi}}}$$

- Power spectrum in the original frame

$$\hat{\mathcal{P}}_\gamma^{\rm GR} = \frac{2H_*^2}{\pi^2 M_{\rm Pl}^2 \bar{\Phi}_*^2}\left(\frac{k}{k_*}\right)^{\hat{n}_\gamma^{\rm GR}} \left(1+\epsilon_\Omega\right)^2\left[1+\mathcal{E}^{\rm GR}(\epsilon_H+\epsilon_{\bar{\Phi}})\right],$$

$$\hat{n}_\gamma^{\rm GR} = -2\frac{\epsilon_H+\epsilon_{\bar{\Phi}}}{1-(\epsilon_H+\epsilon_{\bar{\Phi}})},$$

- Matching conditions:

$$\mathcal{P}_{\gamma(0)}^{\rm gen} = \frac{2H_*^2}{\pi^2 M_{\rm Pl}^2 \bar{\Phi}_*^2} \implies \bar{\Phi}_* = \frac{\sqrt{2}H_*}{\pi M_{\rm Pl}}\left(\mathcal{P}_{\gamma(0)}^{\rm gen}\right)^{-\frac{1}{2}}$$

$$n_\gamma^{\rm gen} = -\frac{2\left(\epsilon_H+\epsilon_{\bar{\Phi}}\right)}{1-\epsilon_H-\epsilon_{\bar{\Phi}}} \implies \epsilon_{\bar{\Phi}} = -\frac{2\epsilon_H+(1-\epsilon_H)n_\gamma^{\rm gen}}{2-n_\gamma^{\rm gen}}$$

$$1+\mathcal{E}^{\rm gen} = \left(1+\epsilon_\Omega\right)^2\left(1+\mathcal{E}^{\rm GR}\right) \implies \epsilon_\Omega = \sqrt{\frac{1+\mathcal{E}^{\rm gen}}{1+\mathcal{E}^{\rm GR}}}-1$$

There is a one-parameter family of “Einstein frames”.

Thank you for your attention!

“Tracking dark energy with nonmininal coupling to gravity”

by Yi-Peng Wu

[JGRG25(2015)2a4]

JGRG 25 @ YITP
December 8, 2015

TRACKING DARK ENERGY WITH NONMINIMAL COUPLING TO GRAVITY

Yi-Peng Wu

Institute of Physics, Academia Sinica

in collaboration with Chao-Qiang Geng & Chung-Chi Lee

EVIDENCE OF DARK ENERGY

PLANCK 2015

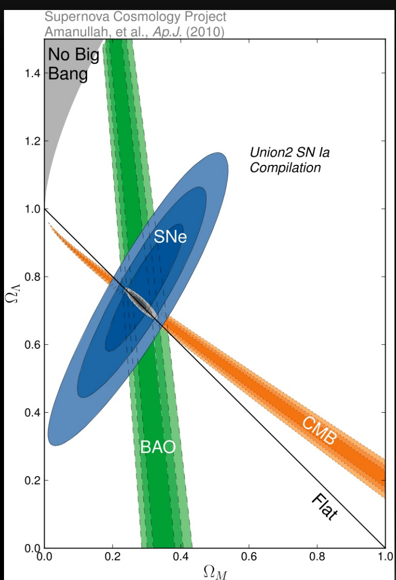

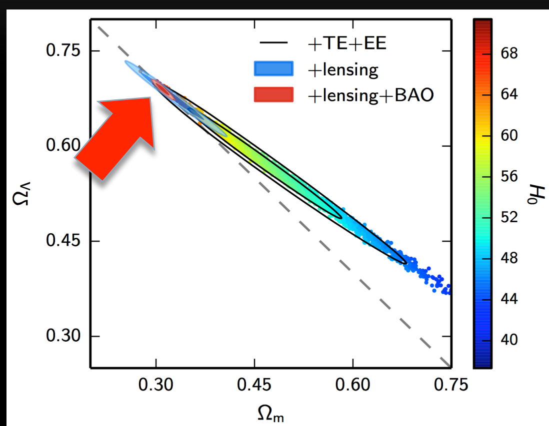

$$w = -1.019 \pm^{0.075}_{0.080} \; (95\% \text{ CL})$$

ΛCDM (w = -1) is consistent with all latest experiments.

COSMIC COINCIDENCE PROBLEM

$$\left(\frac{\rho_{\mathrm{DE}}^{(0)}}{\rho_m^{(0)}}\right) \sim O(1)$$

In the ΛCDM model:

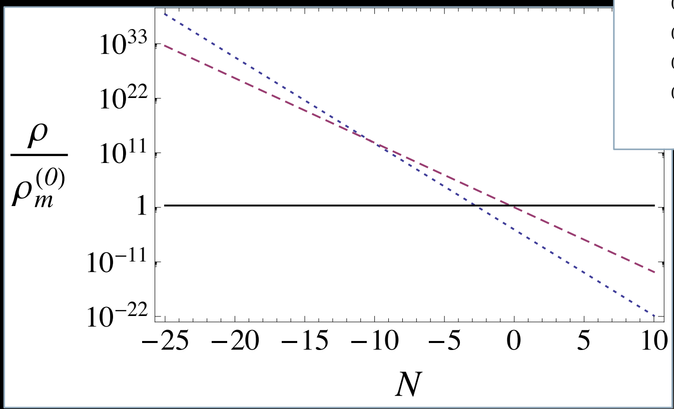

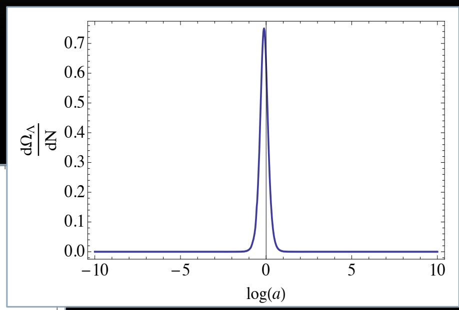

Amendola & Tsujikawa

COSMIC COINCIDENCE PROBLEM

Dark energy candidates:

quintessence, phantom, quintom,…
k-essence, ghost-condensate,…
galileon, generalized galileon,…
f(R), f(G), f(T),…
scalar tensor, teleparallel dark energy,…
……

Quintessence may give an answer?

TRACKER DARK ENERGY

Zlatev, Wang & Steinhardt, 1999

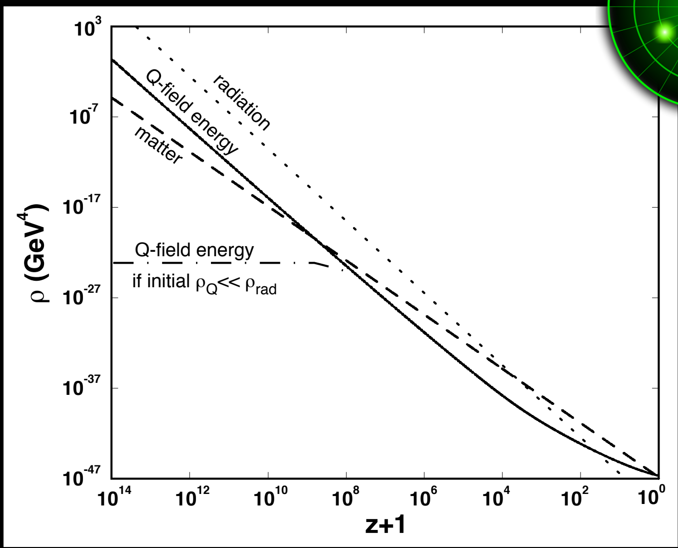

Is the tracker field compatible with observations?

TRACKER DARK ENERGY

$$V(\phi) \sim \phi^{-\alpha}, \quad \alpha > 0$$

Bludman, 2004

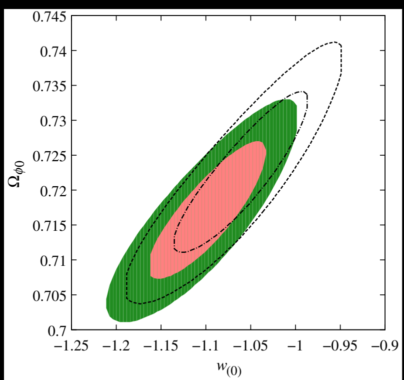

$$w_{(0)} = -2/(\alpha + 2)$$

$$\boxed{\alpha < 0.107}$$

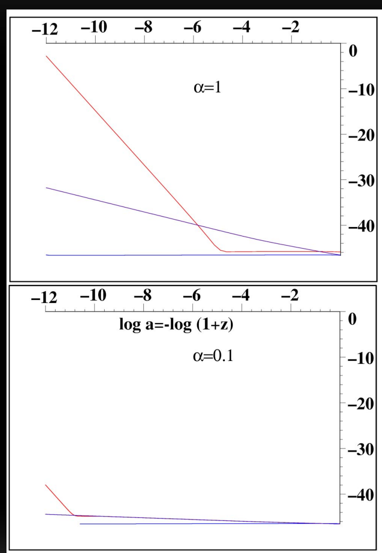

Chiba, Felice & Tsujikawa, 2013

A viable tracker field would only reproduce the coincidence problem!

EXTENDED QUINTESSENCE

Perrotta, Baccigalupi & Matarrese, 2000

$$\mathcal{L}_\phi = F(\phi)R - \frac{1}{2}(\nabla\phi)^2 - V(\phi)$$

$$\Box\phi + F_\phi R - V_\phi = 0$$

$$F(\phi) = \frac{1}{2\kappa^2} + \frac{1}{2}\xi\phi^2$$

TRACKER DARK ENERGY WITH GRAVITY

$$\ddot{\phi} + 3H\dot{\phi} + V_\phi - 6\xi\left(\dot{H} + 2H^2\right)\phi = 0$$

R - boost

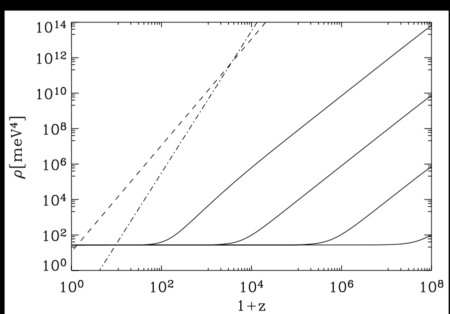

Slow - roll

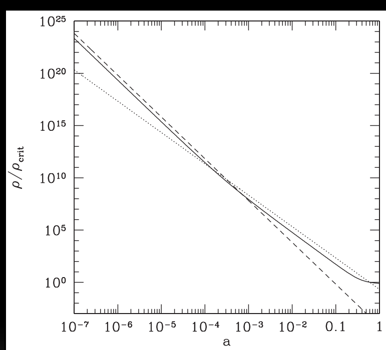

Matarrese, Baccigalupi & Perrotta, 2004

Chiba, Siino & Yamaguchi, 2010

TRACKER DARK ENERGY WITH GRAVITY

$$\ddot{\phi} + 3H\dot{\phi} + \cancel{V_\phi} - 6\xi\left(\dot{H} + 2H^2\right)\phi = 0$$

R - boost

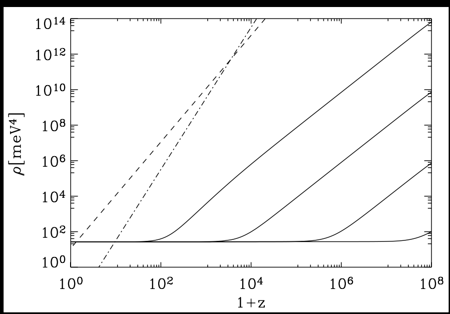

Matarrese, Baccigalupi & Perrotta, 2004

Slow - roll

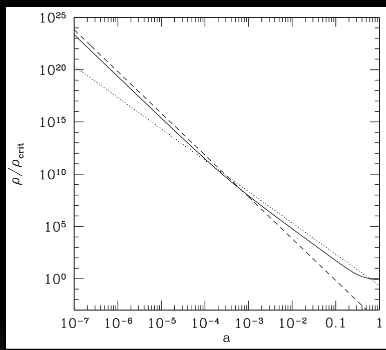

Chiba, Siino & Yamaguchi, 2010

In both cases, the tracker solutions are potential-independent!

TRACKER DARK ENERGY WITH GRAVITY

$$\ddot{\phi} + 3H\dot{\phi} + \cancel{V_\phi} - 6\xi\left(\dot{H} + 2H^2\right)\phi = 0$$

Gravity induced tracking solutions:

$$\phi(N) = C_+ e^{L_+ N} + C_- e^{L_- N}$$

Uzan, 1999

$$L_\pm(w,\xi) = -\frac{3}{4}(1-w) \pm \sqrt{\frac{9}{16}(1-w)^2 + 3\xi(1-3w)}$$

Although the cosmic coincidence is released..

- A viable model requires $V(\phi) \to \Lambda$.
- Ω_ϕ^{nc} must be highly suppressed.

$$\rho_\phi = V(\phi) + \rho_\phi^{nc}$$

TRACKER DARK ENERGY WITH GRAVITY

$$V(\phi) = V_0$$

Geng, Lee & Wu, in prep.

$$\phi(N) = C_+ e^{L_+ N} + C_- e^{L_- N}$$

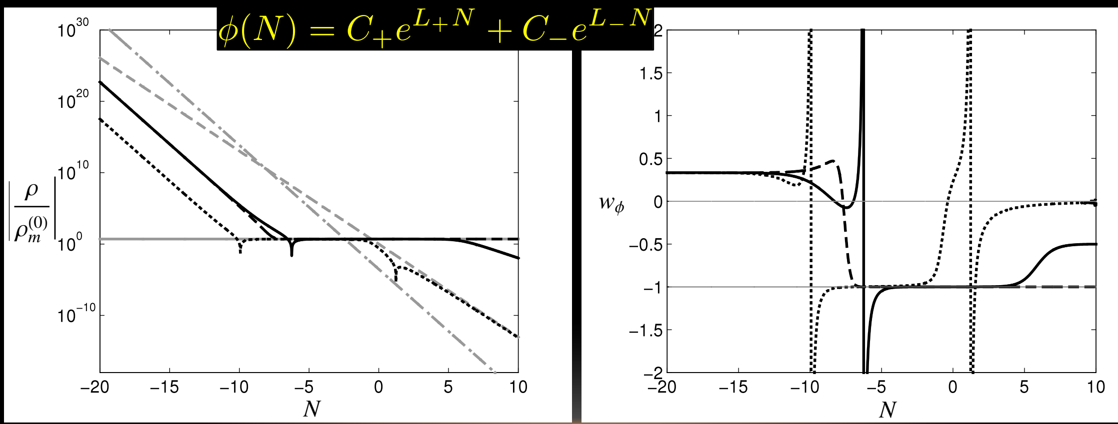

TRACKER DARK ENERGY WITH GRAVITY

$$V(\phi) = V_0$$

Geng, Lee & Wu, in prep.

$$w = \frac{4\xi}{3(1+4\xi)}, \quad (\xi > \frac{3}{2})$$

$$\phi(N) = C_+ e^{L_+ N} + C_- e^{L_- N}$$

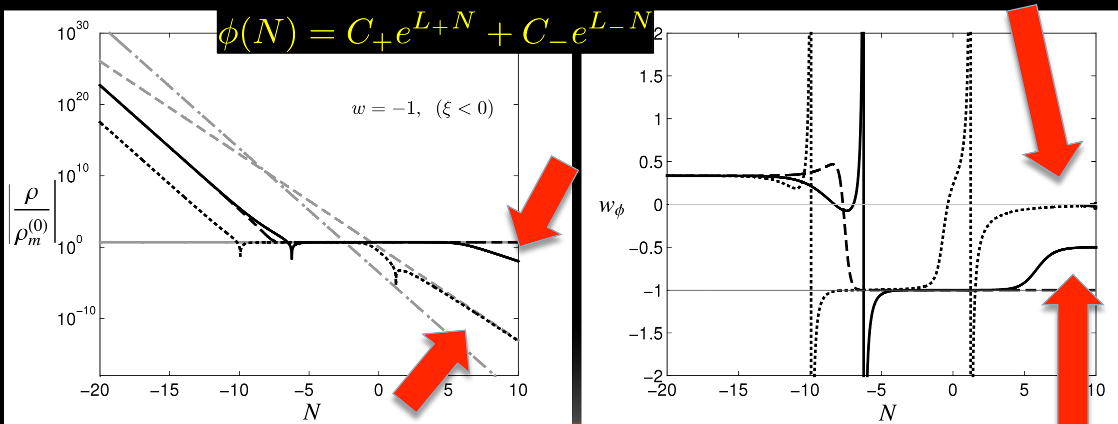

There exist new attractor solutions!

$$w = \frac{-3+2\xi}{3(1+2\xi)}, \quad (0 < \xi < \frac{3}{2})$$

TRACKER DARK ENERGY WITH GRAVITY

$$V(\phi) = V_0\, e^{-\lambda\kappa\phi}$$

Geng, Lee & Wu, in prep.

$$\phi_f = -\frac{2}{\lambda} + \sqrt{\frac{4}{\lambda^2} - \frac{1}{\xi}}, \quad \text{and} \quad H_f^2 = \frac{\kappa^2 V_0}{3(1+\xi\phi_f^2)} e^{-\lambda\phi_f}$$

(I) $\xi < 0$

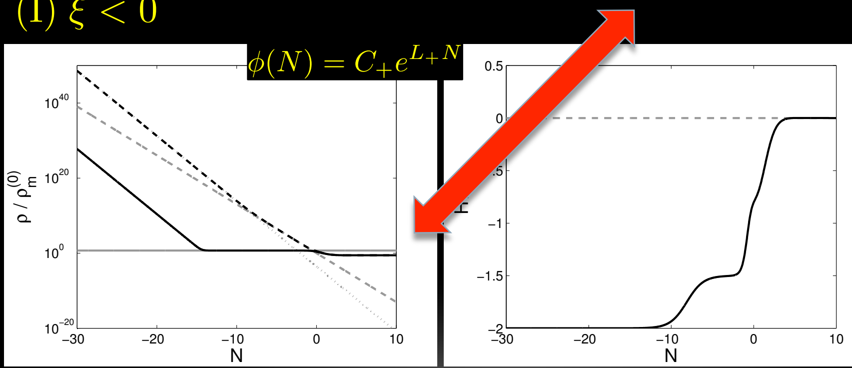

There exist new attractor solutions!

TRACKER DARK ENERGY WITH GRAVITY

$$V(\phi) = V_0\, e^{-\lambda\kappa\phi}$$

Geng, Lee & Wu, in prep.

$$w = \frac{-3+2\xi}{3(1+2\xi)}$$

(II) $\xi > 0$

$$w = \frac{4\xi}{3(1+4\xi)}$$

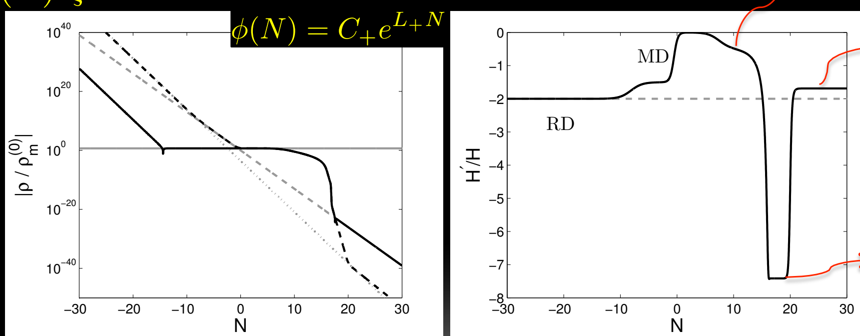

$$w = 1 + 8\xi + 4\sqrt{\frac{2\xi}{3}}(1+6\xi)$$

There exist new attractor solutions!

DARK ENERGY & COSMIC DOOMSDAY

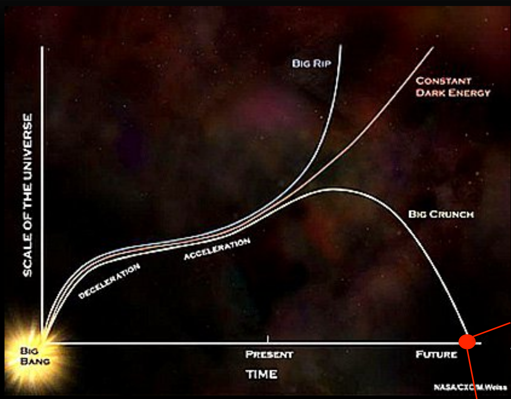

DARK ENERGY & COSMIC DOOMSDAY

$$V(\phi) = V_0 \left(1 - \beta\kappa\phi\right)$$

Kallosh et. al, 2003

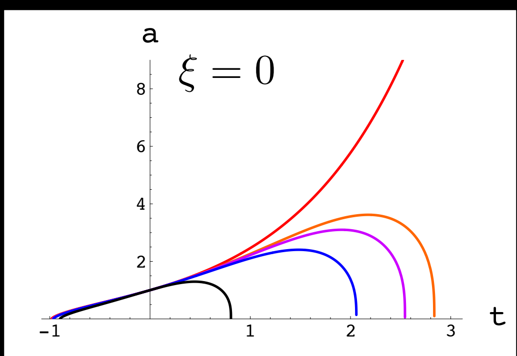

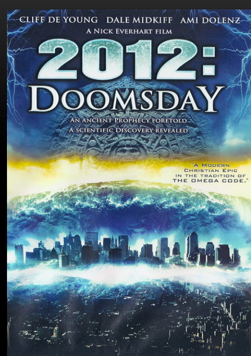

$$t_c > 56 \times 10^9 \text{ years}$$

Ferreira & Avelino, 2015

DARK ENERGY & COSMIC DOOMSDAY

$$V(\phi) = V_0 (1 - \beta\kappa\phi)$$

Geng, Lee & Wu, in prep.

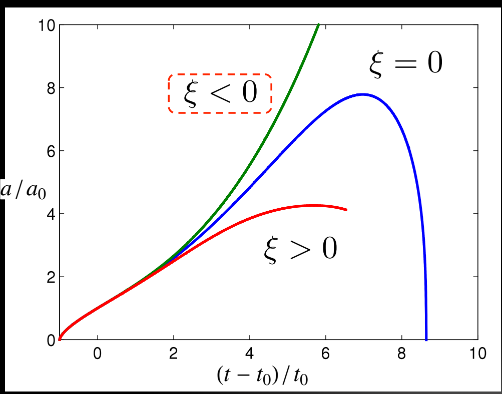

$$\xi < -\frac{3\beta^2}{4} \quad \Rightarrow \quad t_c \to \infty$$

Gravity can save our universe!

TRACKER DARK ENERGY WITH GRAVITY

$$\rho_\phi = V(\phi) + \rho_\phi^{nc}$$

Although the cosmic coincidence is released..

- A viable model requires $V(\phi) \to \Lambda$.
- Ω_ϕ^{nc} must be highly suppressed.
- How much Ω_ϕ^{nc} is allowed today?

Constraints from large scales:

TABLE I. Priors for cosmological parameters.

Parameter	Prior
Baryon density	$0.5 < 100\Omega_b h^2 < 10$
CDM density	$10^{-3} < \Omega_c h^2 < 0.99$
Neutrino mass	$0.01 < \Sigma m_\nu < 2$ eV
Spectral index	$0.9 < n_s < 1.1$
Tensor-to-Scalar ratio	$0 < r < 1$

TABLE II. Parameters for the marginalized confidence regions in Fig. 4 (95% C.L.)

Parameter	$\xi = 0.1$	$\xi = 0.3$	ΛCDM
Baryon density	$100\Omega_b h^2 = 2.21 \pm 0.05$	$100\Omega_b h^2 = 2.21^{+0.05}_{-0.01}$	$100\Omega_b h^2 = 2.22^{+0.04}_{-0.05}$
CDM density	$\Omega_c h^2 = 0.119^{+0.003}_{-0.004}$	$\Omega_c h^2 = 0.118^{+0.004}_{-0.003}$	$\Omega_c h^2 = 0.118 \pm 0.003$
Neutrino mass	$\Sigma m_\nu < 0.245$ eV	$\Sigma m_\nu < 0.245$ eV	$\Sigma m_\nu < 0.211$ eV
Spectral index	$n_s = 0.964 \pm 0.011$	$n_s = 0.964^{+0.011}_{-0.012}$	$n_s = 0.963^{+0.012}_{-0.009}$
Tensor-to-Scalar ratio	$r < 0.116$	$r < 0.118$	$r < 0.125$
Potential	$V_0/\rho_\phi < 1.046$	$V_0/\rho_\phi < 1.178$	–

$$V(\phi) = V_0$$

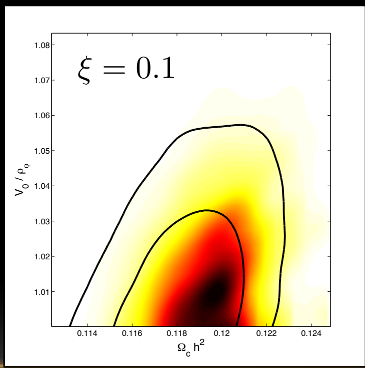

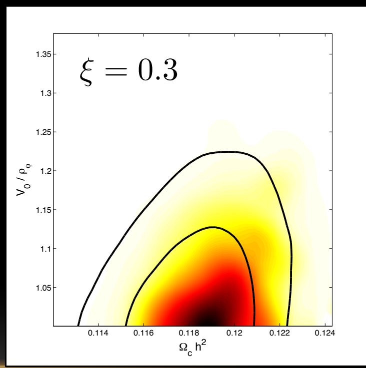

Constraints from the Moon:

Dickey et al, 1994

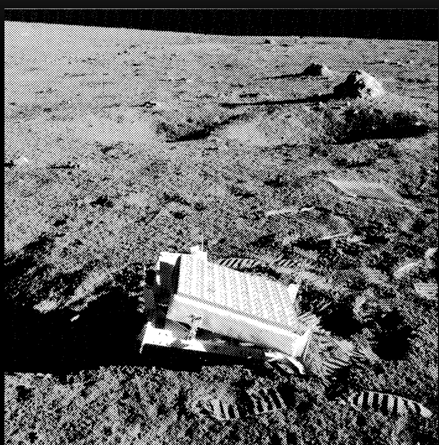

$$\left|\frac{\dot{G}_{\rm eff}}{G_{\rm eff}}\right| < 1.3 \times 10^{-12} {\rm yr}^{-1}$$

Williams et al, 2006

$$G_{\rm eff} = \frac{G}{1 + \xi\kappa^2\phi^2}\frac{1+4Q}{1+3Q}$$

$$Q = \frac{2\xi^2\kappa^2\phi^2}{1+\xi\kappa^2\phi^2}$$

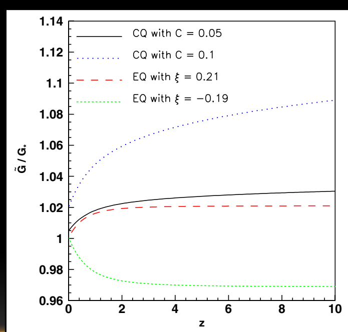

Pettorino & Baccigalupi, 2008

Constraints from Solar System:

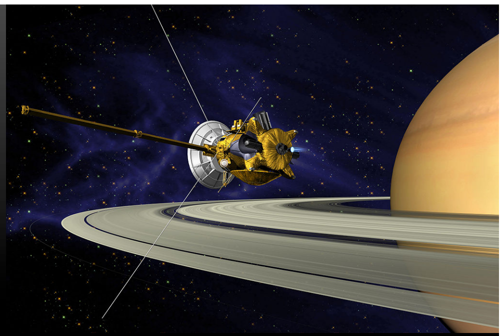

Bertotti et al, 2003

$$\omega_{\rm BD} = \frac{F}{2F_\phi^2} \geq 4 \times 10^4$$

$$F(\phi) = \frac{1}{2\kappa^2} + \frac{1}{2}\xi\phi^2 \qquad \Rightarrow \phi_0^2 \leq \frac{1}{160000\xi^2 - \xi}$$

TABLE III. Solar System constraints to today's parameters

Parameter	$\xi = 0.1$	$\xi = 1$	$\xi = -0.1$
Attractor	$w = -0.78$	$w = -0.11$	$w = -1$
Field value	$\lvert\phi_0\rvert \leq 0.025$	$\lvert\phi_0\rvert \leq 2.5 \times 10^{-3}$	$\lvert\phi_0\rvert \leq 0.025$
ξ-density	$\lvert\Omega_{\phi 0}^{nc}\rvert \leq 9.4 \times 10^{-5}$	$\lvert\Omega_{\phi 0}^{nc}\rvert \leq 2.9 \times 10^{-5}$	$\lvert\Omega_{\phi 0}^{nc}\rvert \leq 2.7 \times 10^{-5}$
ξ-domination	≥ 179.0 Gyr	≥ 31.7 Gyr	–

$$|\xi\phi_0| < 10^{-2}$$

SUMMARY

- We study the future evolution of an extended quintessence field since driving the late-time cosmic acceleration.
- New attractor solutions are found, depending on ξ, in sufficiently flat potentials that can give rise to proper cosmology.
- In the typical cosmic doomsday model with a linear potential, these new attractors can prevent the ultimate collapse of the Universe.
- We apply joint CMB, BAO, Type-Ia supernovae and Solar System measurements to constrain the simplest scenario with a constant potential.
- At most 0.004% (0.01%) of today's dark energy density can be contributed by gravity for ξ ~ 1 (0.1).
- If "ξ" does exist, it may drastically change the fate of our Universe.

Thank you for your attention!

“Real & false loss of coherence in weak gravity”

by Fumika Suzuki

[JGRG25(2015)2a5]

REAL & FALSE LOSS OF COHERENCE IN WEAK GRAVITY

Fumika Suzuki

UBC & IMS

National Institutes of Natural Sciences Institute for Molecular Science

The 25th Workshop on General Relativity and Gravitation in Japan

What is decoherence?

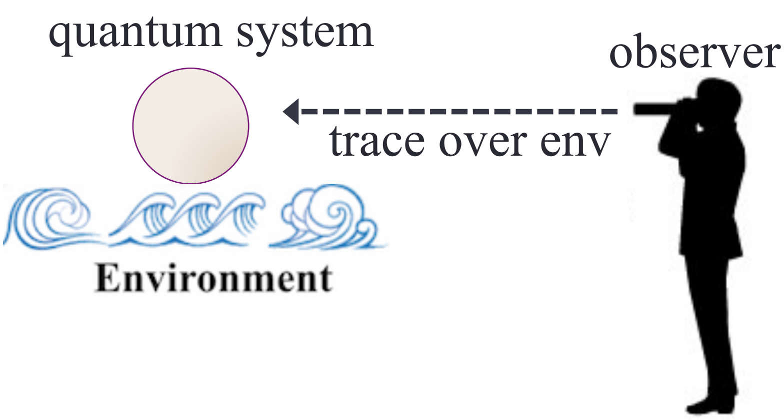

density matrix ρ $\xrightarrow{\text{trace over env}}$ reduced density matrix ρ_{red}

$$-\mathrm{tr}(\rho_{\text{red}} \ln \rho_{\text{red}}) \neq 0$$

Oscillator bath model

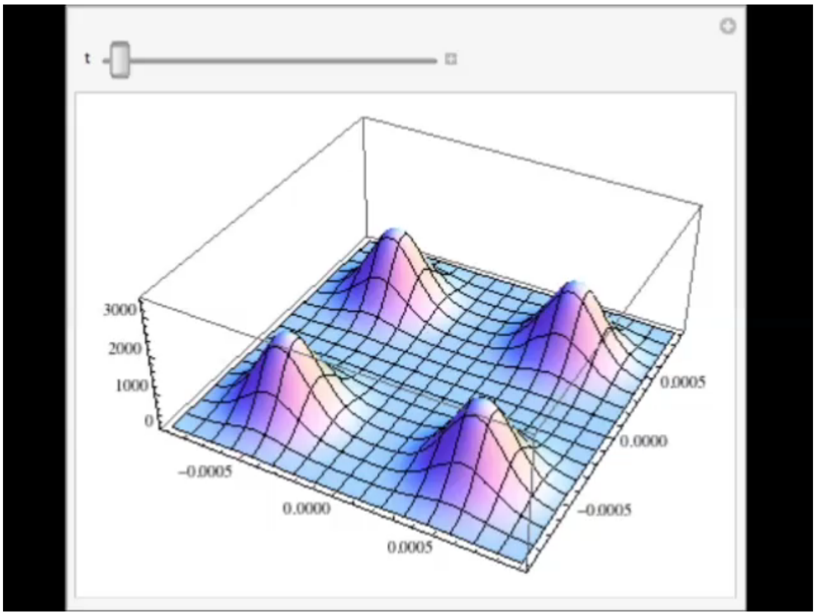

QED (Photon bath)

$$S = S_{\text{sys}} + S_{\text{int}} + S_{\text{photon}}$$

$$S_{\text{photon}} = -\frac{1}{4}\int d^4 r F^{\mu\nu} F_{\mu\nu}$$

$$S_{\text{int}} = \int d^4 r J^\mu A_\mu$$

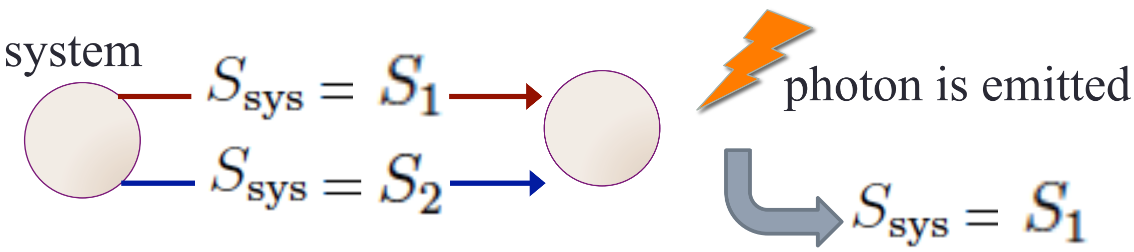

QED (Reduced density matrix propagator)

$$W(x_{\rm i}, x_{\rm f}; x'_{\rm i}, x'_{\rm f}) = \int_{x_{\rm i}}^{x_{\rm f}} \mathcal{D}x \int_{x'_{\rm i}}^{x'_{\rm f}} \mathcal{D}x' \exp(i\, S_{\rm sys}(x) - i\, S_{\rm sys}(x'))\mathcal{F}(x, x')$$

where the influence functional is

$$\mathcal{F}(\mathrm{x},\mathrm{x}') = \exp\Big[-\frac{i}{2}\int_0^T d^4r \int d^3\mathrm{r}' \frac{\rho(\mathbf{r},t)\rho(\mathbf{r}',t)}{4\pi|\mathbf{r}-\mathbf{r}'|} + \frac{i}{2}\int_0^T d^4r' \int d^3\mathrm{r}' \frac{\rho'(\mathbf{r},t)\rho'(\mathbf{r}',t)}{4\pi|\mathbf{r}-\mathbf{r}'|}$$
$$+\frac{i}{2}\int_0^T d^4r \int_0^t d^4r' [J^i(r) + J'^i(r)]\gamma_{ij}(r-r')[J^j(r') - J'^j(r')]$$
$$-\frac{1}{4}\int_0^T d^4r \int_0^t d^4r' [J^i(r) - J'^i(r)]\eta_{ij}(r-r')[J^j(r') - J'^j(r')]\Big]$$

with the correlation functions $\eta_{ij}(r-r') = P_{ij}\displaystyle\int \frac{d^3\mathbf{k}}{(2\pi)^3|\mathbf{k}|}\cos(|\mathbf{k}|(t-t'))e^{i\mathbf{k}\cdot(\mathbf{r}-\mathbf{r}')}$

$$\gamma_{ij}(r-r') = P_{ij}\int \frac{d^3\mathbf{k}}{(2\pi)^3|\mathbf{k}|}\sin(|\mathbf{k}|(t-t'))e^{i\mathbf{k}\cdot(\mathbf{r}-\mathbf{r}')}$$

QED (Influence functional)

$$\mathcal{F}(\mathrm{x},\mathrm{x}') = \exp\Big[-\frac{i}{2}\int_0^T d^4r \int d^3\mathrm{r}' \frac{\rho(\mathbf{r},t)\rho(\mathbf{r}',t)}{4\pi|\mathbf{r}-\mathbf{r}'|} + \frac{i}{2}\int_0^T d^4r' \int d^3\mathrm{r}' \frac{\rho'(\mathbf{r},t)\rho'(\mathbf{r}',t)}{4\pi|\mathbf{r}-\mathbf{r}'|}$$
$$\underbrace{\boxed{+\frac{i}{2}\int_0^T d^4r \int_0^t d^4r' [J^i(r) + J'^i(r)]\gamma_{ij}(r-r')[J^j(r') - J'^j(r')]}}_{\textit{dissipation}}$$
$$\underbrace{\boxed{-\frac{1}{4}\int_0^T d^4r \int_0^t d^4r' [J^i(r) - J'^i(r)]\eta_{ij}(r-r')[J^j(r') - J'^j(r')]}}_{\textit{decoherence}}\Big]$$

False loss of coherence

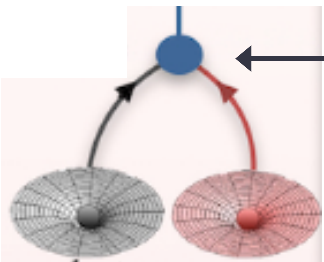

Coherence is restored again

Reduced density matrix loses its coherence

W. G. Unruh, In Relativistic quantum measurement and decoherence, eds H. P. Breuer and F. Petruccione (2000)

Linearized gravity (Graviton bath)

$$S = S_{\mathrm{sys}} + S_{\mathrm{int}} + S_{\mathrm{grav}}$$

$$S_{\mathrm{grav}}(h_{\mu\nu}) = \int d^4r \Big[-\frac{1}{2}\partial_\rho h_{\mu\nu}\partial^\rho h^{\mu\nu} + \partial_\rho h_{\mu\nu}\partial^\nu h^{\mu\rho} - \partial_\nu h^{\mu\nu}\partial_\mu h + \frac{1}{2}\partial^\mu h \partial_\mu h \Big],$$

$$S_{\mathrm{int}}(h_{\mu\nu}, T_{\mu\nu}) = \frac{\kappa}{2}\int d^4r h_{\mu\nu}T^{\mu\nu}$$

$$\kappa = (32\pi G)^{1/2}$$

F. S. and F. Q, J. Phys.: Conf. Ser. 626, 012039 (2015)

Linearized gravity (Influence functional)

$$\begin{aligned}
\mathcal{F}(x,x') \\
= \exp\Big[& \Phi(T_{00,\mathbf{x}};T^{00}_{\mathbf{x}}) - \Phi(T_{00,\mathbf{x}'};T^{00}_{\mathbf{x}'}) + \Phi(T^{i}{}_{i,\mathbf{x}};T^{00}_{\mathbf{x}}) - \Phi(T^{i}{}_{i,\mathbf{x}'};T^{00}_{\mathbf{x}'}) + \Phi(T_{i0,\mathbf{x}};T^{i0}_{\mathbf{x}}) - \Phi(T_{i0,\mathbf{x}'};T^{i0}_{\mathbf{x}'}) \\
& + \Phi(T_{0i,\mathbf{x}};T^{0i}_{\mathbf{x}}) - \Phi(T_{0i,\mathbf{x}'};T^{0i}_{\mathbf{x}'}) + \Phi(T_{00,\mathbf{x}};T^{i}{}_{i,\mathbf{x}}) - \Phi(T_{00,\mathbf{x}'};T^{i}{}_{i,\mathbf{x}'}) + \Phi(T^{i}{}_{i,\mathbf{x}};T^{i}{}_{i,\mathbf{x}}) - \Phi(T^{i}{}_{i,\mathbf{x}'};T^{i}{}_{i,\mathbf{x}'}) \\
& + i\int_0^{\mathrm{T}} d^4r \int_0^t d^4r' (T^{ij}_{\mathbf{x}}(r) + T^{ij}_{\mathbf{x}'}(r))\gamma_{ij,kl}(r-r')(T^{kl}_{\mathbf{x}}(r') - T^{kl}_{\mathbf{x}'}(r')) \\
& - \int_0^{\mathrm{T}} d^4r \int_0^t d^4r' (T^{ij}_{\mathbf{x}}(r) - T^{ij}_{\mathbf{x}'}(r))\eta_{ij,kl}(r-r')(T^{kl}_{\mathbf{x}}(r') - T^{kl}_{\mathbf{x}'}(r')) \Big]
\end{aligned}$$

dissipation & dec
by grav waves

$$\Phi(T_{\mu\nu,\mathbf{x}};T^{\mu\nu}_{\mathbf{x}}) \propto -iG\int d^4r \int d^3\mathbf{r}' \frac{T_{\mu\nu,\mathbf{x}}(\mathbf{r}',t')T^{\mu\nu}_{\mathbf{x}}(\mathbf{r},t)}{|\mathbf{r}-\mathbf{r}'|}$$

with the correlation functions

$$\gamma_{ij,kl}(r-r') = \frac{G}{4\pi^2}\int \frac{d^3k}{|\mathbf{k}|}\sin(|\mathbf{k}|(t-t'))e^{i\mathbf{k}\cdot(\mathbf{r}-\mathbf{r}')}\Pi_{ij,kl}(\mathbf{k})$$

$$\eta_{ij,kl}(r-r') = \frac{G}{4\pi^2}\int \frac{d^3k}{|\mathbf{k}|}\cos(|\mathbf{k}|(t-t'))e^{i\mathbf{k}\cdot(\mathbf{r}-\mathbf{r}')}\Pi_{ij,kl}(\mathbf{k})$$

External observer/internal observer

QM/QFT/QED: Measurements are made from the outside

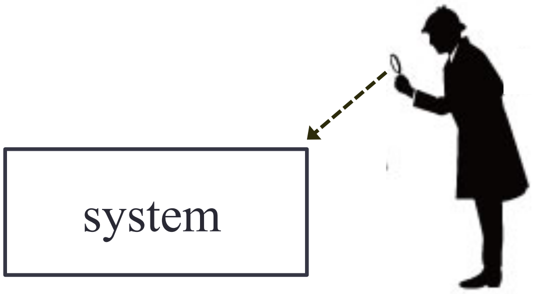

Gravity: Measurements are made from the inside

External time/internal time

QM/QFT/QED/Newtonian physics (external time):
Time flows equably from place to place

Gravity (internal time):
Inequable flow of time from place to place
Time arises from interactions of matters

Summary

❖Photon bath: dipole moment radiation➔real loss of coherence
Coulomb field ➔ false loss of coherence

❖Graviton bath: quadrupole moment radiation ➔ real
gravitational field➔ false in Newtonian limit?

? Interpretation of gravitational decoherence
with external/internal observer+time

Acknowledgements
Thank you for advices: G. W. Semenoff and W. G. Unruh
Thank you for support: Sasakawa Scientic Research Grant ,
the research foundation for opto-science and technology

“Derivative-dependent metric transformation and physical degrees of freedom”

by Yota Watanabe

[JGRG25(2015)2a6]

Derivative-dependent metric transformation and physical degrees of freedom

Yota Watanabe (Kavli IPMU)

Based on

arXiv:1507.05390,

PRD **92**, 084027 (2015)

Collaboration with

Guillem Domènech, Shinji Mukohyama,

Ryo Namba, Atsushi Naruko, Rio Saitou

Outline of talk

I. Derivative-dependent transformation (trf.)

→ # of phys. dof. changes apparently

II. Prove it does not change if trf. is invertible

III. Suggest a broader class of theories

which contain $\dot{N}$ in unitary gauge

Motivations of frame trf.

Inflation / Dark Energy: various models

Non-minimally coupled scalar-tensor theories are considered.

It is useful to transform a frame into

- Einstein frame: kinetic term of metric → GR
- matter frame: free matter moves along geodesics

Construction of general theory

Suppose $I_{\mathrm{mat}} = I_{\mathrm{mat}}[g_{\mu\nu}, \psi]$, $I_{\mathrm{grav}} = I_{\mathrm{grav}}[\tilde{g}_{\mu\nu}, \phi]$ (e.g. EFT).

Different whole theories ← different relations btw. $g_{\mu\nu}$ and $\tilde{g}_{\mu\nu}$

(trf.)

Derivative-dependent trf.

Consider **disformal trf.** $\tilde{g}_{\mu\nu} = \mathcal{A} g_{\mu\nu} + \mathcal{B} \partial_\mu \phi \partial_\nu \phi$

$\mathcal{A}, \mathcal{B}$: scalars composed by ϕ and its derivatives

Derivative & perturbative expansion around $\partial_\mu \phi \neq 0$

⇩ (as EFT of inflation/DE)

X itself is not necessarily small, even if the perturb. of X is small.
$= -g^{\mu\nu} \partial_\mu \phi \partial_\nu \phi$

Hence we must in general consider X-dependences,

$$\tilde{g}_{\mu\nu} = \mathcal{A}(\phi, X) g_{\mu\nu} + \mathcal{B}(\phi, X) \partial_\mu \phi \partial_\nu \phi$$

Neglecting $\nabla_\mu X$ is a consistent truncation to EFT of inflation/DE

Appearance of higher-derivatives

$$\tilde{g}_{\mu\nu} = \mathcal{A}(\phi, X) g_{\mu\nu} + \mathcal{B}(\phi, X) \partial_\mu \phi \partial_\nu \phi$$

$$I = \int d^4x \sqrt{-\tilde{g}} [\tilde{R}/2 + P(\phi, \tilde{X})] \quad \text{(3 dof.)}$$

$$\Downarrow$$

- $\mathcal{A} = \mathcal{A}(\phi), \mathcal{B} = \mathcal{B}(\phi, X)$: sub-class of GLPV theory (3 dof.)

  broader than Horndeski
- $\mathcal{A} = \mathcal{A}(\phi, X), \mathcal{B} = \mathcal{B}(\phi, X)$:

  → $\nabla_\mu X \nabla^\mu X$ ($\dot{N}^2$ in unitary gauge) appears

  apparently beyond GLPV theory (which does not contain $\dot{N}$)

ϕ-EoM: 2nd-order $\xrightarrow[\mathcal{A} = \mathcal{A}(\phi, X)]{}$ higher-order (4 dof.?)

Purpose of this study

- However, # of phys. dof. should not change

  as long as trf. has inverses $\tilde{g}^{\mu\nu}, g_{\mu\nu} = g_{\mu\nu}(\tilde{g})$:

$$\mathcal{A}(\mathcal{A} - \mathcal{B}X)(\mathcal{A} - \mathcal{A}_X X + \mathcal{B}_X X^2) \neq 0$$

  cf. $(\mathcal{A}, \mathcal{B}) = (X, 0)$ is not invertible in "mimetic" theory

- The existence of non-trivial constraints wrt. $\dot{N}$ was pointed out

  at linear perturbation level Gleyzes, Langlois, Vernizzi (2014)

→ We prove that # of phys. dof. does not change

as long as trf. is invertible, both in simple and general cases

Proof (simple case)

Tranformed Einstein-Hilbert action in unitary gauge

$$I_{\rm EH}^{\rm unitary} = \int dt d^d x N\sqrt{\gamma}\left\{A_4(t,N)\left[K^2 - K^i_j K^j_i + (d-1)KL + \frac{d(d-1)}{4}L^2\right]\right.$$
$$\left. + B_4(t,N)\left[R^{(d)} - (d-1)D^2 \ln\mathcal{A} - \frac{(d-1)(d-2)}{4}D_i \ln\mathcal{A} D^i \ln\mathcal{A}\right]\right\}$$

$$L = \frac{\mathcal{A}_N}{\mathcal{A}}\left(\frac{\dot{N}}{N} - \frac{N^i}{N}D_i N\right) + \frac{\mathcal{A}_t}{\mathcal{A}N}$$

Canonical momenta

$$\pi_i \equiv \frac{\delta I}{\delta \dot{N}^i} = 0, \quad \pi_N \equiv \frac{\delta I}{\delta \dot{N}} = \frac{\mathcal{A}_N}{\mathcal{A}}\sqrt{\gamma}A_4(d-1)\left(K + \frac{d}{2}L\right) \neq 0,$$

$$\pi_{ij} \equiv \frac{\delta I}{\delta \dot{\gamma}_{ij}} = \sqrt{\gamma}A_4\left(K\gamma^{ij} - K^{ij} + \frac{d-1}{2}\gamma^{ij}L\right)$$

→ less constraint, more dof.?

Primary constraints

$$\pi_i, \quad \tilde{\pi}_N \equiv \pi_N - \frac{\mathcal{A}_N}{\mathcal{A}}\gamma_{ij}\pi^{ij}$$

→ non-trivial constraint instead of π_N

Proof (simple case)

Secondary constraints

$$\dot{\pi}_i \approx 0 \quad \rightarrow \quad \mathcal{H}_i \equiv -2\sqrt{\gamma}\gamma_{ij}D_k\left(\pi^{jk}/\sqrt{\gamma}\right)$$
$$\dot{\tilde{\pi}}_N \approx 0 \quad \rightarrow \quad \mathcal{C} \equiv \mathcal{C}[B_{4N}, A_{2N}, A_{4N}, \cdots]$$

$2d$ 1st-class constraints: $\pi_i, \mathcal{H}_i + \pi_N \partial_i N$

2 2nd-class constraints: $\tilde{\pi}_N \equiv \pi_N - \frac{\mathcal{A}_N}{\mathcal{A}}\gamma_{ij}\pi^{ij}, \ \mathcal{C}$

$$\#\ \text{of phys. dof.} = \frac{1}{2}[\underbrace{(d^2 + 3d + 2)}_{\text{dim. of phase space}} - 2(2d) - 2] = \underbrace{\frac{d^2 - d - 2}{2}}_{\text{transverse traceless tensor modes}} + 1$$

> We have usual scalar-tensor dof. since non-trivial constraint $\pi_N - \frac{\mathcal{A}_N}{\mathcal{A}}\gamma_{ij}\pi^{ij}$ and its time consistency condition are 2nd class

General case

- Suppose
$$I=\int d^{d+1}x\left[\frac{1}{2}\mathcal{K}_{AB}\dot{\Phi}^A\dot{\Phi}^B+M_A\dot{\Phi}^A+V\right]$$
w/ $\mathcal{K}_{AB}, M_A, V$ are functions of t, Φ^C

- e.g.) higher-derivative theory
$$I=\int d^{d+1}xL\left(g_{\mu\nu},R_{\alpha\beta\gamma\delta},\nabla_\mu R_{\alpha\beta\gamma\delta},\cdots,\nabla_{(\mu_1}\cdots\nabla_{\mu_m)}R_{\alpha\beta\gamma\delta}\right)$$
can be cast into the form:

$\mathcal{R}$'s: auxiliary fields

$$\begin{aligned}I'=\int d^{d+1}x[&L\left(g_{\mu\nu},\mathcal{R}_{\alpha\beta\gamma\delta},\mathcal{R}_{\mu_1\alpha\beta\gamma\delta},\cdots,\mathcal{R}_{\mu_1\cdots\mu_m\alpha\beta\gamma\delta}\right)\\&+\Lambda^{\alpha\beta\gamma\delta}\left(\mathcal{R}_{\alpha\beta\gamma\delta}-R_{\alpha\beta\gamma\delta}\right)+\Lambda^{\mu\alpha\beta\gamma\delta}\left(\mathcal{R}_{\mu\alpha\beta\gamma\delta}-\nabla_\mu\mathcal{R}_{\alpha\beta\gamma\delta}\right)\\&+\cdots+\Lambda^{\mu_1\cdots\mu_m\alpha\beta\gamma\delta}(\mathcal{R}_{\mu_1\cdots\mu_m\alpha\beta\gamma\delta}-\nabla_{(\mu_m}\mathcal{R}_{\mu_1\cdots\mu_{m-1})\alpha\beta\gamma\delta})]\end{aligned}$$

Λ's: Lagrange multipliers

2nd -order derivatives in $R_{\alpha\beta\gamma\delta}$ can be 1st -order by integration by parts

Essence of Proof (general case)

Suppose

- $I=\int d^{d+1}x\left[\frac{1}{2}\mathcal{K}_{AB}\dot{\Phi}^A\dot{\Phi}^B+M_A\dot{\Phi}^A+V\right]$
- $\tilde{\Phi}^A=F^A(\Phi,t)\quad\leftrightarrow\quad\Phi^A=G^A(\tilde{\Phi},t)$ (trf. is invertible)

➡ $$\tilde{I}=\int d^{d+1}x\left[\frac{1}{2}\tilde{\mathcal{K}}_{AB}\dot{\tilde{\Phi}}^A\dot{\tilde{\Phi}}^B+\tilde{M}_A\dot{\tilde{\Phi}}^A+\tilde{V}\right]$$
w/ $\tilde{\mathcal{K}}_{AB},\tilde{M}_A,\tilde{V}:\ (G^A,\text{quantities before trf.})$

We can show trf. preserves

- primary constraints $\{\tilde{\mathcal{C}}_\alpha\}=\{\mathcal{C}_\alpha\}$
- Poisson brackets $\left\{\tilde{\Phi}^A(x),\tilde{\Pi}_B(y)\right\}_{\mathrm{P}}=\delta^A_B\delta^d(x-y),\cdots$
- Time evolution $\left\{\tilde{\mathcal{O}},\tilde{H}\right\}_{\mathrm{P}}+\left(\frac{\partial\tilde{\mathcal{O}}}{\partial t}\right)_{\tilde{\Phi},\tilde{\Pi}}=\{\mathcal{O},H\}_{\mathrm{P}}+\left(\frac{\partial\mathcal{O}}{\partial t}\right)_{\Phi,\Pi}$

➡ preserve
- Secondary constraints
- Constraint algebra

➡ # of phys. dof.

Suggestion of general theory

- The simple case suggests a broader class

$$I = \int d^{d+1}x\sqrt{-g}\mathcal{L}\big(t; N, K + \alpha\partial_\perp N, K^{\mathrm{T}}_{ij}, \gamma_{ij}, D_i\big) \text{ in unitary gauge}$$

scalar made of N, γ_{ij}, D_i

$\frac{1}{N}(\dot{N} - N^i\partial_i N)$

$K^{\mathrm{T}}_{ij} = K_{ij} - \frac{1}{d}K\gamma_{ij}$

$\rightarrow \quad \pi_N \neq 0$

- Non-trivial primary constraint

$$\pi_N - \frac{2}{d}\alpha\gamma_{ij}\pi^{ij} = 0$$

would eliminate 1 dof. in general

- Broader class than GLPV or more general EFT theories with same # of dof. containing $\dot{N}$!

Summary

- Trf. btw. metrics in mat. & grav. sectors define the whole theory. In the EFT of inflation/DE, coefficients of trf. must in general depend on X. Then # of phys. dof. changes apparently.

- Proved it does not change as long as trf. is invertible by studying constraint structure in simple & general cases.

- Suggested a broader class with TT tensor + 1 dof. which contain $\dot{N}$ in unitary gauge.

“Black hole-magnetize neutron star merger : Mass ejection and short gamma-ray burst”

by Kenta Kiuchi

[JGRG25(2015)2b1]

Black hole-magnetize neutron star merger: Mass ejection and short gamma-ray burst

Kenta Kiuchi (YITP)

Collaboration with Yuichiro, Sekiguchi (Toho) ,
Koutarou Kyutoku (Riken), Masaru Shibata (YITP),
Keisuke Taniguchi (Ryukyu)

Ref.) Kiuchi et al. 15 PRD 92, 064034(2015)

YUKAWA INSTITUTE FOR THEORETICAL PHYSICS

K computer

Visualization by Tomohide Wada (Riken)

Motivation

Gravitational waves = Ripples of the spacetime

- Verification of GR
- The EOS of neutron star matter (Lattimer & Parakash 07)
- The central engine of short gamma-ray bursts (Narayan et al. 92)
- A possible site of the r-process synthesis (Lattimer & Schramm 74)

Advanced LIGO will observe ~10 events / yr.

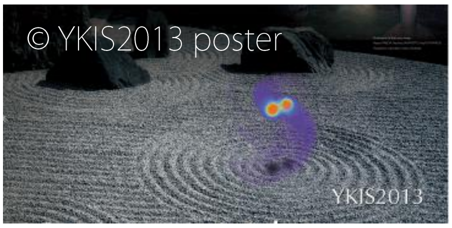

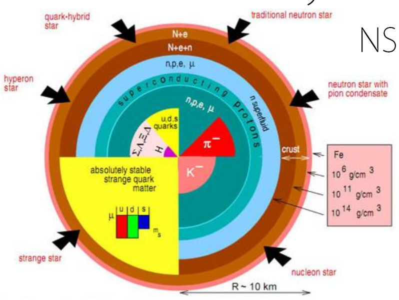

NS interior

Image of gamma-ray burst

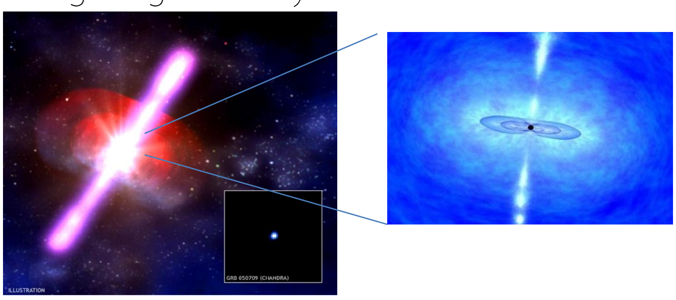

Colliding Neutron Stars Produce Gold ?

Overview of Black Hole (BH) – Neutron Star (NS) merger

Q: Tidal disruption or not ? (Mass ratio, BH spin, EOS of NS)

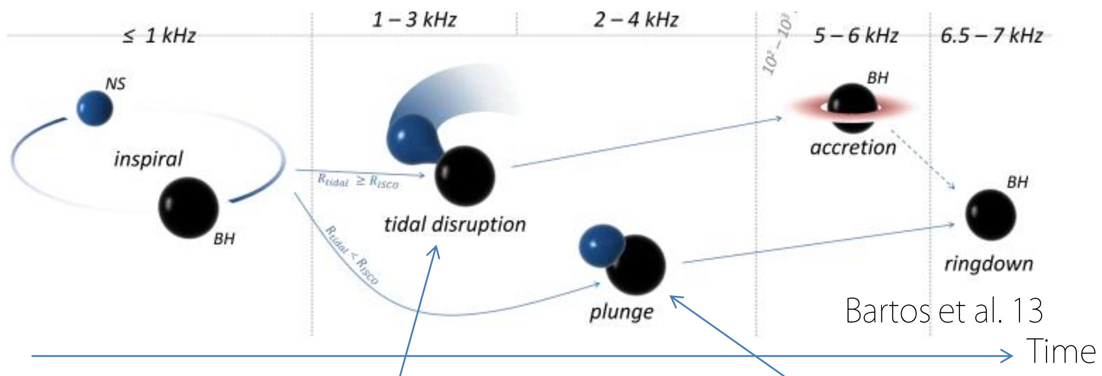

GW forms (Kyutoku et al. 11) *More detailed classification

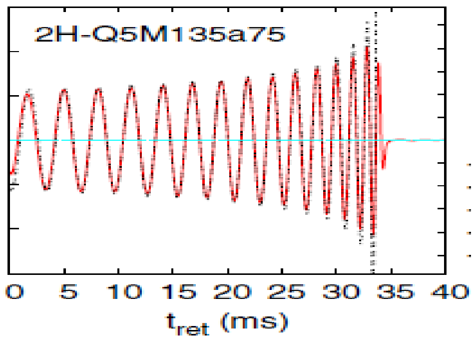

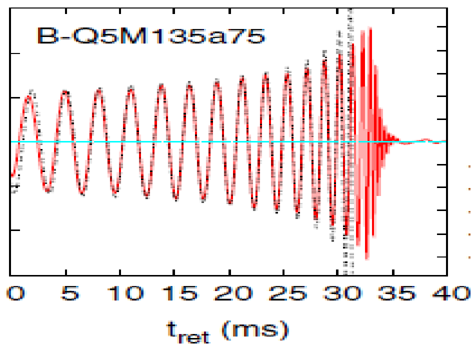

BH – torus systems

A key ingredient = "viscosity"

EOM : $\partial_t(\rho R^2\Omega)+\partial_A(\rho R^2\Omega v_A-\eta R^2\partial_A\Omega)=0$ (A=R, z)

ρ=density, Ω=angular velocity, η=dynamical viscosity

⇒ ▶ Angular momentum transfer by the viscous term.

▶ Energy dissipation due to the viscosity

Q. What is the "viscosity" in BH-torus systems ?

A. Magnetohydrodynamical turbulence ;

$q=q_{ave}+\delta q$ s.t. $\langle q\rangle = q_{ave}$ and $\langle\delta q\rangle=0$ where $\langle\cdot\rangle$ denotes the time average.

EOM : $\partial_t\langle\rho R^2\Omega\rangle+\partial_A(\langle\rho R^2\Omega v_A\rangle+\rho R W_{A\varphi})=0$ (A=R, z)

$W_{A\varphi}=\langle\delta v_A\delta v_\varphi-B_A B_\varphi/4\pi\rho\rangle$: Reynolds+Maxwell stress

Q. What produces the turbulence ?

A. Magnetohydrodynamical instability ; The magnetorotational intability (MRI) is a powerful amplification mechanism (Balbus & Hawley 91) . Unstable for $\nabla\Omega<0$ and growth rate $\propto\Omega$

Q & A cont. and what we have to do

Q. Does magnetic field exist in BH-NS binaries ?

A. Yes . The presence of the magnetic fields is one of the most characteristic properties of NSs.

Therefore, it is mandatory to perform BH-magnetized NS merger simulations.

Recipe of Numerical Relativity

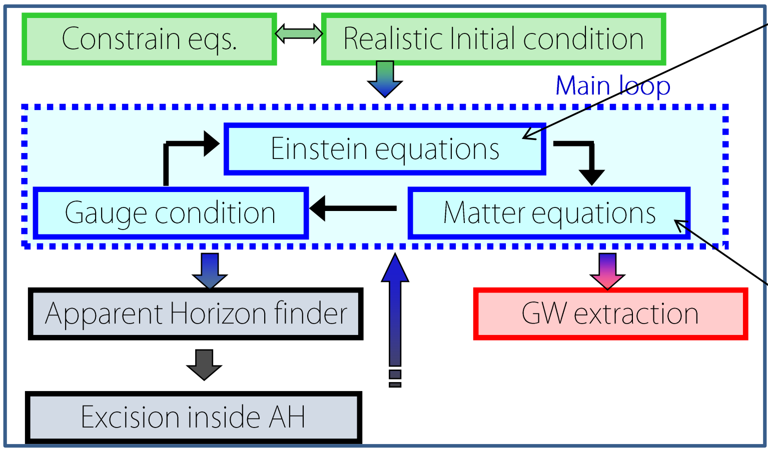

BSSN formulation
(Shibata & Nakamura 95, Baumgrte-Shapiro 99)

- GR hydro.
- GR magneto hydro.
- GR radiation hydro.
- GR radiation magneto hydro.

Slide courtesy of Sekiguchi

Difficulty in MHD simulations

- A short wavelength mode has a high growth rate.
- Turbulent eddies are killed by a numerical viscosity.

Mandatory to do an in-depth resolution study, which is lacking in a bunch of the simulations .

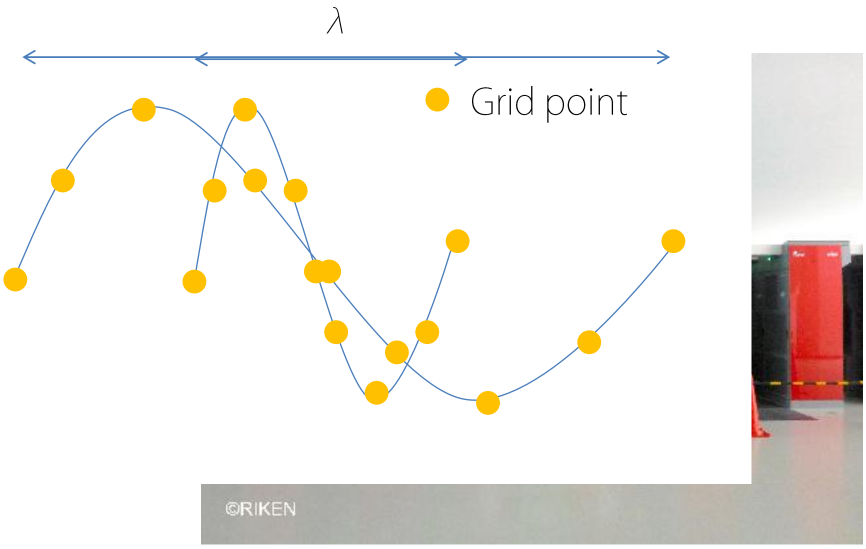

- Total peak efficiency is 10.6 PFLOPS (663,552 cores)

Simulation set-up

- High resolution ; Δx=120m, N=1028^3 (K ; 32,768 cores)
- Middle resolution ; Δx = 160m, N=756^3 (XC30 ; 4,096 cores)
- Normal resolution ; Δx = 202m, N=612^3 (XC30 ; 4,096 cores)
- Low resolution ; Δx = 270m, N=448^3 (FX10 ; 3,456 cores)

c.f. highest-res. in BH-magnetized NS simulation is $\Delta x \approx$260m, N =140^3

<u>Fiducial model</u>

- EOS : APR4 ($M_{max} \approx 2.2 M_\odot$), $M_{NS} = 1.35\ M_\odot$
- M_{BH}/M_{NS} : 4
- BH spin : 0.75
- B_{max} : 10^{15}G

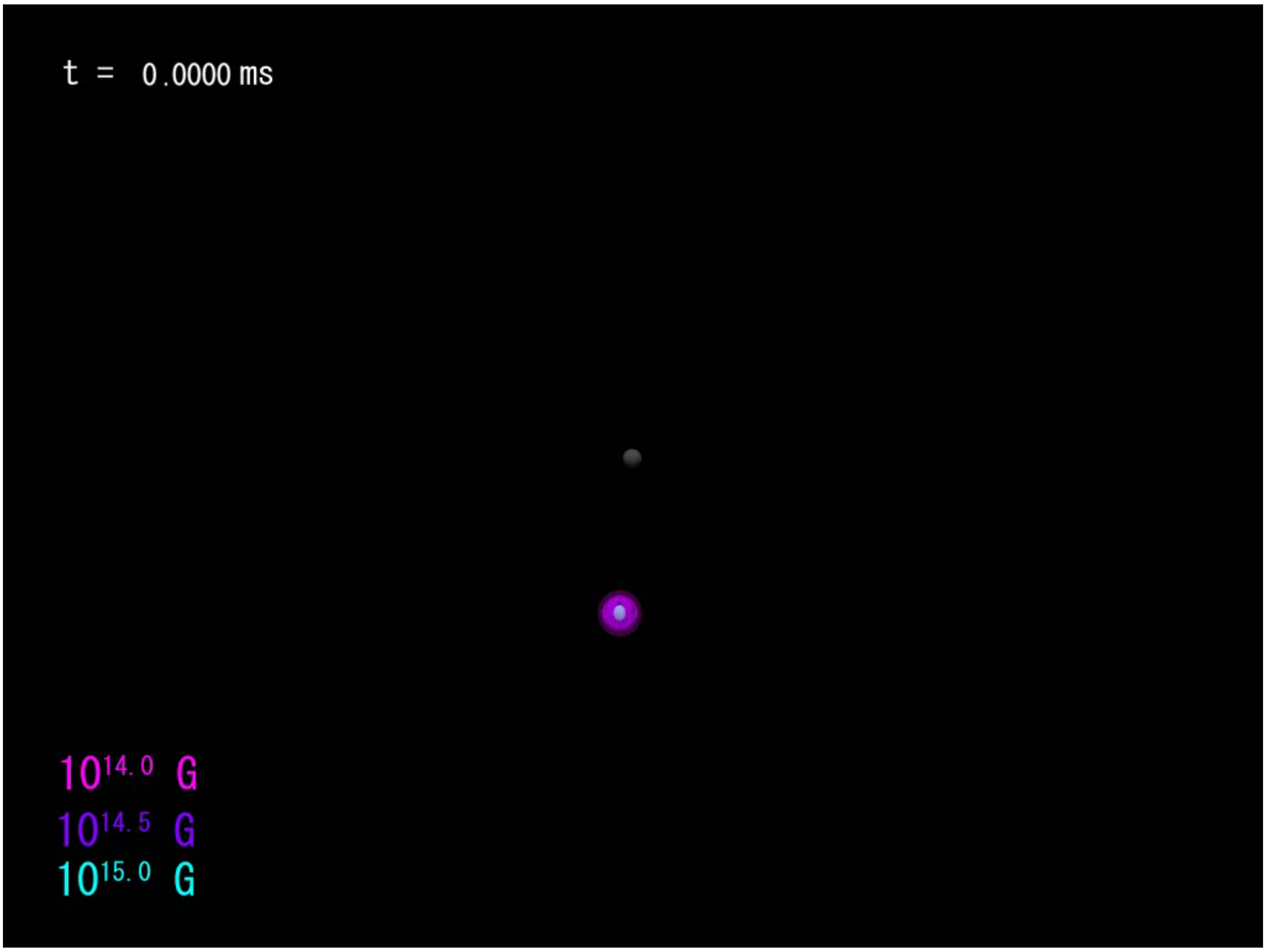

Ejecta time evolution

Ejecta $\stackrel{\mathrm{def}}{=}$ Gravitationally unbounded fluid element (u_t<-1)

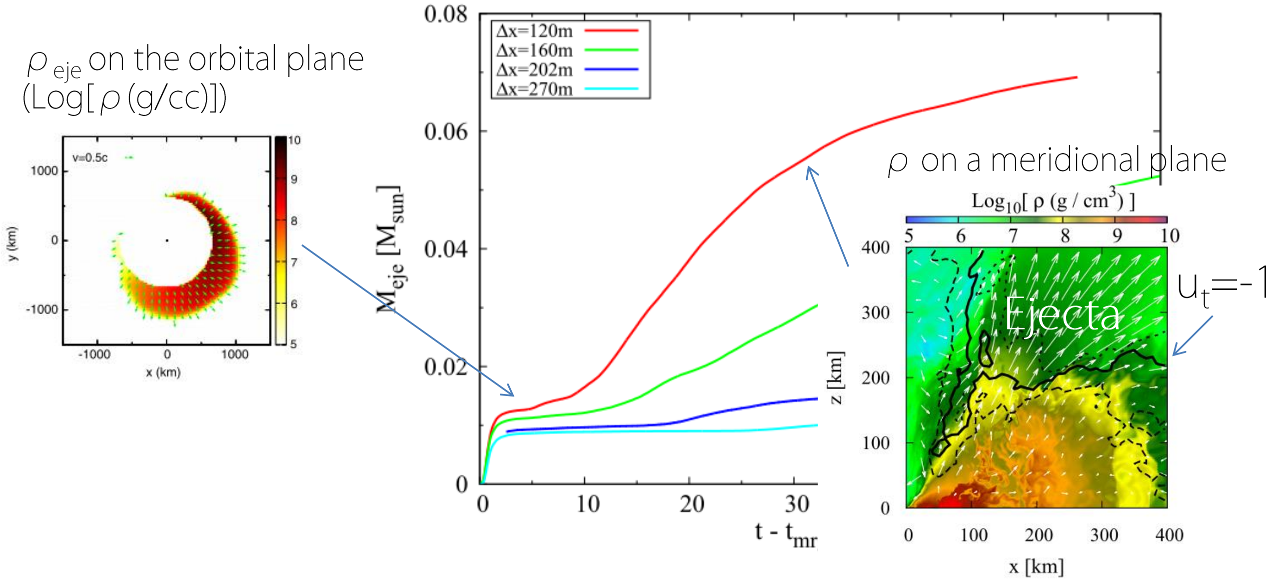

- Dynamical ejecta due to tidal disruption for t ≲ 10ms
- A new component for t ≳ 10ms ; Torus wind

Does the magetorotational instability switch on ?

Magnetic field energy evolution

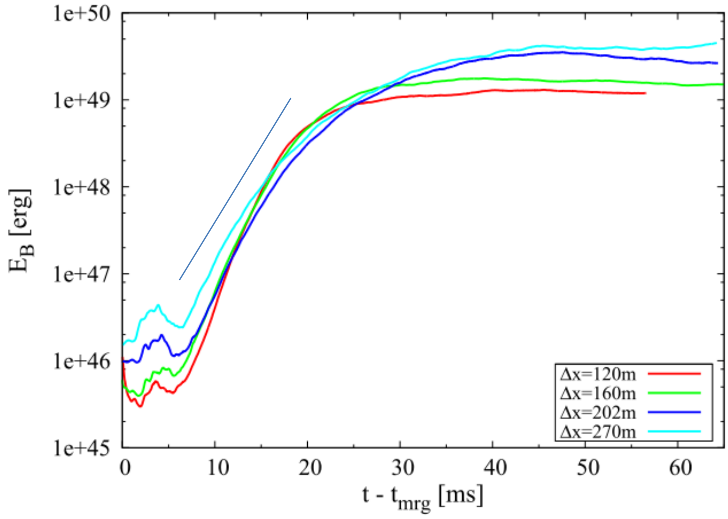

Yes. The magnetic-field energy is exponentially growing for 10 ms $\lesssim t \lesssim$ 20 ms.
$\Rightarrow$ The growth rate agrees approximately with the linear perturbation of non-axisymmetic MRI(Balbus & Hawley 92) and the turbulent state is realized.

Is the effective turbulent "viscosity" really produced ?

Energy spectrum of the turbulence

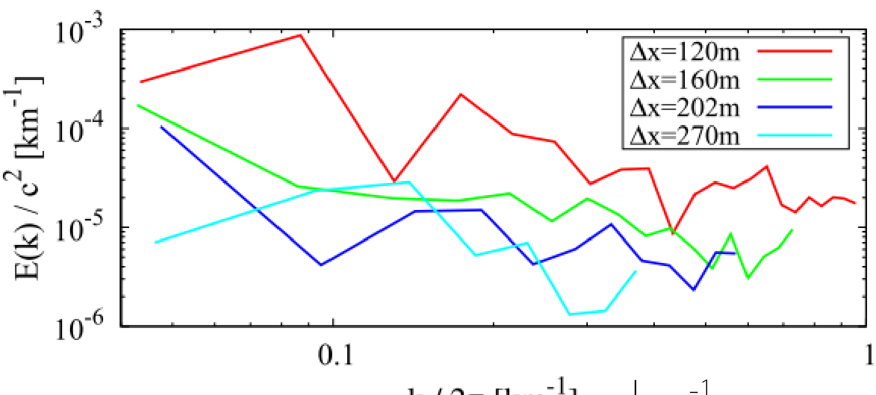

$k / 2\pi$ [km^{-1}] $= l_{edd}^{-1}$

▶The spectrum amplitude is higher in the higher-res. runs.

The effective turbulent viscosity is $\sim \delta v\, l_{edd}$ and $E(k) \propto \delta v^2$
$\Rightarrow$ For a given scale l_{edd}, the effective turbulent "viscosity" increases with increasing the resolution.

So, the answer is Yes.

Is the energy transferred outward and thermalized ?

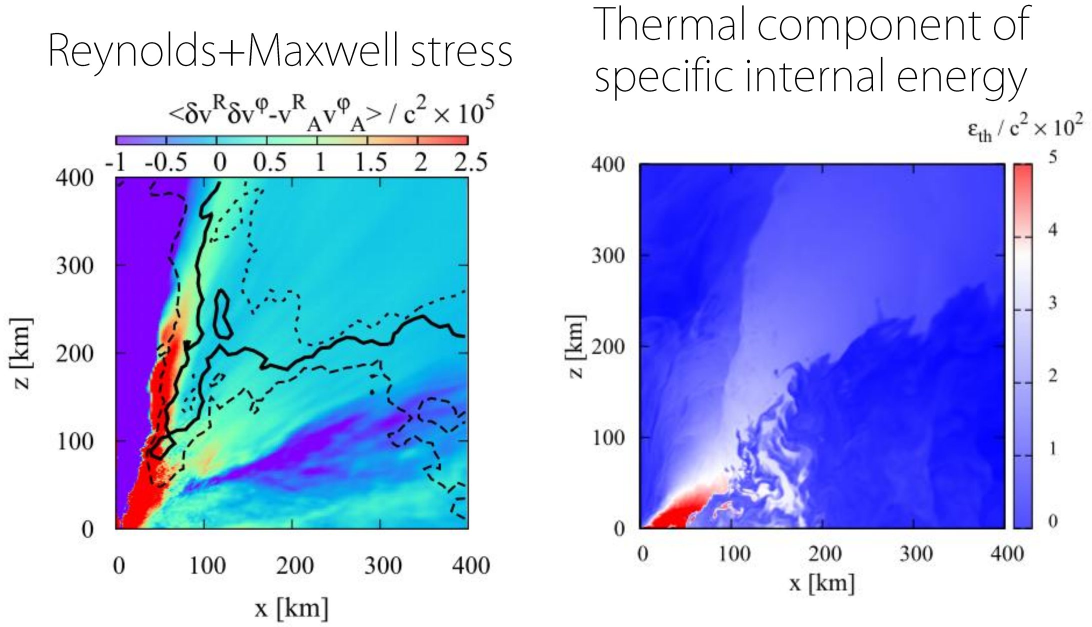

Yes.

▶The energy is transferred outward.

▶Efficient energy conversion to the thermal energy is realized in the vicinity of the inner edge of the torus.

Mechanism of turbulence driven torus wind

▶The realistic high viscosity enhances the mass accretion inside the torus and converts the mass accretion energy to thermal energy efficiently.

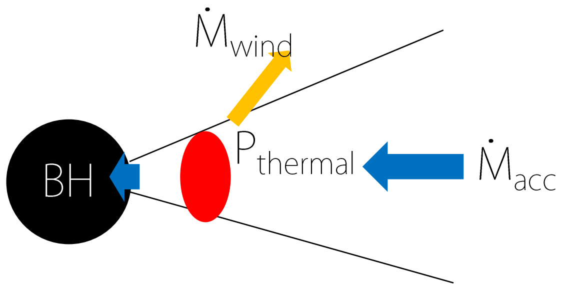

In the absence of the effective turbulent viscosity,

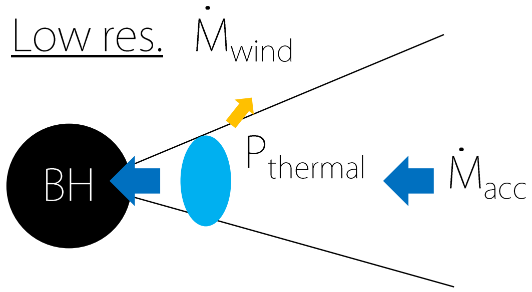

Natural consequence of the torus wind

Density P / P_{mag}

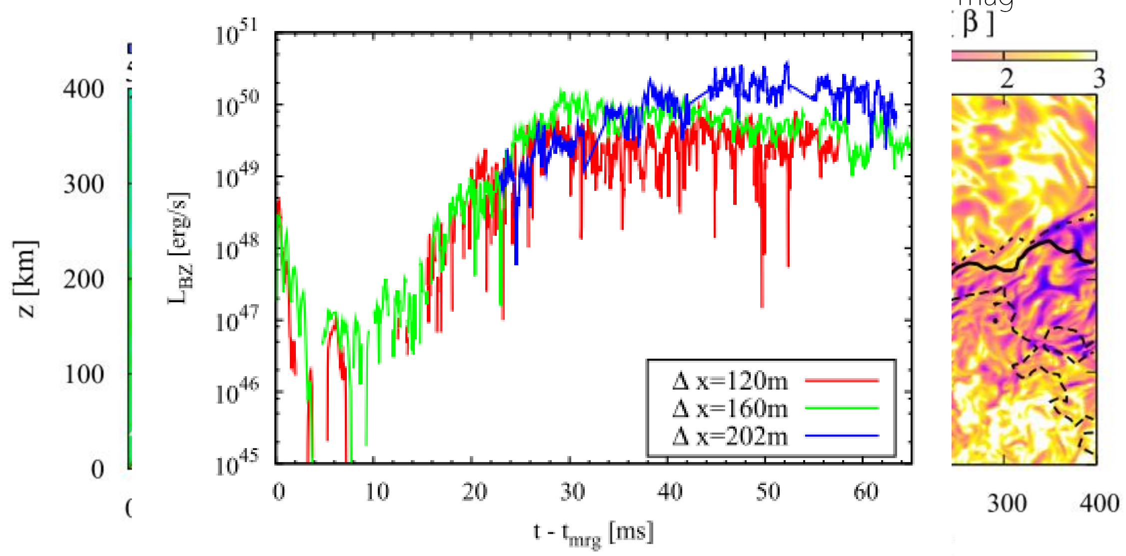

- Funnel wall formation by the torus wind
- Torus wind ⇒ Coherent poloidal B-field ⇒ Formation of a low plasma beta region ⇒ Formation of the magnetosphere
- The BH rotational energy is efficiently extracted as the outgoing Poynting flux ; ≈ 2 × 10^{49} erg/s (Blandford-Znajek 77)

R-process nucleosynthesis in BH-NS merger

- Nucleosynthesis in the BH-NS merger

Electron fraction Y_e of the dynamical ejecta is ≲ 0.1
⇒ Reproduce the third peak of the solar abundance

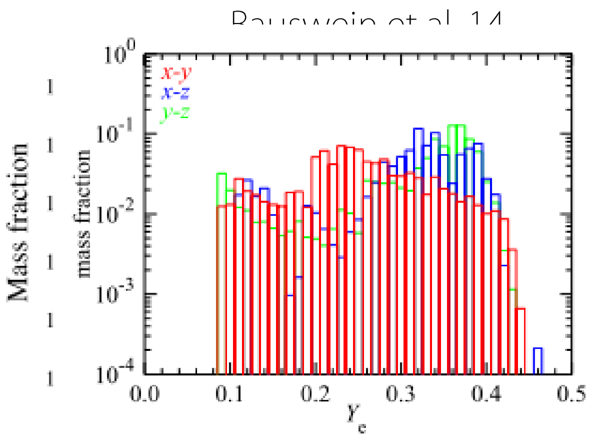

Wanajo et al. 14

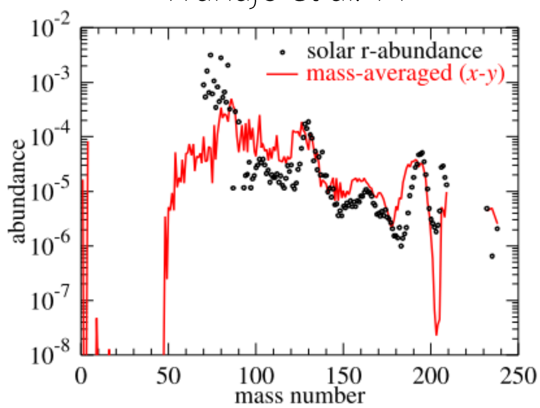

- Torus wind is hot ⇒ Y_e would be high due to the weak interaction.
- Mixture of the dynamical and wind component could reproduce the solar abundance (BH-NS: Just et al. 15, NS-NS: Sekiguchi et al. 15, Wanajo et al. 14)

Radioactively-powered electromagnetic emission

Heating due to the radioactive decay of R-process elements
⇒ Strong electromagnetic transient (Li & Paczynski 98, Kulkarni 05, Metzger & Berger 12)

Discovery of the excess in the near infrared band in GRB130603B (Berger et al. 13, Tanvir et al. 13)

A bunch of theoretical models (Kasen et al. 13, Barnes & Kasen 13, Tanaka & Hotokezaka 13, Takami et al. 14, Kisaka et al. 15)

▶ The amount of the torus wind mass is larger than that of the dynamical ejecta mass in our model.
⇒ Torus wind component could play a leading part of the radioactively-powered emission in BH-NS mergers.

Summary

▶ We performed high-resolution GRMHD simulations of a BH-NS merger on K.

▶We self-consistently show a series of the processes composed of tidal disruption of the NS, accretion torus formation, the magnetic field amplification due to the non-axisymmetric MRI, thermal driven torus wind, subsequent formation of the funnel wall and BH magnetoshpere, and high Blandford-Znajek luminosity.

▶ We discussed the implications to a central engine of short gamma-ray bursts, r-process nucleosynthesis, and radioactively-powered electromagnetic emission.

Effective potential u_t

$W \equiv \ln(-u_t) \Rightarrow W = -GM_{BH}/(R^2+z^2)^{1/2} + l^2/2R^2$
M_{BH}: Black hole mass, l : specific angular momentum

With u_t =-1 and l = const., W becomes a parabolic shape.

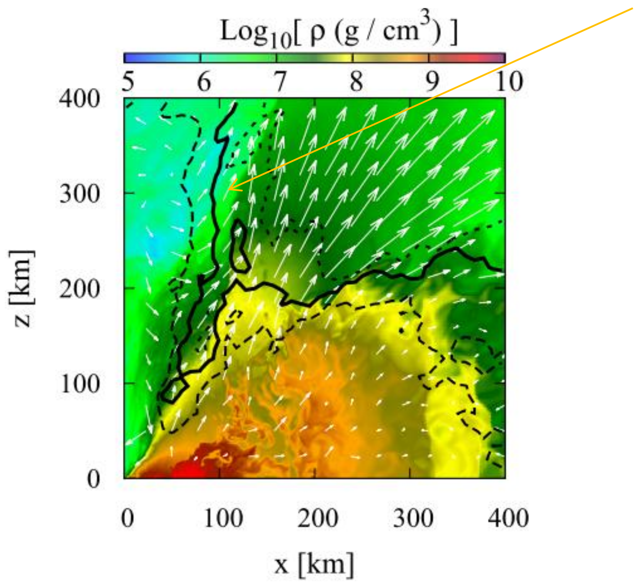

Fixed Mesh Refinement vs Adaptive Mesh Refinement

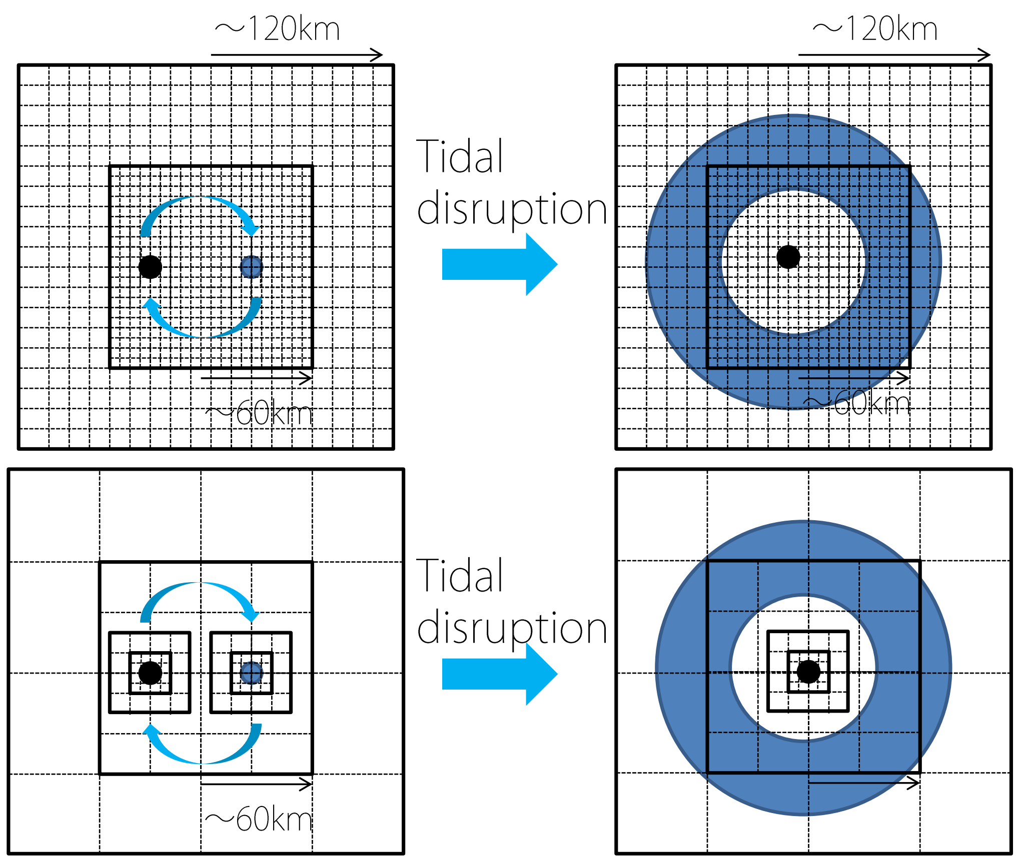

“Rotational Properties of Hypermassive Neutron Stars from Binary Mergers”

by Kentaro Takami

[JGRG25(2015)2b2]

Rotational Properties of Hypermassive Neutron Stars from Binary Mergers

Kentaro Takami

Kobe City College of Technology（KCCT）

Collaborators : Matthias Hanauske and Luciano Rezzolla

The 25th Workshop on General Relativity and Gravitation,
07-11 December 2015.

Introduction

Observation of Neutron Stars

A large number of pulsars have been observed:

$\rightarrow \quad N_{\text{tot}} \sim 2500.$

Abdo+ 2013

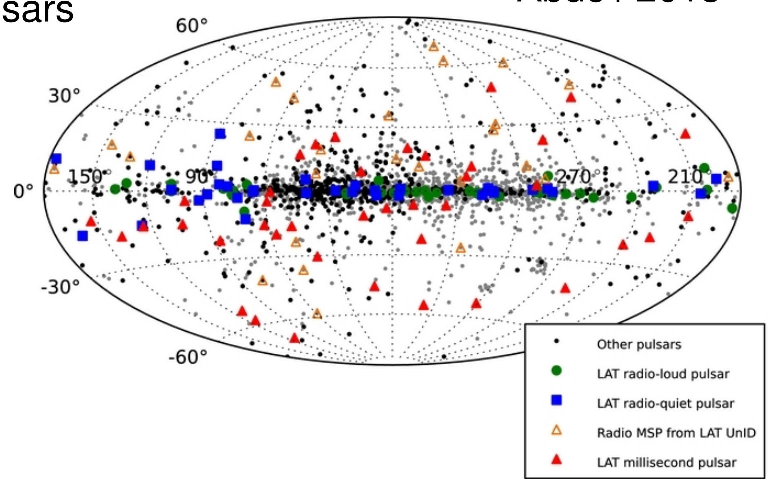

Introduction Methodology Results Conclusions

Observation of Neutron Stars

A large number of pulsars have been observed:

$\rightarrow \quad N_{\text{tot}} \sim 2500.$

Abdo+ 2013

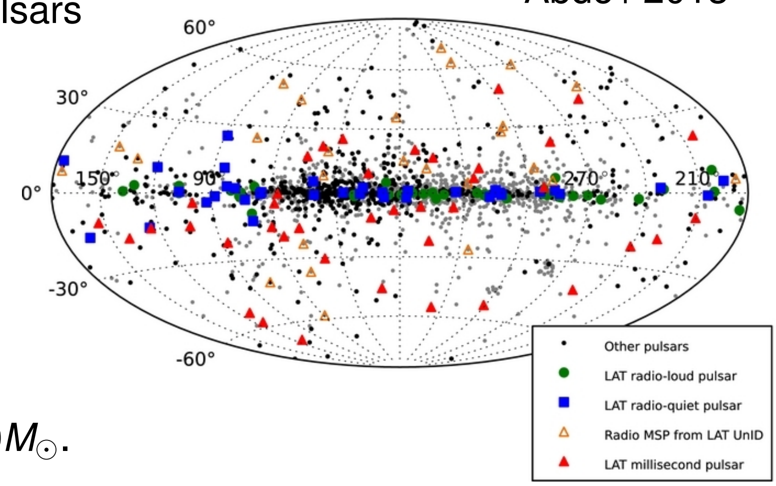

The masses are $\lesssim 2.0 M_{\odot}$.

Observation of Neutron Stars

A large number of pulsars have been observed:

$\rightarrow \quad N_{\mathrm{tot}} \sim 2500.$

Abdo+ 2013

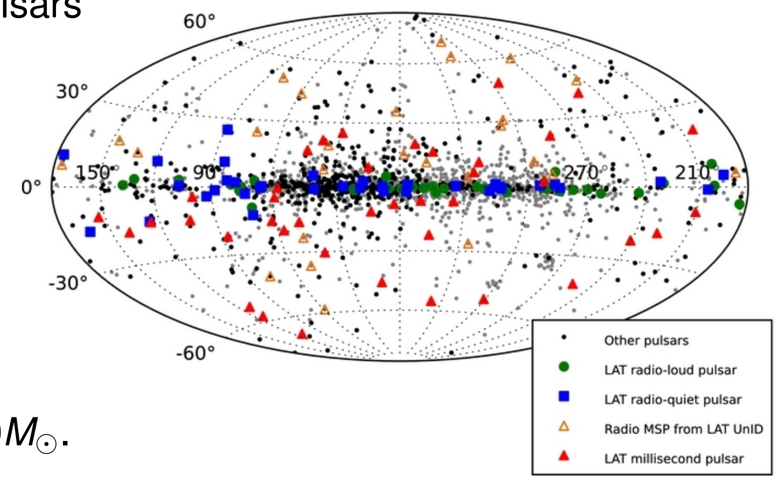

The masses are $\lesssim 2.0 M_{\odot}$.

They are uniformly rotating neutron stars (NSs).

Uniformly Rotating Neutron Star

A NS with uniform rotation can uniquely be constructed by *e.g.* , KEH code (Komatsu+ 1989) and RNS code (Stergioulas 1997), when we specified

- the axis ratio, central rest-mass density and EOS,

  or

- the rotational rate and total baryon mass and EOS.

e.g. , for polytropic EOS with $K = 100$ and $\Gamma = 2$

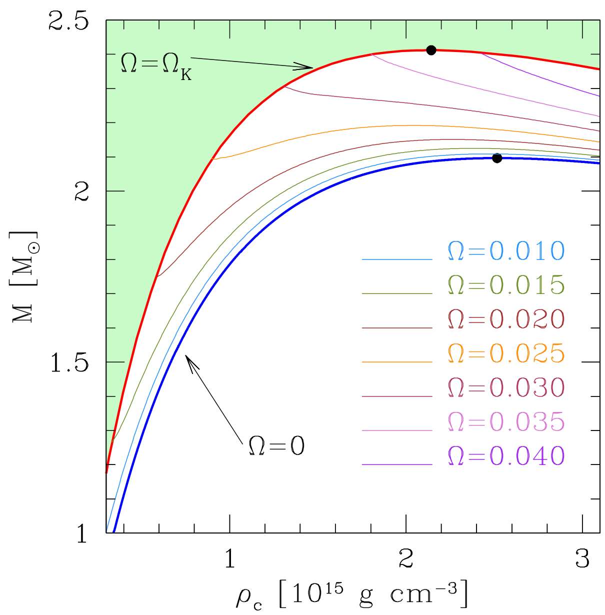

Rezzolla+ 2013

Differentially Rotating Neutron Star

- A newly born NS in a supernova event,
  or
- a NS in a remnant of a binary NS merger,

is not uniformly but differentially rotating.

Introduction Methodology Results Conclusions

Differentially Rotating Neutron Star

- A newly born NS in a supernova event,
  or
- a NS in a remnant of a binary NS merger,

is not uniformly but differentially rotating.

It can give a variety of interesting properties to a NS,

e.g. , ...
by the differentially rotating effects, we can expect that it is a hyper massive neutron star (HMNS) with

$M > M_{\max} \sim 2.0 M_{\odot}$,

which lead the complicate dynamics such as a

HMNS $\Longrightarrow$ BH + torus + ? $\Longrightarrow$ BH.

Differentially Rotating Neutron Star

A NS with differential rotation cannot uniquely be constructed, because there is a rotation profile for the differential rotation.

1

Introduction Methodology Results Conclusions

Differentially Rotating Neutron Star

A NS with differential rotation cannot uniquely be constructed, because there is a rotation profile for the differential rotation.

There is only one rotation profile[1] suggested by Eriguchi+ 1985, which is usually referred as "*j*-constant law":

$$\frac{j}{1 - j\Omega} = \widehat{A}^2(\Omega_c - \Omega) \ .$$

1

Differentially Rotating Neutron Star

A NS with differential rotation cannot uniquely be constructed, because there is a rotation profile for the differential rotation.

There is only one rotation profile[1] suggested by Eriguchi+ 1985, which is usually referred as "*j*-constant law":

$$\frac{j}{1-j\Omega} = \hat{A}^2(\Omega_c - \Omega)\ .$$

1

e.g. , for polytropic EOS with $K = 100$ and $\Gamma = 2$

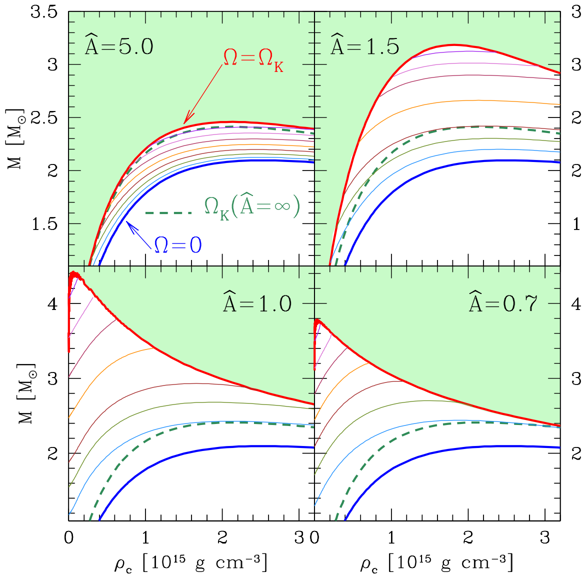

Rezzolla+ 2013

Introduction Methodology Results Conclusions

Differentially Rotating Neutron Star

A NS with differential rotation cannot uniquely be constructed, because there is a rotation profile for the differential rotation.

There is only one rotation profile[1] suggested by Eriguchi+ 1985, which is usually referred as "*j*-constant law":

$$\frac{j}{1-j\Omega} = \hat{A}^2(\Omega_c - \Omega)\ .$$

e.g. , for polytropic EOS with $K = 100$ and $\Gamma = 2$

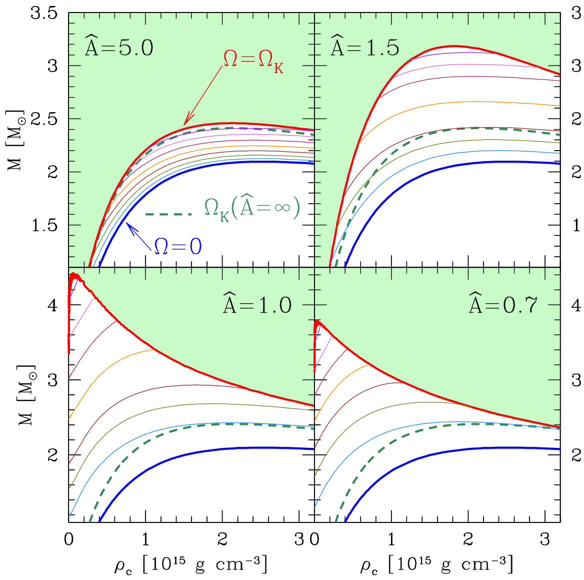

Rezzolla+ 2013

[1] Recently Galeazzi+ 2012 extend to the generalized *j*-constant law :
$\frac{j}{1-j\Omega} = [\frac{R_0^2}{\Omega_c^\alpha}\Omega(\Omega^\alpha - \Omega_c^\alpha)]/[1 - \frac{R_0^2}{\Omega_c^\alpha}\Omega^2(\Omega^\alpha - \Omega_c^\alpha)]\ .$

Differentially Rotating Neutron Star

The most of studies are using an axisymmetric initial models with *j*-constant law as a typical HMNS:

Introduction Methodology Results Conclusions

Differentially Rotating Neutron Star

The most of studies are using an axisymmetric initial models with *j*-constant law as a typical HMNS:

e.g. , ...

MRI in HMNS

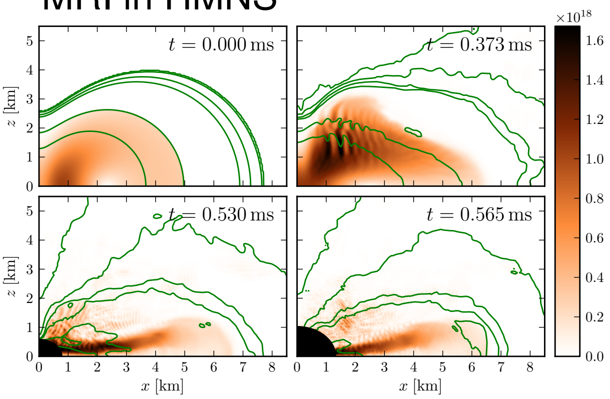

Siegel+ 2013

Short GRB jet from HMNS

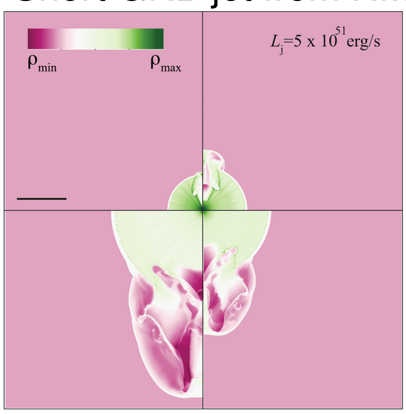

Murguia-Berthier+ 2014

Differentially Rotating Neutron Star

The most of studies are using an axisymmetric initial models with *j*-constant law as a typical HMNS:

However it seems that a differentially rotating NS with *j*-constant law is completely far from a realistic HMNS computed by a BNS-merger simulation.

Introduction Methodology Results Conclusions

Differentially Rotating Neutron Star

The most of studies are using an axisymmetric initial models with *j*-constant law as a typical HMNS:

However it seems that a differentially rotating NS with *j*-constant law is completely far from a realistic HMNS computed by a BNS-merger simulation.

We have the detail studies about the rotational properties of HMNSs by using full-GR BNS-merger simulations.

Methodology

Introduction Methodology Results Conclusions

Numerical Method

All of our calculations have been performed in full general relativity.

< spacetime evolution >

McLachlan code which is a part of publicly available Einstein Toolkit (Löffler+2012).

- BSSNOK formalism (Nakamura+1987, Shibata+1995, Baumgarte+1998)
- 4th-order finite differencing method

< fluid evolution >

Whisky code which is our privately developed code (Baiotti+ 2005).

- finite-volume method
- HLLE approximate Riemann solver
- PPM reconstruction
- 4th-order Runge-Kutta scheme

Equation of State

"hybrid" equation of state (EOS)

based on a piecewise polytropic (PP) EOS augmented by an ideal gas:

$$p = p_{\rm c} + p_{\rm th} , \quad \varepsilon = \varepsilon_{\rm c} + \varepsilon_{\rm th} ,$$

where

$$\begin{aligned}
p_{\rm th} &= (\Gamma_{\rm th} - 1)\, \rho\, \varepsilon_{\rm th} && : \text{ideal gas} , \\
p_{\rm c} &= K_i\, \rho^{\Gamma_i} && : \text{piecewise polytropic EOS} , \\
K_{\ell+1} &= K_\ell\, \rho_\ell^{(\Gamma_\ell - \Gamma_{\ell+1})} && : \text{continuity of pressure} , \\
\varepsilon_{\rm c} &= \varepsilon_i + \frac{K_i}{\Gamma_i - 1}\, \rho^{(\Gamma_i - 1)} && : \text{first law of thermodynamics} .
\end{aligned}$$

Our Models

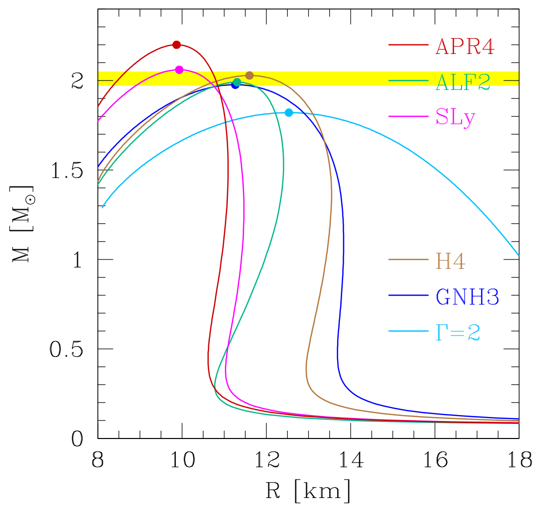

- Observed maximum mass is $2.01 \pm 0.04 M_\odot$ for PSR J0348+0432 (Antoniadis+2013).

As realistic nuclear EOSs, we use 5 different EOSs, *i.e.* , APR4, ALF2, SLy, H4 and GNH3.

For each of EOS, we consider

- a low-mass model ($M = 1.25 + 1.25\, M_\odot$), and
- a high-mass model ($M = 1.35 + 1.35\, M_\odot$).

Results

Dynamics

In corotating frame,

rest-mass density angular velocity

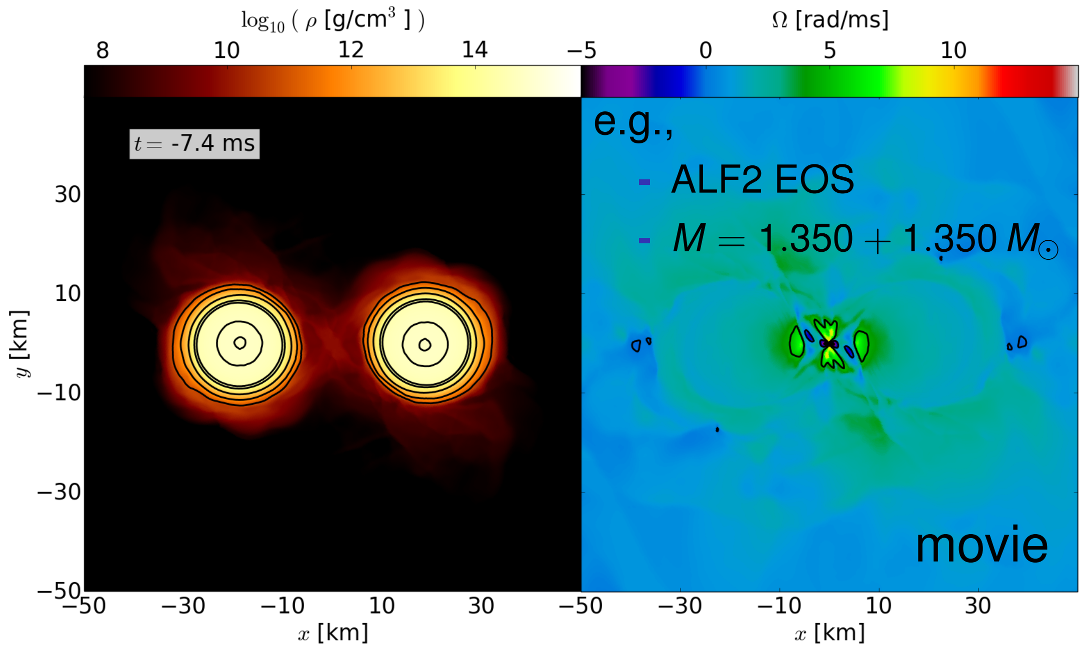

Properties

Averaged angular velocity profile of HMNS which is defined by

$$\bar{\Omega}(r,t) = \int_{t-\Delta t/2}^{t+\Delta t/2} \int_{-\pi}^{\pi} \Omega(r,\phi,t')\, d\phi\, dt' \, .$$

Introduction Methodology **Results** Conclusions

Properties

e.g. , high-mass model with ALF2 EOS

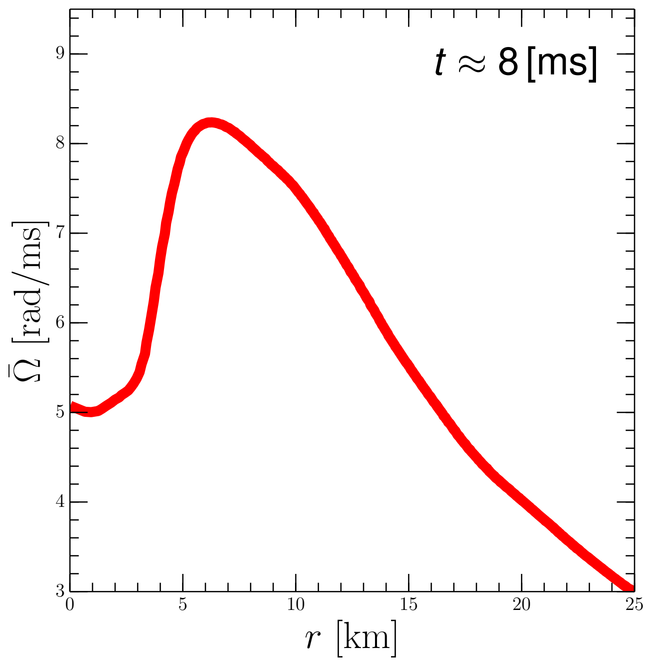

Averaged angular velocity profile of HMNS which is defined by

$$\bar{\Omega}(r,t) = \int_{t-\Delta t/2}^{t+\Delta t/2} \int_{-\pi}^{\pi} \Omega(r,\phi,t')\, d\phi\, dt' \, .$$

Properties

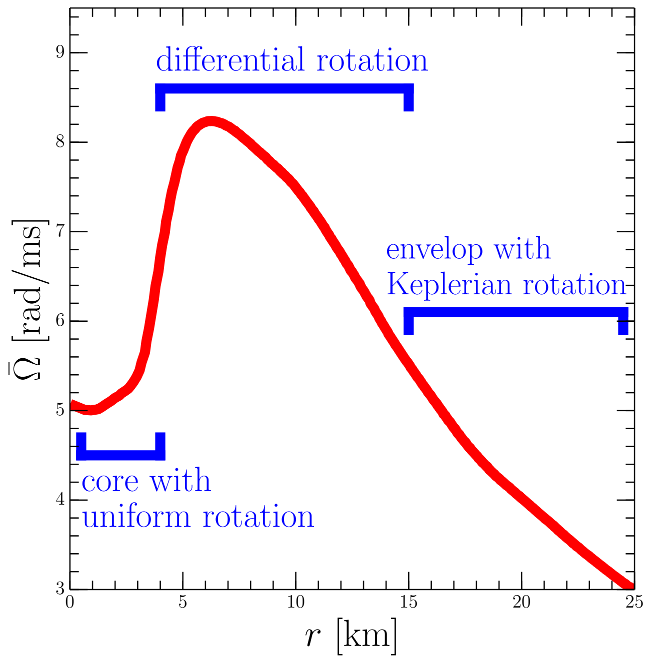

Averaged angular velocity profile of HMNS which is defined by

$$\bar{\Omega}(r,t) = \int_{t-\Delta t/2}^{t+\Delta t/2} \int_{-\pi}^{\pi} \Omega(r,\phi,t')\,d\phi\,dt' \ .$$

The structure consists of 3 different regions:

- core with uniform rotation,
- differential rotation,
- envelope with Keplerian rotation.

Introduction Methodology **Results** Conclusions

Properties

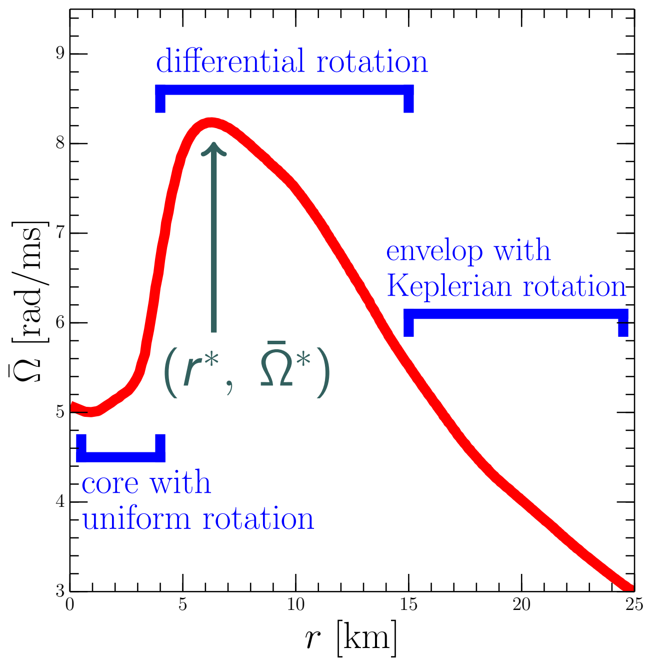

Averaged angular velocity profile of HMNS which is defined by

$$\bar{\Omega}(r,t) = \int_{t-\Delta t/2}^{t+\Delta t/2} \int_{-\pi}^{\pi} \Omega(r,\phi,t')\,d\phi\,dt' \ .$$

The structure consists of 3 different regions:

- core with uniform rotation,
- differential rotation,
- envelope with Keplerian rotation.

Properties

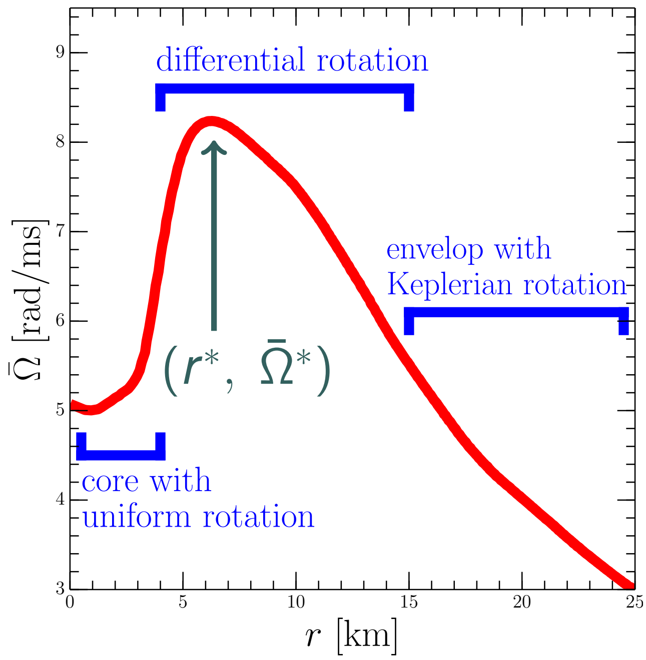

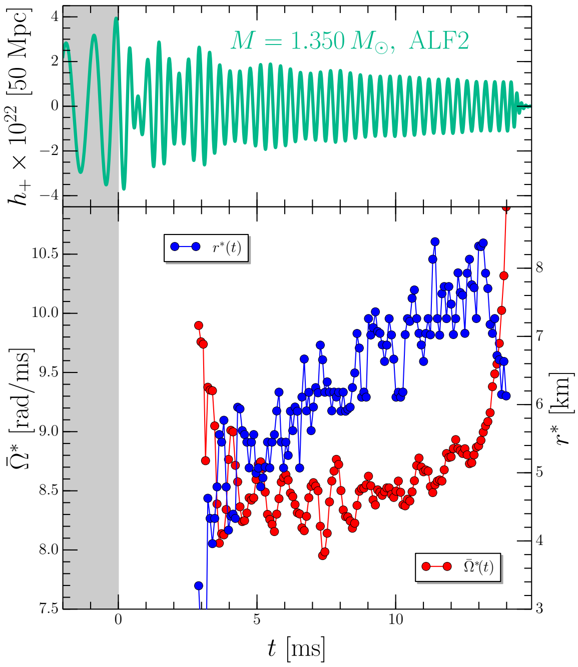

Introduction Methodology Results Conclusions

Properties

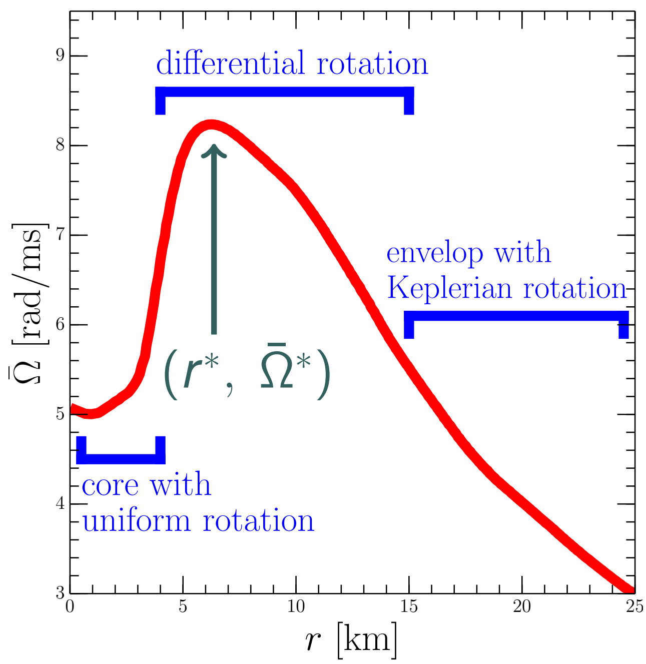

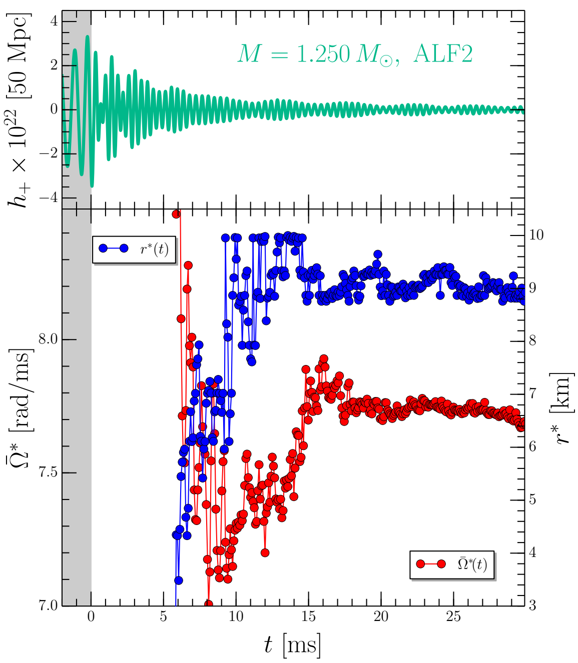

Properties

Common features and the correlation relations.

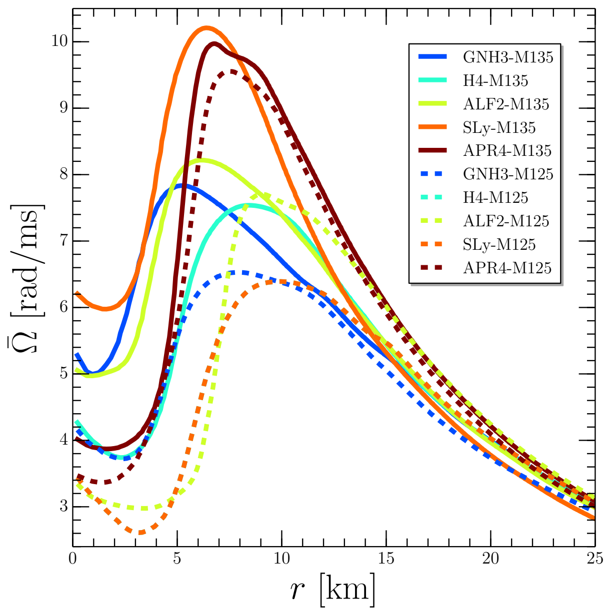

Introduction Methodology **Results** Conclusions

Properties

Common features and the correlation relations.

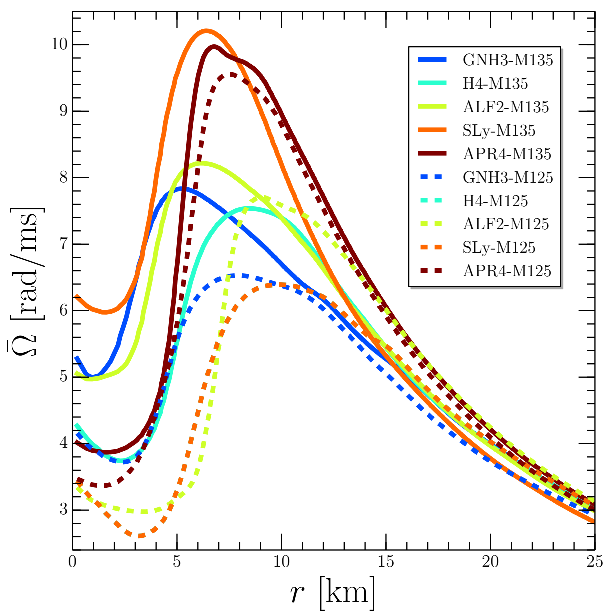

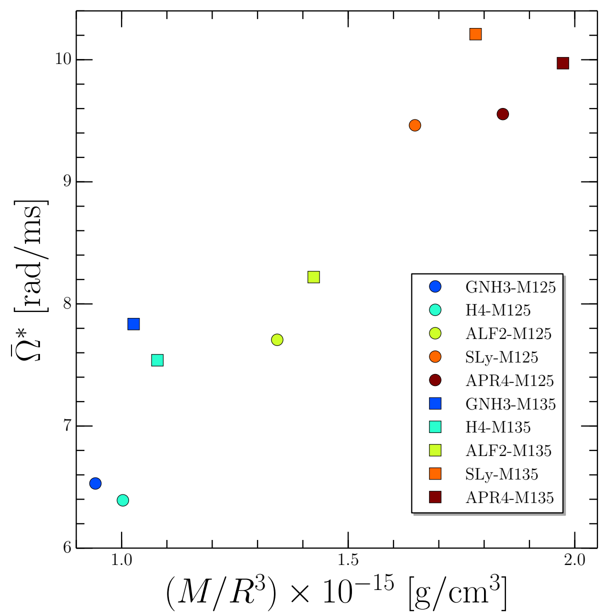

Properties

Common features and the correlation relations.

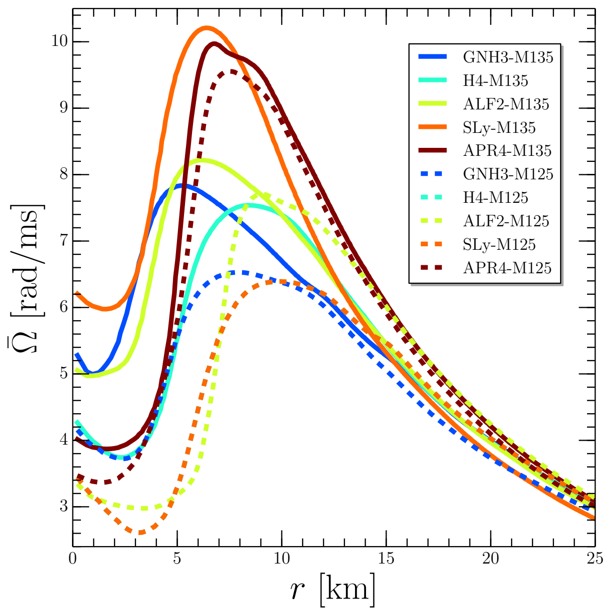

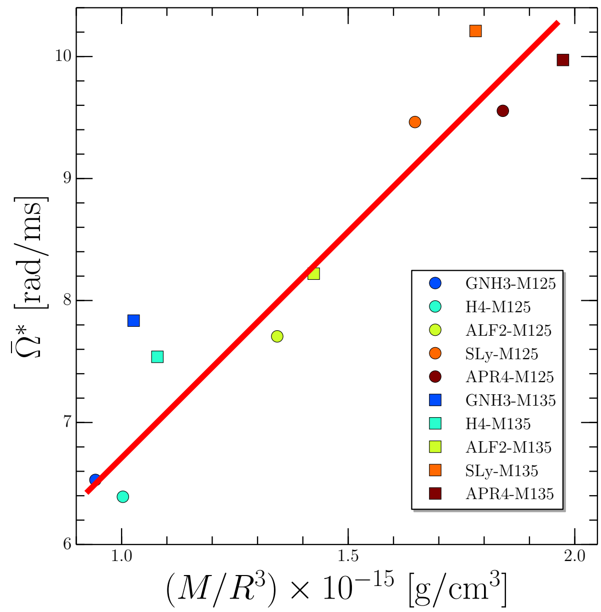

Introduction Methodology Results Conclusions

Properties

Common features and the correlation relations.

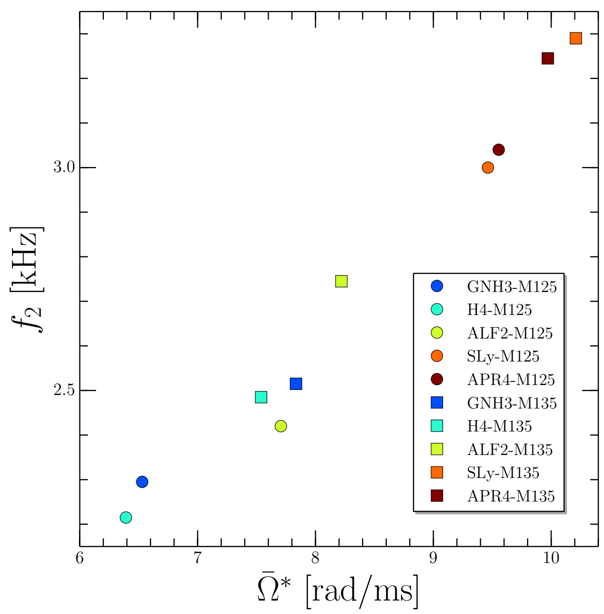

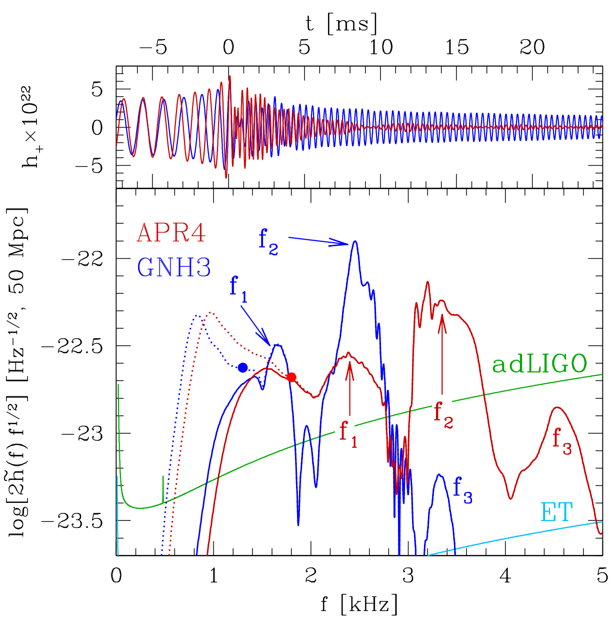

Properties

Common features and the correlation relations.

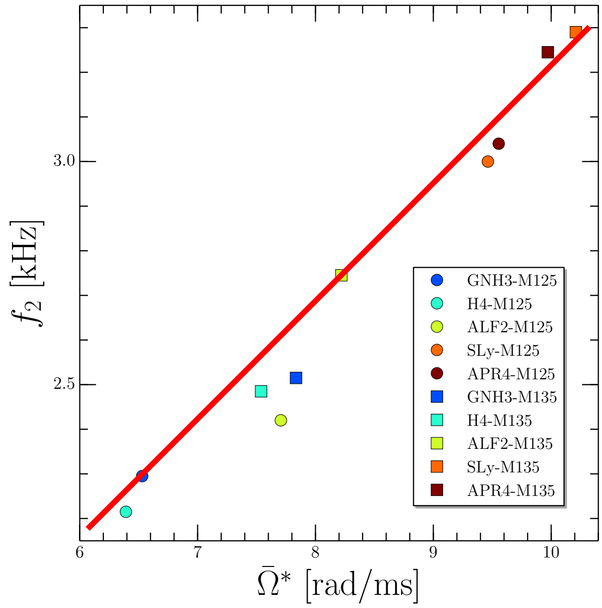

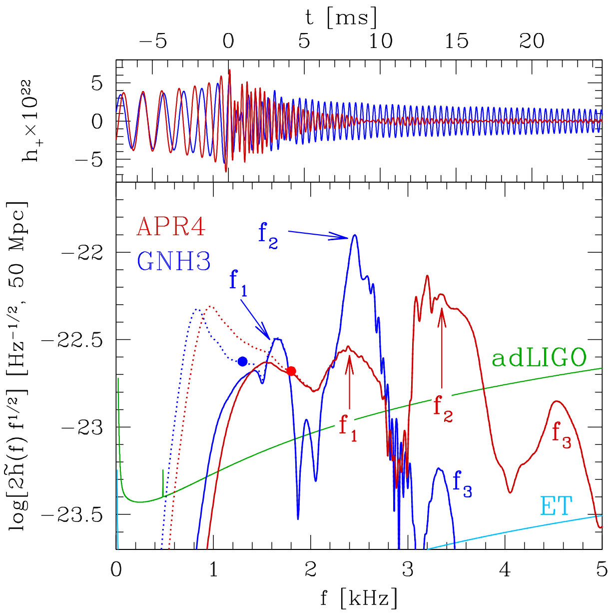

Conclusions

Conclusions

Remarks

- we have found that the rotational profile consist of 3 different regions:
  - **(i)** core with uniform rotation,
  - **(ii)** differential rotation,
  - **(iii)** envelope with Keplerian rotation.
- we have found that several universal correlations
  - **(a)** (M/R^3) vs $\bar{\Omega}^*$,
  - **(b)** $\bar{\Omega}^*$ vs f_2 .

Future Works

- instead of j-constant law, we construct new realistic rotation law for a HMNS and implement it to a ID codes to create a rotating neutron star.

“Reducing orbital eccentricity in initial data of black hole-neutron star binaries in the puncture framework”

by Koutarou Kyutoku

[JGRG25(2015)2b4]

Reducing orbital eccentricity in initial data of black hole-neutron star binaries in the puncture framework

Koutarou Kyutoku RIKEN, iTHES

Kyutoku, Shibata, Taniguchi PRD 90 064006 (2014)

Kyutoku, Shibata, Taniguchi in preparation

Gravitational waves from BH-NS

Promising target for Advanced LIGO, KAGRA…

Probe to the neutron star
- equation of state

radius, tidal deformability

Probe to the black hole
- effect of the spin
- quasinormal modes

http://gwcenter.icrr.u-tokyo.ac.jp/wp-content/themes/lcgt/images/img_abt_lcgt.jpg

Role of numerical relativity

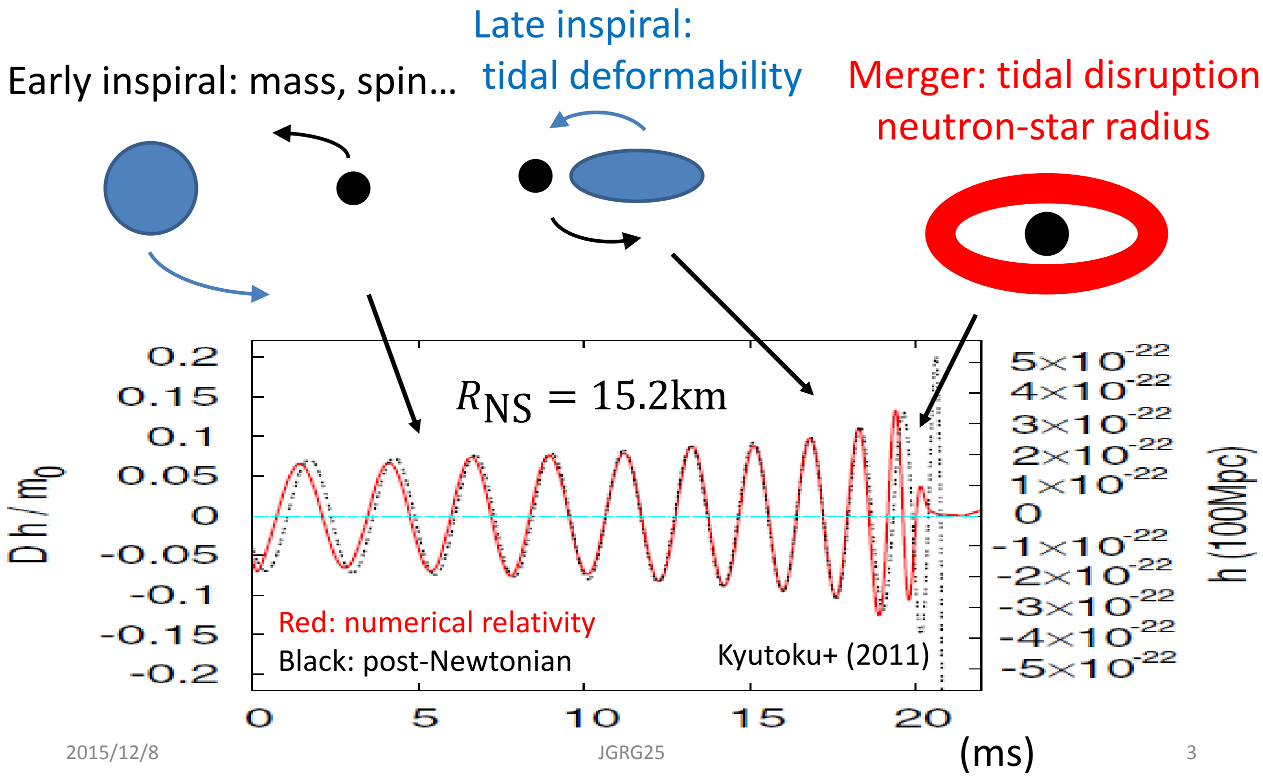

Initial data

Initial data are essential for numerical relativity

Gravitational side: Einstein's constraint equations

The induced metric γ_{ij} and extrinsic curvature K_{ij}

- assume conformal flatness $\gamma_{ij} = \psi^4 f_{ij}$
- maximal slicing $K_{ij} = \psi^{-2}\hat{A}_{ij}$, $f^{ij}\hat{A}_{ij} = 0$

Hydrodynamic side: hydrostatic equations

- some form of timelike symmetry is assumed to have a first integral of Euler's equation

Residual eccentricity

NS-NS/BH-NS simulations have suffered from unphysical “residual eccentricity” of $e \sim 0.01$ (except excision-method with nonprecessing spins)

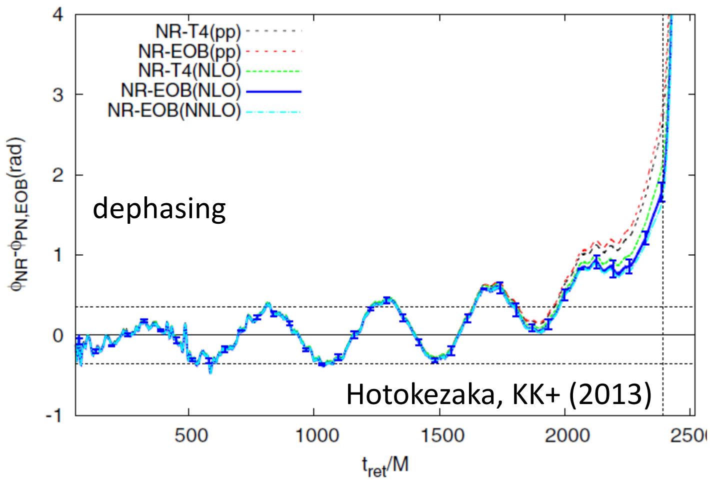

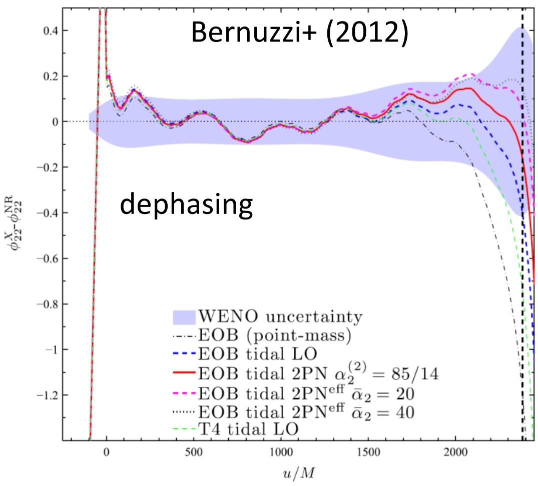

Why does the eccentricity remain?

Imperfection of helically symmetric initial data (the binary is stationary in its corotating frame)

Helical Killing vector

$$\xi^a = (\partial_t)^a + \Omega\left(\partial_\varphi\right)^a$$

No radiation reaction

= no approaching motion

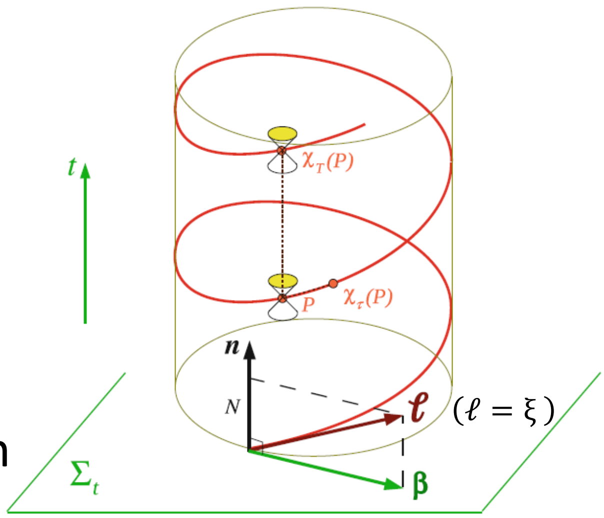

Gourgoulhon (2012)

Modify the symmetry vector

Incorporate a relative approaching velocity

$$\xi^a = (\partial_t)^a + \Omega(\partial_\varphi)^a + v(\partial_x)^a$$

and tune the orbital angular velocity

so that the binary smoothly begins the inspiral

Low-eccentricity orbits may be obtained with appropriate (Ω, v)

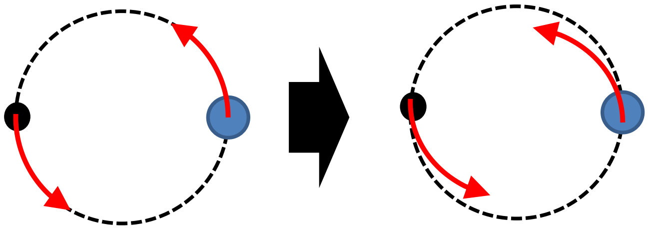

Iterative correction

Fit the evolution of orbital frequency by

$$\dot{\Omega}(t) = A_0 + A_1 t + B\cos(\omega t + \phi)$$

A: secular evolution due to radiation reaction

B: modulation due to the eccentricity etc.

modify (Ω, v) of initial data iteratively to remove modulation

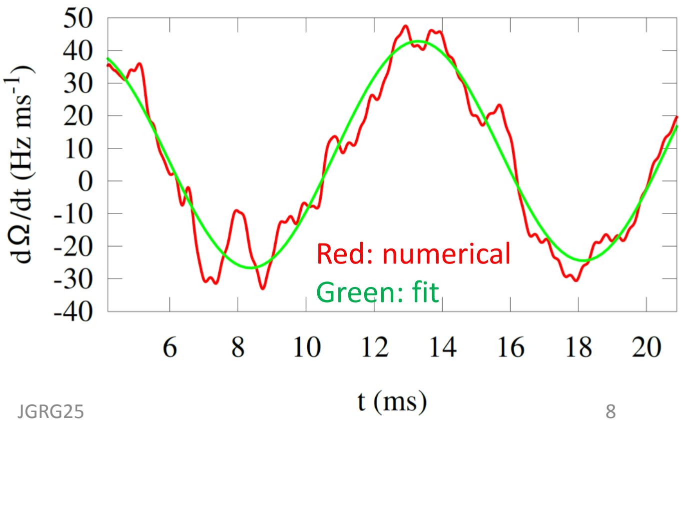

Choice of center-of-mass for BH-NS

The location of "center-of-mass" of the system is not determined uniquely for the puncture method

- corotation condition: $\beta^{\varphi} = -\Omega$ at the puncture

baseline, because we also assume $\beta^{r} = -v_{\mathrm{BH}}$

- PN-J method: require $J_{\mathrm{num}}(\Omega) = J_{\mathrm{PN}}(\Omega)$

better than the above for helically symmetry (and we have adopted), though phenomenological

just for comparison in today's results

Nonprecessing system

BH spin parallel to the orbital angu. mom. or zero

4%->0.1% smoothly by 3 iterations (more for spinning)

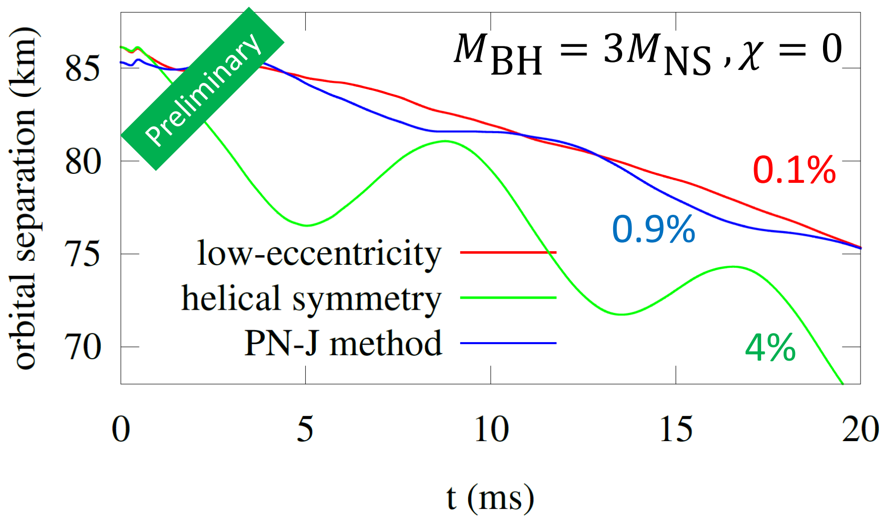

Precessing system

BH spin misaligned w.r.t the orbital angu.mom.
1.5%->0.7% not smoothly: down->up->down

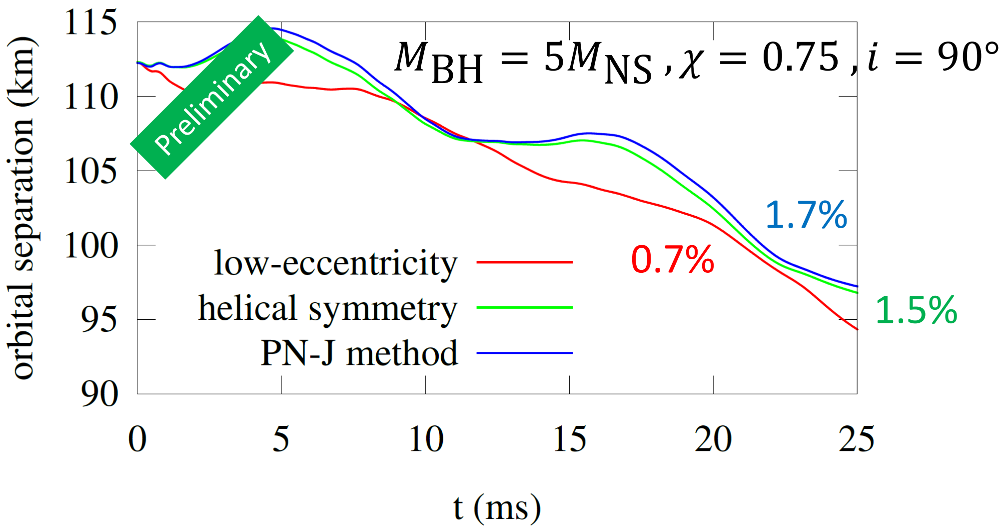

Required improvement

Some mixing of spin-induced modulation?
- the eccentricity is a bit too small from the beginning compared to nonprecessing systems

Comparisons with post-Newton orbital dynamics
(and why starts from periastron, not apastron?)

Efficiency is not high even for aligned-spin cases
-> iterative estimation should be improved
include more parameters, choose time windows…

Summary

- We develop a method to remove residual eccentricities in initial data of black hole-neutron star binaries in the puncture framework.
- For nonprecessing binaries, the method seems to work well.
- For precessing binaries, the method does not work as well as for nonprecessing binaries, possibly due to the spin-induced modulation. Improvements are necessary.

"Gravitational waves from precessing black hole-neutron star mergers"

by Kyohei Kawaguchi

[JGRG25(2015)2b5]

Gravitational Waves From Precessing Black Hole-Neutron Star mergers

Kyohei Kawaguchi[A], Kotarou Kyutoku[B], Hiroyuki Nakano[C], Hirotada Okawa[A,D], Masaru Shibata[A], Keisuke Taniguchi[E]

A:Yukawa Institute for Theoretical Physics B:Interdisciplinary Theoretical Science Research Group, RIKEN C:Department of Physics, Kyoto University D:Advanced Research Institute for Science and Engineering, Waseda University E: Department of Physics, University of the Ryukyus

2015.12.8

JGRG25 @ Kyoto University

Gravitational waves from BHNS mergers

・The dynamics of a BHNS merger depends on the parameter of the binary.

$M_{\rm NS}$	$Q := \dfrac{M_{\rm BH}}{M_{\rm NS}}$	$\chi := \dfrac{S_{\rm BH}}{M_{\rm BH}^2}$	$i_{\rm tilt} := \cos^{-1}\left(\dfrac{\mathbf{S}_{\rm BH}\cdot\mathbf{L}}{S_{\rm BH}L}\right)$	$\mathcal{C} := \dfrac{M_{\rm NS}}{R_{\rm NS}}$
NS mass	mass ratio	dimensionless spin	spin orientation	NS compactness

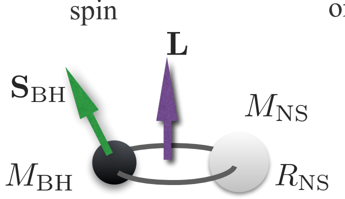

・The gravitational waves from a BHNS merger contains the information of the binary.

Particularly, the gravitational waves in the late inspiral and the merger phase reflects the property of the NS.

> In this talk, I focus on the gravitational waves in the merger phase, based on the results of recent numerical-relativity simulations.
> (K. Kyutoku et. al 2015, KK et al. 2015)

The effects of the NS

・The NS structure affects both phase and amplitude of the gravitational waveforms.

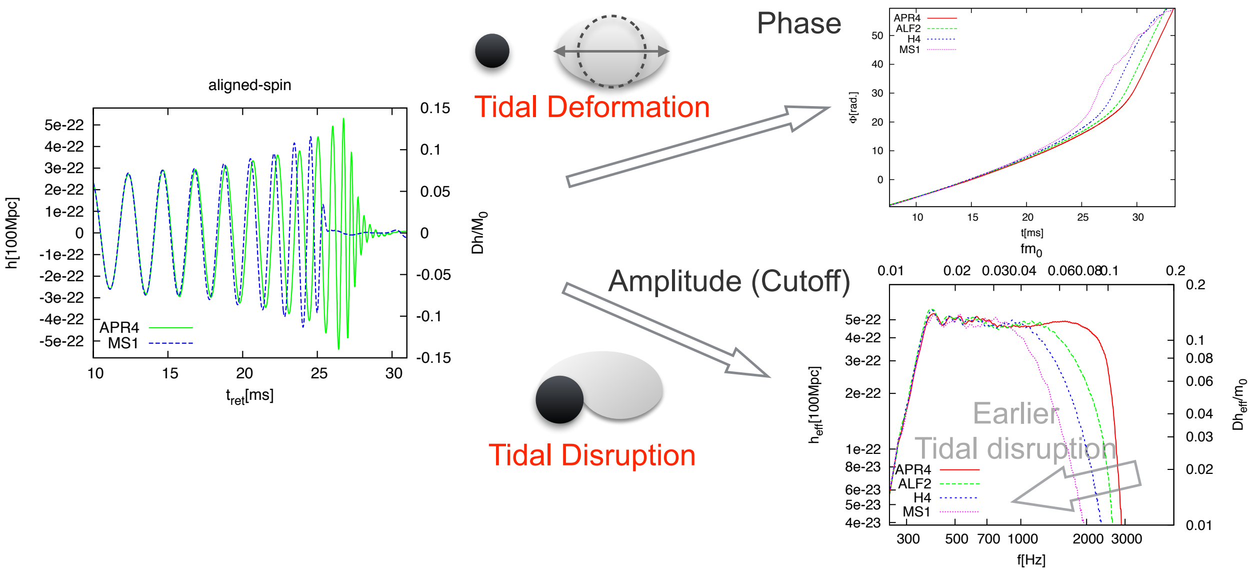

・We can get the informations of the NS structure if we could extract these effects from the waveforms.

The orbital precession

・The misalignment of the BH spin and the orbital angular momentum of the binary leads to the orbital precession.

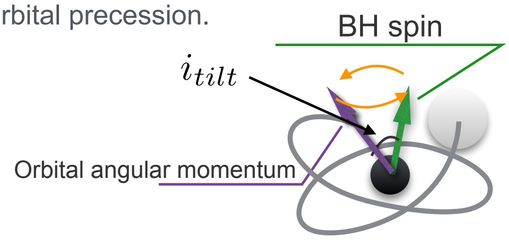

・The orbital precession makes it difficult to separate the effect which comes from the NS structure from the waveform by modulating the both phase and amplitude.

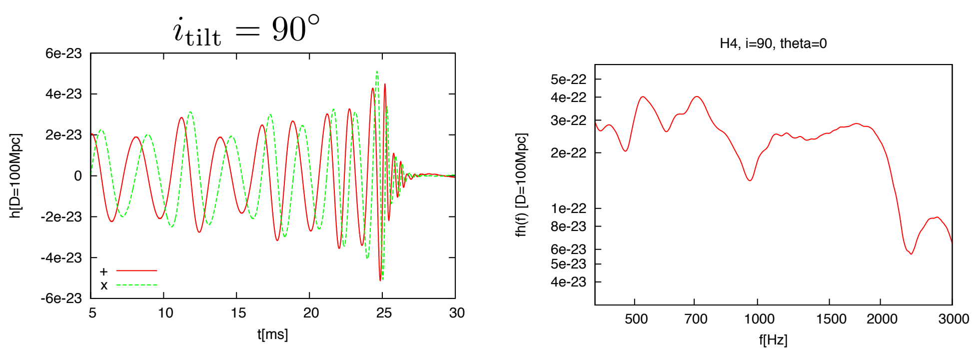

The purpose and the motivation

- The parameter space for BHNS mergers becomes very large if we consider the misalignment of the BH.
- In presence of the orbital precession, the links between the binary parameters and the shape of the waveforms.

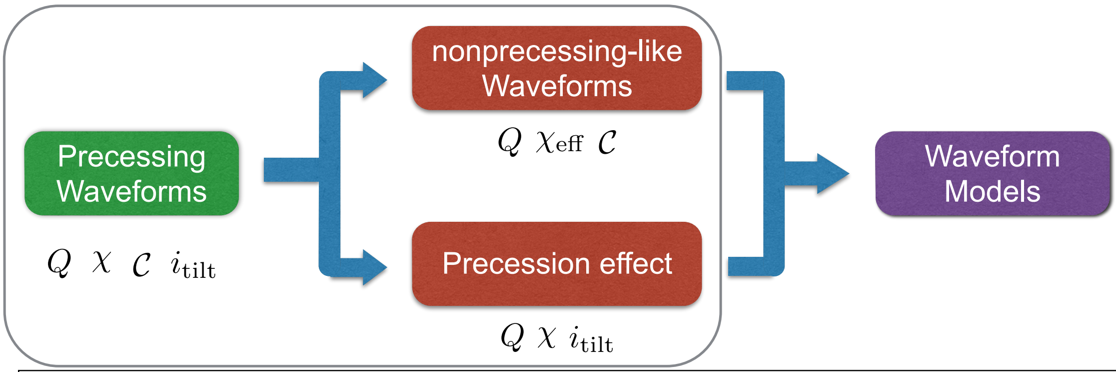

It can be useful if we could separate the effect of the orbital precession from the complicated precessing waveforms.

Quadrupole Alignment (QA)

- The angular velocity of the orbital precession is always smaller by an order of magnitude than the angular velocity of the orbital motion in the simulation.

$$\omega_{\rm prec} \ll \Omega_{\rm orb}$$

→ the waveform observed from the observer which always faces the instantaneous orbital plane may be similar to the one which can be obtained from non-precessing binary.

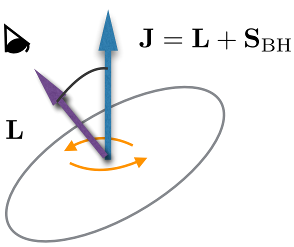

$$\tilde{h}_{lm} = \sum_{m'} h_{lm'} D^{l}_{m'm}(\mathcal{R}^{-1})$$

$\mathcal{R}$: rotation matrix

$$\begin{aligned} h(\theta,\phi) &= \sum_{l,m} h_{lm}\ {}_{-2}Y_{lm}(\theta,\phi) \\ &= \sum_{l,m} \tilde{h}_{lm}\ {}_{-2}\tilde{Y}_{lm}(\theta,\phi) \end{aligned}$$

${}_{-2}\tilde{Y}_{lm}(\theta,\phi)$:Spin Weighted Harmonics with its axis with $\hat{z}' = \mathcal{R}\hat{z}$

We can obtain this waveform and the axis of the instantaneous orbital plane by finding the axis which maximize the amplitude of the dominant (l,m)=(2,±2) modes in the rotated frame.

$$\max_{\mathcal{R}} \left| \tilde{h}_{22} + \tilde{h}^{*}_{2-2} \right|$$

(e.g. *Shcmidt et al.* 2012)

Treatment for spin-misalignment correction

・The effect of precession can not be completely removed only by QA because of the presence of the 1.5 PN spin-misalignment correction.

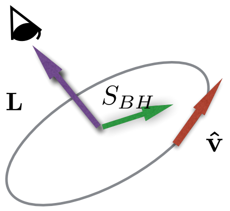

$$\frac{|\tilde{h}_{22}| - |\tilde{h}_{2-2}|}{|\tilde{h}_{22}| + |\tilde{h}_{2-2}|} \approx -v^2 \frac{\mathbf{S}\cdot\hat{\mathbf{v}}}{2M^2} \approx v^2 \chi \sin i_{\mathrm{tilt}}$$

(ref. Boyle et al. 2014)

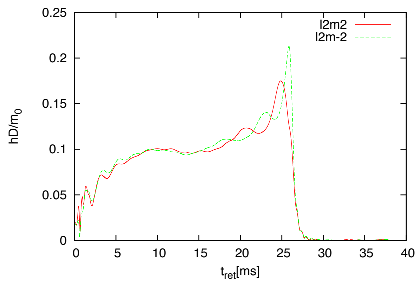

・The spin-misalignment correction contribute to the waveforms with the opposite sign in (l,m)=(2,+2) and (2,-2) mode in the leading order, therefore, it can be separated by making an addition and a subtraction between these modes.

"QA+ waveforms"

$$\tilde{h}'_{22} := \frac{\tilde{h}_{22} + \tilde{h}^*_{2-2}}{2} \qquad \tilde{h}^{\mathrm{tilt}}_{22} := \frac{\tilde{h}_{22} - \tilde{h}^*_{2-2}}{2}$$

Result

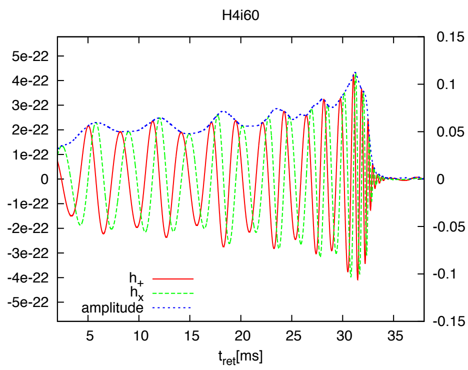

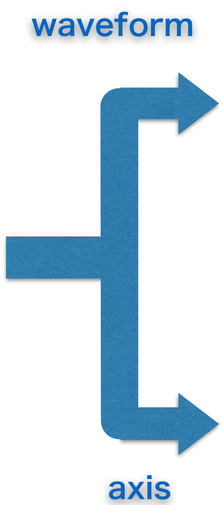

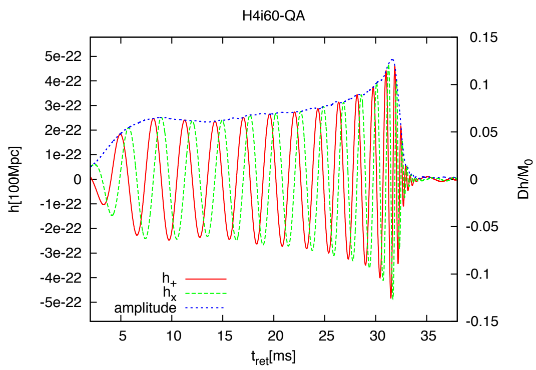

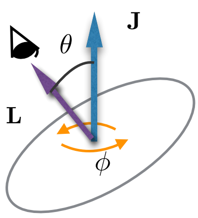

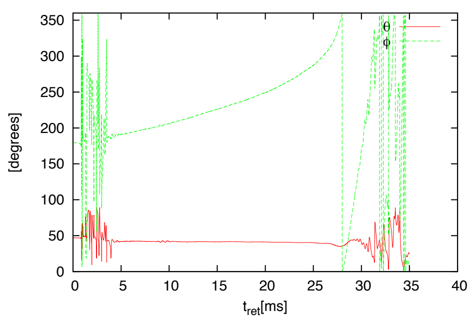

QA+ v.s. spin-aligned waveforms

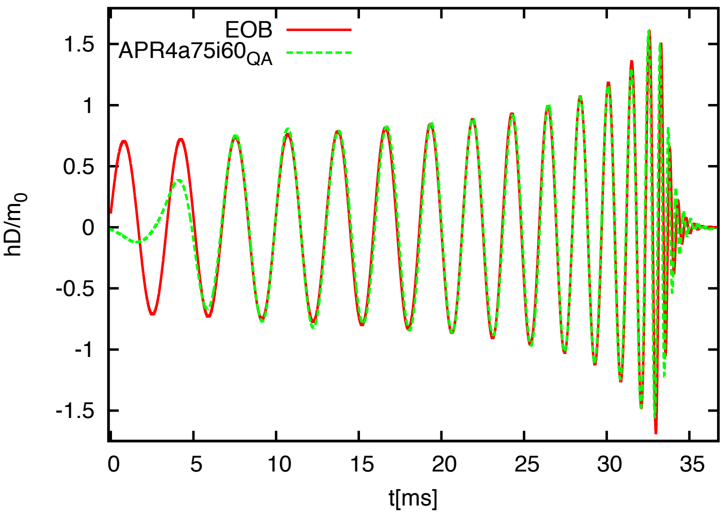

・The QA+ waveforms are similar to the spin-aligned waveforms with the same total mass, the same mass ratio and the same effective spin parameter, $\chi_{\rm eff} := \chi \cos i_{\rm tilt}$.

Result

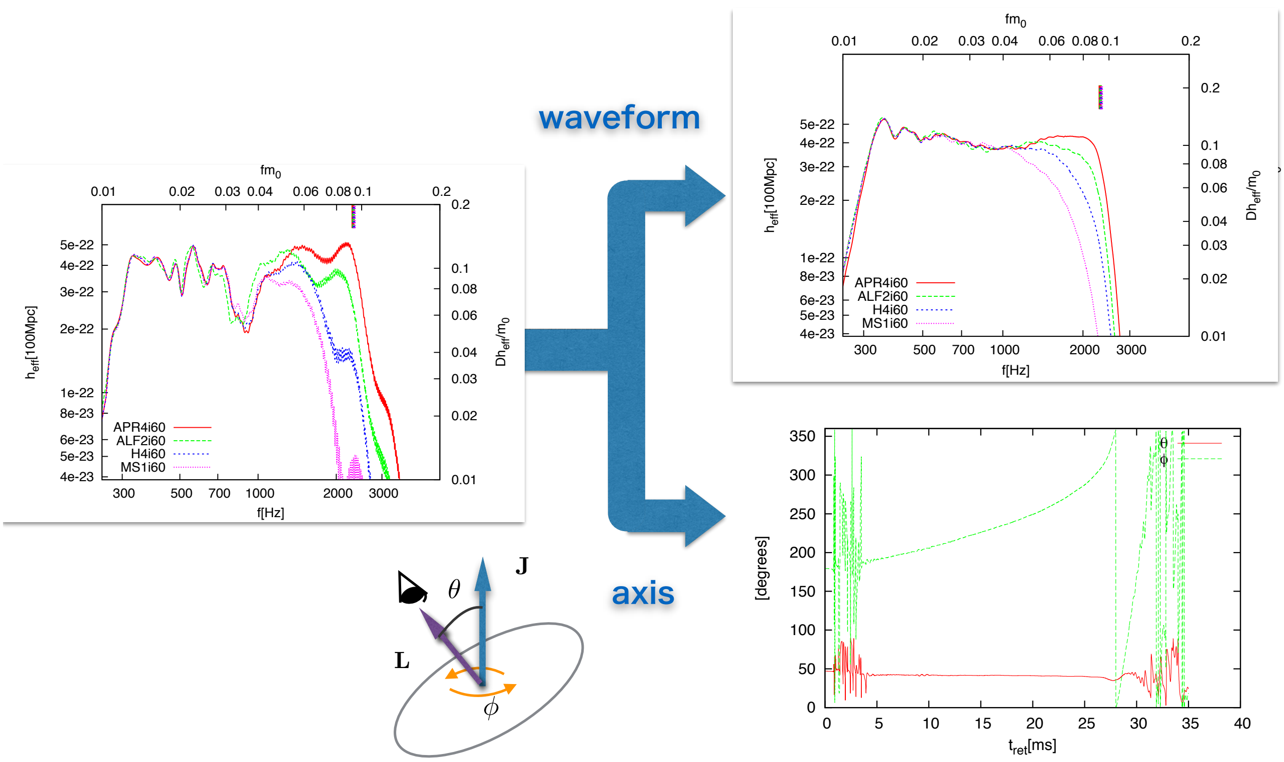

Cutoff Frequency

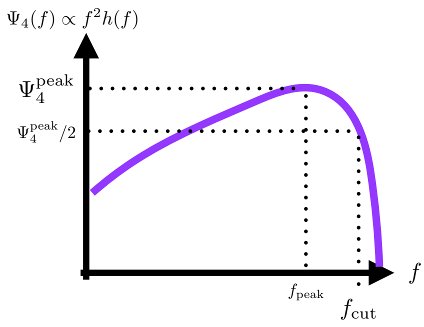

$Q = 5$
$\chi = 0.75$
$M_{\rm NS} = 1.35 M_\odot$

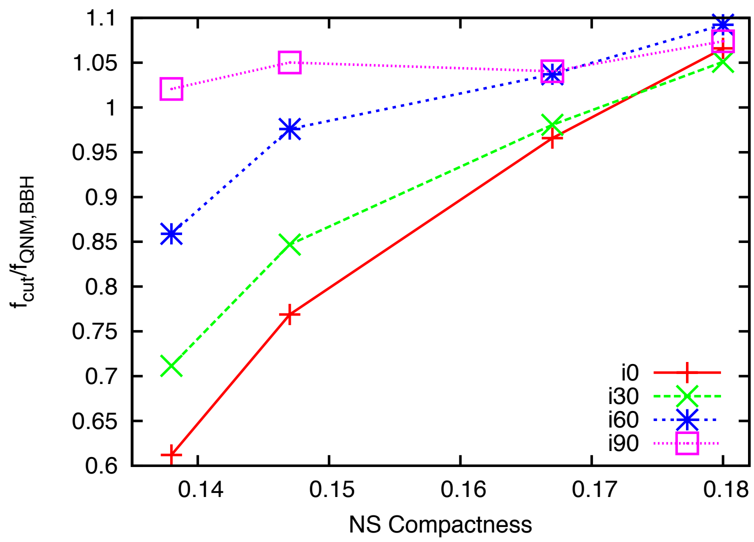

- The dependance of the cutoff frequency on the NS compactness is clear seen.

Summary

- The QA+ method can be useful for separating the effect of the orbital precession from the precessing BHNS waveforms in the merger phase.
- The QA+ waveforms may have some connection to the non-precessing BHNS waveforms.
- The dependence of cutoff frequency on the NS compactness is clearly seen in the QA+ spectra.

“The detection rate of Inspiral and QNMs of Pop III BH-BHs which can confirm or refute the GR in the strong gravity region”

by Tomoya Kinugawa

[JGRG25(2015)2b6]

The detection rate of Inspiral and QNMs of Pop III BH-BHs which can confirm or refute the GR in the strong gravity region

Tomoya Kinugawa (Kyoto univ.), Akinobu Miyamoto (Osaka city univ.),
Nobuyuki Kanda (Osaka city univ.), Takashi Nakamura (Kyoto univ.)

arXiv:1505.06962 accepted to MNRAS

Introduction

Pop III star and Pop III binary

- **Population III (Pop III) stars** are the first stars after the Bing Bang.
- Binary fraction of Pop III stars ～1/2
  (Stacy et al. 2013, Susa et al. 2014)
- Merger timescale due to gravitational radiation may be so long that Pop III binaries merge at the present day.

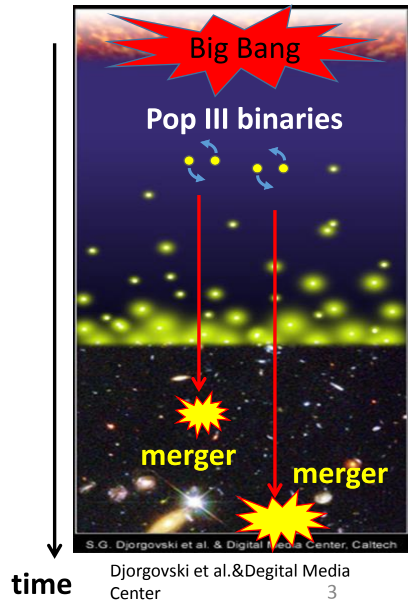

Djorgovski et al.&Degital Media Center

3

The differences between Pop III and Pop I

	Pop I stars (Sun like stars)	Pop III stars
Metallicity	2%	0
Radius	Large	Small
Typical mass	Small (~1 Msun)	Large (~10-100 Msun)
Wind mass loss	Present	Absent

Pop III binaries are easier to be massive compact binary

4

Method

How to calculate Pop III binaries?

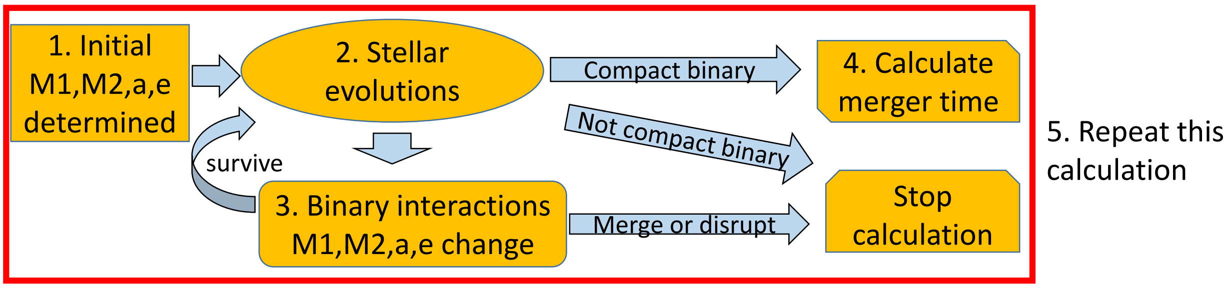

1. Initial condition of binary are decided by Monte Carlo method with initial distribution functions
   (primary mass: M1, secondary mass: M2, separation: a, orbital eccentricity: e)
2. We calculate evolution of stars
3. If star fulfills the condition of binary interactions (BIs), we calculate BIs and change M1, M2, a, e .
   - If binary merges or disrupts due to BIs before binary becomes compact binary, we stop calculation.
   - If binary survives from BIs, we calculate stellar evolutions again.
4. If binary becomes compact binary (NS-NS, NS-BH, BH-BH), we calculate when binary merge due to GW.
5. We repeat these calculations and take the statistics of compact binary mergers.

Binary Interactions

- Tidal friction
- Common envelope
- Mass transfer
- Supernova effect
- Gravitational radiation

Change
M1,M2,a, e

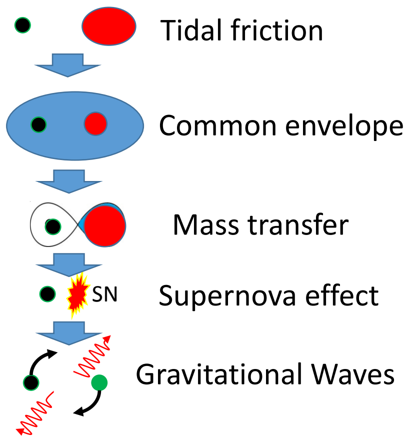

We need to specify some parameters to calculate these effects.

We use the parameters adopted for Pop I population synthesis in Our standard model.

Pop III binary population synthesis

We simulate 10^6 Pop III-binary evolutions and estimate how many binaries become compact binary which merges within Hubble time.

Initial conditions are decided by Monte Carlo method with initial distribution functions

e.g. standard model

- Initial parameter (M1,M2,a,e) distribution function P(x)

M1 : Flat ($10\ M_{\odot} < M < 100\ M_{\odot}$)

q=M2/M1 : P(q)=const. (0<q<1)

a : $P(a) \propto 1/a$ ($a_{min} < a < 10^6 R_{\odot}$)

e : $P(e) \propto e$ (0<e<1)

The same distribution functions adopted for Pop I population synthesis

Results

Results

The numbers of the compact binaries which merge within Hubble time for 10^6 binaries

NSNS	NSBH	BHBH
0	50	115056

- A lot of Pop III BH-BH binaries form and merge within Hubble time

Pop III chirp mass distribution

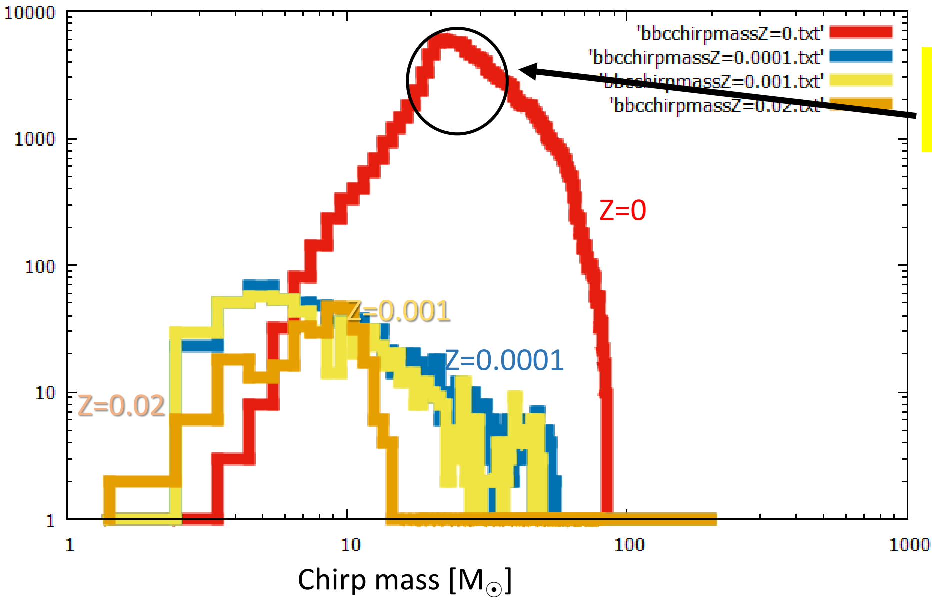

Typical chirp mass
M∼30 M⊙

e.g. Pop I, Pop II
(Z=0.02,0.001,0.0001)
IMF:Salpeter

Typical mass ∼10 M⊙

11

Detection range of KAGRA

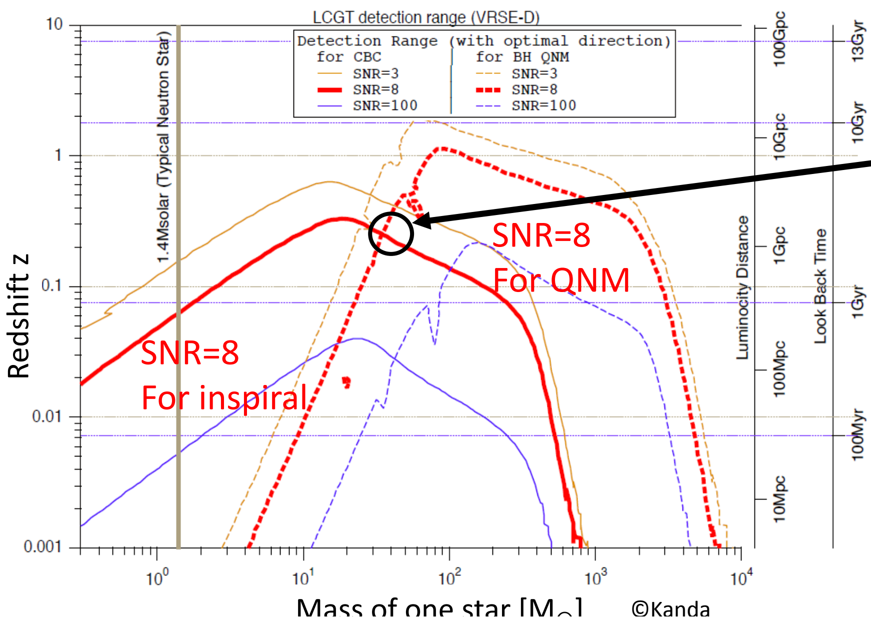

M_{BH}∼30M⊙
SNR=8

Luminocity distance
∼1.5 Gpc

Redshift z∼0.28

12

Detection rate

Detection rate of the inspiral and QNM (a/M=0.70) by 2nd generation detectors

$$N \sim 180 \left(\frac{SFR_p}{10^{-2.5}}\right)\left(\frac{f_b/(1+f_b)}{0.33}\right)\boxed{\mathrm{Err_{sys}}}\ [\mathrm{yr}^{-1}]$$

SFRp is the peak value of Pop III SFR ($10^{-2.5}$ Msun/yr/Mpc^3),
f_b is the initial binary fraction (1/2),
$\mathrm{Err_{sys}}$ = 1 corresponds to adopting distribution functions and the binary evolution for Pop I stars.

To evaluate the robustness of the chirp mass distribution and the range of $\mathrm{Err_{sys}}$, we examine the dependence of the results on the unknown parameters and the distribution functions.

Errsys

	Errsys
Standard	1 (180 /yr)
IMF($10M_\odot$<M< $100\ M_\odot$ or $140\ M_\odot$) Flat,M^{-1},Salpeter	0.42~3.4
Initial eccentricity distribution f(e)∝e,const.,$e^{-0.5}$	0.94~3.4
SN natal kick V=0,100,300 km/s	0.2~3.4
Common envelope αλ=0.01,0.1,1,10	0.21~3.4
Mass transfer (mass loss fraction) β=0, 0.5, 1	0.67~4
Worst	0.046

- On the other hand, the typical chirp mass is not changed.

Pop III BH-BH

- Errsys=0.046~4

  ⇒**Detection rate R～8.3-720 $\left(\frac{SFR_{peak}}{10^{-2.5}}\right)\left(\frac{f_b/(1+f_b)}{0.33}\right)$ [yr^{-1}]**

- Chirp mass **M～30 $M_{\odot}$**

Details are described in Kinugawa et al. 2015 arXiv:1505.06962

We might detect the Pop III BH-BH by GW

1. The chirp mass distribution might distinguish Pop III from Pop I, Pop II
2. We might check the GR by BH QNM from Pop III BH-BH
   (For the details, **Nakano**'s poster P23)

“Gravitational Collapse of a Collisionless Particle System in an Expanding Universe”

by Chulmoon Yoo

[JGRG25(2015)3a1]

Gravitational Collapse of a Collisionless Particle System in an Expanding Universe

Yoo, Chulmoon（Nagoya U.）

with Tomohiro Harada（Rikkyo U.）
Hirotada Okawa（Waseda U.）

Tabel of Contents

◎Motivation: PBH formation with pressureless matter

◎Simulation with collisionless particle system

◎Test: comparison with the LTB solution

◎An example of Non-spherical collapse

Motivation: PBH with Pressureless Matter

PBH in Dust Universe

◎**Primordial black holes(PBHs)**

- In principle, it can be formed in any stage after inflation
- Observational bound for PBH abundance
- PBHs in radiation dominated era are mainly considered
- What about preheating era?

◎**PBH during preheating**

- There are several related works on estimation of PBH abundance
- Roughly, the universe is matter dominated(effectively dust)
- Threshold for PBH production is different from that in radiation era

◎**PBH formation in dust universe**

- With spherical sym. PBH may easily form
- Asphericity grows and is essential（Lin-Mestel-Shu instability）
- Elongation, flattening may preclude BH formation(Hoop conjecture)

5

Dust Collapse

◎**Simulation with collisionless particles(asympt. flat)**

- **Axisymmetric collapse**[Shapiro-Teukolsky(1991)]
- **Full 3D with BSSN**[Shibata(1999)]
- **(5D axisymmetric**[Yamada-Shinkai(2011)]**)**
- **For large ellipticity, naked singularity forms before BH formation** [Nakamura-Shapiro-Teukolsky(1988)]

◎**Extension to expanding backgrounds**

- **Periodic boundary condition(T^3 topology, EdS background)**
- **Initial data with a compensated density inhomogeneity**

◎**Final Goal**

- **Threshold for the ellipticity**

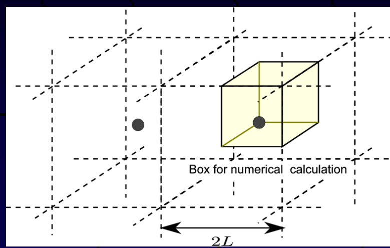

6

Simulation with Collisionless Particles

Collisionless Particles

◎Particle motions

- Timelike geodesics
- Four velocity: $u_a^\mu = E_a(n^\mu + V_a^\mu)$

◎Energy momentum

- $T^{\mu\nu} = -\sum_a m_a \frac{\delta^3(\vec{x}-\vec{x}_a)}{u_a^\lambda n_\lambda \sqrt{\gamma}} u_a^\mu u_a^\nu$

$$\rho := n_\mu n_\nu T^{\mu\nu} = \sum_a m_a E_a \frac{\delta^3(\vec{x}-\vec{x}_a)}{\sqrt{\gamma}}$$

$$J^i := -\gamma^i_\mu n_\nu T^{\mu\nu} = \sum_a m_a E_a V_a^i \frac{\delta^3(\vec{x}-\vec{x}_a)}{\sqrt{\gamma}}$$

$$S^{ij} := \gamma^i_\mu \gamma^j_\nu T^{\mu\nu} = \sum_a m_a E_a V_a^i V_a^j \frac{\delta^3(\vec{x}-\vec{x}_a)}{\sqrt{\gamma}}$$

◎Smoothing

- $\delta^3(\vec{x}-\vec{x}_a) \to f_{sp}(|\vec{x}-\vec{x}_a|, r_s)$

Spline Kernel

◎Smoothing

- $\delta^3(\vec{x}-\vec{x}_a) \to f_{sp}(|\vec{x}-\vec{x}_a|, r_s)$

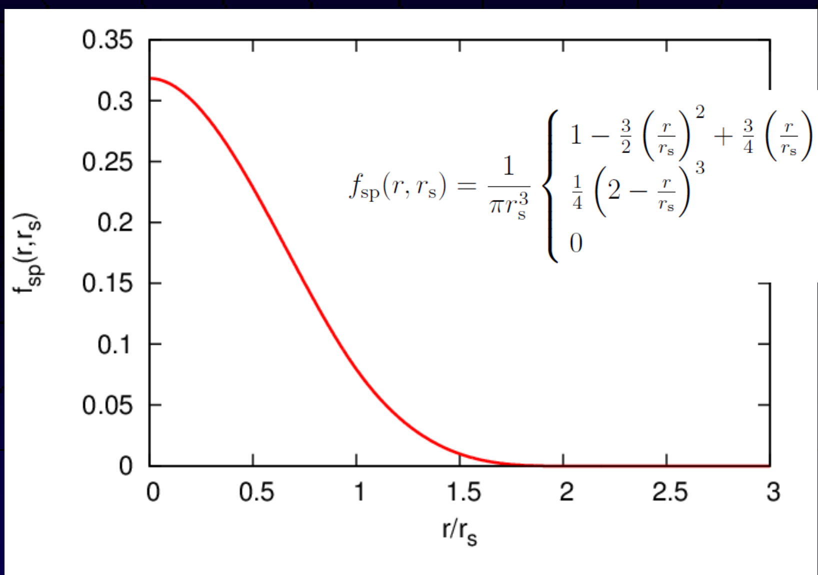

$$f_{\rm sp}(r, r_{\rm s}) = \frac{1}{\pi r_{\rm s}^3} \begin{cases} 1 - \frac{3}{2}\left(\frac{r}{r_{\rm s}}\right)^2 + \frac{3}{4}\left(\frac{r}{r_{\rm s}}\right)^3 & \text{for } 0 \le \frac{r}{r_{\rm s}} \le 1 \\ \frac{1}{4}\left(2 - \frac{r}{r_{\rm s}}\right)^3 & \text{for } 1 \le \frac{r}{r_{\rm s}} \le 2 \\ 0 & \text{for } 1 < \frac{r}{r_{\rm s}} \end{cases}$$

9

Flow of Time Evolution

◎Initial data for geometry and particles(skip)

◎2nd order leap frog with BSSN (with time filtering)

◎Constant-mean-curvature(CMC) condition for α(lapse)

◎Flow of evolution

1-1. Evolve geometrical variables except for α(lapse)

1-2. Evolve particle variables solving geodesic eqs.
*2nd order interpolation for geometry at particle position

2. Set energy momentum tensor
*No α-dependence in our expression

3. Set α by solving the elliptic eq. of CMC condition

10

Coordinate

◎Numerical region

・$0 \leq X, Y, Z \leq L$
(X, Y, Z:Cartesian)

・with reflection boundary

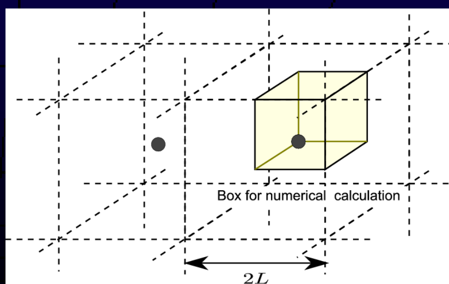

◎Inhomogeneous grid

- To keep fine resolution in collapsing region
- Inhomogeneous grid $x^i = (x, y, z)$

$$X^i = f(x^i) \text{ for } i = x, y, z \quad \text{with } f(x) = x - \frac{A}{1+A}\frac{L}{\pi}\sin\left(\frac{\pi}{L}x\right)$$

- Compatible with the boundary cond.
- Same numerical region($0 \leq x, y, z \leq L$)
- $\left(\frac{dX^i}{dx^i}\right)_{\text{boundary}} \Big/ \left(\frac{dX^i}{dx^i}\right)_{\text{center}} = 1 + 2A$

11

Test:
Comparison with LTB

JGRG25@Kyoto

Chulmoon Yoo

12

Animation

◎**Number of particles: 10^4**

- **We plot 1/10 of them**

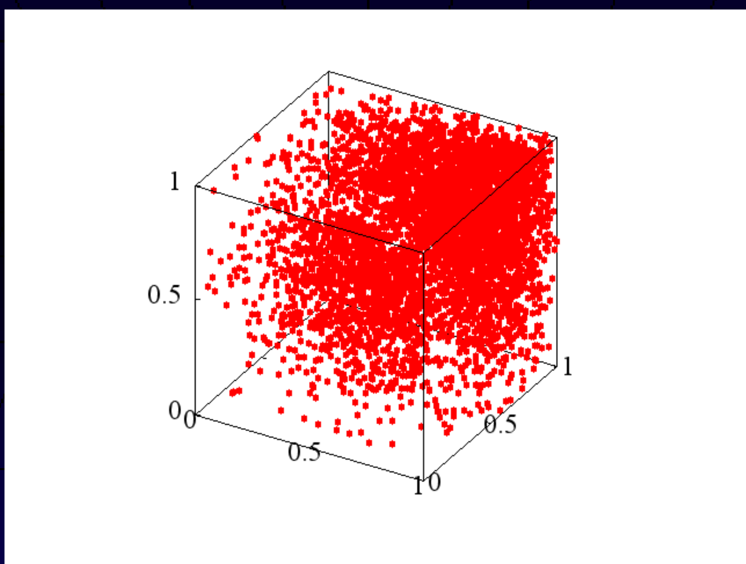

***time interval is not constant**

JGRG25@Kyoto

Chulmoon Yoo

13

Lapse

◎Lemaitre-Tolman-Bondi: spherical dust solution

- Assuming only growing mode

◎Evolution of Lapse α

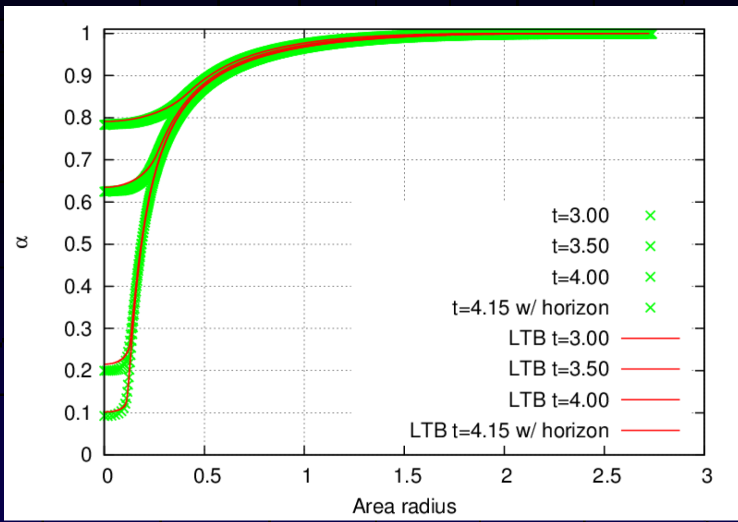

14

Expansion

◎Value of expansion on spheres(approximately)

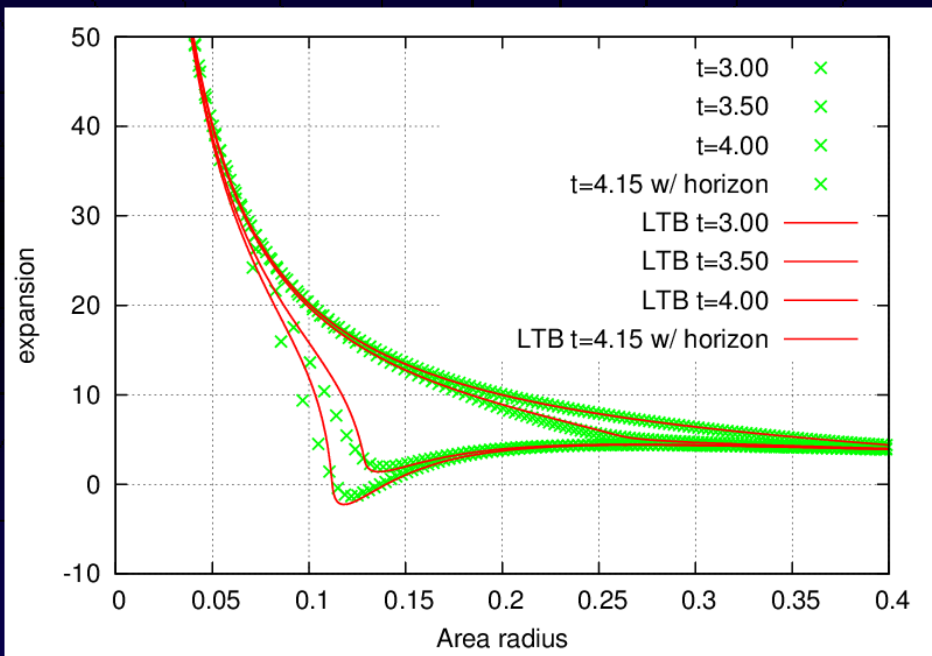

15

An Example of Non-spherical Collapse

JGRG25@Kyoto Chulmoon Yoo

16

Initial Data

◎A simple initial data

- Conformally flat: $dl^2 = \Psi^4 \delta_{ij} dx^i dx^j$
- Energy momentum: $T_{\mu\nu} = \rho u_\mu u_\nu = \rho n_\nu n_\nu$
- Extrinsic curvature: $K_{ij} = \frac{1}{3} K \delta_{ij}$ with K being constant
  $\Rightarrow$ trivial Mom. constraint
- Hamiltonian constraint: $\Delta\Psi - \frac{1}{12} K^2 \Psi^5 + 2\pi\rho\Psi^5 = 0$
- Density profile

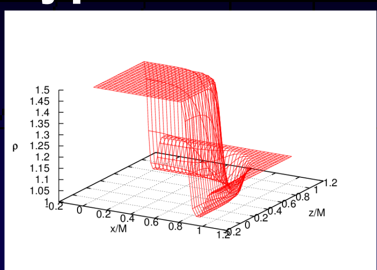

$\longrightarrow$ Random distribution of particles

JGRG25@Kyoto Chulmoon Yoo

17

Examples

◎Spherical vs Nonspherical (two examples)

- **Spherical**

  $w_x = w_y = w_z = 0.5L$

- **Nonspherical**

  $w_x = w_y = 0.7L, w_z = 0.5L$

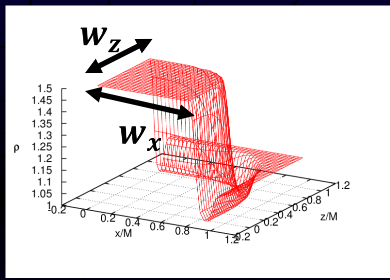

- **Horizon is formed in both cases**
- **Constraint violation at the time of horizon formation**
  →next slide

18

Constraint violation

◎Spherical vs Nonspherical

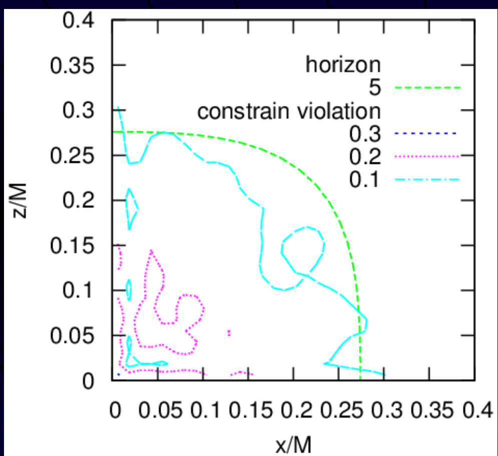

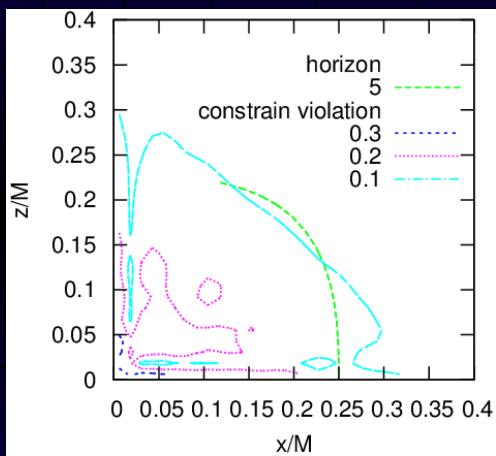

- **Horizon formation is harder for nonspherical cases…?**
- **What about curvature invariant…?**

19

To do list

◎More realistic initial data

- Based on approximate solutions in long-wavelength limit

◎Calculation of curvature invariant

◎Check the threshold for BH formation

◎....many others...

JGRG25@Kyoto Chulmoon Yoo

20

My Expectation

◎Non-spherical collapse is general

◎Curvature singularity appears before horizon formation

Naked singularity in the early universe!

◎Unknown high energy physics may take place there...(?)

GUT physics, stringy effects, quantum gravity etc

Thank you!

JGRG25@Kyoto Chulmoon Yoo

"Stationary bubbles and their tunneling channels toward trivial geometry"

by Guillem Domènech Fuertes

[JGRG25(2015)3a2]

Tunnelling of stationary bubbles and information loss paradox

Guillem Domènech

YITP, Kyoto University

in collaboration with: P. Chen, M. Sasaki, D. Yeom

guillem.domenech@yukawa.kyoto-u.ac.jp

December 8, JGRG, 京都

Information Loss Paradox

Long standing problem (already 40 years!)

- What is it?

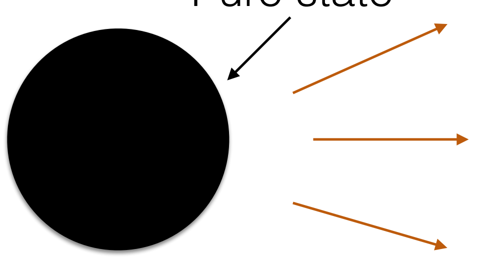

$$T \sim \frac{1}{M}$$

- It seems to me that it may well be due to a lack of Quantum Gravity. Why people keeps attacking it?

It may lead to some hints of quantum gravity.

Information Loss Paradox

Different (not yet definitive) solutions:

- Firewalls (Almheiri, Marolf, Polchinski & Sully +13)
- Black Hole Complementarity (Susskind +93)
- Regular black hole picture (A. Ashtekar & M. Bojowald +05). Planck size remnants.
- AdS/CFT
- Other universe inside a black hole (Yeom +09)
- Quantum entanglement (Horowitz +03)
- Effective loss of information (Maldacena +03, Hawking +05)

Effective Loss of Information

What is the idea behind? Euclidean Path Integrals

- Sum over all configurations

$$\langle \mathrm{out}|\Psi|\mathrm{in}\rangle = \int Dg\ D\psi_a\ \mathrm{e}^{\frac{i}{\hbar}S[g,\psi_a]}$$

- If there is one configuration with trivial topology, information is conserved (Maldacena 03, Hawking 05). A classical observer sees a definite geometry, therefore sees a loss of information.

- In practice, we need a semiclassical approximation. WKB approximation. $P \sim \mathrm{e}^{-S_E}$

- Goal: Build a concrete example. First, we need the thin-shell formalism…

Thin Shell (Spherical Symmetry)

Set up: Israel 1966

- Outside / Inside metric: (AdS)-Schwarzschild

$$ds_{\pm}^2 = -f_{\pm}(R)dT^2 + \frac{1}{f_{\pm}(R)}dR^2 + R^2 d\Omega^2 \qquad f_{\pm}(R) = 1 - \frac{2M_{\pm}}{R} + \frac{R^2}{\ell_{\pm}^2}$$

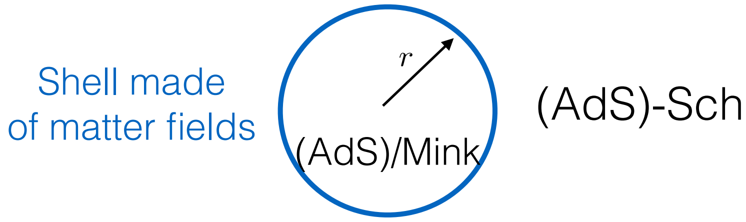

- Identifying the extra piece with a perfect fluid: EOM

$$\epsilon_- \sqrt{\dot{r}^2 + f_-(r)} - \epsilon_+ \sqrt{\dot{r}^2 + f_+(r)} = 4\pi r \sigma \qquad \sigma(r) = \frac{\sigma_0}{r^{2(1+w)}}$$

Parameters: $M_+ \, , \, \ell_{\pm} \, , \, \sigma \, , \, w = \lambda/\sigma$ (No singularity $M_- = 0$)

Luckily, there is a more intuitive way to look at it…

Effective potential

… we can treat it as a particle in 1-d with E=0!

$$\dot{r}^2 + V(r) \;=\; 0.$$

For a true vacuum bubble in AdS background with a constant tension it has a general shape:

(w=-1)

Sasaki & Yeom 14

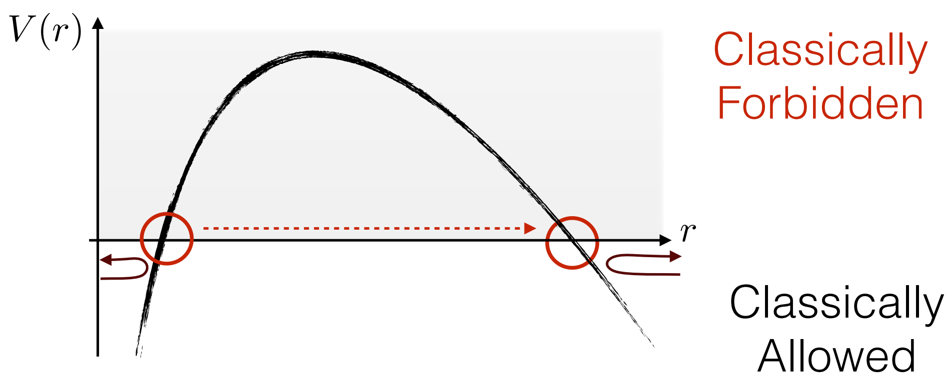

What about non-perturbative effects?

Thin-shell tunneling

Penrose diagram:

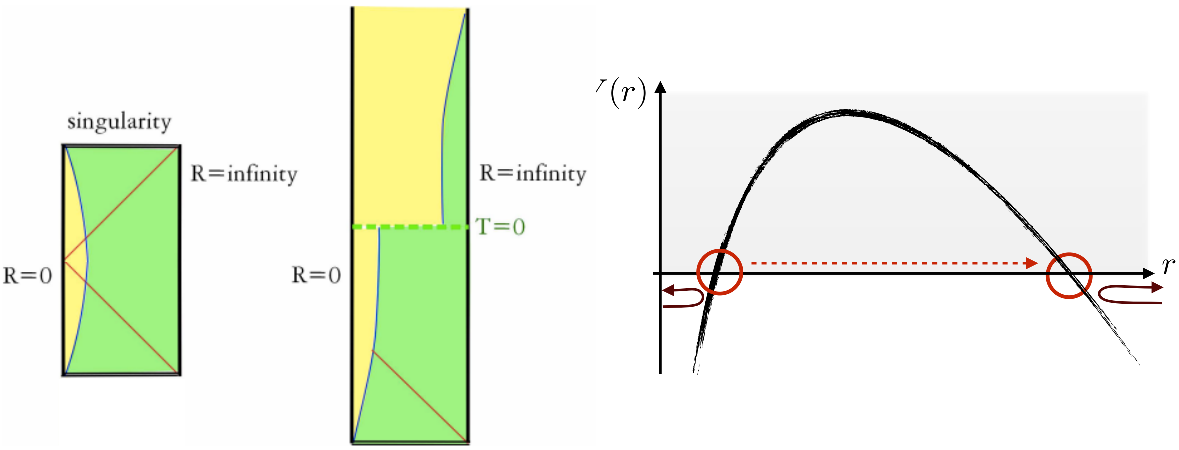

The shell can tunnel to expanding region, leaving nothing but trivial topology behind! Initial conditions?

Main points

We want a thin-shell that:

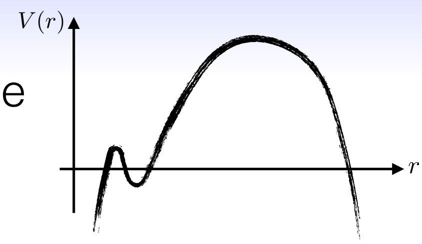

- Starts from a well-defined initial state
- Stationary and Stable
- Tunnels either into Black Hole or Expands to Infinity

We need 4 zeros in the potential.

What kind of physical situation?

- Last stages of star collapse: Stable system, suffers phase transition and forms a BH.
  Modify the tension. GD, Sasaki & Yeom 14

Modifying the tension (1)

Building the number of zeros: GD, Sasaki & Yeom 14

$$\sqrt{\cancel{\dot{r}^2} + f_-(r)} - \sqrt{\cancel{\dot{r}^2} + f_+(r)} = 4\pi r\sigma$$

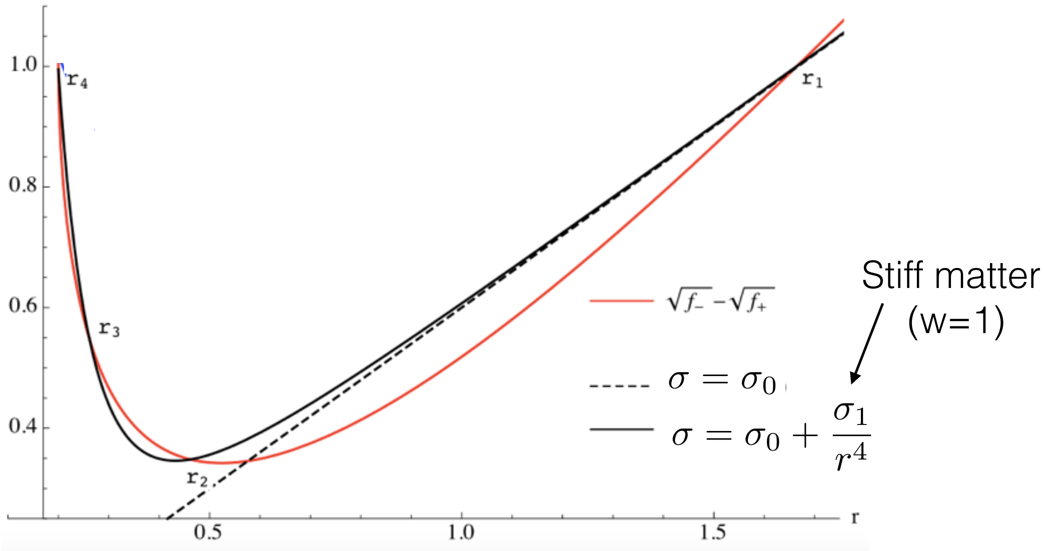

Modifying the tension (2)

It also works when in/out is Minkowsky, although we need to tune more the tension.

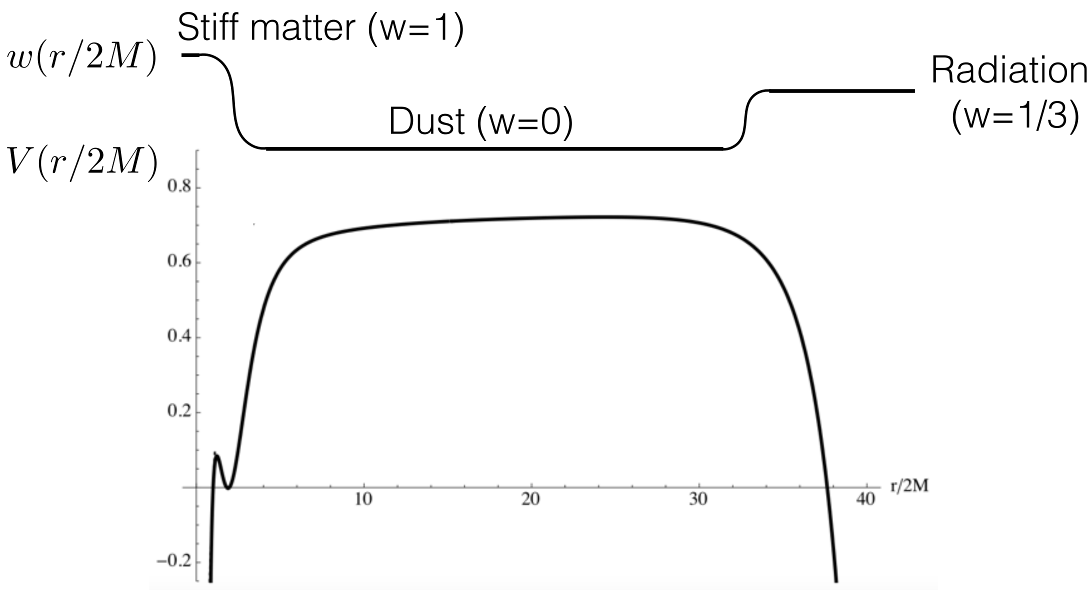

Implications

- A classically stable stationary thin-shell may tunnel, by quantum effects, into a black hole or expands to infinity.

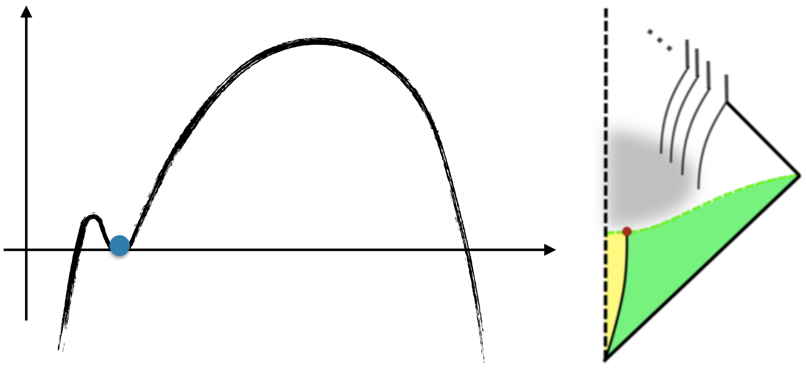

$$P \sim \mathrm{e}^{-a\frac{M^2}{M_{pl}^2}}$$

- There is no loss of information in terms of the wave function. There is always a history where the shell expands to infinity, although exponentially and planck mass suppressed.

Summary

- By modifying the tension (like star collapse) we built a stationary thin-shell which, by quantum effects, tunnels into a black hole or expands to infinity.

- In this example, there is no loss of information. However, a classical observer fins an effective loss of information.

- Effective loss of information (Euclidean Path Integrals) may solve the information loss paradox.

- However, there are still open issues: How general the solution is? How do we define expectation values?

Thank you!

Thin Shell

Israel 1966

Joining two geometries (solutions to Einstein equations)

1. Continuity of the metric:

$$g^{+}_{\alpha\beta} - g^{-}_{\alpha\beta} = [g_{\alpha\beta}] = 0$$

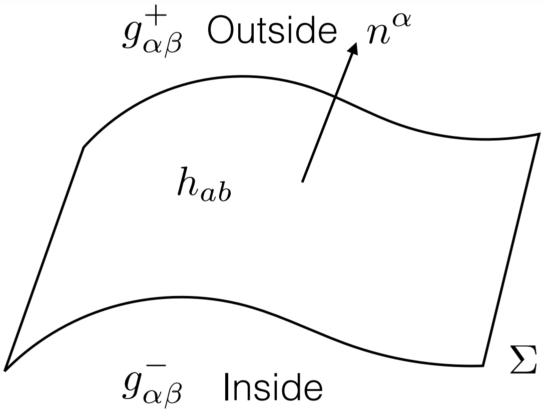

2. Einstein Equations?

$$G_{\mu\nu} = \kappa T_{\mu\nu} + S_{\mu\nu}\ \delta(\ell)$$

$$S_{ab} = \frac{1}{8\pi}\left([K_{ab}] - [K]\, h_{ab}\right)$$

3. Describes a thin-shell! Identify as Perfect Fluid:

$$S_{ab} = (\sigma + \lambda) u_a u_b + \lambda\ h_{ab}$$

Thin Shell (Spherical Symmetry)

Set up: Israel 1966

- Outside / Inside metric: (AdS)-Schwarzschild

$$ds^2_\pm = -f_\pm(R)dT^2 + \frac{1}{f_\pm(R)}dR^2 + R^2 d\Omega^2 \qquad f_\pm(R) = 1 - \frac{2M_\pm}{R} + \frac{R^2}{\ell^2_\pm}$$

- Intrinsic geometry thin-shell:

$$ds^2 = -dt^2 + r^2(t)d\Omega^2$$

- Identifying the extra piece with a perfect fluid: EOM

$$\epsilon_- \sqrt{\dot{r}^2 + f_-(r)} - \epsilon_+ \sqrt{\dot{r}^2 + f_+(r)} = 4\pi r \sigma \qquad \sigma(r) = \frac{\sigma_0}{r^{2(1+w)}}$$

Parameters: $M_+ \,,\, \ell_\pm \,,\, \sigma \,,\, w = \lambda/\sigma$ (No singularity $M_- = 0$)

Luckily, there is a more intuitive way to look at it…

Effective potential

… we can treat it as a particle in 1-d with E=0!

$t \to -i\tau$ $\qquad -\dot{r}^2 + V(r) = 0$ $\qquad$ Wick rotation

In AdS background with a constant tension it has a general shape: What about non-perturbative effects?

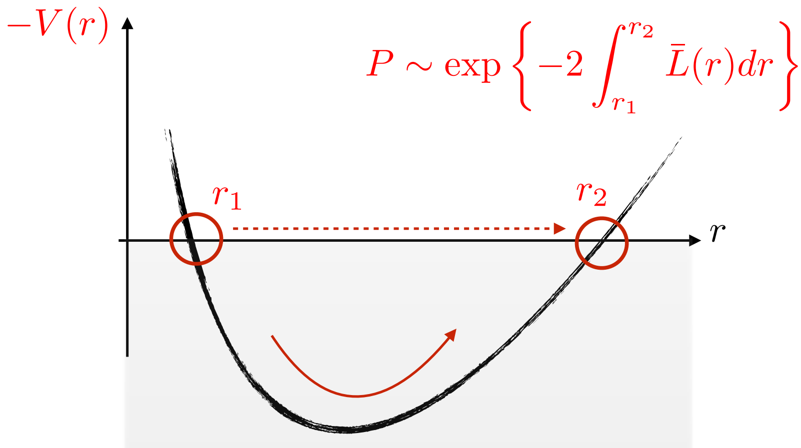

Minkowsky case

$$w(\bar{r}) = \begin{cases} \frac{1}{2}\tanh\left[\mu_1\left(\bar{r}_1 - \bar{r}\right)\right] + \frac{1}{2} & \bar{r} < \bar{r}_m \\ \frac{1}{6}\tanh\left[\mu_2\left(\bar{r} - \bar{r}_2\right)\right] + \frac{1}{6} & \bar{r} > \bar{r}_m \end{cases}$$

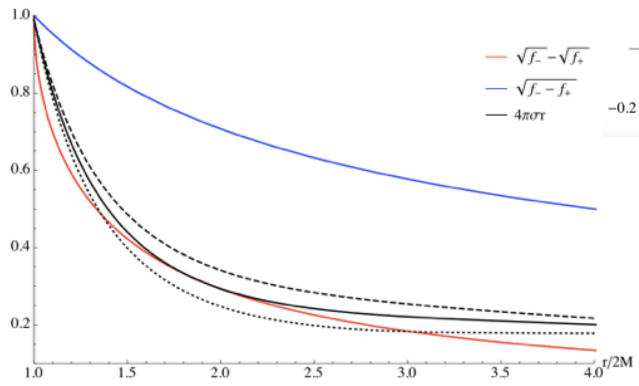

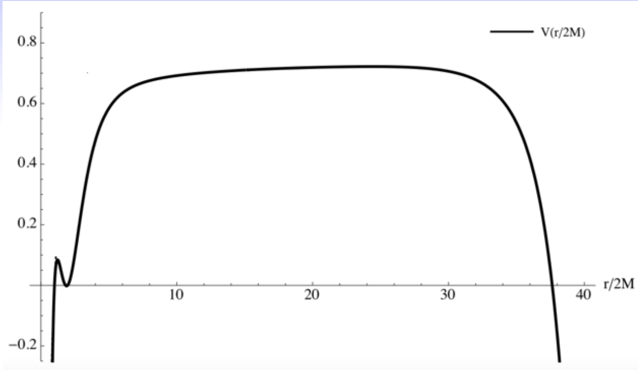

$$\frac{P_{\text{expand}}}{P_{\text{BH}}} \sim \mathrm{e}^{-27.1 M^2/M_{\text{Pl}}^2}$$

$$B_{\text{BH}} \approx 0.3\ M^2/M_{\text{Pl}}^2 \qquad \text{and} \qquad B_{\text{expand}} \approx 27.4\ M^2/M_{\text{Pl}}^2$$

“Gravitational Baryogenesis after Anisotropic Inflation”

by Mitsuhiro Fukushima

[JGRG25(2015)3a3]

3a3

Gravitational Baryogenesis after Anisotropic Inflation

The 25th Workshop on General Relativity and Gravitation in Japan
—Kyoto Univ. YITP—

Department of Physics, Waseda University,
Mitsuhiro FUKUSHIMA

Collaborators

Waseda Institute for Advanced Study, Waseda University,
Shuntaro MIZUNO

Department of Physics, Waseda University,
Kei-ichi MAEDA

Introduction – Gravitational Baryogenesis (GBG)

H.Davoudiasl, R.Kitano, G.D.Kribs, H.Murayama, P.J.Steinhardt (2004)

Inspired from supergravity

$$S_{\rm int} = \frac{1}{M_*^2}\int d^4x\sqrt{-g}\,\underline{(\partial_\mu R)\, J_B^\mu}$$

Expansion of the universe

Dynamically CPT violating interaction

R Ricci scalar curvature

J_B^μ Baryon current

M_* Cut-off mass scale

n_B Baryon number density

s Entropy density

Sakharov's criteria

1. Baryon number violation
2. C and CP violation
3. Departure from equilibrium

⟺ Baryogenesis in thermal equilibrium

Based on CPT invariance

Baryon asymmetry

$$Y_B \equiv \frac{n_B}{s} \propto \left.\frac{\dot{R}}{M_*^2 T}\right|_{T_D}$$

T_D Temperature at B-violation decouple

Introduction – Problem and Improvement of GBG

✓ Gravitational Baryogeneis cannot generate sufficient baryon asymmetry in the original form.

$$Y_{B,obs} \simeq 10^{-10}$$

Assumption

- Standard thermal history of the universe
- Low reheating temperature constrained by gravitino problem

$$T_{RD} \lesssim 10^9 \mathrm{GeV}$$

$$Y_B \propto \left. \frac{\dot{R}}{M_*^2 T} \right|_{T_D}$$

need some enhancement mechanisms $\dot{R} \nearrow$

➢ ***Anisotropic background metric can enhance baryon asymmetry***

Kh.Saaidi, H.Hossienkhani (2009); V.Fayaz, H.Hossienkhani (2013).

Assumption

- ✓ Bianchi Type I (anisotropic) background
- ✓ Isotropic matter fields → Their model can be used as long as anisotropy is sufficiently small
- Origin of anisotropy is not mentioned, thus the magnitude of it is unknown

From a realistic perspective, we check the possibility of Gravitational baryogenesis.

Anisotropic Inflationary model M.Watanabe, S.Kanno, J.Soda (2009).

Improvement by changing background metric

What changes can be expected within the anisotropic universe?

$$Y_B \propto \left. \frac{\dot{R}}{M_*^2 T} \right|_{T_D}$$

I. Increasing time derivative of Ricci scalar curvature

(Previous research)

flat FLRW

$$\dot{R} = -\sqrt{3}(1+w)(1-3w)\frac{\rho^{3/2}}{M_{pl}^3}$$

$p = w\rho$ EoS parameter

Bianchi Type I metric

$$ds^2 = -dt^2 + A(t)^2 dx^2 + B(t)^2 dy^2 + C(t)^2 dz^2$$

Shear scalar

$$\Sigma^2 = \frac{1}{6}\left[\left(\frac{\dot{A}}{A}\right)^2 + \left(\frac{\dot{B}}{B}\right)^2 + \left(\frac{\dot{C}}{C}\right)^2\right] - \frac{1}{2}H^2$$

$$\dot{R} = -\sqrt{3}(1+w)(1-3w)\frac{\rho}{M_{pl}^3}\sqrt{\rho + \boxed{3M_{pl}^2\Sigma^2}}$$

(isotropic matter field case)

II. Increasing decoupling temperature of B-violating interaction

Improvement by changing background metric

What changes can be expected within the anisotropic universe?

I. Increasing time derivative of Ricci scalar curvature

II. Increasing decoupling temperature of B-violating interaction

Decoupling Temperature

- B-violating interaction $\mathcal{O}_B$ (mass dimension $D = 4 + n$ operator) $n > 0$

→ Reaction rate $\Gamma_B = \dfrac{T^{2n+1}}{M_B^{2n}}$ M_B mass scale of $\mathcal{O}_B$

Decouple occurs at $H \gtrsim \Gamma_B$

Friedmann Eq.

$$H^2 = \Sigma^2 + \frac{1}{3M_{pl}^2}\rho \sim \Sigma^2 + \frac{T^4}{M_{pl}^2}$$

$$Y_B \approx \frac{T_D^6}{M_*^2 M_{pl}^3 T_{RD}} \quad \text{Reheating}$$

(decoupling time)

$$Y_B \approx (1-3w)\frac{T_D^5}{M_*^2 M_{pl}^3} \quad \text{RD}$$

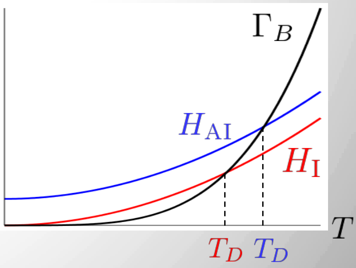

→ Both two effects enhance baryon asymmetry

Model Setting – Anisotropic Inflation

M.Watanabe, S.Kanno, J.Soda (2009).

Based on context of supergravity

Coupling inflaton with vector field

$$\mathcal{S} = \int d^4x\sqrt{-g}\left[\frac{M_{pl}^2}{2}R - \frac{1}{2}(\partial_\mu\phi)(\partial^\mu\phi) - V(\phi) \boxed{- \frac{1}{4}f(\phi)^2 F_{\mu\nu}F^{\mu\nu}}\right]$$

gauge kinetic function

$$f(\phi) = \exp\left[\frac{2c}{M_{pl}^2}\int\frac{V}{V_\phi}d\phi\right]$$

$$c > 1$$

c Inflaton-vector coupling parameter

Anisotropic matter field $A_\mu dx^\mu = v(t)dx$

→ The anisotropic hair in the inflationary universe can exist.
There is an attractor solution of the stable anisotropic inflation model.

Ansatz: ***Axial symmetric Bianchi Type I metric***

$$ds^2 = -dt^2 + e^{2\alpha}\left[e^{-4\beta}dx^2 + e^{2\beta}\left(dy^2 + dz^2\right)\right]$$

$H = \dot{\alpha}$ Hubble parameter $\boxed{\Sigma = \dot{\beta}}$ Shear parameter

Basic Equations (Anisotropic Inflation Model)

Ex) $V = \frac{1}{2} m^2 \phi^2$ chaotic inflation model

$$\rho_m = \rho_\phi + \rho_v$$
$$p_m = w \rho_m$$

Basic equations

$$H^2 = \Sigma^2 + \frac{1}{3M_{pl}^2} \rho_m$$

$$\dot{\Sigma} = -3H\Sigma + \frac{1}{M_{pl}^2} \Delta p_v$$

$$\dot{\rho}_\phi + 3H(\rho_\phi + p_\phi) = -\Gamma_v \rho_v$$

$$\dot{\rho}_v + \underbrace{3H\rho_v\left(\frac{4}{3} + \frac{4\Sigma}{3H}\right)}_{3H\rho_v + H_i p_v^i} = \Gamma_v \rho_v$$

$$\Gamma_v \equiv \frac{2c}{M_{pl}^2} \phi \dot{\phi}$$

$$\rho_\phi = \frac{1}{2}\dot{\phi}^2 + \frac{1}{2} m^2 \phi^2$$
$$\rho_v = \frac{\dot{v}^2}{2} f^2 e^{-2\alpha + 4\sigma}$$

$$\bar{p}_v \equiv \frac{1}{3}(p_v^x + p_v^y + p_v^z) = \frac{1}{3}\rho_v$$
$$\Delta p_v \equiv p_v^y - \bar{p}_v = \frac{2}{3}\rho_v$$
$$-p_v^x = p_v^y = p_v^z = \rho_v$$

Evolution of Anisotropy: Σ/H

$$f(\phi) = \exp\left[\frac{c}{2M_{pl}^2}\phi^2\right]$$

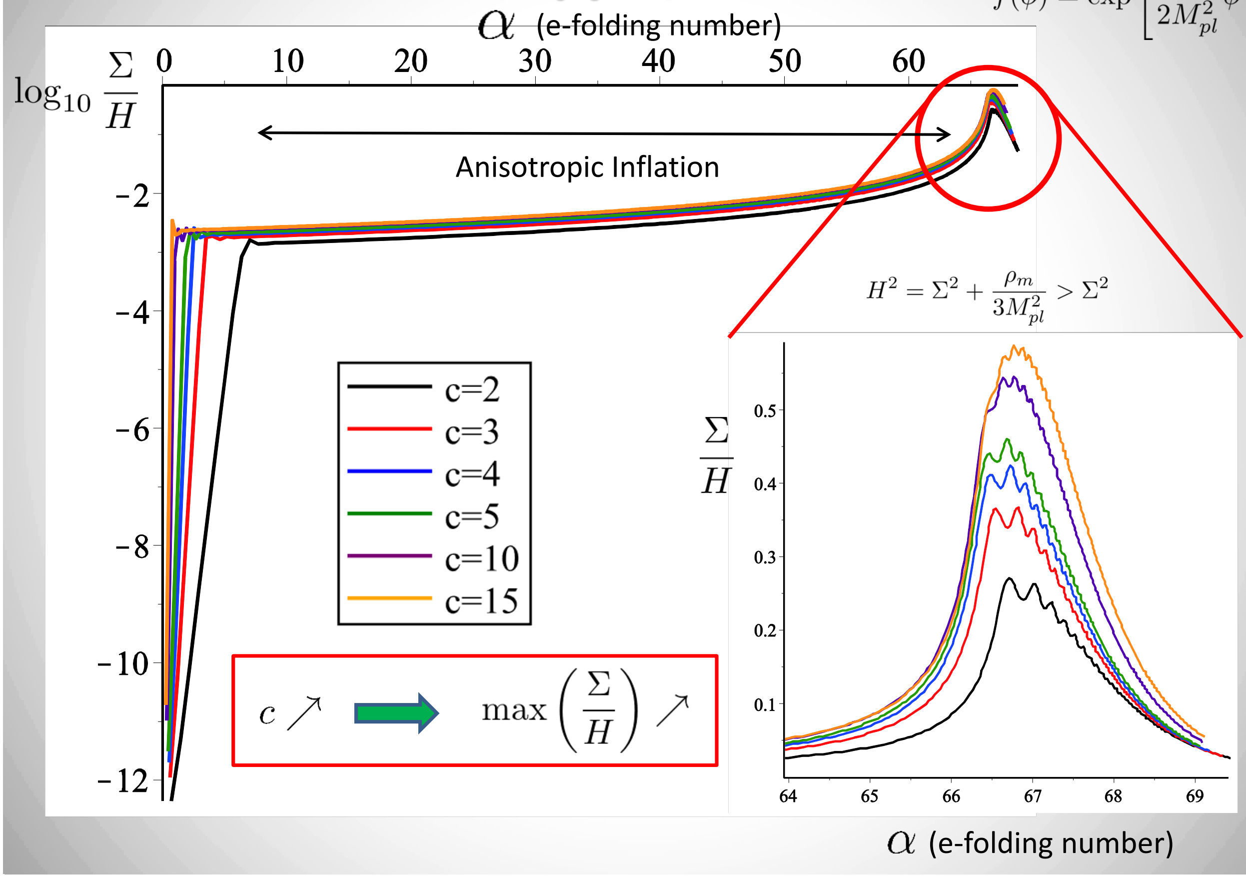

Calculation of Ricci Scalar in Anisotropic Universe

$$R = 6\dot{H} + 12H^2 + 6\Sigma^2 = 3(1-3w)(H^2 - \Sigma^2)$$

$$Y_B \propto \left.\frac{\dot{R}}{M_*^2 T}\right|_{T_D}$$

$$H^2 = \Sigma^2 + \frac{1}{3M_{pl}^2}\rho_m$$

$$\dot{H} = -3\Sigma^2 - \frac{1}{2M_{pl}^2}(1+w)\rho_m$$

$$\dot{\Sigma} = -3H\Sigma + \frac{1}{M_{pl}^2}\Delta p_v$$

Derive $\dot{R}$ with including effect of anisotropic matter field

Enhancement by shear term

$$\dot{R} = -\frac{\sqrt{3}}{M_{pl}^3}(1-3w)(1+w)\rho_m\sqrt{\rho_m \boxed{+ 3M_{pl}^2\Sigma^2}} - \frac{6}{M_{pl}^2}(1-3w)\boxed{\Delta p_v \Sigma} - \frac{3}{M_{pl}^2}\rho_m \boxed{\dot{w}}$$

FLRW universe

$$\dot{R} = -\sqrt{3}(1+w)(1-3w)\frac{\rho^{3/2}}{M_{pl}^3}$$

Effect of shear evolution by anisotropic vector pressure

Effect of dominant matter changing

Calculation of $\dot{R}$ during Reheating phase

Assumption

- B-violation decouple occurs during reheating phase ↔ Radiation Dominant phase
- Gradual reheating ← In order to survive anisotropic components
- Radiations are created from only inflaton

$$\dot{\rho}_v + 3H\rho_v\left(\frac{4}{3} + \frac{4\Sigma}{3H}\right) = \Gamma_v \rho_v$$

$$\dot{\rho}_r + (4-3\varepsilon)H\rho_r = \Gamma_\phi \rho_\phi$$

$$\dot{\rho}_\phi + 3H\rho_\phi = -\Gamma_v\rho_v - \Gamma_\phi\rho_\phi$$

Trace anomaly

$$w_r = \frac{1}{3} - \varepsilon$$

$$\Gamma_v \equiv \frac{2c}{M_{pl}^2}\phi\dot{\phi} \to 0$$ neglectable in this phase

$$\dot{R} = -\frac{\sqrt{3}}{M_{pl}^3}(1-3w)(1+w)\rho_m\sqrt{\rho_m + 3M_{pl}^2\Sigma^2} - \frac{6}{M_{pl}^2}(1-3w)\Delta p_v\Sigma - \frac{3}{M_{pl}^2}\rho_m\dot{w}$$

Partially cancel

$\dot{w}$

$$w \equiv \frac{p_m}{\rho_m} = \frac{p_\phi + \bar{p}_v + p_r}{\rho_\phi + \rho_v + \rho_r} = \frac{1}{3}\frac{\rho_v + (1-3\varepsilon)\rho_r}{\rho_\phi + \rho_v + \rho_r}$$

$\dot{R}$ at reheating phase

$$\boxed{\dot{R} = -\sqrt{3}\frac{\rho_\phi\sqrt{\rho_m + 3M_{pl}^2\Sigma^2}}{M_{pl}^3} - \frac{\Gamma_\phi\rho_\phi}{M_{pl}^2}} + \varepsilon\left[-4\sqrt{3}\frac{\rho_r\sqrt{\rho_m + 3M_{pl}^2\Sigma^2}}{M_{pl}^3} + 3\frac{\Gamma_\phi\rho_\phi}{M_{pl}^2}\right]$$

Generated baryon asymmetry: Reheating case

Ex) dim.6-operators, reheating

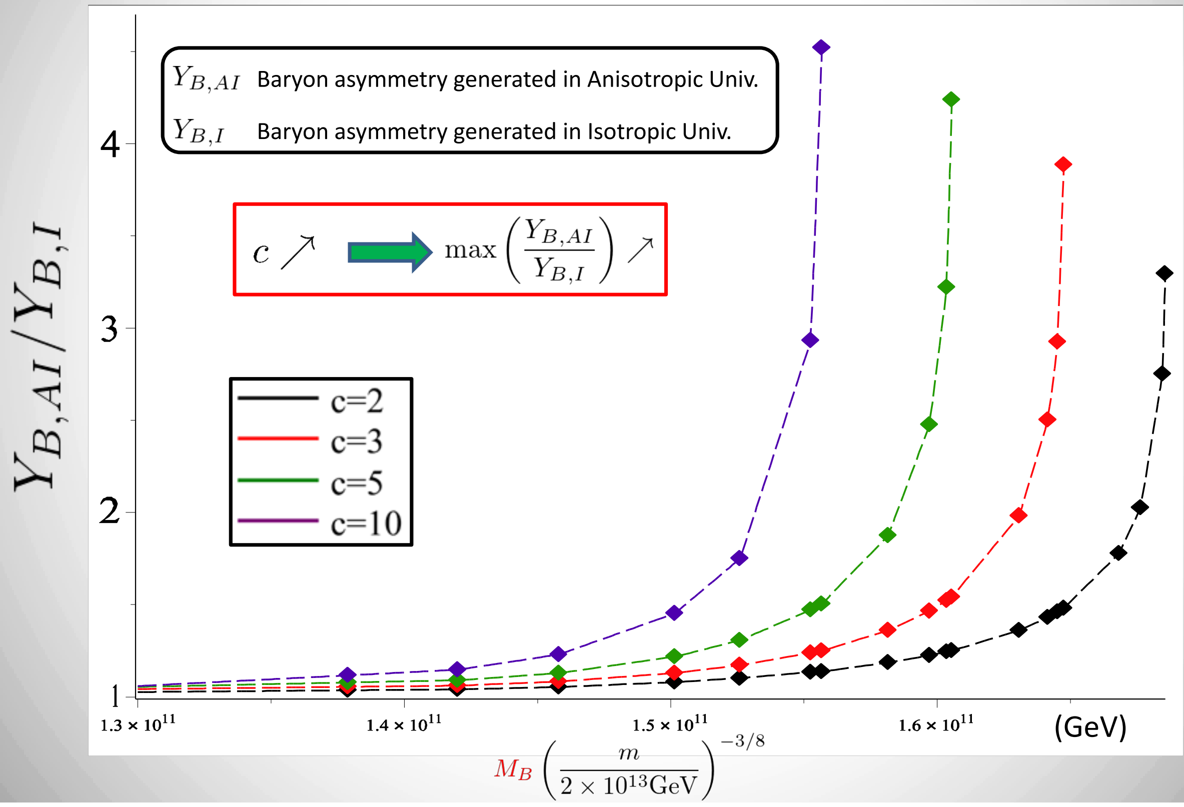

Can anisotropic universe generate sufficient baryon asymmetry?

(Regardless of the observational constraint on parameter c)

✓ From previous slide, the difference of generated baryon asymmetry between aniso-/isotropic Universe is only $\mathcal{O}(1)$.

$M_* \lesssim$ LHC scale ← (FLRW case)

problematic

$Y_B \propto M_*^{-2}$

→ $\mathcal{O}(1)$ enhancement is too small

FLRW, dim.6-operators, reheating

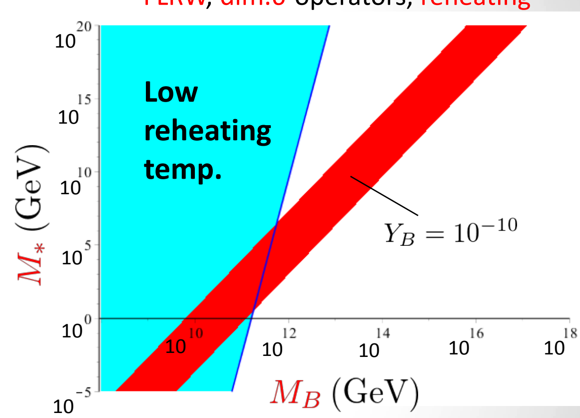

✓ From anisotropic inflation model, the shear of the universe can grow up to comparable level with the matter fields. (Even if c is very large)

$$\boxed{\frac{\Sigma}{H}(t_e) \simeq \sqrt{\frac{3c-1}{21c-3}}} \qquad H^2 = \Sigma^2 + \frac{1}{3M_{pl}^2}\rho_m$$

→ The enhancement is much less than the requirement.

Constraint on coupling parameter c

Statistical Anisotropy in Curvature perturbation

$$P(\mathbf{k}) = P(k)\left[1 + h_*(\hat{\mathbf{k}}\cdot\hat{\mathbf{v}})\right]$$

Analytical Prediction

M.Watanabe, S.Kanno, J.Soda (2010)

$$h_* = 24\left(1-\frac{1}{c}\right)N_k^2$$

Observational Result

J.Kim, E.Komatsu (2013)

$$h_* = 0.002 \pm 0.016 \ (68\%\mathrm{CL})$$

(Planck 2013)

$$1-\frac{1}{c} \lesssim 10^{-7}\times\left(\frac{|h_*|}{10^{-2}}\right)\left(\frac{N_k}{60}\right)^{-2} \qquad \boxed{c\approx 1}$$

Anisotropy of the universe during inflationary phase is strongly restricted to be small.

Summary

- ✓ Gravitational baryogenesis cannot generate sufficient baryon asymmetry within the low reheating temperature which is constrained from gravitino problem.

But…

- ✓ Anisotropic background metric can enhance generated baryon asymmetry.
  (through increasing $\dot{R}$ and T_D)

Anisotropic inflation

- ✓ Anisotropy of the Universe exponentially grows at the end of inflation.

- ✓ Generated baryon asymmetry Y_B increases with large c (large anisotropy).

But…

- ✓ In this model, the amount of baryon asymmetry Y_B can be enlarged at most $\mathcal{O}(1)$.
- ✓ Moreover, anisotropy is strongly restricted to be small from CMB observation.

⟹ Expectable enhancement is too small to solve above problem.

Appendix

Original research

H.Davoudiasl, R.Kitano, G.D.Kribs, H.Murayama, P.J.Steinhardt (2004).

$$Y_B \approx \frac{T_{\rm RD}^5}{M_*^2 M_{pl}^3}\left(\frac{M_B^{2n}}{M_{pl}T_{\rm RD}^{2n-1}}\right)^{(9w+7)/(4n-3w-1)}$$

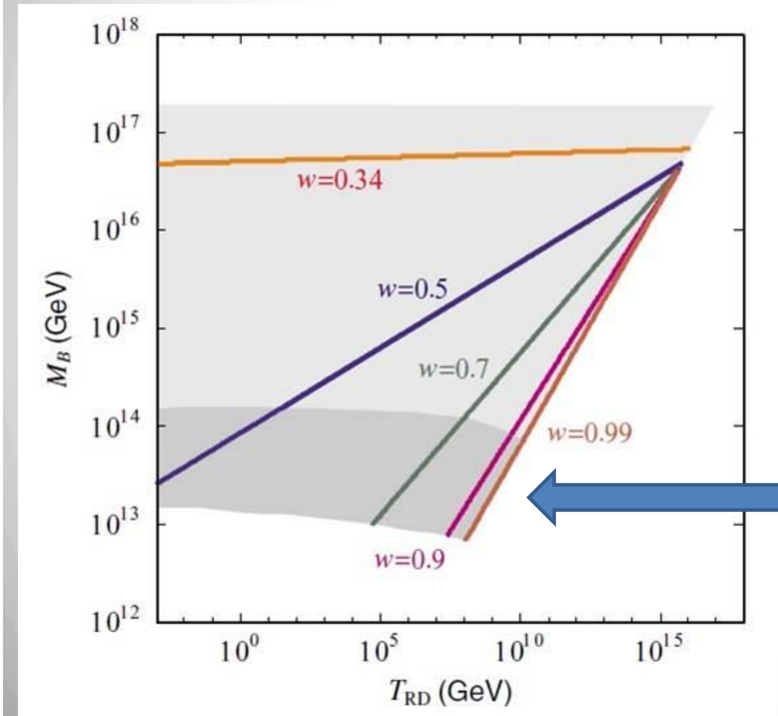

T_{RD} Reheating temperature

M_B mass scale associated with B-violating interaction

w Equation of State parameter

$$p = w\rho$$

$w > 1/3$ "Strange" matter dominant

Allowed region
restricted by gravitino problem

Generated baryon asymmetry by Gravitational Baryogenesis

$$S_{\text{int}} = \frac{1}{M_*^2}\int d^4x\sqrt{-g}\,(\partial_\mu R)\,J_B^\mu \xrightarrow{\text{CP odd}}$$

Difference energy shift

$$\Delta E_i(t) = \frac{\dot{R}(t)}{M_*^2}b_i \equiv V_0(t)b_i$$

$$\mu_b = -\mu_{\bar{b}}$$

Baryon number density

$$n_B(t) = \sum_i b_i g_{b_i}\int \frac{4\pi p^2 dp}{(2\pi)^3}\left[\exp\left(\frac{\sqrt{p^2+m_i^2}+b_iV_0(t)}{T(t)}\right)\mp 1\right]^{-1}$$

b_i baryon number

g_{b_i} spin states

One fermionic baryon

asymmetry is frozen when B-violating interaction is decoupled

$$n_B(t) \simeq -\left.\frac{g_b\dot{R}(t)}{6M_*^2}T^2(t)\right|_{t=t_D}$$

T_D Temperature at B-violation decouple

$$s = \frac{2\pi^2 g_*}{45}T^3$$

$$Y_B \simeq -\frac{15g_b}{4\pi^2 g_*}\left.\frac{\dot{R}}{M_*^2T}\right|_{T_D} \propto \left.\frac{\dot{R}}{M_*^2T}\right|_{T_D}$$

Generated Baryon asymmetry

observable $Y_{B,obs} \simeq 10^{-10}$

Gravitino problem

$$T_{RD} \lesssim 10^9\,\text{GeV}$$

Ex2) dim.6-operators, radiation dominant

$$Y_B \simeq (1-3w)\frac{M_B^{20/3}}{M_*^2 M_{pl}^{14/3}}$$

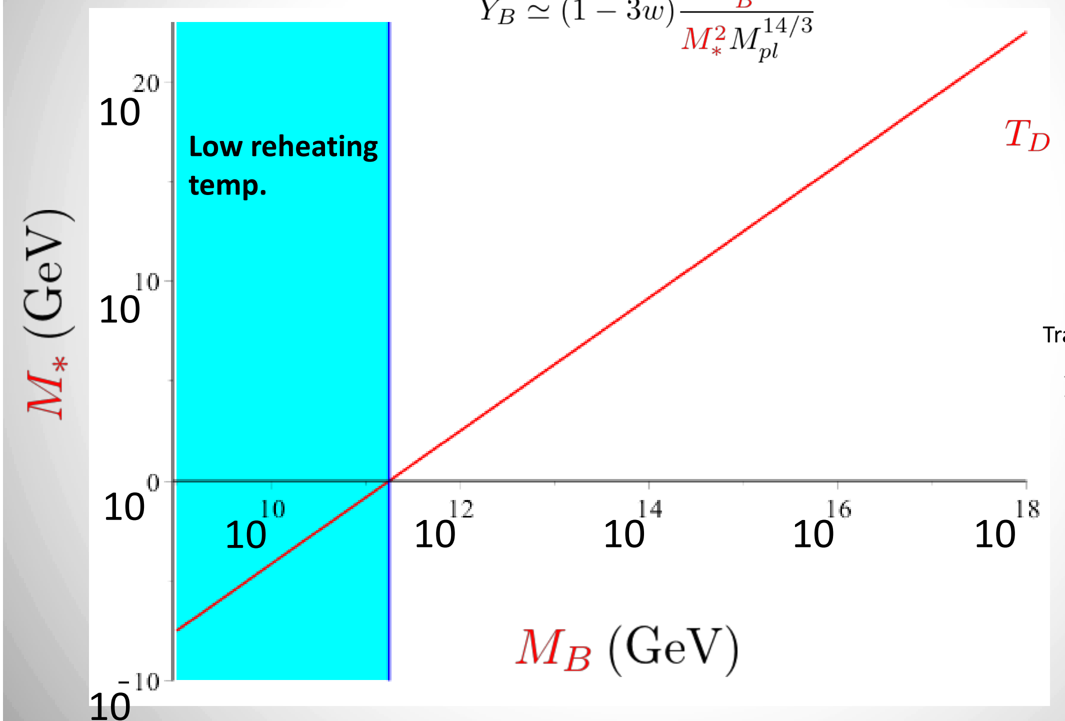

$$T_D < T_{RD} < M_I$$

Trace anomaly

$$1-3w \simeq 10^{-1}$$

$$T_D \simeq \frac{M_B^{4/3}}{M_{pl}^{1/3}}$$

Enhanced baryon asymmetry by huge shear $\rho \ll 3M_{pl}\Sigma^2$

Ex) dim.6-operators, radiation dominant

$$Y_B \approx (1-3w)\frac{\Sigma^{8/5}M_B^{12/5}}{M_*^2 M_{pl}^2}$$

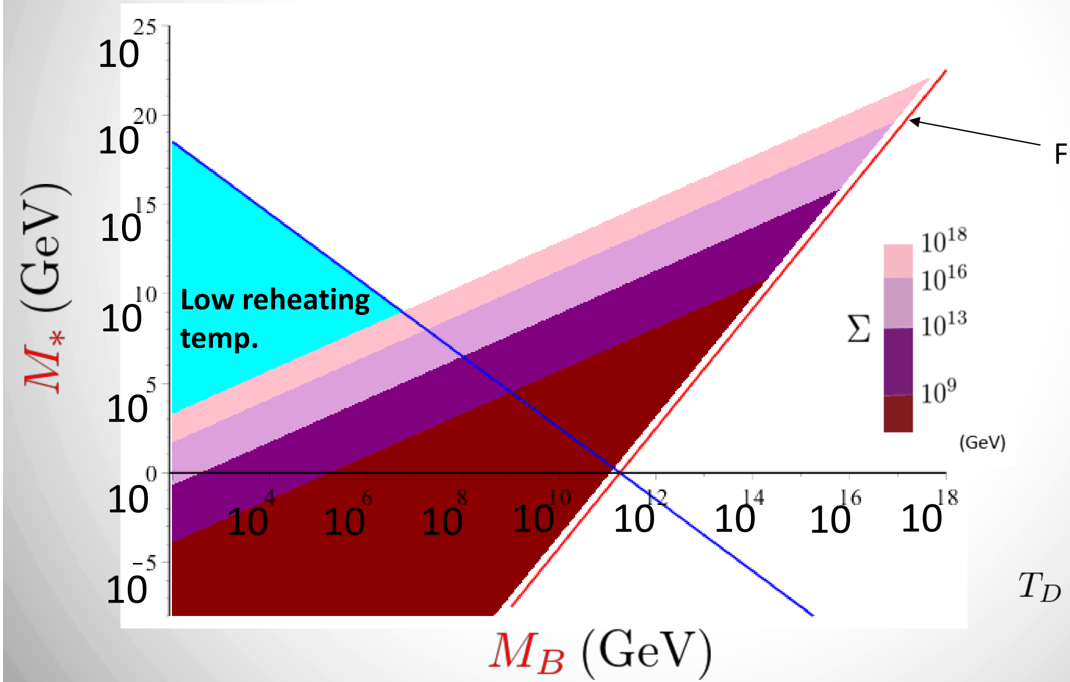

$$T_D \simeq \Sigma^{1/5}M_B^{4/5}$$

Maximum value of Anisotropy -c dependence-

Slow-roll parameter

$$\epsilon_H \equiv -\frac{\dot{H}}{H^2} = \frac{18M_{pl}^2\Sigma^2 + 3(1+w)\rho_m}{6M_{pl}^2\Sigma^2 + 2\rho_m}$$

$\epsilon_H(t_e) = 1$ Accelerating expansion end

During accelerating expansion

$$0 < \Sigma^2 < -\frac{1}{12M_{pl}^2}(1+3w)\rho_m$$

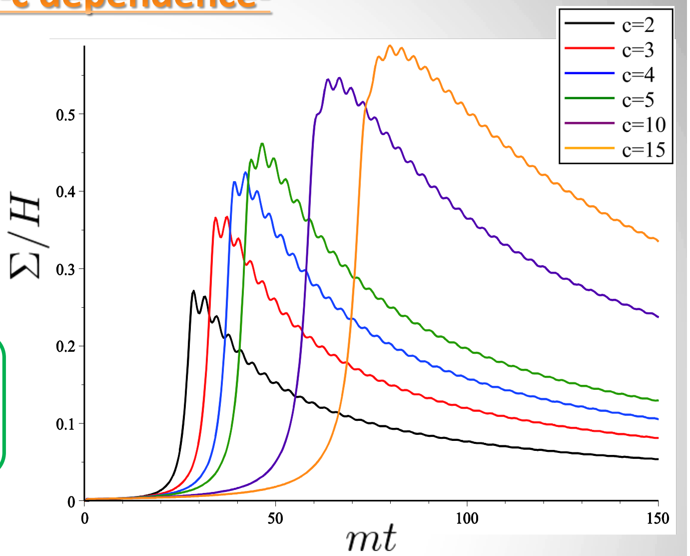

Anisotropy

$$\frac{\Sigma}{H} = \sqrt{\frac{\Sigma^2}{\Sigma^2 + \frac{1}{3M_{pl}^2}\rho_m}} < \sqrt{-\frac{1+3w}{3(1-w)}} \xrightarrow{-1<w<-1/3} 0 < \frac{\Sigma}{H} < \frac{1}{\sqrt{3}}$$

Using first-order approximation: $w(t_e) \equiv \frac{p_\phi + \bar{p}_v}{\rho_\phi + \rho_v} \simeq -\frac{5c-1}{9c-1}$ $\Rightarrow$ $\boxed{\frac{\Sigma}{H}(t_e) \simeq \sqrt{\frac{3c-1}{21c-3}}}$

During Inflation (First-order Approximation)

$H(t) \simeq -\frac{m^2}{3c}t + H_0$ $\Delta p_v \simeq \frac{c-1}{3c^2}m^2M_{pl}^2$ $\phi(t) \simeq -\frac{\sqrt{6}mM_{pl}}{3c}t + \frac{\sqrt{6}M_{pl}}{m}H_0$

Anisotropy increases with large c

Maximum value of Anisotropy -c dependence-

Anisotropy

$$\frac{\Sigma}{H} = \sqrt{\frac{\Sigma^2}{\Sigma^2 + \frac{1}{3M_{pl}^2}\rho_m}} < \sqrt{-\frac{1+3w}{3(1-w)}} \xrightarrow{-1<w<-1/3} 0 < \frac{\Sigma}{H} < \frac{1}{\sqrt{3}}$$

$$w = \frac{p_\phi + \bar{p}_v}{\rho_\phi + \rho_v} = \frac{3w_\phi + r_v}{3 + 3r_v} \qquad t_e = \frac{3cH_0}{m^2} - \frac{\sqrt{3c}}{m} \qquad \rho_\phi(t_e) = \frac{1+3c}{3c^2}m^2 M_p^2$$

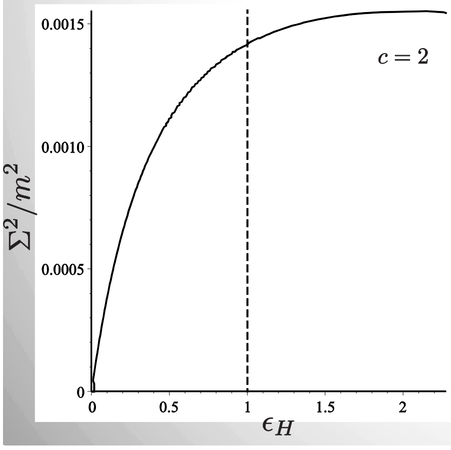

$$w_\phi = \frac{1-3c}{1+3c} \qquad r_v = \frac{3}{2}\frac{c-1}{1+3c}$$

$$w(t_e) \equiv \frac{p_\phi + \bar{p}_v}{\rho_\phi + \rho_v} \simeq -\frac{5c-1}{9c-1} \Rightarrow \boxed{\frac{\Sigma}{H}(t_e) \simeq \sqrt{\frac{3c-1}{21c-3}}}$$

Anisotropy increases with large c

Generated baryon asymmetry: Radiation Dominated case

Ex2) dim.6-operators, radiation dominant

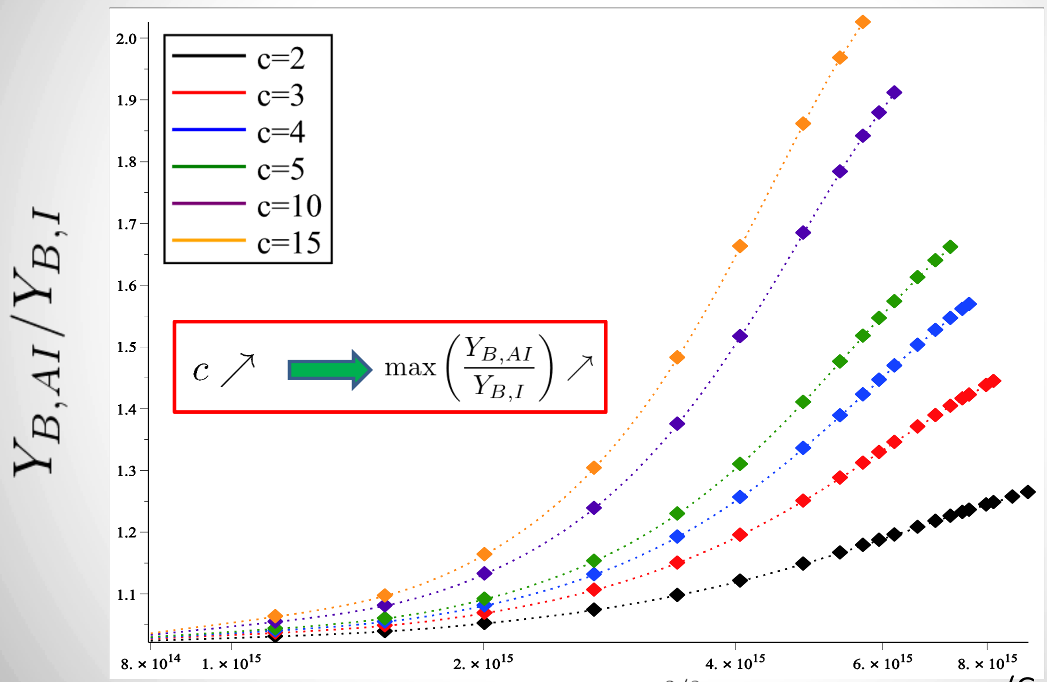

$$M_B\left(\frac{m}{2\times 10^{13}\text{GeV}}\right)^{-3/8} \text{ (GeV)}$$

“Fermionic Schwinger current in 4-d de Sitter spacetime”

by Takahiro Hayashinaka

[JGRG25(2015)3a4]

Fermionic Schwinger current in 4-d de Sitter spacetime

Takahiro Hayashinaka (RESCEU, Univ. Tokyo)
Work in preparation with :
Tomohiro Fujita (Stanford), Jun'ichi Yokoyama (RESCEU)

8, Dec. JGRG25 in kyoto

Outline

- Background
  - Large scale magnetic field and magnetogenesis
- Models for magnetogenesis
- Schwinger effect in de Sitter space
  - E.o.m. in gravitational/electric background field
  - Renormalized VEV of current operator
- Summary

Magnetic field in our universe

- There are magnetic fields in every scales (stellar - extragalactic).
- Extragalactic (or cosmological) magnetic fields were found (A. Neronov, I. Vovk, Science, 328, 73 (2010)).
- The strength of this cosmological magnetic fields is very low, but they got lower limit $|B_k| \geq 10^{-20\,\sim\,-18}$ for $k \sim 1\mathrm{Mpc}^{-1}$.
- The origin is still unknown.

Magnetogenesis

- Inflationary generation of the seed magnetic fields.
- Produced from quantum fluctuation in the early universe
- In the FLRW universe, B scales as $|B_k| \propto a^{-2}$.

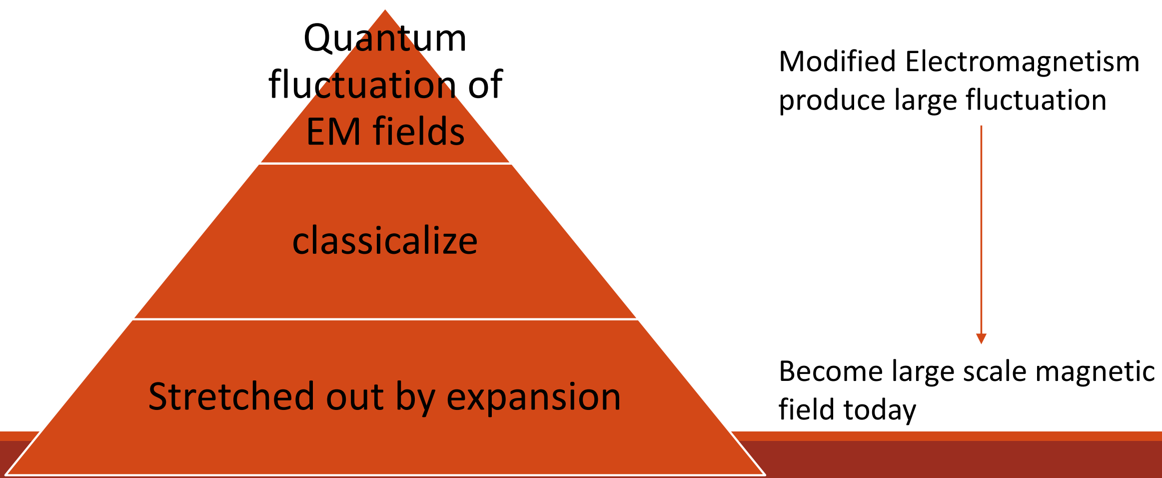

Why modified EM?

- Usual EM action has the conformal invariance
- Work in de Sitter spacetime ($g_{\mu\nu} = a^2\eta_{\mu\nu}$)

$$\mathcal{L} = -\frac{1}{4}\eta^{\mu\alpha}\eta^{\nu\beta}F_{\mu\nu}F_{\alpha\beta} \longrightarrow -\frac{1}{4}\sqrt{-g}g^{\mu\alpha}g^{\nu\beta}F_{\mu\nu}F_{\alpha\beta} = -\frac{1}{4}\eta^{\mu\alpha}\eta^{\nu\beta}F_{\mu\nu}F_{\alpha\beta}$$

- Nothing happens!
- We have to break the conformal invariance by hand

Model for magnetogenesis

- Conformal invariance
  - No electromagnetic field generation occurs
- Conformal invariance breaking model
  - fFF(IFF) model
    - Coupling between a scalar (not necessary inflaton) and EM kinetic term
    - = Model with time-dependent effective coupling
    - We assume the scalar field depends only on the conformal time

$$\mathcal{L} \supset -\frac{1}{4}g^{\mu\alpha}g^{\nu\beta}\underline{f^2(\eta)}F_{\mu\nu}F_{\alpha\beta} \qquad f(\eta) = f_0\left(\frac{a}{a_f}\right)^{\alpha}$$

Canonical variables

Effective coupling constant

Effective coupling

- fFF model has a time-dependent effective coupling

$$D_\mu = \partial_\mu + ieA_\mu = \partial_\mu + i(e/f)(fA_\mu)$$

$f \propto (a/a_f)^\alpha$

- When $\alpha > 0$, e/f is large in the early time.
  - =strong coupling
- When $\alpha < 0$, e/f is small in the early time.
  - =weak coupling

J. Martin, J. Yokoyama, JCAP 01 025 (2008)

Problem of the fFF model

- Strong coupling region
  → calculation is not reliable.
- Weak coupling region
  → produce electric field too much, not magnetic field
  Called "backreaction problem" because it breaks the inflation.
  V. Demozzi, V. Mukhanov, H. Rubinstein, JCAP 08, 025 (2009)
- However, Schwinger effect (charged particle production) may be effective when the strong electric field exists.

Schwinger Effect

- One of the non-perturbative QED effect
  - Strong backgraound fields can produce particles from vacuum.
- Schwinger's original discussion (1951)
  - Determine the effective lagrangian (EH Lagrangian) from QED action.

$$\mathcal{L} = -\mathcal{F} - \frac{1}{8\pi^2}\int_0^\infty \frac{\mathrm{d}s}{s^3}\mathrm{e}^{-m^2 s}\left[(es)^2 \frac{\Re\cosh(es\sqrt{2(\mathcal{F}+i\mathcal{G})})}{\Im\cosh(es\sqrt{2(\mathcal{F}+i\mathcal{G})})} - \frac{2}{3}(es)^2\mathcal{F} - 1\right]$$

$$\left(\ \mathcal{F} \equiv \frac{1}{2}(\boldsymbol{B}^2 - \boldsymbol{E}^2),\ \mathcal{G} \equiv \boldsymbol{E}\cdot\boldsymbol{B}\ \right)$$

  - Imaginary part of the effective action occurs.

Effective action

$$\mathrm{e}^{i\Gamma} = \langle 0; \text{final} | 0; \text{initial} \rangle$$

Physics of particle production (in Minkowski)

Electric field Energy $eEd \sim \dfrac{eE}{m} \sim m$ Particle energy

(Compton wave length $d = \dfrac{1}{m}$)

Typical strength scale of particle production is given by

$$eE_{\mathrm{Sch}} \sim m^2$$

Induced Current

- The produced particles run along the electric background field, then the electrical current is induced.
- We consider following analytic case

Dirac eq.

$$(i\gamma^a \partial_a - eA_a\gamma^a - ma)\xi(\eta, \boldsymbol{x}) = 0.$$

Background field

$$A_z = -\frac{E}{H}a(\eta) = \frac{E}{H^2\eta}$$

Induced current

$$e\left\langle 0 \left| \hat{\bar{\xi}}\gamma^3\hat{\xi} \right| 0 \right\rangle = -e\int \frac{\mathrm{d}^3k}{(2\pi)^3} \sum_{s=1,2} v^\dagger_{\boldsymbol{k},s}\gamma^0\gamma^3 v_{\boldsymbol{k},s}.$$

Adiabatic subtraction

- Solution of the Dirac eq.

$$\hat{\xi}(\eta, \boldsymbol{x}) = \mathrm{e}^{-iHLz}\int \frac{\mathrm{d}^3k}{(2\pi)^3} \sum_{s=1,2}\left[\hat{b}_{\boldsymbol{k},s}u_{\boldsymbol{k},s}(\eta)\mathrm{e}^{i\boldsymbol{k}\cdot\boldsymbol{x}} + \hat{d}^\dagger_{\boldsymbol{k},s}v_{-\boldsymbol{k},s}(\eta)\mathrm{e}^{-i\boldsymbol{k}\cdot\boldsymbol{x}}\right]$$

is used to evaluate the VEV of the induced current and this is indeed (UV-) divergent. To renormalize it, we subtract the adiabatic expansion (also known as WKB exoansion) of the quantity.

WKB solution for Fermion

- e.o.m. for the mode function (KG type equation for the Dirac) is given by

$$\left(\hbar^2\partial_\eta^2 + \omega_k^2(\eta) - i\hbar\sigma(\eta)\right)\zeta(\eta) = 0.$$

- Usual ansatz for WKB expansion $\zeta \stackrel{!}{=} \frac{1}{\sqrt{\Omega_k(\eta)}} e^{-i/\hbar \int d\eta' \Omega_k(\eta')}$ does not work.

- The correct ansatz of the WKB expansion is given by

$$\zeta = \sqrt{\frac{\sigma}{2\omega^2(\sigma+\omega')}}\left(1+\hbar F^{(1)}+\hbar^2 F^{(2)}+\cdots\right) e^{-i/\hbar\int d\eta'(\omega+\hbar\omega^{(1)}+\hbar^2\omega^{(2)}+\cdots)},$$

and this gives the correct behavior in large momentum limit.

Induced Current 1

VEV of the current induced by charged scalar in 2 dimensional dS spacetime
M. Fröb et al. **JCAP 1404 (2014) 009**

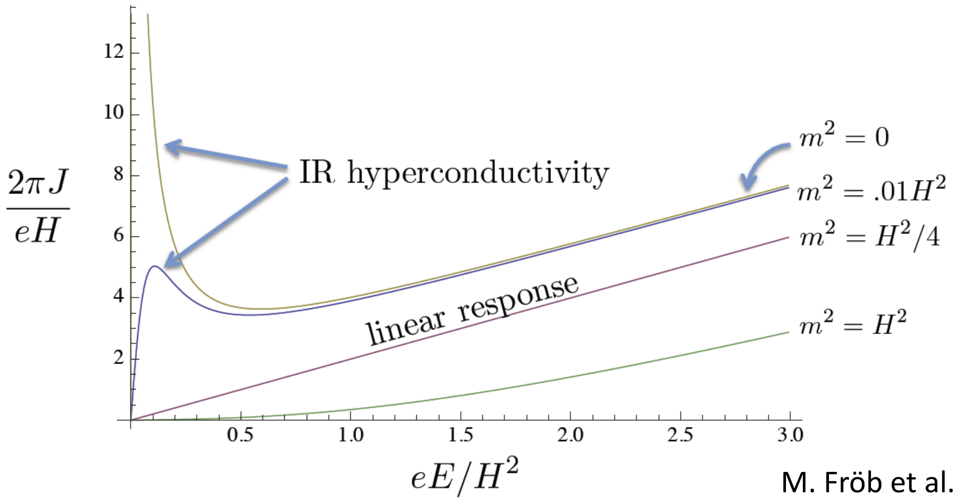

M. Fröb et al. (2014)

Induced Current 2

VEV of the current induced by charged scalar in 4 dimensional dS spacetime

Kobayashi, Afshordi, JHEP 1410 (2014) 166

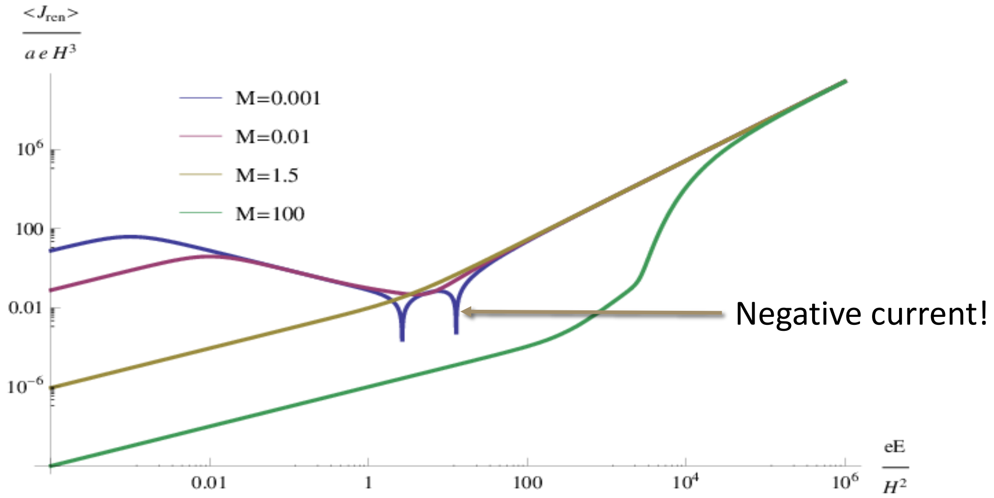

Induced Current 3

VEV of the current induced by Dirac fermion in 2 dimensional dS spacetime

C. Stahl et al. arXiv:1507.01686

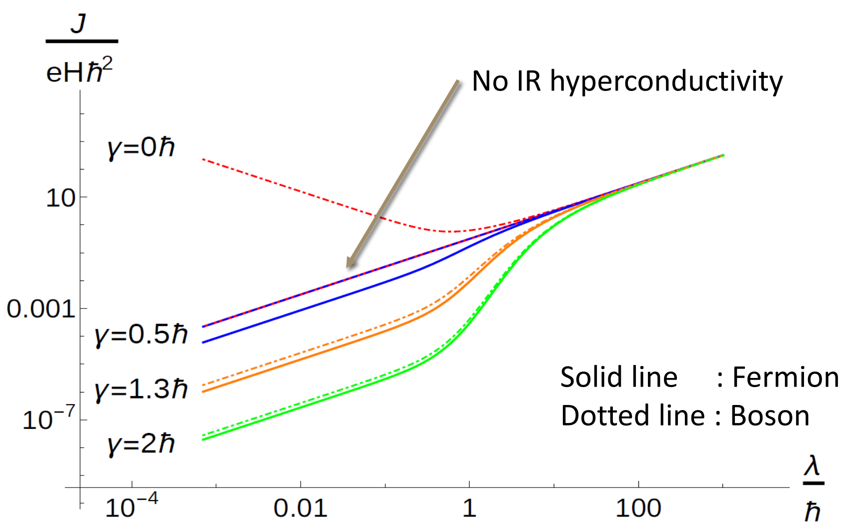

C. Stahl et al. (2015)

Induced Current 4 - preliminary

VEV of the current induced by Dirac femrmion in 4 dimensional dS spacetime

- now proceeding
- We find the negative current also happens in this case.

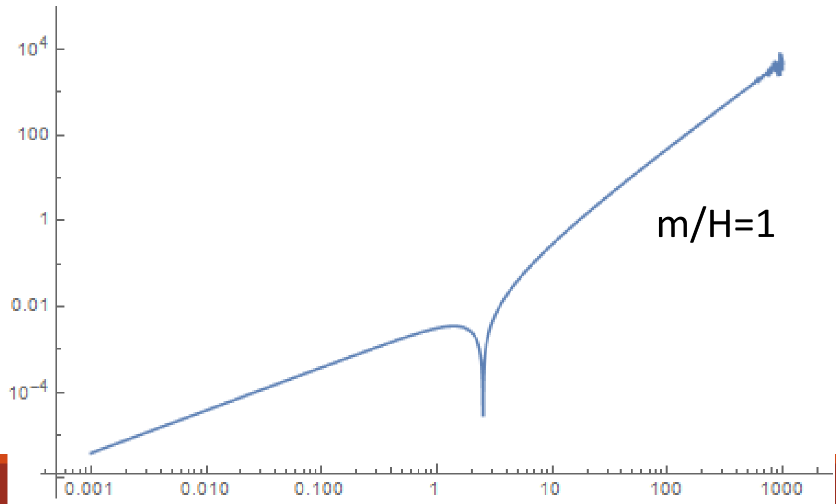

Summary

- Inflationary magnetogenesis does not go well so far.
- The over production of the electric field breaks the inflation.
- Schwinger effect may remove the cause.

- Property of Schwinger effect in dS spacetime is quite different from that in Minkowski spacetime.
- Even the negative current appears in 4-dimensional case regardless of the spin of the charged particle .

“Designing Anisotropic Inflation with Form Fields”

by Asuka Ito

[JGRG25(2015)3a5]

Designing Anisotropic Inflation with Form Fields

Asuka Ito (Kobe Univ.)

with Jiro Soda (Kobe Univ.)

Ref: arXiv:1506.02450

Introduction

Cosmic no-hair conjecture (1983 R.M.Wald)

→ An anisotropic hair vanishes during the inflationary expansion.

Counter example (2010 M.Watanabe, S.Kanno, J.Soda.)

Introduction

Cosmic no-hair conjecture (1983 R.M.Wald)

→ An anisotropic hair vanishes during the inflationary expansion.

Anisotropic universe was not realistic…

Counter example (2010 M.Watanabe, S.Kanno, J.Soda.)

2/12

Introduction

Cosmic no-hair conjecture (1983 R.M.Wald)

→ An anisotropic hair vanishes during the inflationary expansion.

Anisotropic universe was not realistic…

Counter example (2010 M.Watanabe, S.Kanno, J.Soda.)

→ If there is a gauge field coupled with inflaton, inflationary universe can become anisotropic.

Introduction

Cosmic no-hair conjecture (1983 R.M.Wald)

→ An anisotropic hair vanishes during the inflationary expansion.

Anisotropic universe was not realistic…

Counter example (2010 M.Watanabe, S.Kanno, J.Soda.)

→ If there is a gauge field coupled with inflaton, inflationary universe can become anisotropic.

Anisotropic universe is realized generally !

Anisotropy & Observation

Power spectrum of curvature perturbation

$$P(\vec{k}) = P(k)\ \left[(1 + g\sin(\theta)^2)\right]$$ (θ is zenith angle)

$g = 0$ → Isotropic

Now constraint for g from CMB is $|g| < 0.02$ … small.

Anisotropy & Observation

Power spectrum of curvature perturbation

$$P(\vec{k}) = P(k)\ \left[(1 + g\sin(\theta)^2)\right] \quad (\ \theta \text{ is zenith angle }\ )$$

$g = 0$ → **Isotropic**

Now constraint for g from CMB is $|g| < 0.02$ ... small.

However, recently precise observation could prove anisotropy in the future.

3/12

Anisotropy & Observation

Power spectrum of curvature perturbation

$$P(\vec{k}) = P(k)\ \left[(1 + g\sin(\theta)^2)\right] \quad (\ \theta \text{ is zenith angle }\ )$$

$g = 0$ → **Isotropic**

Now constraint for g from CMB is $|g| < 0.02$ ... small.

However, recently precise observation could prove anisotropy in the future.

From the point of view of precision cosmology,
it is important to investigate anisotropic inflation !

Factor of Anisotropy

gauge field：

2-form field：

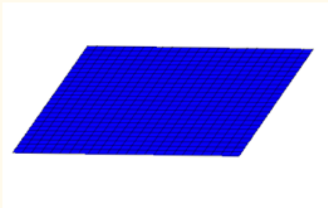

A directional field can become a factor of anisotropy.

4/12

Factor of Anisotropy

gauge field：

2-form field：

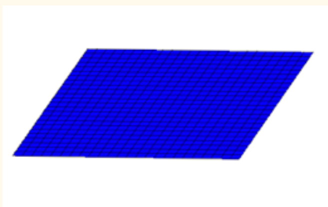

A directional field can become a factor of anisotropy.

⇨ **We consider an inflation model where gauge field and 2-form field (motivated from string theory) exist.**

Only gauge field

action

$$S = \int d^4x\sqrt{-g}\left[\frac{M_p^2}{2}R - \frac{1}{2}(\partial_\mu\phi)(\partial^\mu\phi) - V_0 e^{\lambda\frac{\phi}{M_p}} - \frac{1}{4}f_A^2 e^{2\rho_A\frac{\phi}{M_p}}F_{\mu\nu}F^{\mu\nu}\right]$$

(Functions are exponential type.)

5/12

Only gauge field

action

$$S = \int d^4x\sqrt{-g}\left[\frac{M_p^2}{2}R - \frac{1}{2}(\partial_\mu\phi)(\partial^\mu\phi) - V_0 e^{\lambda\frac{\phi}{M_p}} - \frac{1}{4}f_A^2 e^{2\rho_A\frac{\phi}{M_p}}F_{\mu\nu}F^{\mu\nu}\right]$$

(Functions are exponential type.)

5/12

Only gauge field

action

$$S = \int d^4x\sqrt{-g}\left[\frac{M_p^2}{2}R - \frac{1}{2}(\partial_\mu\phi)(\partial^\mu\phi) - V_0 e^{\lambda\frac{\phi}{M_p}} - \frac{1}{4}f_A^2 e^{2\rho_A\frac{\phi}{M_p}}F_{\mu\nu}F^{\mu\nu}\right]$$

(Functions are exponential type.)

It is known anisotropic power-law solution (exact solution) exists.

((2010) S.Kanno, J.Soda, M.Watanabe)

metric

$$ds^2 = -dt^2 + t^{2\zeta}\left[t^{-4\eta}dx^2 + t^{2\eta}(dy^2 + dz^2)\right]$$

5/12

Only gauge field

action

$$S = \int d^4x\sqrt{-g}\left[\frac{M_p^2}{2}R - \frac{1}{2}(\partial_\mu\phi)(\partial^\mu\phi) - V_0 e^{\lambda\frac{\phi}{M_p}} - \frac{1}{4}f_A^2 e^{2\rho_A\frac{\phi}{M_p}}F_{\mu\nu}F^{\mu\nu}\right]$$

(Functions are exponential type.)

It is known anisotropic power-law solution (exact solution) exists.

((2010) S.Kanno, J.Soda, M.Watanabe)

metric

$$ds^2 = -dt^2 + t^{2\zeta}\left[t^{-4\eta}dx^2 + t^{2\eta}(dy^2 + dz^2)\right]$$

This time, $\eta > 0$, so the shape of anisotropy is…

Only gauge field

oblate type

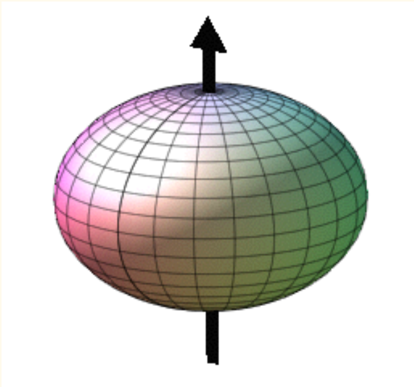

$$P(\vec{k}) = P(k)\ \left[(1 + g\sin(\theta)^2)\right]$$

$$\Rightarrow \quad g > 0$$

Only 2-form field

action

$$\boxed{S = \int d^4x\sqrt{-g}\ [\frac{M_p^2}{2}R - \frac{1}{2}(\partial_\mu\phi)(\partial^\mu\phi) - V_0 e^{\lambda\frac{\phi}{M_p}} - \frac{1}{12}f_B^2 e^{2\rho_B\frac{\phi}{M_p}} H_{\mu\nu\lambda}H^{\mu\nu\lambda}]}$$

(Functions are exponential type.)

Only 2-form field

action

$$S = \int d^4x\sqrt{-g}\,[\frac{M_p^2}{2}R - \frac{1}{2}(\partial_\mu\phi)(\partial^\mu\phi) - V_0 e^{\lambda\frac{\phi}{M_p}} - \frac{1}{12}f_B^2 e^{2\rho_B\frac{\phi}{M_p}} H_{\mu\nu\lambda}H^{\mu\nu\lambda}]$$

(Functions are exponential type.)

7/12

Only 2-form field

action

$$S = \int d^4x\sqrt{-g}\,[\frac{M_p^2}{2}R - \frac{1}{2}(\partial_\mu\phi)(\partial^\mu\phi) - V_0 e^{\lambda\frac{\phi}{M_p}} - \frac{1}{12}f_B^2 e^{2\rho_B\frac{\phi}{M_p}} H_{\mu\nu\lambda}H^{\mu\nu\lambda}]$$

(Functions are exponential type.)

We found anisotropic power-law solution (exact solution) exists like the case of only a gauge field.

metric

$$ds^2 = -dt^2 + t^{2\zeta}\left[t^{-4\eta}dx^2 + t^{2\eta}(dy^2 + dz^2)\right]$$

Only 2-form field

action

$$S = \int d^4x \sqrt{-g}\,\left[\frac{M_p^2}{2}R - \frac{1}{2}(\partial_\mu\phi)(\partial^\mu\phi) - V_0 e^{\lambda\frac{\phi}{M_p}} - \frac{1}{12}f_B^2 e^{2\rho_B\frac{\phi}{M_p}} H_{\mu\nu\lambda}H^{\mu\nu\lambda}\right]$$

(Functions are exponential type.)

We found anisotropic power-law solution (exact solution) exists like the case of only a gauge field.

metric

$$ds^2 = -dt^2 + t^{2\zeta}\left[t^{-4\eta}dx^2 + t^{2\eta}(dy^2+dz^2)\right]$$

This time, $\eta < 0$, so the shape of anisotropy is…

Only 2-form field

prolate type

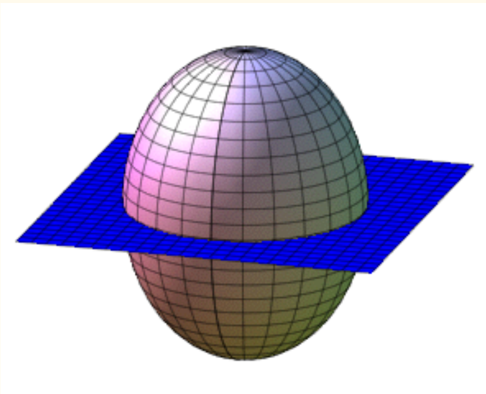

$$P(\vec{k}) = P(k)\ \left[(1 + g\sin(\theta)^2)\right]$$

$$\Rightarrow \quad g < 0$$

Gauge field & 2-form field

action

$$\boxed{S = \int d^4x\sqrt{-g}\,[\frac{M_p^2}{2}R - \frac{1}{2}(\partial_\mu\phi)(\partial^\mu\phi) - V_0 e^{\lambda\frac{\phi}{M_p}} - \frac{1}{4}f_A^2 e^{2\rho_A\frac{\phi}{M_p}}F_{\mu\nu}F^{\mu\nu} - \frac{1}{12}f_B^2 e^{2\rho_B\frac{\phi}{M_p}}H_{\mu\nu\lambda}H^{\mu\nu\lambda}]}$$

9/12

Gauge field & 2-form field

action

$$\boxed{S = \int d^4x\sqrt{-g}\,[\frac{M_p^2}{2}R - \frac{1}{2}(\partial_\mu\phi)(\partial^\mu\phi) - V_0 e^{\lambda\frac{\phi}{M_p}} - \frac{1}{4}f_A^2 e^{2\rho_A\frac{\phi}{M_p}}F_{\mu\nu}F^{\mu\nu} - \frac{1}{12}f_B^2 e^{2\rho_B\frac{\phi}{M_p}}H_{\mu\nu\lambda}H^{\mu\nu\lambda}]}$$

Gauge field & 2-form field

action

$$S=\int d^4x\sqrt{-g}\,[\frac{M_p^2}{2}R-\frac{1}{2}(\partial_\mu\phi)(\partial^\mu\phi)-V_0e^{\lambda\frac{\phi}{M_p}}-\frac{1}{4}f_A^2e^{2\rho_A\frac{\phi}{M_p}}F_{\mu\nu}F^{\mu\nu}-\frac{1}{12}f_B^2e^{2\rho_B\frac{\phi}{M_p}}H_{\mu\nu\lambda}H^{\mu\nu\lambda}]$$

This time, there are four candidates of a stable solution.

isotropic solution

$+$

anisotropic solution

	gauge solution	**(2-form decays)**
	2-form solution	**(gauge decays)**
	hybrid solution	**(both live)**

9/12

Gauge field & 2-form field

action

$$S=\int d^4x\sqrt{-g}\,[\frac{M_p^2}{2}R-\frac{1}{2}(\partial_\mu\phi)(\partial^\mu\phi)-V_0e^{\lambda\frac{\phi}{M_p}}-\frac{1}{4}f_A^2e^{2\rho_A\frac{\phi}{M_p}}F_{\mu\nu}F^{\mu\nu}-\frac{1}{12}f_B^2e^{2\rho_B\frac{\phi}{M_p}}H_{\mu\nu\lambda}H^{\mu\nu\lambda}]$$

This time, there are four candidates of a stable solution.

isotropic solution

$+$

anisotropic solution

	gauge solution	**(2-form decays)**
	2-form solution	**(gauge decays)**
	hybrid solution	**(both live)**

Coupling constants λ , ρ_A , ρ_B
determine which solution becomes stable !

This can be depicted in 3-dimensional figure…

Gauge field & 2-form field

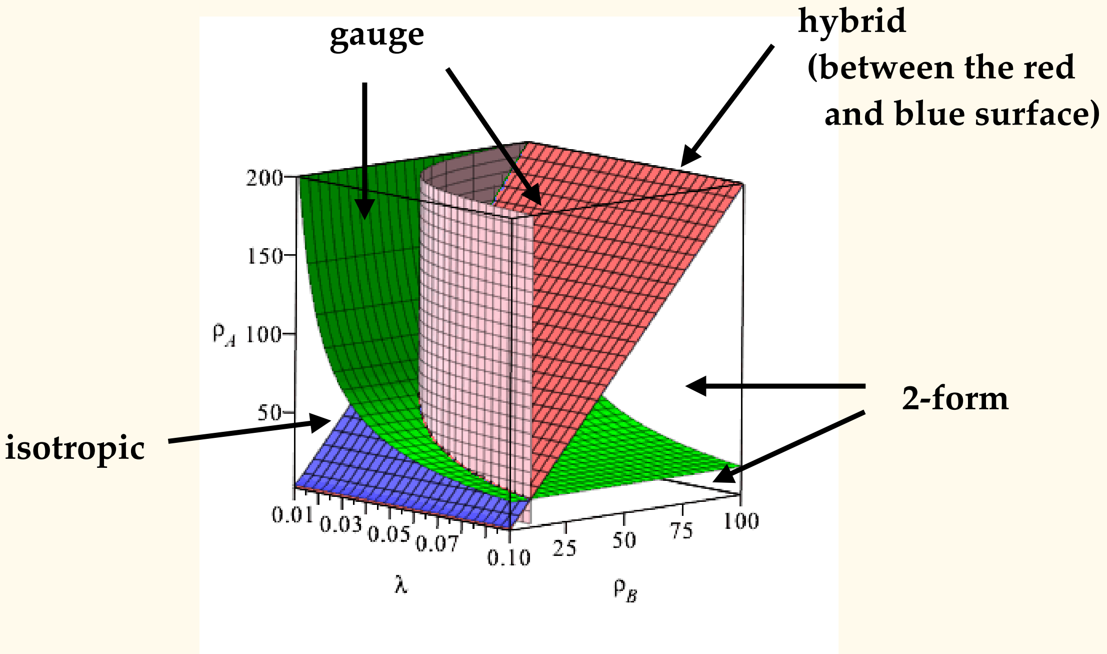

Each surface intersects on a curved line exactly !

In the case of the hybrid solution, which is the shape of anisotropy, oblate or prolate ?

In the case of the hybrid solution, which is the shape of anisotropy, oblate or prolate ?

It is also determined by the coupling constants.

$$S = \int d^4x\sqrt{-g}\,[\frac{M_p^2}{2}R - \frac{1}{2}(\partial_\mu\phi)(\partial^\mu\phi) - V_0 e^{\lambda\frac{\phi}{M_p}} - \frac{1}{4}f_A^2 e^{2\rho_A\frac{\phi}{M_p}}F_{\mu\nu}F^{\mu\nu} - \frac{1}{12}f_B^2 e^{2\rho_B\frac{\phi}{M_p}}H_{\mu\nu\lambda}H^{\mu\nu\lambda}]$$

$2(\rho_A - 2\rho_B) - \lambda \ > 0$ ⇨ **oblate (gauge like)**

< 0 ⇨ **prolate (2-form like)**

Conclusion

- **From the point of view of precision cosmology, it is important to investigate anisotropic inflation.**
- **gauge field & 2-form field can become a factor of anisotropy.**
- **only gauge field** ⇨ **oblate type**
- **only 2-form field** ⇨ **prolate type**
- **gauge field & 2-form field**

In the case of the hybrid solution (both fields live),
Coupling constants λ, ρ_A, ρ_B determine the shape of anisotropy.

Thank you very much!

2-form field

$$\frac{d}{dt}\left[f_B^2 e^{2\rho_B \frac{\phi}{M_p}} e^{-\alpha-4\sigma}\dot{v}_B\right] = 0$$

$$\Longrightarrow \quad \dot{v}_B = p_B f_B^{-2} e^{-2\rho_B \frac{\phi}{M_p}} e^{\alpha+4\sigma} \qquad (\quad p_B = const \quad)$$

scalar field

$$\ddot{\phi} = -3\dot{\alpha}\dot{\phi} - \frac{1}{M_p}\lambda V_0 e^{\lambda\frac{\phi}{M_p}} + \frac{1}{M_p}\rho_B p_B^2 f_B^{-2} e^{-2\rho_B \frac{\phi}{M_p}} e^{-2\alpha+4\sigma} \; .$$

Einstein equations

$$\dot{\alpha}^2 = \dot{\sigma}^2 + \frac{1}{3M_p}\,[\frac{1}{2}\dot{\phi}^2 + V_0 e^{\lambda\frac{\phi}{M_p}} + \frac{1}{2} f_B^{-2} e^{-2\rho_B \frac{\phi}{M_p}} e^{-2\alpha+4\sigma}] \; ,$$

$$\ddot{\alpha} = -3\dot{\alpha}^2 + \frac{1}{M_p} V_0 e^{\lambda\frac{\phi}{M_p}} + \frac{1}{3M_p^2} p_B^2 f_B^{-2} e^{-2\rho_B \frac{\phi}{M_p}} e^{-2\alpha+4\sigma} \; ,$$

$$\ddot{\sigma} = -3\dot{\alpha}\dot{\sigma} + -\frac{1}{3M_p^2} p_B^2 f_B^{-2} e^{-2\rho_B \frac{\phi}{M_p}} e^{-2\alpha+4\sigma} \; .$$

Seeking for the particular solutions…

Phase space

we change the variables as

$$X = \frac{\dot\sigma}{\dot\alpha} \;, \quad Y = \frac{1}{M_p}\frac{\dot\phi}{\dot\alpha} \;, \quad Z_B = \frac{1}{M_p\dot\alpha} p_B f_B^{-1} e^{-\rho_B \frac{\phi}{M_p}} e^{-\alpha+2\sigma} \;.$$

(anisotropy)

$$ds^2 = -dt^2 + e^{2\alpha(t)}\left[e^{-4\sigma(t)}dx^2 + e^{2\sigma(t)}(dy^2 + dz^2)\right]$$

Equations of motion become

$$\frac{dX}{d\alpha} = X[\,3(X^2-1) + \frac{1}{2}Y^2\,] + \frac{1}{6}Z_B^2(X-2) \;,$$
$$\frac{dY}{d\alpha} = (Y+\lambda)[\,3(X^2-1) + \frac{1}{2}Y^2\,] + (\frac{1}{6}Y + \rho_B + \frac{\lambda}{2})Z_B^2 \;,$$
$$\frac{dZ_B}{d\alpha} = Z_B[\,3(X^2-1) + \frac{1}{2}Y^2 - \rho_B Y + 2 + 2X + \frac{1}{6}Z_B^2\,] \;.$$

Setting LHS are 0, we find fixed points (particular solutions)…

Fixed Point (particular solution)

Isotropic fixed point

$$X = 0, \quad Y = -\lambda, \quad Z_B = 0$$

isotropic

Anisotropic fixed point

$$X = \frac{-\lambda^2 - 2\rho_B\lambda + 2}{\lambda^2 + 5\rho_B\lambda + 6\rho_B^2 + 4} \;,$$
$$Y = \frac{-6(\lambda + \rho_B)}{\lambda^2 + 5\rho_B\lambda + 6\rho_B^2 + 4} \;,$$
$$Z_B^2 = \frac{9(\lambda^2 + 2\rho_B\lambda - 2)(6\rho_B^2 + 4\rho_B\lambda + 4)}{\lambda^2 + 5\rho_B\lambda + 6\rho_B^2 + 4} \;.$$

anisotropic

$\lambda^2 + 2\rho_B\lambda - 2 > 0$ is needed for existence of this fixed point.

To find the dynamics of general solution,
we study the stability of fixed points !

Stability of fixed point

The results are below.

	condition of stability of fixed point
Isotropic	$\lambda^2 + 2\rho_B\lambda - 2 < 0$
Anisotropic	$\lambda^2 + 2\rho_B\lambda - 2 > 0$

← corresponding to the existence condition.

Coupling constants λ , ρ_B determine which solution become stable!

In the case, $\lambda^2 + 2\rho_B\lambda - 2 > 0$

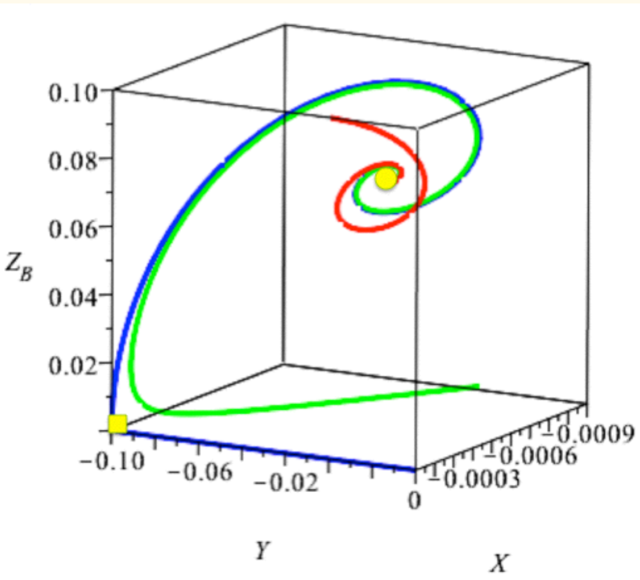

anisotropic fixed point → attractor

isotropic fixed point → saddle point

existence condition

Isotropic	$\lambda^2 < 6$
gauge	$\lambda^2 + 2\rho_A\lambda - 4 > 0$
2-form	$\lambda^2 + 2\rho_B\lambda - 2 > 0$
Hybrid	$\lambda^2 - 4 + \lambda(2\rho_A - \rho_B) + 2\rho_B(\rho_A - 2\rho_B) > 0$ $3\lambda^2 - 8 + 4\lambda(\rho_A + \rho_B) - 4\rho_A(\rho_A - 2\rho_B) > 0$

stability condition

Isotropic	$\lambda^2 + 2\rho_A\lambda - 4 < 0$, $\lambda^2 + 2\rho_B\lambda - 2 < 0$
gauge	$3\lambda^2 - 8 + 4\lambda(\rho_A + \rho_B) - 4\rho_A(\rho_A - 2\rho_B) < 0$
2-form	$\lambda^2 - 4 + \lambda(2\rho_A - \rho_B) + 2\rho_B(\rho_A - 2\rho_B) < 0$
Hybrid	$\lambda^2 - 4 + \lambda(2\rho_A - \rho_B) + 2\rho_B(\rho_A - 2\rho_B) > 0$ $3\lambda^2 - 8 + 4\lambda(\rho_A + \rho_B) - 4\rho_A(\rho_A - 2\rho_B) > 0$

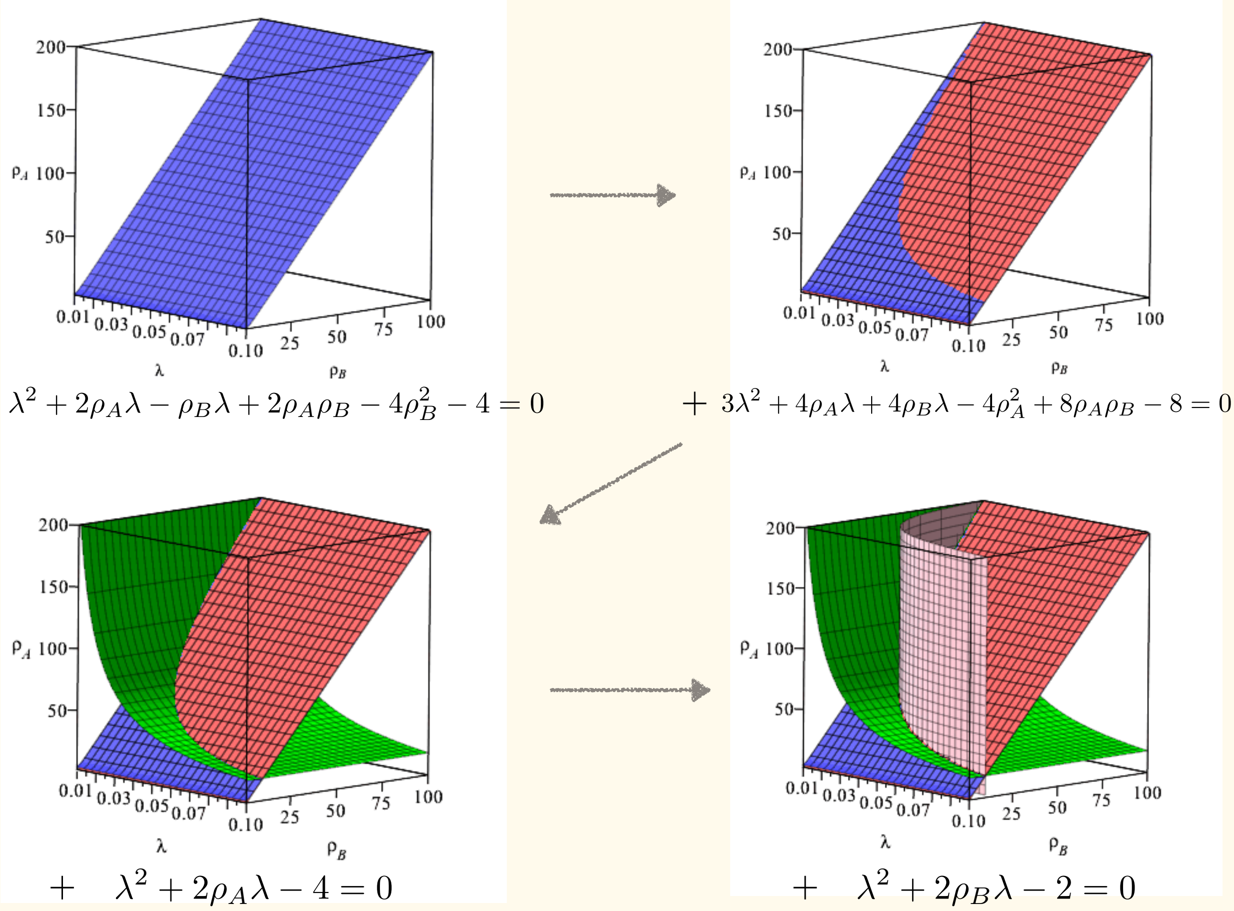

“Black holes as seeds of baby universe”

by Naritaka Oshita

[JGRG25(2015)3a6]

JGRG25 December, 8 @ Kyoto Univ.

YITP YUKAWA INSTITUTE FOR THEORETICAL PHYSICS

Black holes as seeds of baby universe

N. Oshita and J. Yokoyama [gr-qc:1601.03929]
"Creation of an inflationary universe out of a black hole"

東京大学 THE UNIVERSITY OF TOKYO

RESEARCH CENTER FOR THE EARLY UNIVERSE THE UNIVERSITY OF TOKYO RESCEU

Univ. of Tokyo, RESCEU Naritaka Oshita
Univ. of Tokyo, RESCEU Jun'ichi Yokoyama

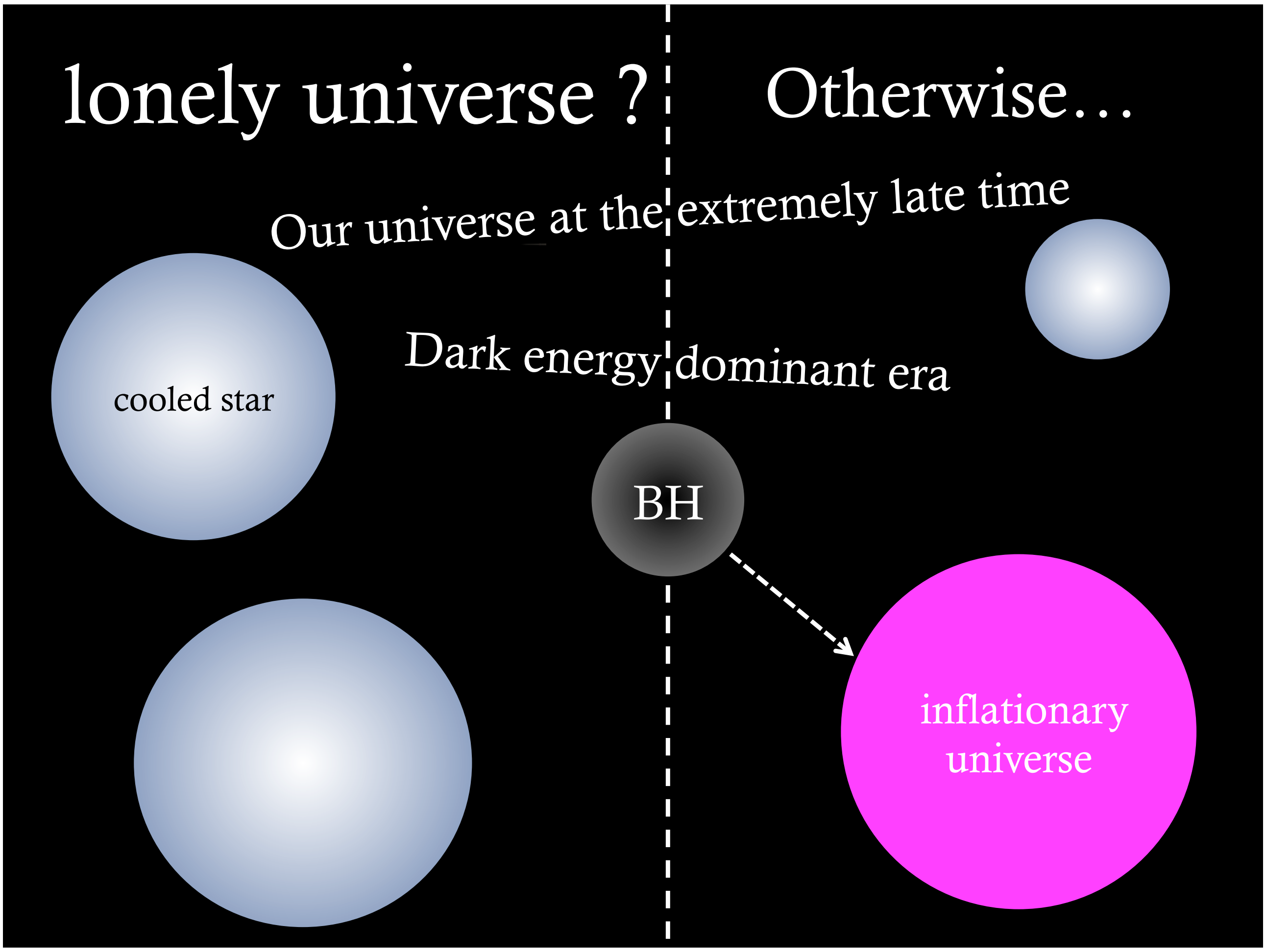

Inflationary universe out of a black hole

Does the heat of a BH catalyzes nucleation of a FVB?

[False Vacuum Bubble]

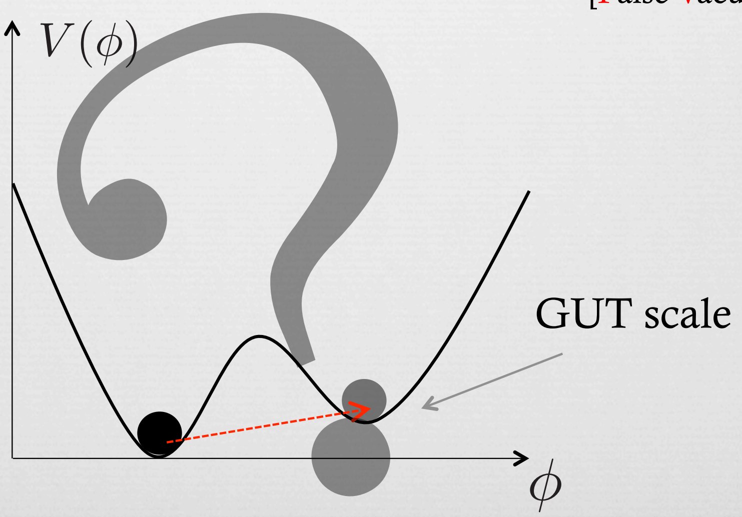

If such a phase transition is induced…

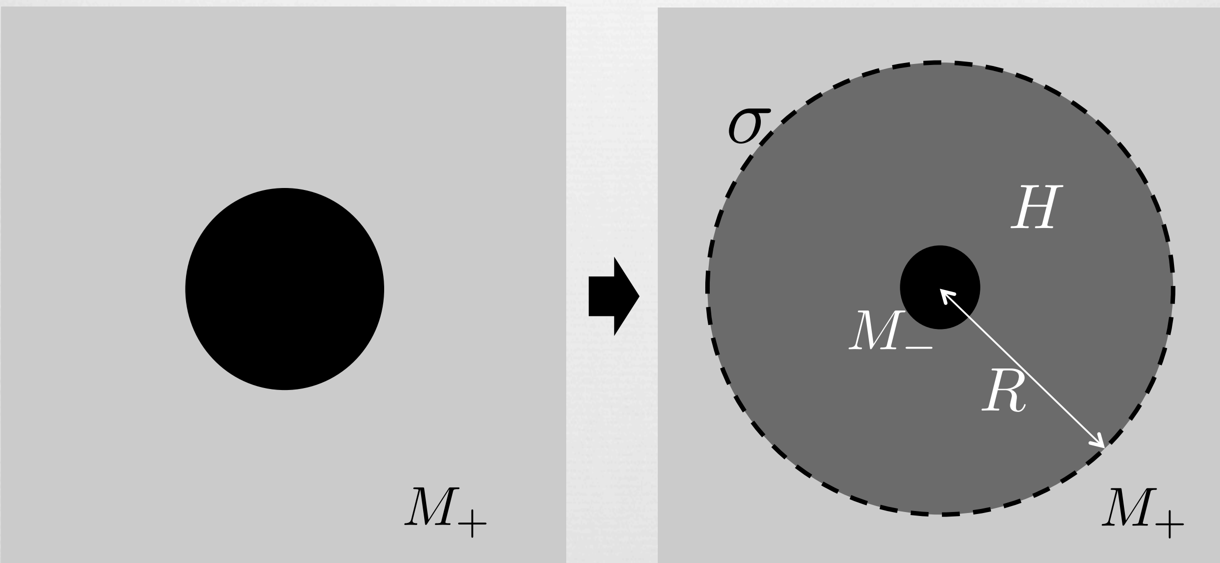

parameters of the FVB

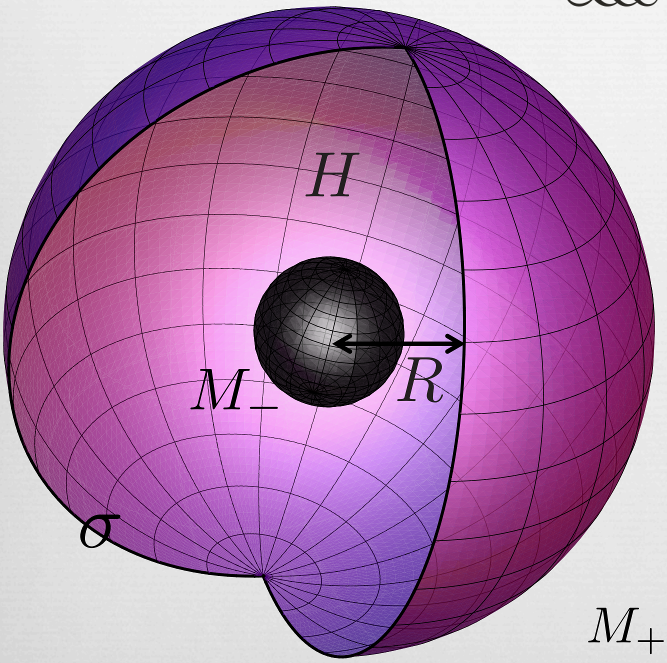

Energy scale of a FVB

$$\chi = \sqrt{(4\pi G\sigma)^2 + H^2}$$

Surface energy / total energy

$$\gamma = \frac{8\pi G\sigma}{\sqrt{(4\pi G\sigma)^2 + H^2}}$$

Dimensionless quantity for R and τ (proper time)

$$z \equiv \frac{\chi^{2/3}}{(2G\Delta M)^{1/3}} R$$

$$\tau' = \frac{\chi^2}{8\pi G\sigma}\tau$$

Israel junction condition

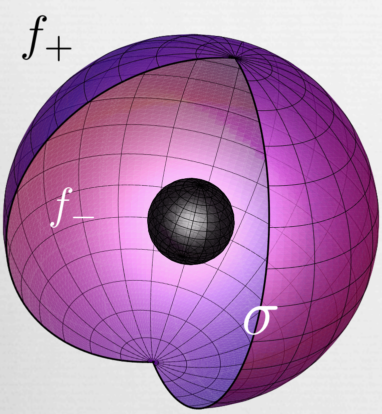

Israel junction condition

$$\beta_- - \beta_+ = 4\pi G\sigma R$$

$$\beta_+ = f_+\dot{\tau}_+ = \pm\sqrt{f_+ + \dot{R}^2}$$

$$\beta_- = f_-\dot{\tau}_- = \pm\sqrt{f_- + \dot{R}^2}$$

Deformation
(Squaring both sides)

$$\boxed{\left(\frac{dz}{d\tau'}\right)^2 - \frac{\gamma^2}{1-r}\frac{1}{z} - \left(\frac{1-z^3}{z^2}\right)^2 = -\frac{\gamma^2}{(2GM_+\chi)^{2/3}(1-r)^{2/3}}}$$

potential V(z)

total energy E

$$ds^2 = f_\pm d\tau^2 + f_\pm^{-1}dr^2 + r^2 d\Omega^2$$

$$f_+ = 1 - \frac{2GM_+}{r} \qquad f_- = 1 - \frac{2GM_-}{r} - H^2 r^2$$

$$r \equiv M_-/M_+$$

Dynamics of a bubble wall
→dynamical system in 1-dim

Solutions for Israel junction condition

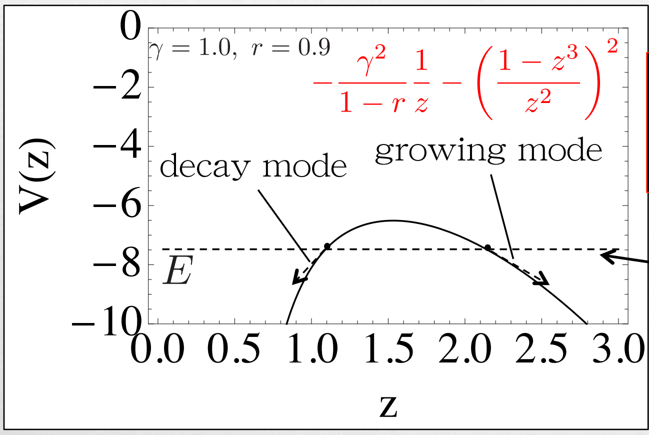

$$\left(\frac{dz}{d\lambda'}\right)^2 + V(z) = E$$

$$-\frac{\gamma^2}{(2GM_+\chi)^{2/3}(1-r)^{2/3}}$$

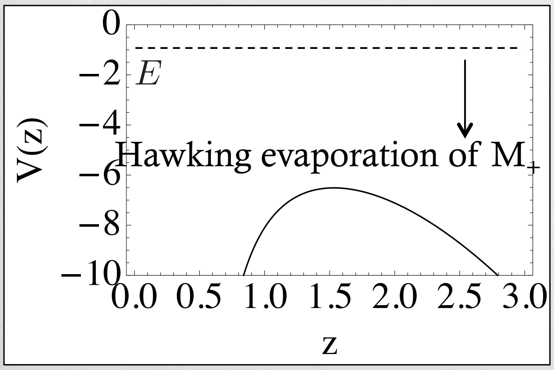

$M_+ \gg 1/(G\chi)$

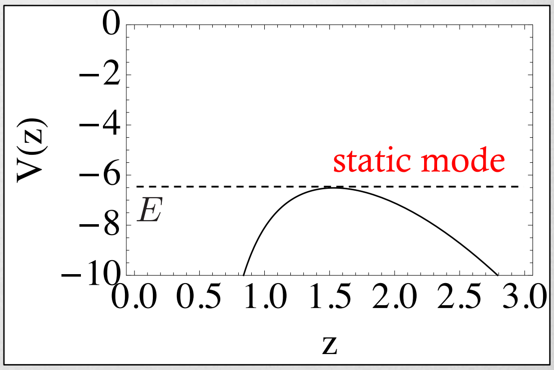

$M_+ = M_C \sim 1/(G\chi) \sim 10^4 M_{\rm Pl}$

Solutions for Israel junction condition

$$\left(\frac{dz}{d\lambda'}\right)^2 + V(z) = E$$

Formula loosing the information of the sign of $\beta_\pm$

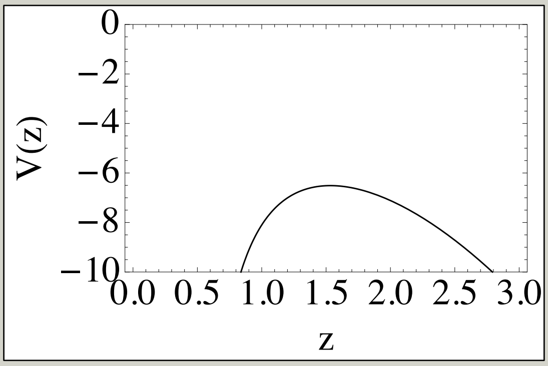

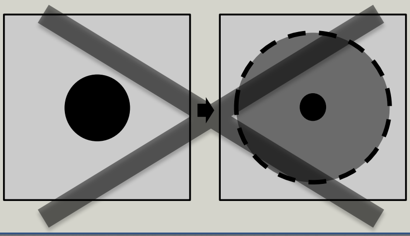

$$\beta_- - \beta_+ = 4\pi G\sigma R$$

Formula including the information of the sign of $\beta_\pm$

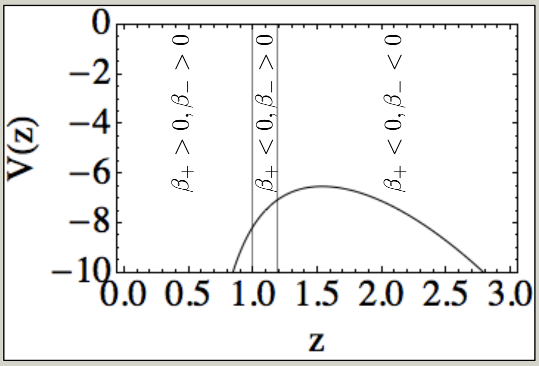

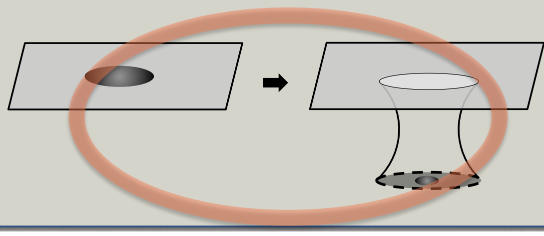

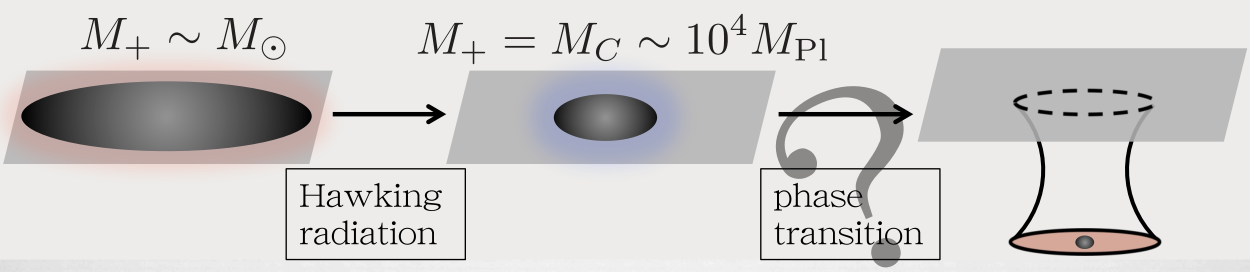

Is it really that such a structure of a FVB is created from a phase transition???

→calculating the decay rate exponent B.

$$\Gamma \propto e^{-B}$$

Entropic interpretation

$$S_{\rm E} = \beta F$$

$$B = \Delta\left(\frac{E}{T}\right) - \Delta S$$

zero at the static bubble $V_{\rm top} = E$

the entropy term affect in the transition rate Γ

$$B < 0 \leftrightarrow \Delta S > 0$$

A BH may transient to a baby universe as soon as its mass reaches at the critical mass.

$\boxed{\text{higher than the temperature of the FV}}$

$GM_{+}\chi < GM_{C}\chi \simeq 0.3$ (for $\gamma \ll 1$)

BHs with high Hawking temperature →Inflationary universe

$\boxed{\text{Baby universe}}$

present time

Hawking radiation

$\sim 10^{56} \times$ cosmological time

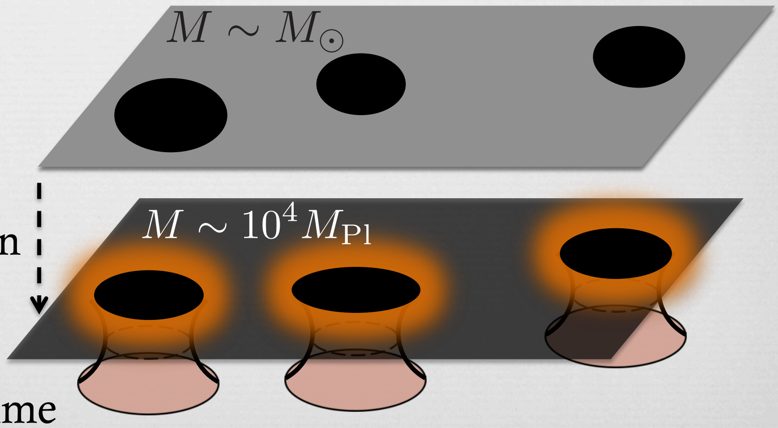

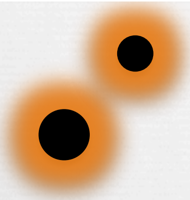

summary

- Calculation of free energy for Schwarzschild spacetime and the system including a false vacuum bubble

  → a BH with higher Hawking temperature above the de Sitter

  temperature induces a phase transition.

- A BH creates a throat including a false vacuum bubble, namely a baby universe
- Inflation would happen when a false vacuum bubble grows and exceeds a de Sitter radius.
- BHs can be regarded as seeds of a baby universe.

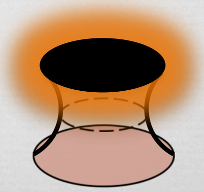

“Probing properties of cosmic strings through Pulsar Timing Arrays”

by Sachiko Kuroyanagi

[JGRG25(2015)3b1]

Probing properties of cosmic strings through Pulsar Timing Arrays

Use of anisotropy of the gravitational wave background

Sachiko Kuroyanagi
(Nagoya U.)

in collaboration with
K. Takahashi, H. Kumamoto, N. Yonemaru
(Kumamoto U.)

2015/12/8 JGRG@Kyoto U.

Pulsar timing array

Robust and unique method of detecting gravitational waves at $10^{-8\sim-9}$Hz

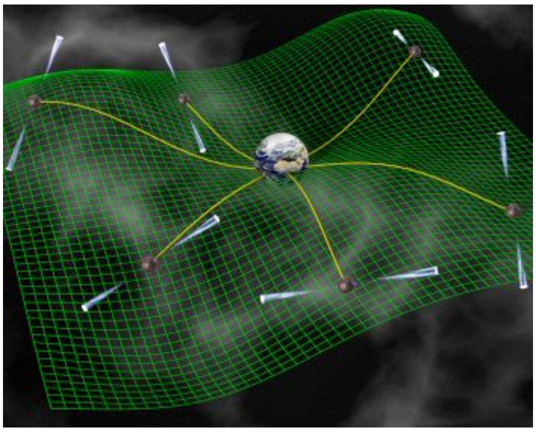

expected to detect gravitational waves
from super massive black hole binaries
or maybe from exotic sources (e.g. cosmic strings)

Cosmic string ?

One dimensional topological defect
generated in the early universe

<u>Generation mechanism</u>

1: Phase transition

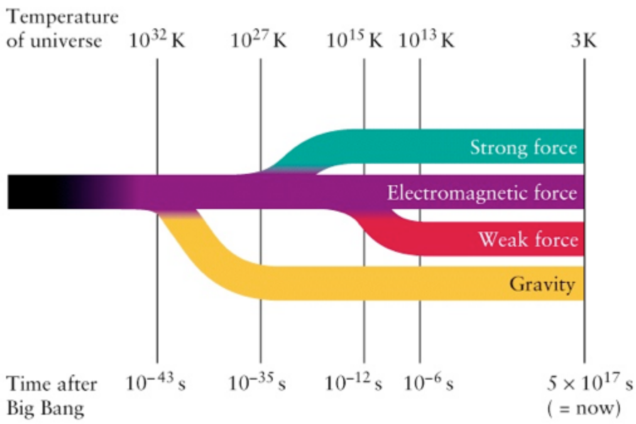

2: Cosmic superstrings

Cosmological size D-strings or F-strings remains after inflation

→ could provide some insight into fundamental physics

Cosmic string ?

infinite string becomes a loop by reconnection

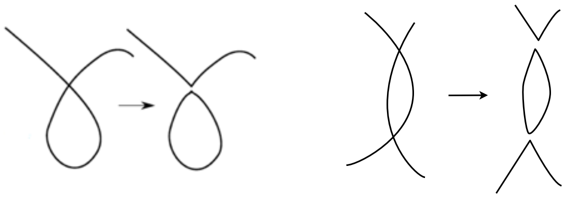

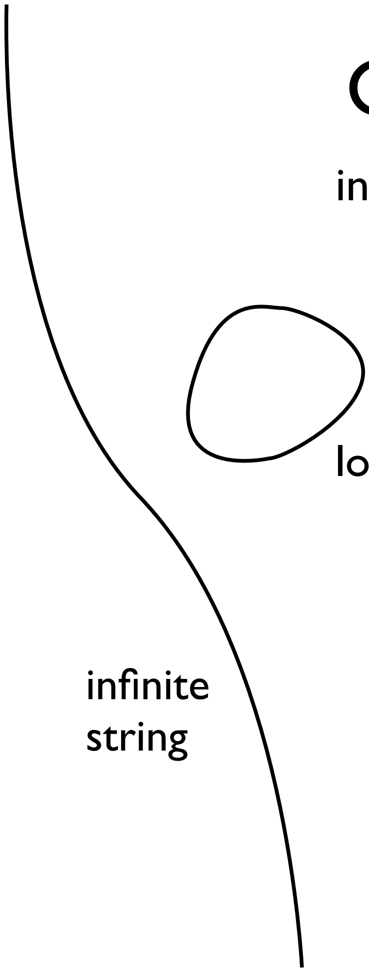

loop

infinite string

strings emit gravitational waves
especially from singular structures

kink

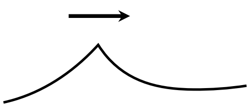

cusp

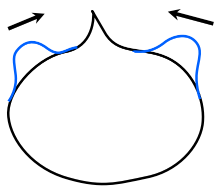

loops lose energy and shrink by emitting
gravitational waves and eventually evaporate

Gravitational waves from cosmic string loops

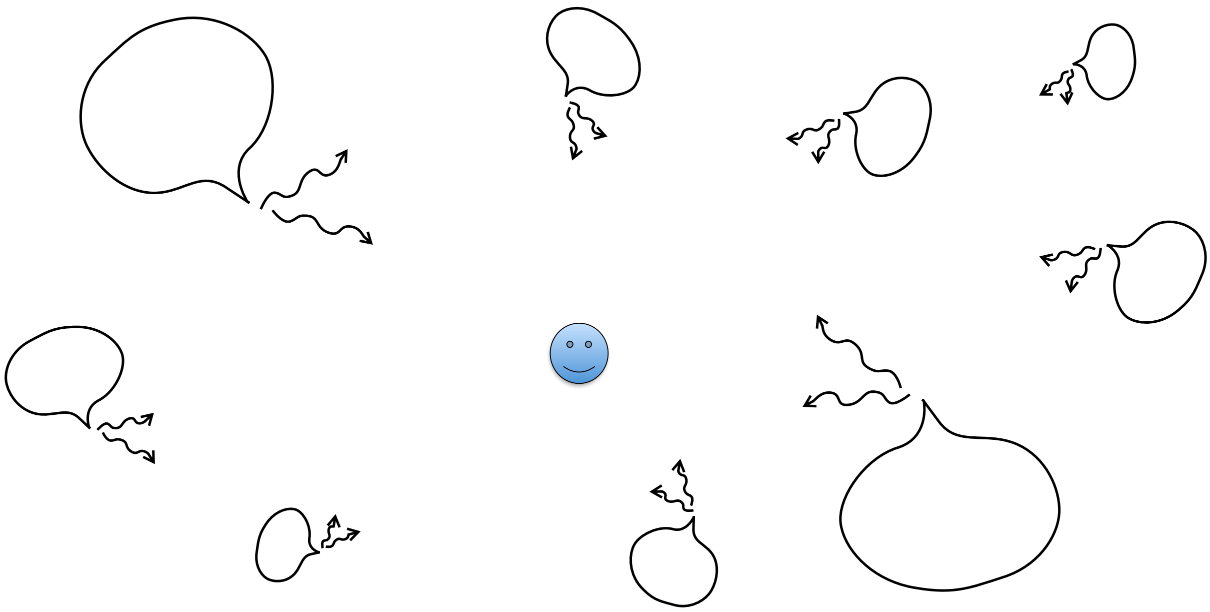

Gravitational waves coming from different directions overlap each other and form gravitational wave background

Spectrum and Sensitivities

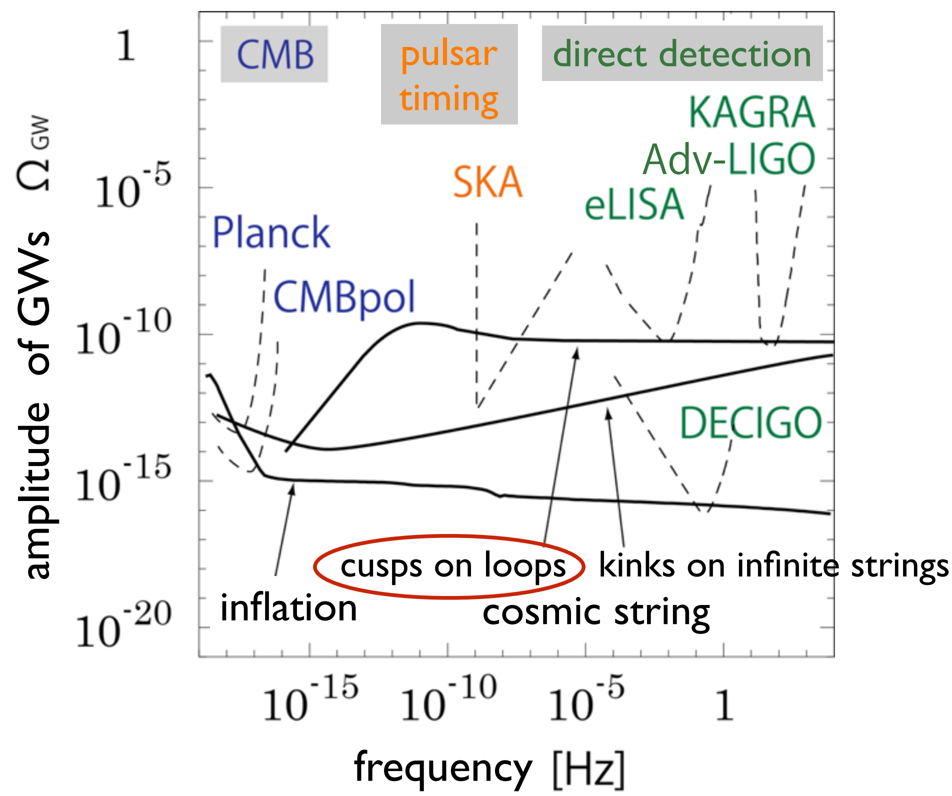

What determines the GW amplitude?

3 main parameters to characterize cosmic string

- $G\mu$: tension = line density
  Generation mechanism
- α : initial loop size $L \sim \alpha H^{-1}$
  Network evolution
- p : reconnection probability
  Phase transition origin: p=1
  Cosmic superstring: p<<1

Detectability in Gμ - α plane

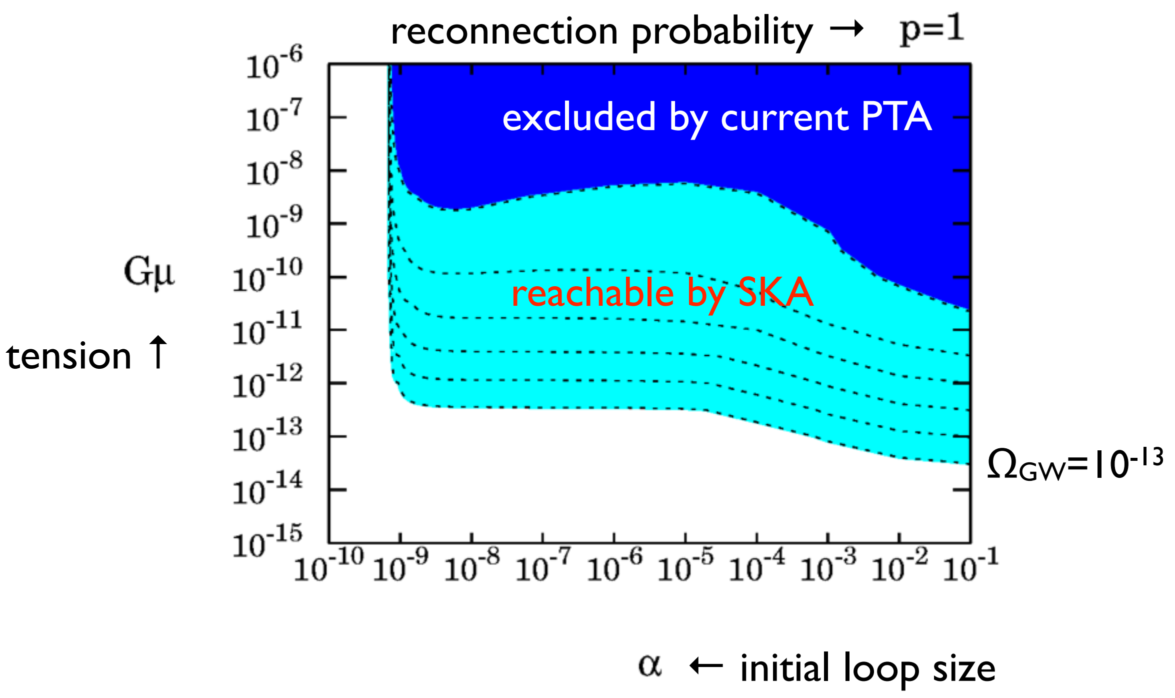

SKA will cover a large parameter space of cosmic string parameters

Gravitational waves from cosmic string loops

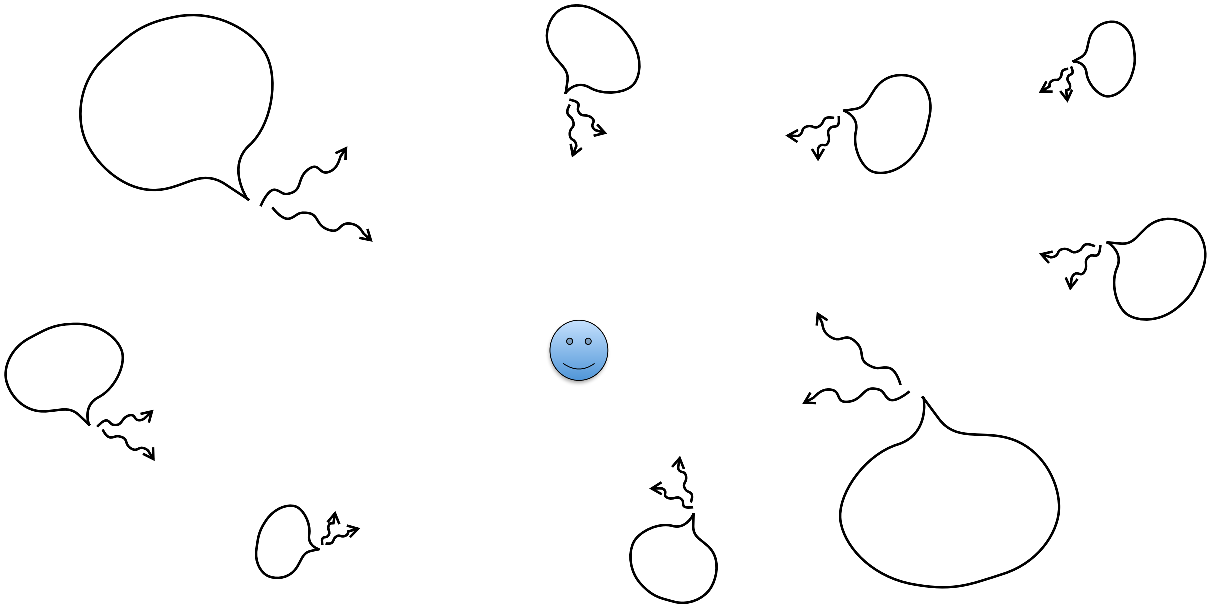

Gravitational waves coming from different directions overlap each other and form gravitational wave background

Anisotropy of gravitational wave background

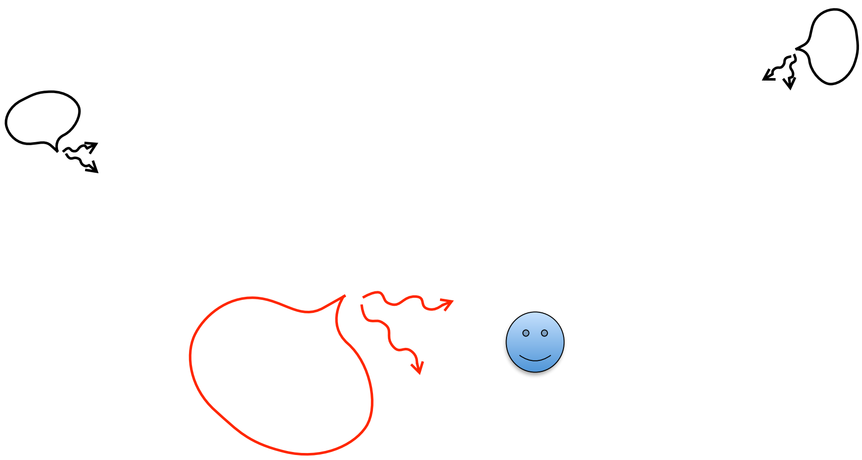

If gravitational wave background is formed by a few bursts, it becomes anisotropic

Anisotropy of gravitational wave background

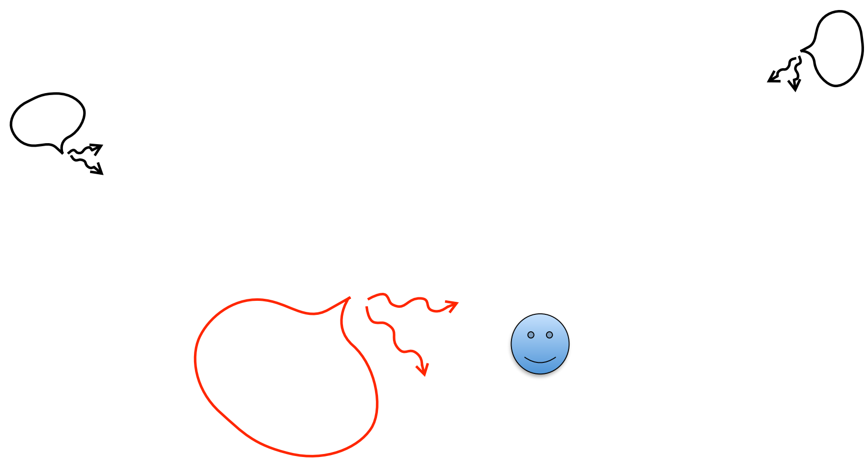

Can we extract information of cosmic strings from anisotropy of the gravitational wave background?

Anisotropy test in PTAs

- Formulations are constructed by
  Mingarelli et. al., PRD 88, 062005 (2013)

GW amplitude: $\Omega_{\rm gw}(f) = \dfrac{8\pi^2}{3H_0^2} f^3 H(f) \displaystyle\int d\hat{\Omega} P(\hat{\Omega})$

$P(\hat{\Omega}) \equiv \displaystyle\sum_{lm} c_l^m Y_l^m(\hat{\Omega})$ ← Spherical harmonic expansion

- Simulation study in a context of GWs from **SMBH binaries**
  Taylor & Gair, PRD 88, 084011 (2013)

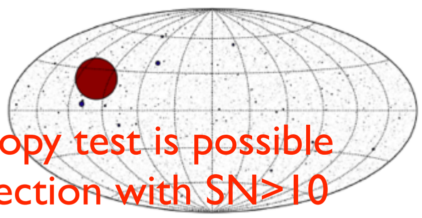

Anisotropy test is possible
for detection with SN>10

angular power spectrum: $C_l = \sum_m |c_{lm}|^2/(2l+1)$

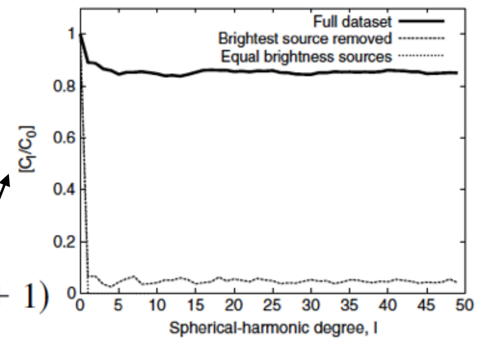

Predictions for cosmic strings

1. predict rate of GW bursts

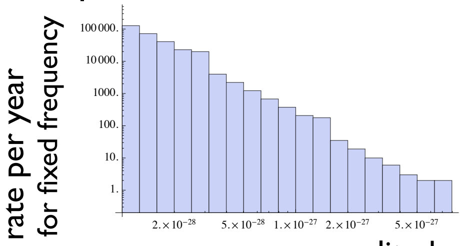

2. randomly distribute the source

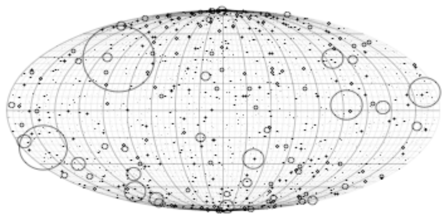

3. make100 realizations

$$c_{lm} = \sum_{i=1}^{N} \rho_i Y_{lm}(\hat{\Omega}_i)$$

$$C_l = \sum_m |c_{lm}|^2/(2l+1)$$

4. calculate anisotropy levels

log normal distribution?

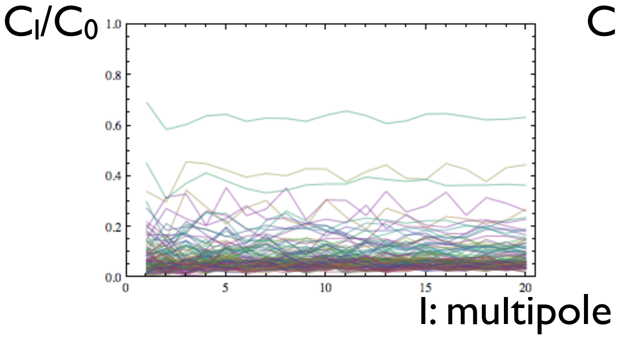

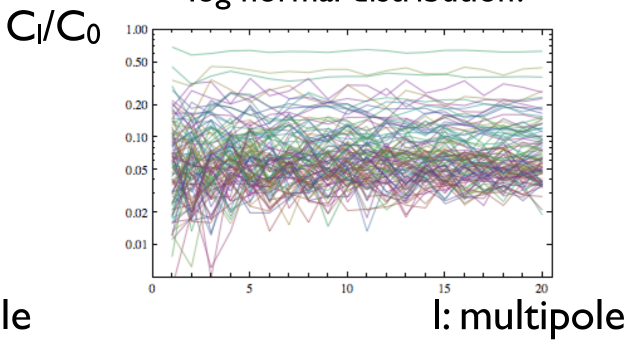

assumed $f=(10\mathrm{yr})^{-1}$

$G\mu = 10^{-11}$, $p=1$

Anisotropy level

with 2σ error bar

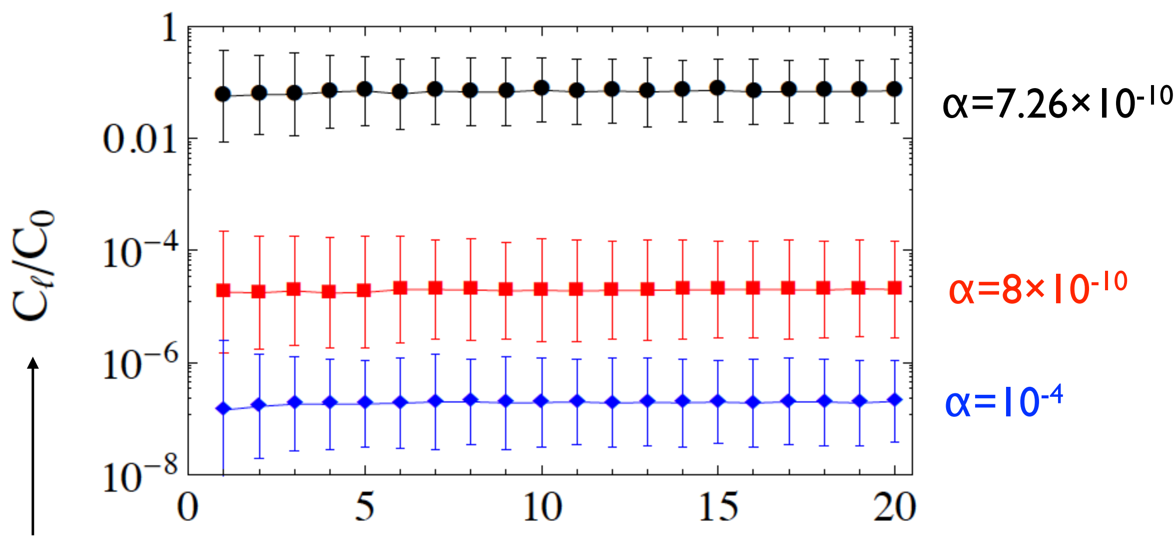

$$C_l = \sum_m |c_{lm}|^2/(2l+1)$$

We get large anisotropy for smaller value of α

(smaller initial loop size)

Dipole component α dependence

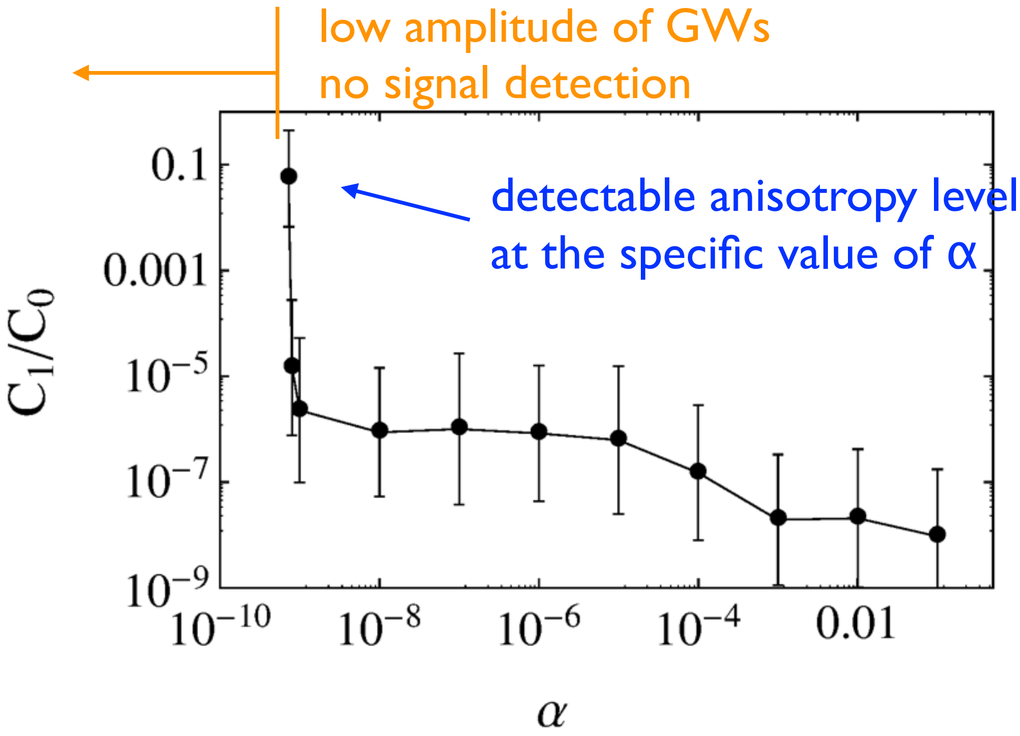

Interpretation

large α = long lifetime

network consists of
mixture of old and new loops

small α = short lifetime

loops evaporate soon after
their formation

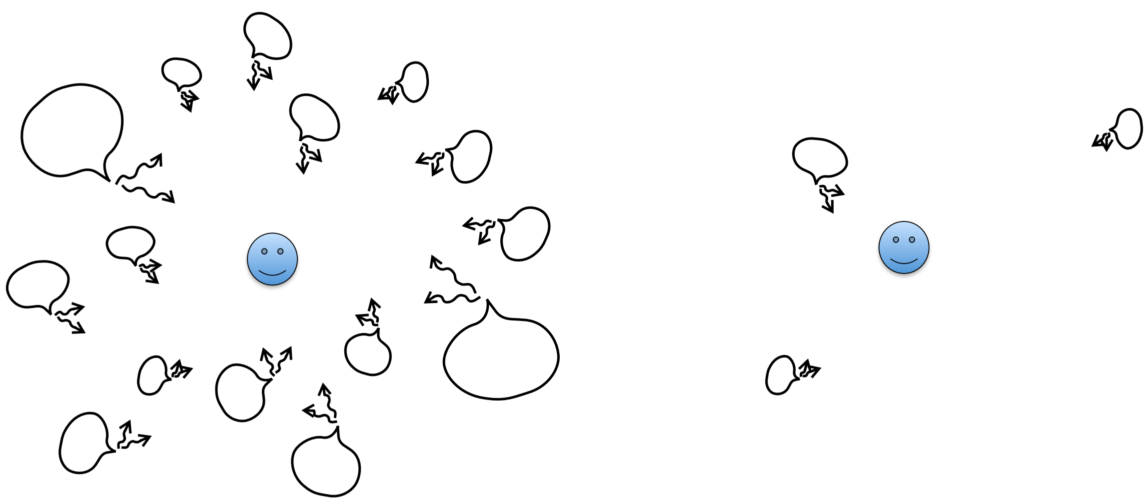

→ isotropic GWs

→ anisotropic GWs

Observation frequency dependence

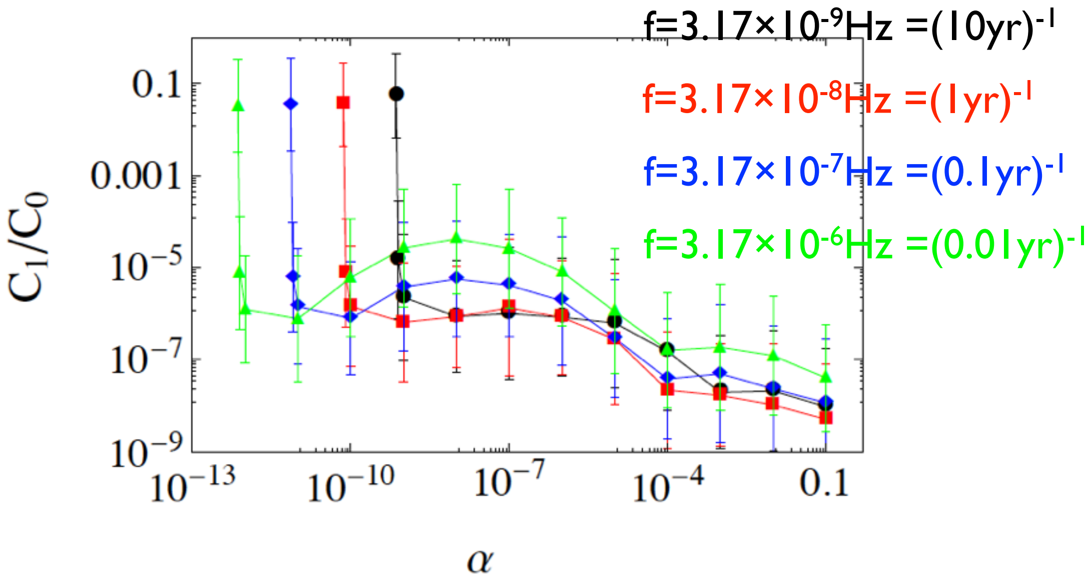

The peak position changes for different observation frequency

When loops evaporate soon after the formation by emitting GWs,

$\boxed{\text{frequency of GWs} \sim (\text{initial loop size})^{-1} \propto \alpha^{-1}}$

Observation frequency dependence

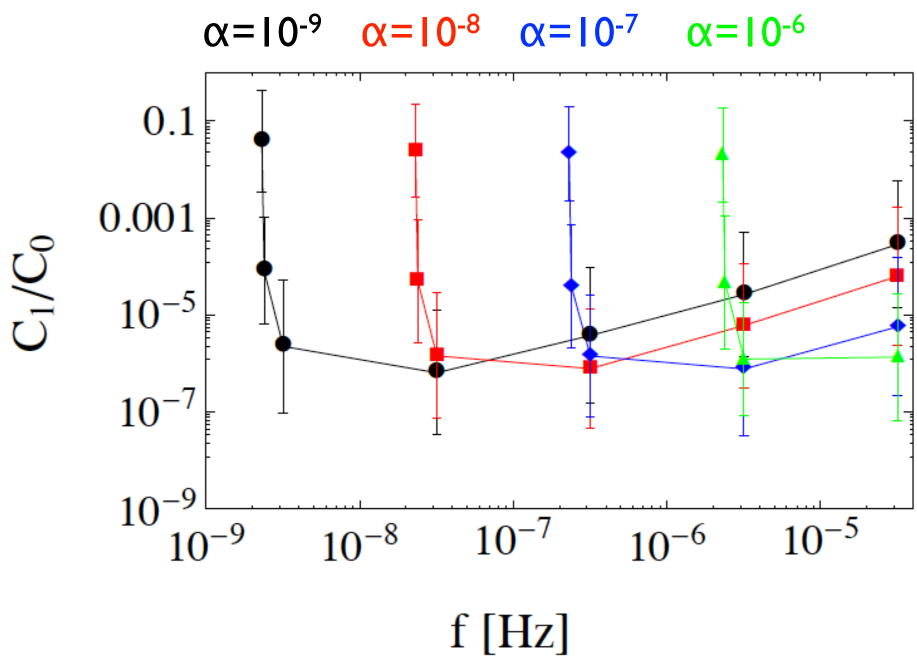

By checking anisotropy at different frequency bands,
it may be possible to obtain implication on the value of α

Summary

- Testing the existence of cosmic string by PTA is important for obtaining implication on fundamental physics.
- SKA will cover a large parameter space of cosmic string parameters.
- Anisotropy of the gravitational wave background can be used to extract information on the initial loop size, which is important for understanding cosmic evolution of the string network.

“Resonant Primordial Gravitational Waves Amplification”

by Chunshan Lin

[JGRG25(2015)3b2]

Resonant Primordial Gravitational Waves Amplification

Chunshan Lin

Yukawa Institute for Theoretical Physics, Kyoto University

Ref: PLB 752 (2016) 84-88, arXiv:1504.01373
by CL and Misao Sasaki

December 18, 2015

I. Introduction

Inflation and Lyth bound

Figure: Planck CMB map 2015 and Starry Night by Vincent van Gogh, June 1889.

Introduction

Future Experiments

Several next-generation satellite missions as well as the ground based experiments and balloons, are aimed at measuring primordial gravitational waves down to $r \sim 10^{-3}$.

Lyth Bound

The tensor-to-scalar ratio is propotional to the variation of the inflaton field during inflation, i.e. $\Delta\phi/M_p \simeq \int dN\sqrt{r/8}$. The threshold

$$\Delta\phi = M_p \quad \Longleftrightarrow \quad r = 2\times 10^{-3}$$

The sizeable amplitude of the primordial gravitational waves requires a super-Planckian excursion of the inflaton, i.e. $\Delta\phi > M_p$. Lyth, 1996

Question

What's the big deal of super/sub-Planckian excursion?

Introduction

Answer

It is a big deal! It is a matter of the validity of our effective field theory.

$$V(\phi) = \frac{1}{2}m^2\phi^2 + \lambda\phi^4 + \sum_n c_n \cdot \frac{\phi^n}{\Lambda^{n-4}}.$$

- $\Delta\phi > M_p$, the above perturbative expansion breaks down and we lose the predictability of our theory.
- Classically arguably that $V = \frac{1}{2}m^2\phi^2$, but the higher order terms can always be generated by quantum loop correction, because inflaton has to couple to standard model field to reheat universe.

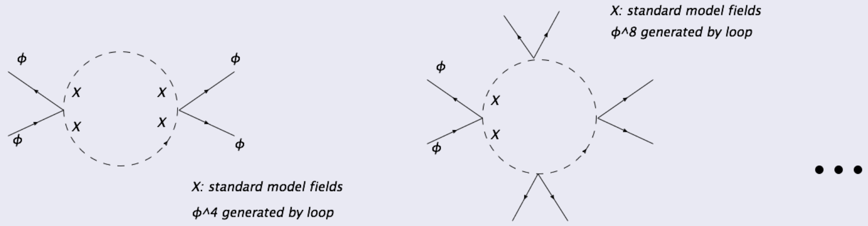

Introduction

Highlight

The detection of the primordial tensor perturbation with its amplitude larger than the threshold value $r = 2 \times 10^{-3}$ has a profound impact on our understanding of fundamental physics.

During early epoch of universe,

1. Quantum field theory needs to be modified???
2. General relativity needs to be modified???

Here we modify gravity.

Introduction

The idea

Minimally extend GR to a theory with non-vanishing graviton mass.

1. Scalar modes are the same as GR + single field slow roll inflation;
2. Vector modes remain non-dynamical, the same as GR;
3. Tensor modes receive a mass correction.

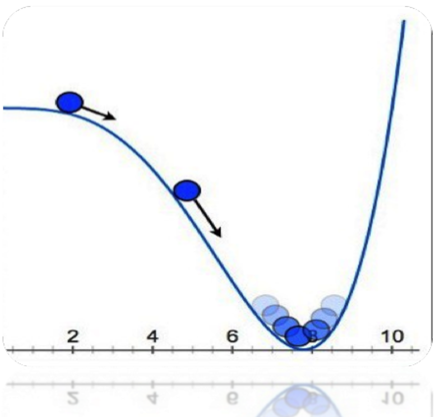

graviton mass $m_g^2(\phi)$: coherent oscillation of inflaton during reheating leads to coherent oscillation of graviton mass, and gives rise to the resonant amplification of primordial gravitational waves.

III. Minimally Extended Inflation in Massive Gravity

Massive Gravity Theories: one of workable examples

- We consider a massive gravity theory with 2+1=3 d.o.f

$$S = M_p^2 \int d^4x\sqrt{-g}\left[\frac{1}{2}\mathcal{R} + m_g^2\mathcal{F}\left(N,\ h^{ij}\right)\right].$$

General covariance is non-linearly recovered by 4 *Stückelberg* fields

$$\varphi^0 = f(t), \quad \varphi^i = x^i, \quad i = 1, 2, 3.$$

with internal symmetry

$$\varphi^i \to \Lambda^i_j\varphi^j, \qquad \varphi^i \to \varphi^i + \xi^i\left(\varphi^0\right).$$ Dubovsky 2004

At 1st derivative level, there are 2 ingredients respect the symmetry,

$$\begin{aligned} X &= g^{\mu\nu}\partial_\mu\varphi^0\partial_\nu\varphi^0 = N^{-2}, \\ Z^{ij} &= g^{\mu\nu}\partial_\mu\varphi^i\partial_\nu\varphi^j - \frac{g^{\mu\nu}\partial_\mu\varphi^0\partial_\nu\varphi^i \cdot g^{\lambda\rho}\partial_\lambda\varphi^0\partial_\rho\varphi^j}{X} = h^{ij}. \end{aligned}$$

Massive inflation

- To minimize our model, we identify the time-like *Stückelberg* field with inflaton scalar $\varphi^0 = \phi$. We write down the action with enhanced global symmetry $\varphi^i \to \text{constant} \cdot \varphi^i$,

$$S = \int d^4x\sqrt{-g}\left[\frac{M_p^2}{2}\mathcal{R} - \frac{1}{2}g^{\mu\nu}\partial_\mu\phi\partial_\nu\phi - V(\phi) - \frac{9}{8}M_p^2 m_g^2(\phi)\frac{\bar{\delta}Z^{ij}\bar{\delta}Z^{ij}}{Z^2}\right],$$

  - $\bar{\delta}Z^{ij}$ is a traceless tensor defined by

$$\bar{\delta}Z^{ij} \equiv Z^{ij} - 3\frac{Z^{ik}Z^{kj}}{Z},$$

    thus it doesn't contribute to the background energy momentum tensor.
  - We assume the functional dependence of graviton mass

$$m_g^2(\phi) = \frac{\lambda\phi^2}{1+(\phi/\phi_*)^4},$$

    without losing generality, we assume $\phi = 0$ after reheating.

Massive inflation

- As usual, we consider a flat FLRW background,

$$ds^2 = -dt^2 + a^2 d\mathbf{x}^2.$$

- Due to the $SO(3)$ symmetry, we can decompose the metric perturbation into scalar, vector, and tensor modes. These modes are completely decoupled at linear order,

$$\begin{aligned} g_{00} &= -(1+2\alpha)\ , \\ g_{0i} &= a(t)\left(S_i + \partial_i\beta\right)\ , \\ g_{ij} &= a^2(t)\left[\delta_{ij} + 2\psi\delta_{ij} + \partial_i\partial_j E + \frac{1}{2}(\partial_i F_j + \partial_j F_i) + \gamma_{ij}\right]\ , \end{aligned}$$

  - α, β, ψ and E are scalar;
  - S_i and F_i are vectors, $\partial_i S^i = \partial_i F^i = 0$;
  - γ_{ij} is tensor $\gamma^i_i = \partial_i\gamma^{ij} = 0$.

Massive Inflation: tensor perturbation

- The 2nd action for the tensor perturbation reads (with FRW ansatz)

$$S_T^{(2)} = \frac{M_p^2}{8}\int dtd^3xa^3\left[\dot{\gamma}_{ij}\dot{\gamma}^{ij} - \left(\frac{k^2}{a^2} + m_g^2\right)\gamma_{ij}\gamma^{ij}\right].$$

We see that the graviton receives a mass correction. We quantize the tensor mode as

$$\gamma_{ij}(x) = \sum_{s=\pm}\int d^3k\left[a_{\boldsymbol{k}}e_{ij}(\boldsymbol{k},s)\gamma_k e^{i\boldsymbol{k}\cdot\boldsymbol{x}} + h.c.\right],$$

$a_{\boldsymbol{k}}$ is the annihilation operator
$e_{ij}(\boldsymbol{k},s)$ is the polarization tensor $e_{ij}(k,s)e^{ij}(k,s') = \delta_{ss'}$.

- The equation of motion for the tensor modes reads

$$\ddot{\gamma}_k + 3H\dot{\gamma}_k + \left(\frac{k^2}{a^2} + m_g^2\right)\gamma_k = 0.$$

Massive Inflation: tensor perturbation

- During inflation stage,

$$m_g^2 \simeq \lambda\phi_*^2(\phi_*/\phi_i)^2 \sim H^2\epsilon \ll H_i^2.$$

It also avoids the exponential suppression due to the mass term. The inflationary tensor spectrum is calculated by

$$\mathcal{P}_\gamma = \frac{2H^2}{\pi^2M_p^2}\left(\frac{k}{aH}\right)^{2m_g^2/3H^2},$$

with the tilt

$$n_t \simeq -2\epsilon + \frac{2m_g^2}{3H_i^2},$$

where $\epsilon \equiv -\dot{H}/H^2$ is the slow-roll parameter.
Significantly, the tensor spectrum has the blue tilt if $m_g^2 > 3H^2\epsilon$.

Massive Inflation: tensor perturbation

- At the reheating stage, the inflaton oscillates around the potential minimum, and gradually decays to radiation,

$$V(\phi) \simeq \frac{1}{2} M^2 \phi^2 + \cdots .$$

where M is the mass of the inflaton during reheating.
Asymptotically for large $Mt \gg 1$, we have

$$\phi_r \simeq \frac{\phi_*}{\sqrt{3\pi} Mt} \sin(Mt) \exp\left(-\frac{1}{2}\Gamma Mt\right),$$

where subscript "r" stands for "reheating", and $e^{-\Gamma Mt}$ characterize the decay of inflation during reheating.

- The EoM of gravitational waves becomes a Mathieu-type equation,

$$\frac{d^2\gamma_k}{dx^2} + \frac{2}{x}\frac{d\gamma_k}{dx} + \frac{\xi \cdot e^{-\Gamma x}}{x^2} \sin^2(x)\gamma_k = 0,$$

where $x \equiv Mt$ and $\xi \equiv \frac{\lambda \phi_*^2}{3\pi M^2}$.
$\frac{\xi \cdot e^{-\Gamma x}}{x^2} \gg 1$ gives rise to broad parametric resonance.

Massive Inflation: tensor perturbation

remark I

- To avoid the exponential suppression,
  the graviton mass $\ll$ Hubble constant during inflation;
- To have broad parametric resonance,
  the graviton mass $\gg$ Hubble constant during reheating;

Both of two conditions could be easily satisfied if $\phi_* \ll M_p$. It is also the condition of validity of our EFT, which is automatically satisfied for many small field inflationary models.

remark II

The functional dependence of m_g^2 doesn't have to be $m_g^2(\phi) = \frac{\lambda\phi^2}{1+(\phi/\phi_*)^4}$.
It would be very interesting to ask what kind of coupling form could be naturally induced from some more fundamental theory.

Massive Inflation: tensor perturbation

- We numerically solve the Mathieu equation

$$\frac{d^2\gamma_k}{dx^2} + \frac{2}{x}\frac{d\gamma_k}{dx} + \frac{\xi \cdot e^{-\Gamma x}}{x^2}\sin^2(x)\gamma_k = 0,$$

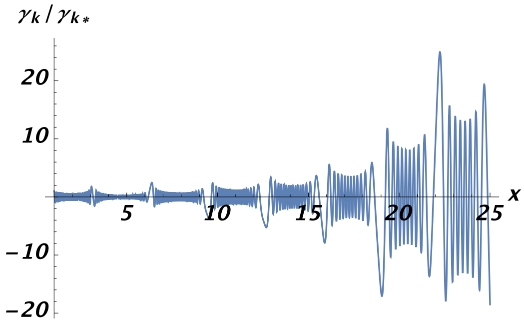

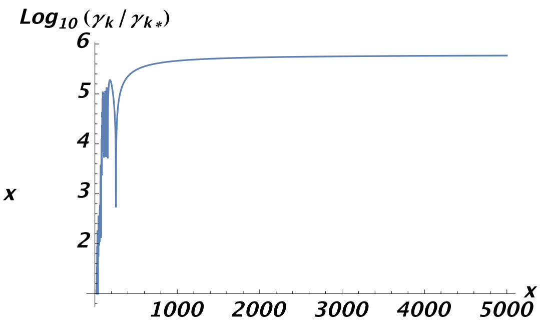

The horizontal axis is $x \equiv Mt$ and the vertical axis is the relative amplitude of the tensor modes γ_k/γ_{k*}. The parameters are $\xi = 10^6$ and $\Gamma = 0.05$, with the initial condition $d\gamma_k/dx|_{x=1} = 0$.

Massive Inflation: tensor perturbation

- Resonant amplification factor depends on 2 parameters: ξ and Γ,

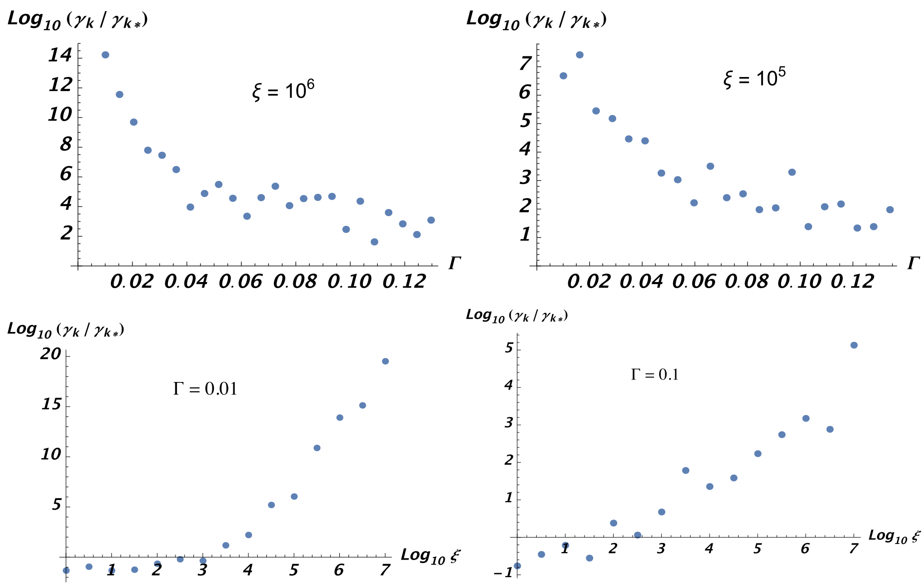

The vertical axes is $Log_{10}(\gamma_k/\gamma_{k*})$ evaluated at $x = 1000$.

Massive Inflation: tensor perturbation

Several remarks

- The tensor power spectrum is almost scale-invariant, as long as the graviton mass during inflation is small enough,

$$\mathcal{P}_\gamma^{obs} = A \times \mathcal{P}_\gamma^{inf} = A \times \frac{2H^2}{\pi^2 M_p^2}\left(\frac{k}{aH}\right)^{2m_g^2/3H^2},$$

  where A is the resonant amplification factor, it is normally very large.
- After reheating, inflaton stays at the bottom of potential and thus $m_g^2 \to 0$.
  - Scalar and tensor modes just simply decouple in the limit $m_g^2 \to 0$;
  - There is no vDVZ discontinuity (Dubovsky, 2004);

  Therefore GR is recovered after reheating.
- We have checked that vector modes remain non-dynamical, the same as the ones in GR.

Massive inflation: vector perturbation

- We adopt the unitary gauge, the fluctuations of $SO(3)$ *Stückelberg* scalar fields $\delta\varphi^i = 0$. The 2nd action of the vector perturbation reads

$$S_V^{(2)} = \frac{1}{16}M_p^2 \int a^3k^2\left[\dot{F}_i\dot{F}_i - m_g^2 F_iF_i - \frac{4S_i\dot{F}_i}{a} + \frac{4S_iS_i}{a^2}\right].$$

  Varying this action with respect to S_i gives rise to a constraint

$$S_i = \frac{1}{2}a\dot{F}_i.$$

  Using this solution back in the action, we get

$$S_V^{(2)} = -\frac{1}{16}M_p^2 m_g^2 \int a^3k^2F_iF_i.$$

  Kinetic term for vector perturbation was canceled out. It is by no mean of an accident, because the kinetic term of vector modes are prohibited by internal symmetry $\varphi^i \to \varphi^i + \xi^i\left(\varphi^0\right)$.

Massive inflation: scalar perturbation

- The scalar perturbations

$$\begin{aligned} g_{00} &= -(1+2\alpha) \ , \qquad g_{0i} = a(t)\partial_i\beta \ , \\ g_{ij} &= a^2(t)\left[\delta_{ij} + 2\psi\delta_{ij} + \partial_i\partial_j E\right] \ , \end{aligned}$$

Integrate out the non-dynamical modes, we get (in the $\delta\phi = 0$ gauge)

$$S_s^{(2)} = M_p^2 \int a^3\epsilon\left(\dot{\psi}^2 - \frac{k^2}{a^2}\psi^2\right),$$

Exactly the same as GR + a single scalar field. In this gauge, ψ is identical to the curvature perturbation on the comoving slicing, $\mathcal{R}_c$, and the power spectrum is given by

$$\mathcal{P}_{\mathcal{R}} = \frac{H^2}{8\pi^2\epsilon M_p^2}.$$

Sasaki 1986, Mukhanov 1988

Massive inflation: scalar perturbation

- Thus the tensor-to-scalar ratio we observe today is

$$r = \frac{A \times \mathcal{P}_\gamma^{inf}}{\mathcal{P}_{\mathcal{R}}} = 16\epsilon \times A,$$

where A is the resonant amplification factor of the tensor modes during reheating. Thus during 60 e-folds, ϕ traverses a distance

$$\Delta\phi \simeq 15M_p\sqrt{2r/A}.$$

We conclude that the Lyth bound can be explictly evaded!

Summary and Outlook

Summary

Minimally extend GR to a theory with non-vanishing graviton mass.

- Scalar modes are the same as GR + single field slow roll inflation;
- Vector modes remain non-dynamical, the same as GR;
- Tensor modes receive a mass correction. Graivton mass term couples to inflaton, the coherent oscillations of inflaton resonantly amplifies tensor modes during reheating.

Outlook

- At non-linear level, we expect new scalar-scalar and scalar-tensor interaction and interesting features on primordial non-Gaussianity.
- With Chern-Simons term $\mathcal{L}_{CS} \simeq \frac{g}{f}\phi\mathcal{R}\tilde{\mathcal{R}}$ taken into account, we expect a massive resonant production of chiral gravitational waves during reheating. What's its influence to lepto-genesis?
- ... ...

Thanks you!

"Scale-dependent gravitational waves from a rolling axion"

by Ryo Namba

[JGRG25(2015)3b3]

Scale-dependent gravitational waves from a rolling axion

Ryo Namba

Kavli IPMU

The 25th Workshop on General Relativity and Gravitation (JGRG24)
YITP, Kyoto University
December 8, 2015

RN, Peloso, Shiraishi, Sorbo & Unal, arXiv:1509.07521
Mukohyama, RN, Peloso & Shiu, JCAP **1408**, 036 (2014), arXiv:1405.0346
Barnaby, Moxon, RN, Peloso, Shiu & Zhou, Phys. Rev. D **86**, 103508 (2012), arXiv:1206.6117

Outline

1. Introduction
2. Our model
   - Gauge field production
   - Sourcing scalar and tensor
3. Phenomenology
   - Scalar constraints
   - Scale-dependent, parity-violating GW signatures

Outline

1. Introduction
2. Our model
   - Gauge field production
   - Sourcing scalar and tensor
3. Phenomenology
   - Scalar constraints
   - Scale-dependent, parity-violating GW signatures

Introduction

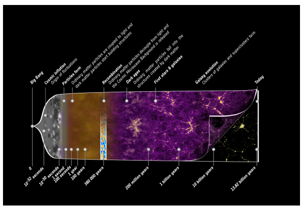

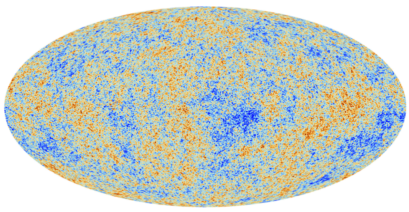

- **Inflation** $\sim$ dominant paradigm for the physics in the primordial universe
- Standard prediction for **gravitational waves (GWs)** from inflation

$$P_{\rm GW}(k) = \left.\frac{2H^2}{\pi^2 M_p^2}\right|_{k=aH} , \qquad E_{\rm inflation} \cong 10^{16}\,{\rm GeV}\left(\frac{r}{0.01}\right)^{1/4}$$

  - Considered as robust evidence of inflation
  - Direct probe of inflationary energy scale
  - Almost scale invariant, slightly red $\sim$ decreasing H
  - If detected, strong evidence for the existence of (quantized) graviton

Crucial assumption

Source of GWs $=$ **vacuum fluctuations** of graviton

A large number of experimental/observational efforts

- Planck, POLARBEAR, BICEP/Keck Array, SPIDER, . . .
- LiteBIRD, Simons Array, EBEX, PIXIE, . . .
- Future experiments aims for $\sigma(r) = \mathcal{O}\left(10^{-3}\right)$

Question of interest

How robust would P $\propto$ H^2 be upon detection?

Sources of Gravitational Waves

$$\left[\frac{\partial^2}{\partial\tau^2} - \nabla^2 - \frac{a''}{a}\right](a\,h_{ij}) = S_{ij} \propto T_{ij}^{TT}$$

Other sources of GW, uncorrelated with the standard vacuum fluctuations

- **Phase transitions**: vacuum bubble collisions, turbulence, . . .
- **Particle production**: interactions in inflationary scenarios
  - Inflaton couplings are necessary for reheating

Such sources might spoil the curvature perturbations

- Approximate scale invariance $\quad n_s = 0.968 \pm 0.006$
- Gaussianity $\quad f_{\rm NL}^{\rm local} = 2.5 \pm 5.7\,,\quad f_{\rm NL}^{\rm equil} = -16 \pm 70\,,\quad f_{\rm NL}^{\rm ortho} = -34 \pm 33$

Planck ’15

Must respect these observational bounds

Outline

1. Introduction
2. Our model
   - Gauge field production
   - Sourcing scalar and tensor
3. Phenomenology
   - Scalar constraints
   - Scale-dependent, parity-violating GW signatures

Criteria of Implementation

Production of particle X

- **X must be coupled to φ only gravitationally**
  - ▷ Sources GW and ζ only through gravity
- **X must be relativistic**
  - ▷ Sources GW without suppressed quadrupole
- **X must have spin $\geq$ 1**
  - ▷ To avoid spin suppression

Barnaby et al '12

$$
\begin{tikzcd}
 & & \delta\varphi \sim \zeta \\
\dot{\sigma}^{(0)} \arrow[r, "\textbf{direct}"] & X \arrow[ur, "\textbf{grav.}"] \arrow[dr, "\text{grav.}"'] & \\
 & & \text{GW}
\end{tikzcd}
$$

Concrete Model

Our model

$$\mathcal{L} = \mathcal{L}_{\text{inflaton}} - \frac{1}{2}(\partial\sigma)^2 - V(\sigma) - \frac{1}{4}F^2 - \frac{\alpha}{4f}\sigma F\tilde{F}$$

Standard — Subdominant — Leads production

Localized production: $V(\sigma) = \frac{\Lambda^4}{2}\left(1 + \cos\frac{\sigma}{f}\right)$

Slow roll: $|\ddot{\sigma}| \ll 3H|\dot{\sigma}|$

$$\frac{\sigma}{f} \cong 2\arctan\left[e^{H\delta(t-t_*)}\right], \quad \delta \equiv \frac{\Lambda^4}{6H^2f^2} \ll 3$$

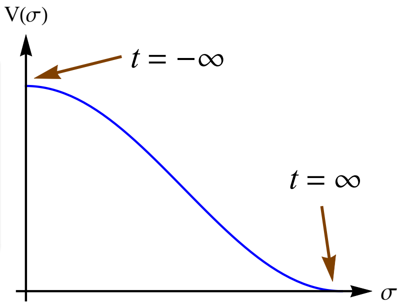

Gauge Field Production

Coupling: $\mathcal{L}_{\text{int}} = -\frac{\alpha}{4f}\sigma F\tilde{F}$

$$\frac{\partial^2}{\partial\tau^2}A_\pm + \left(k^2 \mp 2\, a\, kH\, \xi\right)A_\pm = 0$$

Coupling strength

$$\xi \equiv \frac{\alpha\,\dot{\sigma}}{2\,f\,H} \cong \frac{\xi_*}{\cosh\left[H\delta\,(t-t_*)\right]}$$

- Parity violation
- Derivative coupling

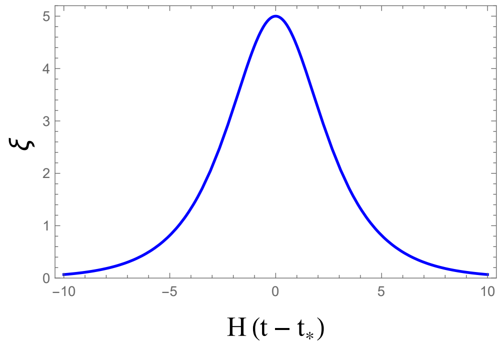

Exponential production

only for one helicity state

at horizon crossing

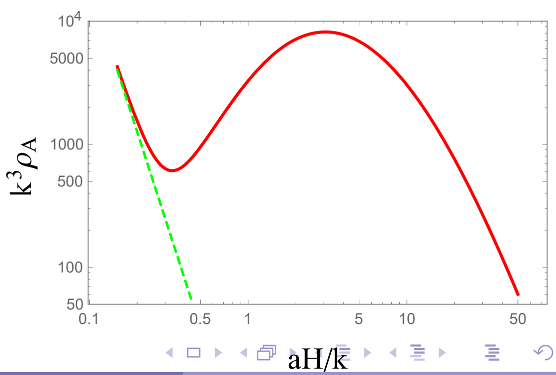

Sourcing Scalar and Tensor Perturbations

Sourcing by the produced particles to

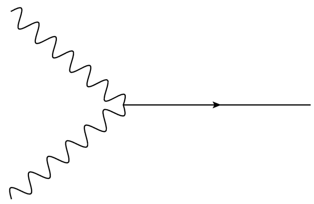

Scalar perturbations

$$\zeta \cong -\frac{H}{\dot{\phi}}\,\delta\phi$$

$$\left(\frac{\partial^2}{\partial\tau^2} - \nabla^2 + \mathcal{M}^2_{\phi\phi}\right)(a\,\delta\phi) + \mathcal{M}^2_{\phi\sigma}\,(a\,\delta\sigma) = -\frac{a^3\dot{\phi}}{4M_p^2 H}\left(\vec{E}\cdot\vec{E} + \vec{B}\cdot\vec{B}\right)$$

$$\left(\frac{\partial^2}{\partial\tau^2} - \nabla^2 + \mathcal{M}^2_{\sigma\sigma}\right)(a\,\delta\sigma) + \mathcal{M}^2_{\sigma\phi}\,(a\,\delta\phi) = \alpha\frac{a^3}{f}\,\vec{E}\cdot\vec{B}$$

Tensor perturbations

$$\delta g_{ij} = a^2\,(\delta_{ij} + h_{ij})$$

$$\left(\frac{\partial^2}{\partial\tau^2} - \nabla^2 + \mathcal{M}^2_{\phi\phi}\right)(a\,h_{ij}) = -\frac{2\,a^3}{M_p^2}\,(E_iE_j + B_iB_j)$$

Outline

1 Introduction

2 Our model
- Gauge field production
- Sourcing scalar and tensor

3 Phenomenology
- Scalar constraints
- Scale-dependent, parity-violating GW signatures

Power Spectra

$$\text{Scalar:}\quad \mathcal{P}_\zeta\,\delta^{(3)}\left(\vec{k}+\vec{k}'\right) \equiv \frac{k^3}{2\pi^2}\left\langle \zeta\left(\vec{k}\right)\,\zeta\left(\vec{k}'\right)\right\rangle$$

$$\text{Tensor:}\quad \mathcal{P}_\lambda\,\delta_{\lambda\lambda'}\,\delta^{(3)}\left(\vec{k}+\vec{k}'\right) \equiv \frac{k^3}{2\pi^2}\left\langle h_\lambda\left(\vec{k}\right)\,h_{\lambda'}\left(\vec{k}'\right)\right\rangle$$

$$\mathcal{P}_\zeta = \underbrace{\mathcal{P}_\zeta^{(0)}}_{\text{vacuum}} + \underbrace{\mathcal{P}_\zeta^{(1)}}_{\text{sourced}}\ ,\quad \mathcal{P}_\lambda = \underbrace{\mathcal{P}_\lambda^{(0)}}_{\text{vacuum}} + \underbrace{\mathcal{P}_\lambda^{(1)}}_{\text{sourced}}$$

$$\text{Decompose:}\quad \mathcal{P}_\zeta^{(1)} = \left[\epsilon_\phi \mathcal{P}_\zeta^{(0)}\right]^2 f_{2,\zeta}\left(\xi_*,\,x_*,\,\delta\right)\ ,\quad x_* \equiv \left.\frac{k}{aH}\right|_{t=t_*}$$

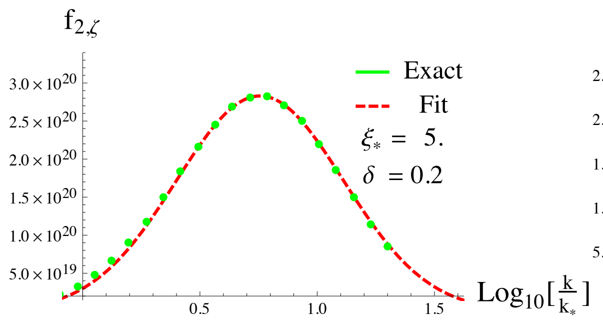

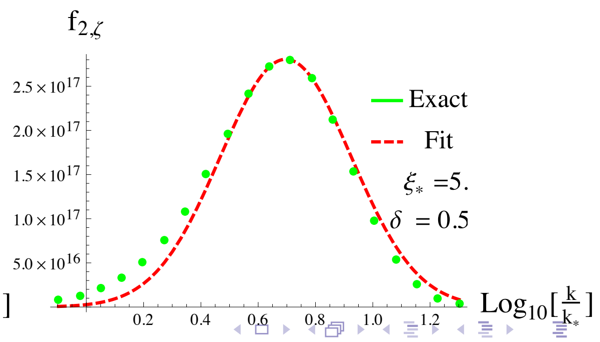

Phenomenology

- Fix all the cosmological parameters as best fit values for WMAP
- Additional parameters:

$$k_* :\ \text{controls the position of the bump} \;\rightarrow\; \text{fix}$$
$$\delta :\ \text{controls the width of the bump} \;\rightarrow\; \text{fix}$$
$$\xi_* :\ \text{controls the peak amplitude of signals} \;\rightarrow\; \text{vary}$$

- Take ξ_*, allowed by 2σ $\rightarrow$ conservative limit on ξ_*

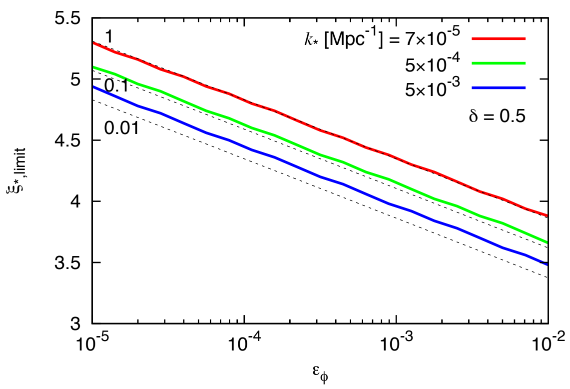

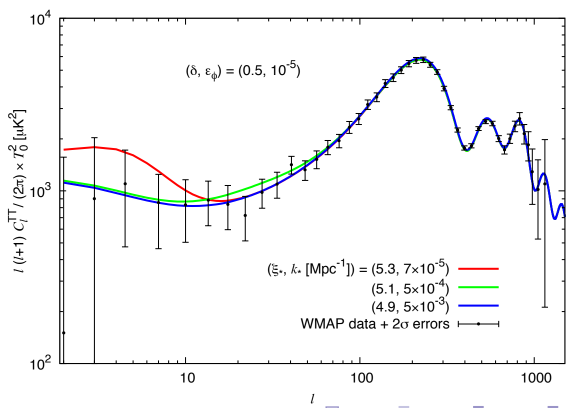

Detection of B-mode and Signal-to-Noise

Fix

$$\epsilon_\phi \equiv \frac{\dot{\phi}^2}{2M_p^2 H^2} = 10^{-5}$$

$$\delta = 0.5$$

$$k_* = \left(7 \times 10^{-5},\, 5 \times 10^{-4},\, 5 \times 10^{-3}\right) \mathrm{Mpc}^{-1}$$

$$\xi_* = \xi_{*,\mathrm{limit}}$$

Signal-to-noise: $$\left(\frac{S}{N}\right)^2_{BB} = \sum_{\ell=2}^{\ell_{\max}} \frac{2\ell+1}{2} \left(\frac{C_\ell^{BB}}{C_{\ell,\mathrm{dat}}^{BB}}\right)^2$$

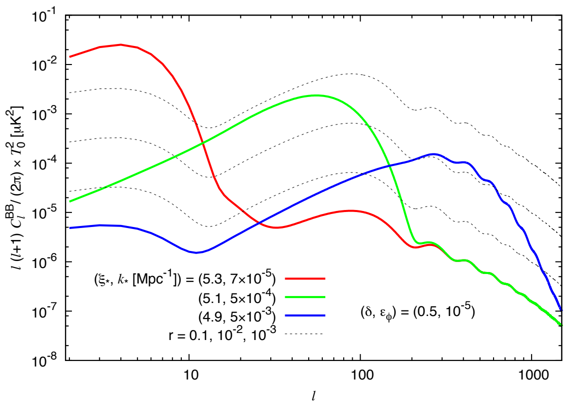

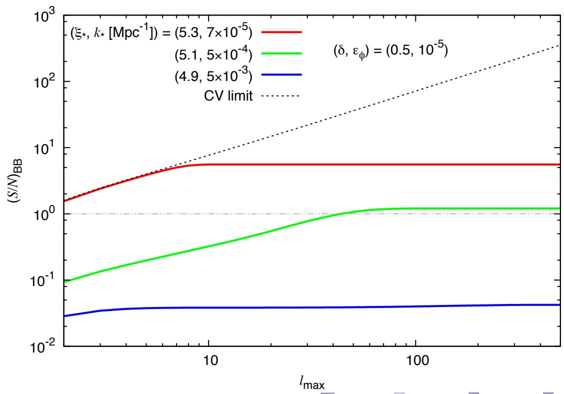

CMB Bispectra

Three-point correlation

$$\langle \zeta\zeta\zeta \rangle \cong \underbrace{\langle \zeta^{(1)}\zeta^{(1)}\zeta^{(1)} \rangle}_{\text{sourced}}, \quad \langle h_\lambda h_\lambda h_\lambda \rangle \cong \underbrace{\langle h_R^{(1)} h_R^{(1)} h_R^{(1)} \rangle}_{\text{sourced}}$$

Signal-to-noise: $$\left(\frac{S}{N}\right)^2_{BBB/TTT} = \sum_{\ell_1,\ell_2,\ell_3}^{\ell_{\max}} \frac{|B_{\ell_1\ell_2\ell_3}^{BBB/TTT}|^2}{6\, C_{\ell_1}^{BB/TT} C_{\ell_2}^{BB/TT} C_{\ell_3}^{BB/TT}}$$

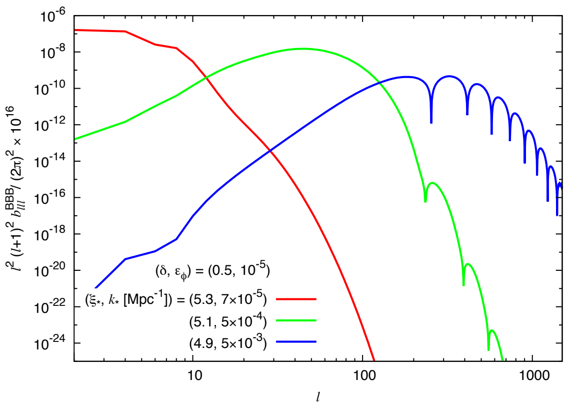

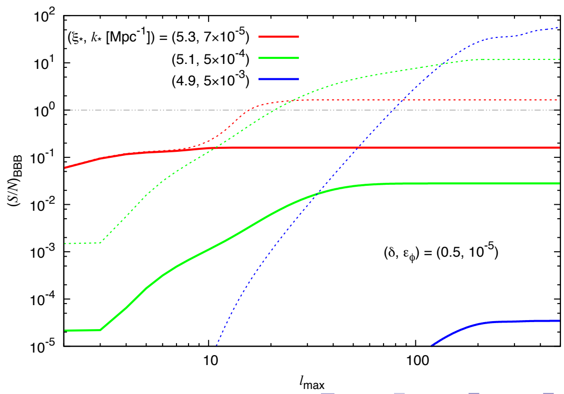

Parity Violation

$\mathcal{L}_{\rm int} = \sigma F\tilde{F}$ breaks parity for $\dot{\sigma} \neq 0$

- Only one polarization of A_μ is produced, A_+
- Only one helicity of h_λ is sourced, h_R
- Non-zero TB (EB) correlation: $\langle a^T a^B \rangle \propto \mathcal{P}_R - \mathcal{P}_L \neq 0$

Signal-to-noise: $$\left(\frac{S}{N}\right)^2_{TB} = \sum_{\ell=2}^{\ell_{\rm max}} (2\ell+1)\, \frac{\left(C_\ell^{TB}\right)^2}{C_\ell^{TT} C_{\ell,{\rm dat}}^{BB}}$$

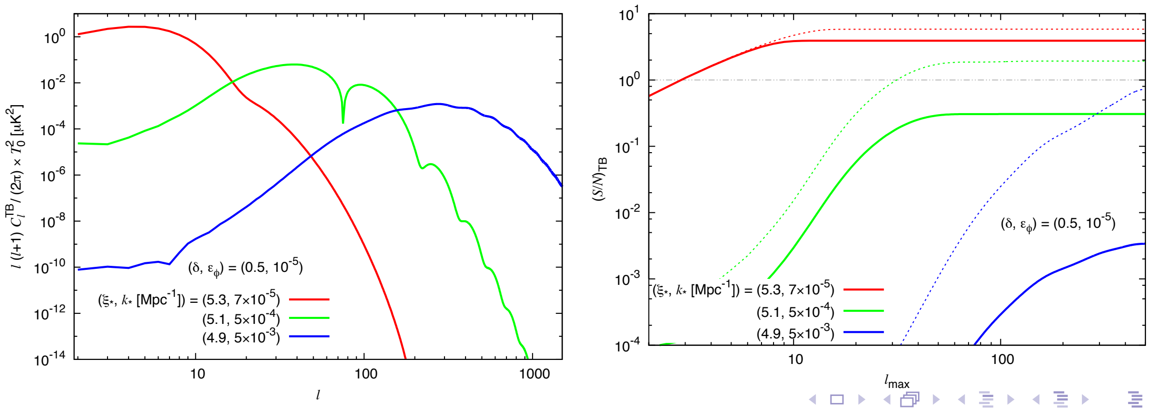

Summary and Outlook

Implications of primordial B-mode/GWs detection

- Standard notion: $E_{\rm inflation} \cong 10^{16}\,{\rm GeV} \times (r/0.01)^{1/4}$
- Future observational improvements: $\sigma(r) = \mathcal{O}\left(10^{-3}\right)$

Particle production in the sector gravitationally coupled to inflaton

$$\mathcal{L}_{\rm int} = -\frac{\alpha}{4f}\,\sigma F\tilde{F}$$

- $\dot{\sigma} \neq 0 \implies A_\mu$ production, breaking parity
- Relative change in $\dot{\sigma} \implies$ localized production

Rich phenomenological features with $S/N > 1$

- Strongly scale-dependent tensor — bump feature
- Parity-violating correlations, $\langle TB \rangle$, $\langle EB \rangle \neq 0$
- Detectable $\langle BBB \rangle$

One of the very few existing examples

- Detectable GWs at CMB scales, uncorrelated with vacuum fluctuations
- Respecting all the strong limits from T modes of CMB

“Axion Bosenova and Gravitational Waves”

by Hirotaka Yoshino

[JGRG25(2015)3b4]

Axion Bosenova
and
Gravitational Waves

Hirotaka Yoshino
Hideo Kodama (KEK)

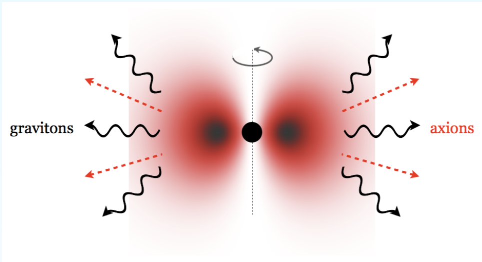

PTP128, 153 (2012);
PTEP2014, 043E02 (2014);
PTEP2015, 061E01 (2015);
CQG32, 214001 (2015).

JGRG25 @ Yukawa Institute at Kyoto University
(Dec 8, 2015)

Contents

- Introduction
- l = m = 1 mode axion cloud

HY and Kodama., arXiv:1505.00714, published in CQG.

- l = m = 2 mode axion cloud
- Summary

Introduction

System of a BH and a scalar field

- AXIVERSE scenario   Arvanitaki et al., PRD81 (2010), 123530.

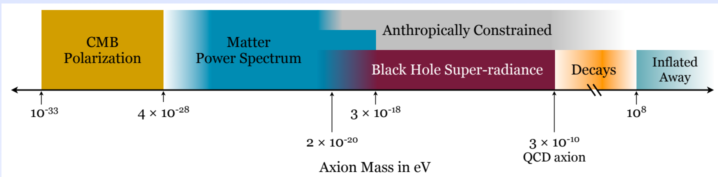

- Interesting phenomena

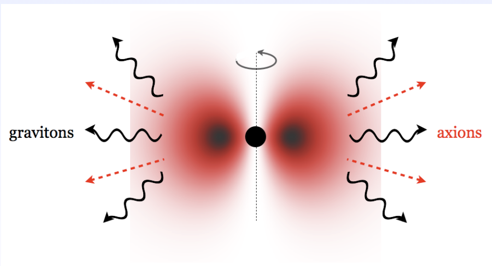

Superradiant instability & BH bomb

- Gravitational waves could be detected

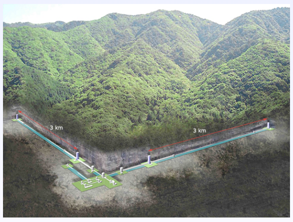

Kerr BH

- Metric

$$ds^2 = -\left(\frac{\Delta - a^2\sin^2\theta}{\Sigma}\right)dt^2 - \frac{2a\sin^2\theta(r^2+a^2-\Delta)}{\Sigma}dtd\phi + \left[\frac{(r^2+a^2)^2-\Delta a^2\sin^2\theta}{\Sigma}\right]\sin^2\theta d\phi^2 + \frac{\Sigma}{\Delta}dr^2 + \Sigma d\theta^2$$

$$\Sigma = r^2 + a^2\cos^2\theta,$$
$$\Delta = r^2 + a^2 - 2Mr.$$

$$J = Ma$$

- Ergo region

$\xi = \partial_t$ becomes spacelike:

$$\xi_a\xi^a = g_{tt} > 0$$

$$E = -p_a\xi^a$$

can be negative

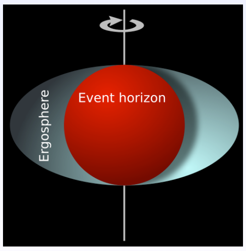

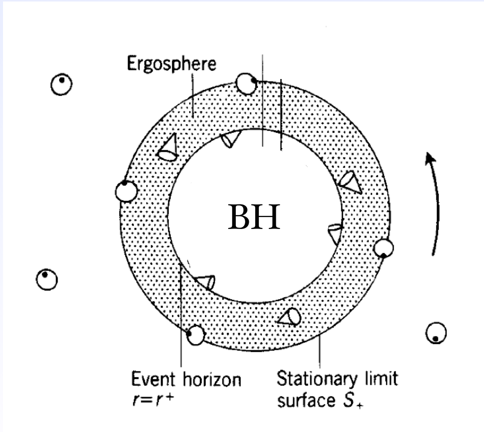

Gravitational Atom

- Massive Klein-Gordon field $\nabla^2\Phi - \mu^2\Phi = 0$

$$\Phi = \mathrm{Re}[e^{-i\omega t}R(r)S(\theta)e^{im\phi}]$$
$$R = \frac{u}{\sqrt{r^2+a^2}}$$

$$\frac{d^2u}{dr_*^2} + \left[\omega^2 - V(\omega)\right]u = 0$$

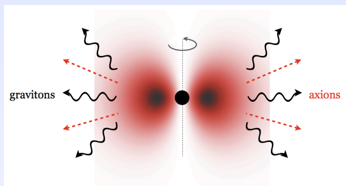

$$\omega = \omega_R + i\,\boxed{\omega_I}$$ Unstable if positive

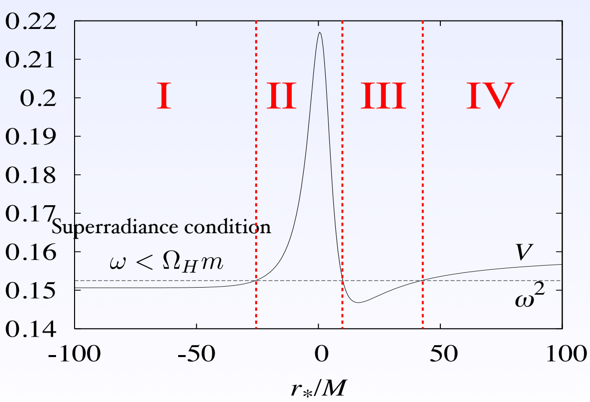

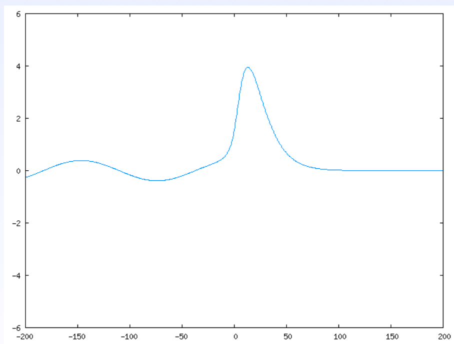

Growth rates

- Calculation by continued fraction method

HY and Kodama., arXiv:1505.00714.

Superradiance condition

$$\omega < \Omega_H m$$
$$\wr\wr$$
$$\mu$$

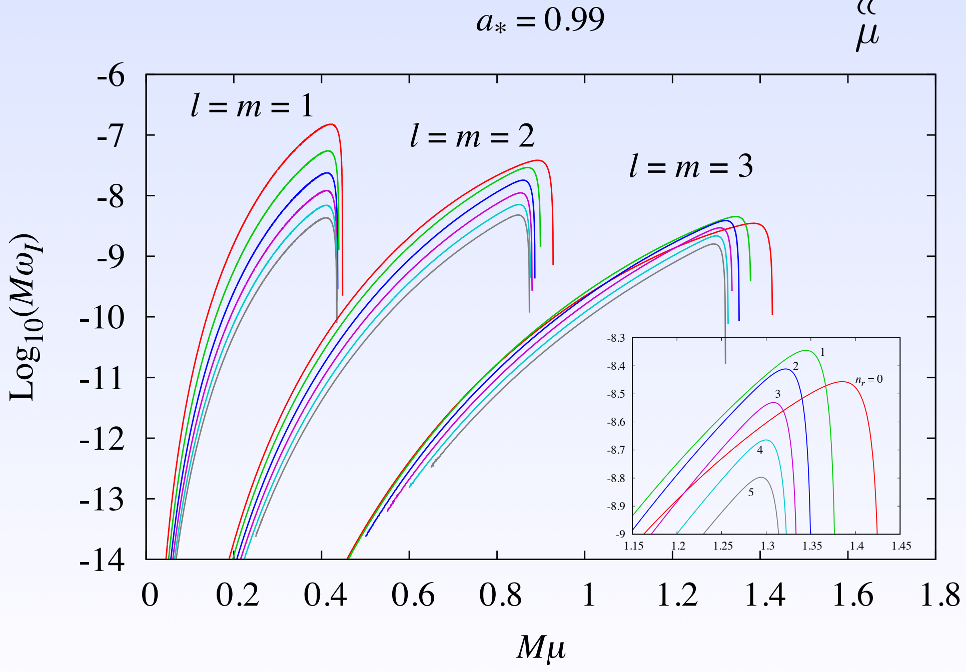

Issues to be considered

- Effect of nonlinear self-interaction

$$V = f_a^2 \mu^2 [1 - \cos(\Phi/f_a)]$$

$$\Rightarrow \quad \boxed{\nabla^2 \varphi - \mu^2 \sin\varphi = 0} \qquad \varphi \equiv \frac{\Phi}{f_a}$$

- Emission of gravitational waves

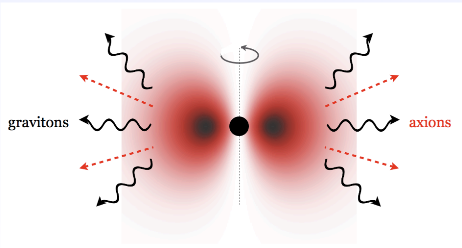

Current status (codes)

- Code to simulate scalar field

  ➪ Fiarly good codes have been developed to simulate scalar field as a test field in the Kerr space-time background with arbitrary rotation parameter.

- Code to simulate GW emission

  ➪ We calculate GWs generated by energy-momentum tensor of the scalar field by solving Teukolsky equation in time domain.

  We have developed the code for the case that the BH is non-rotating.

  HY and Kodama., arXiv:1505.00714.

Current status (results)

- l = m = 1 mode

  ➪ Scalar field : Bosenova occurs,

  GWs : Burst GWs are emitted
  (Indication from Schwarzschild case)

- l = m = 2 mode

  ➪ Scalar field: No bosenova happens,

  GWs: No burst GWs are emitted.
  (Indication from Schwarzschild case)

l = m = 1 mode axion cloud

Simulation (scalar field + GWs)

- Setup HY and Kodama., arXiv:1505.00714.
  - The BH is a Schwarzschild BH
  - $M\mu = 0.3$
  - Initial condition is a quasibound state of Klein-Gordon field with l = m = 1, nr=0
  - Initial amplitude of the scalar field is $\sim$ 0.5

GW emission during “bosenova” (Schwarzschild)

Scalar field

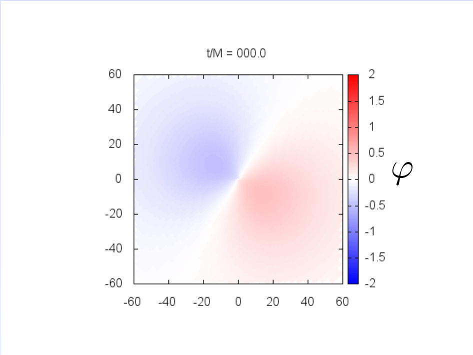

GWs

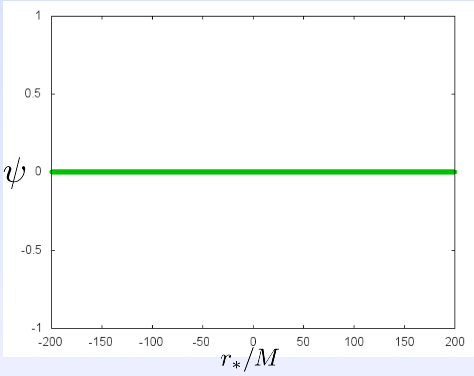

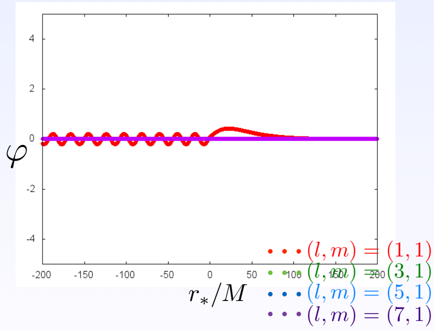

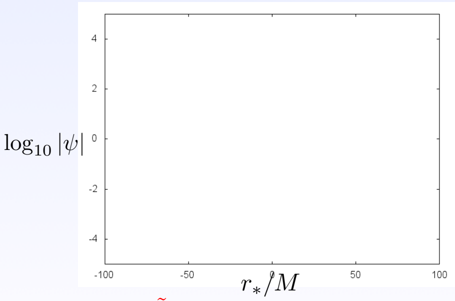

$\cdots$ $(\tilde{\ell}, \tilde{m}) = (2,2)$, real part

$\cdots$ $(\tilde{\ell}, \tilde{m}) = (2,2)$, imaginary part

GW emission during “bosenova” (Schwarzschild)

Scalar field

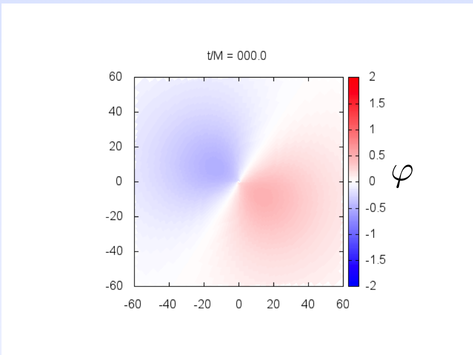

GWs

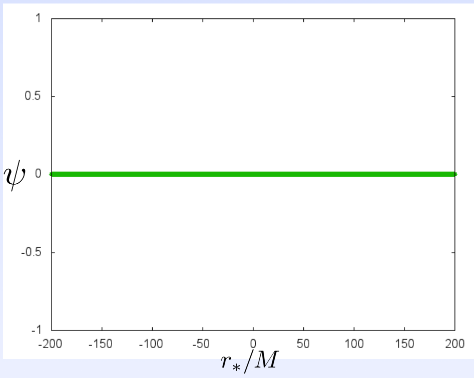

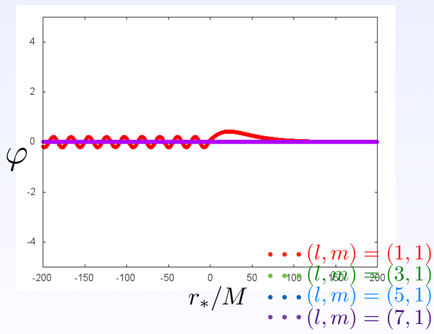

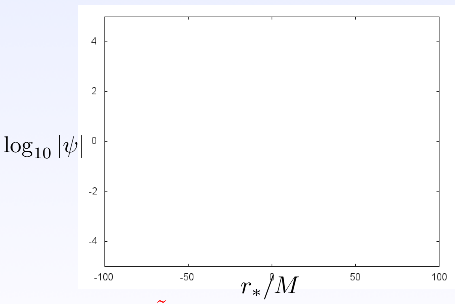

$\cdots$ $(\tilde{\ell}, \tilde{m}) = (2,2)$, real part

$\cdots$ $(\tilde{\ell}, \tilde{m}) = (2,2)$, imaginary part

l = m = 2 mode axion cloud

Simulation (scalar field)

- Setup

HY and Kodama., arXiv:1505.00714.

  - The BH is a rapidly rotating Kerr BH $a/M = 0.99$
  - $M\mu = 0.8$
  - Initial condition is a quasibound state of Klein-Gordon field with l = m = 2, nr=0
  - The initial amplitude is ~ 1

Simulation result (1)

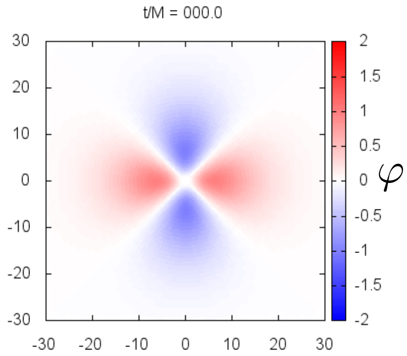

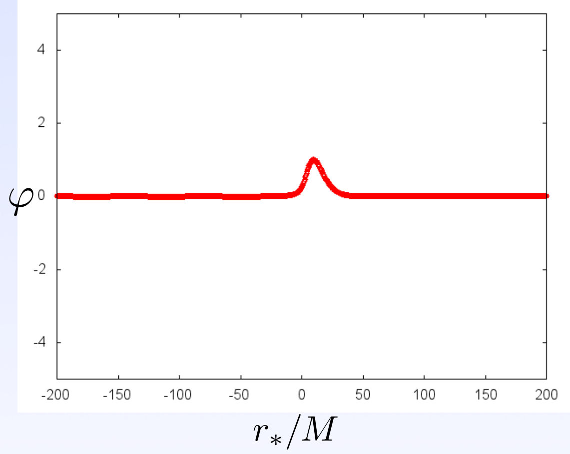

Simulation result (1)

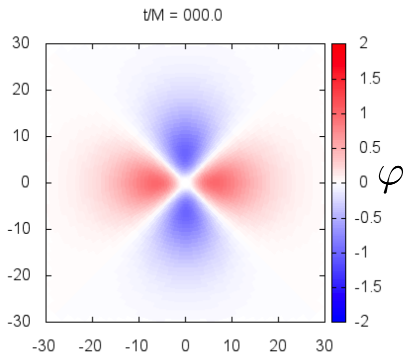

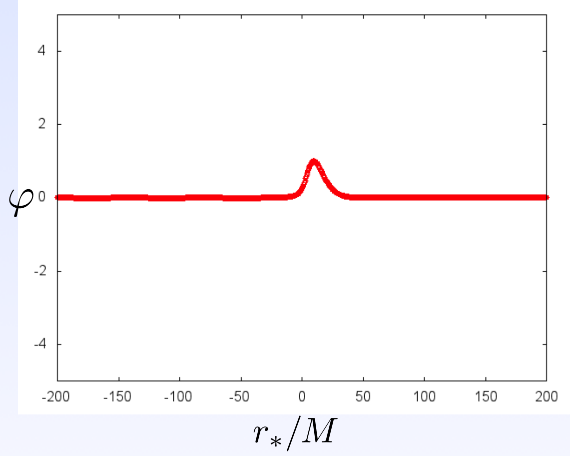

Result of simulation (2)

- The energy and angular momentum continue to be extracted.

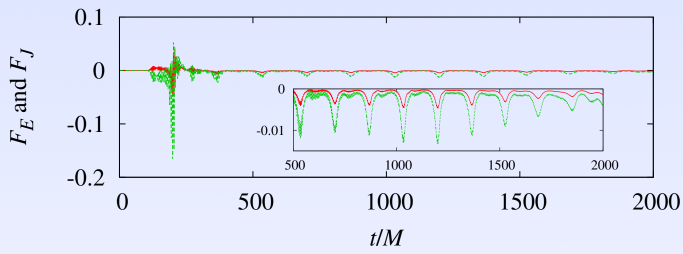

- Energy and angular momentum continues to be emitted to the distant place.

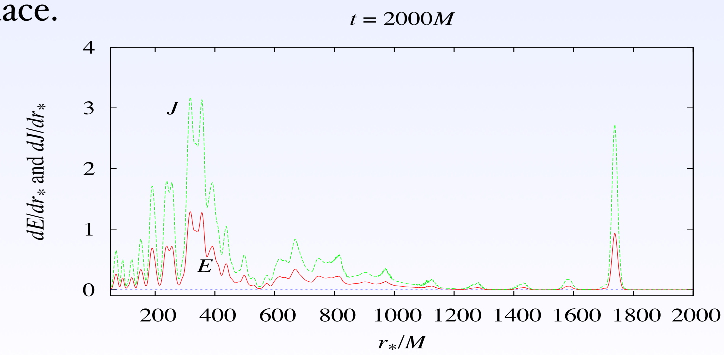

Simulation (scalar field + GWs)

- Setup **TEST SIMULATION**
  - The BH is a Schwarzschild BH
  - $M\mu = 0.6$
  - Initial condition is a quasibound state of Klein-Gordon field with l = m = 2, nr=0
  - Initial amplitude of the scalar field is $\sim$ 0.5

GWs from l = m = 2 axion cloud (Schwarzschild)

TEST SIMULATION

Scalar field

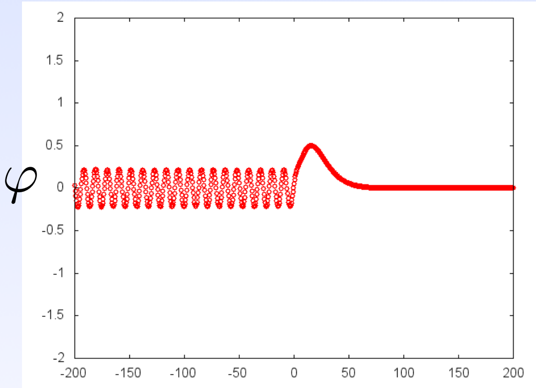

r_*/M

GWs

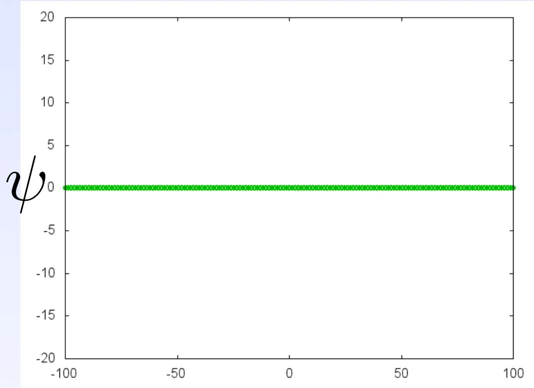

r_*/M

$\cdots\ (\ell, m) = (2, 2)$

$\cdots\ (\tilde{\ell}, \tilde{m}) = (4, 4),$ real part

$\cdots\ (\tilde{\ell}, \tilde{m}) = (4, 4),$ imaginary part

GWs from l = m = 2 axion cloud (Schwarzschild)

TEST SIMULATION

Scalar field

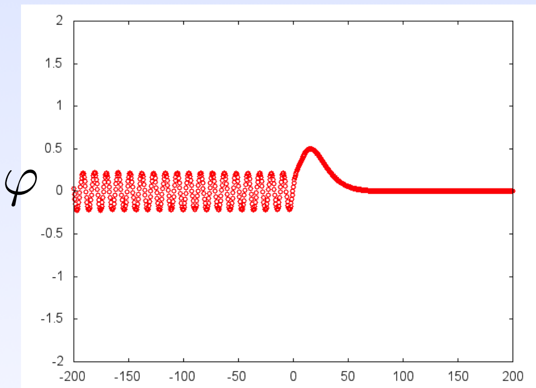

r_*/M

GWs

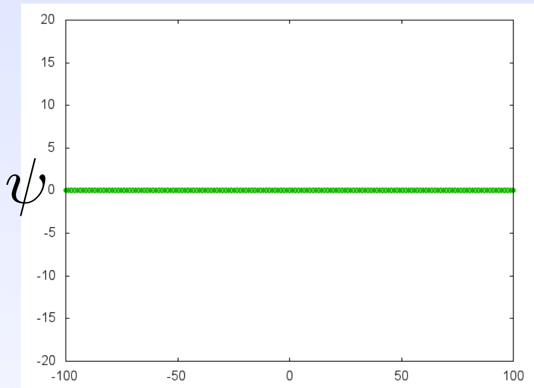

r_*/M

$\cdots\ (\ell, m) = (2, 2)$

$\cdots\ (\tilde{\ell}, \tilde{m}) = (4, 4),$ real part

$\cdots\ (\tilde{\ell}, \tilde{m}) = (4, 4),$ imaginary part

Summary

Summary

The phenomena caused by the scalar field nonlinear self-interaction strongly depend on its mode

- l = m = 1 mode

  ⇨ Scalar field : Bosenova occurs,

  GWs : Burst GWs are emitted.

- l = m = 2 mode

  ⇨ Scalar field: No bosenova happens,

  GWs: No burst GWs are emitted.

Thank you!

“Primordial Chiral Gravitational Waves from a Non-Abelian Gauge Field”

by Ippei Obata

[JGRG25(2015)3b5]

Primordial Chiral Gravitational Waves from a Non-Abelian Gauge Fields

Ippei Obata (Kyoto Univ.)

Collaborator: Jiro Soda (Kobe Univ.)

(working in progress)

JGRG25

Introduction

Primordial GWs from an early Universe

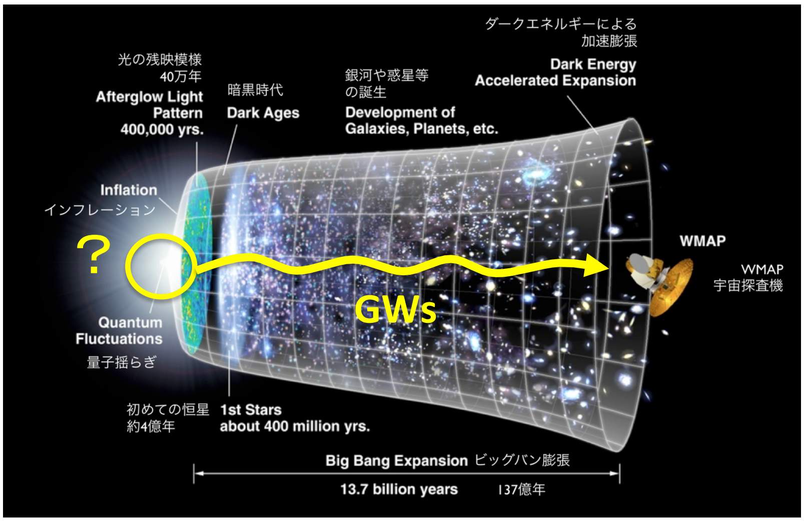

Inflationary energy scale (single field)

$$\Lambda \simeq \underline{10^{16}}\mathrm{GeV}\left(\frac{r}{0.01}\right)^{1/4} \longleftarrow$$

High energy physics?

Primordial GWs from an early Universe

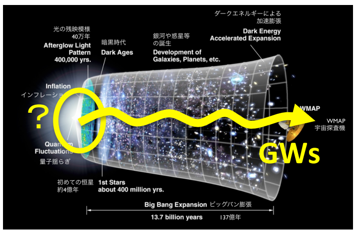

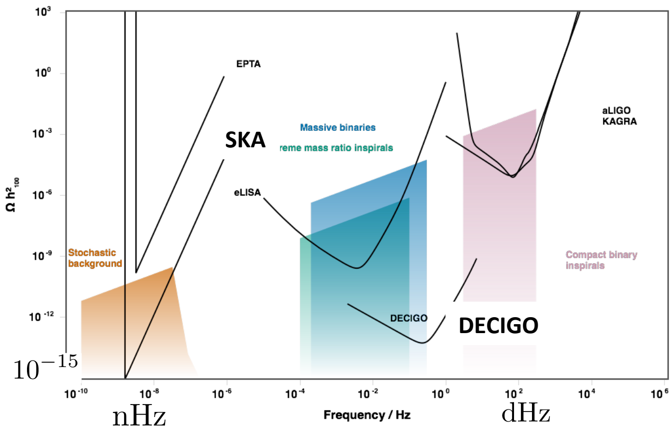

http://rhcole.com/apps/GWplotter/

Energy density of GWs (single field)

$$h_0^2\Omega_{\mathrm{gw}}(f) \simeq \underline{10^{-17}}\left(\frac{\Lambda}{10^{16}\mathrm{GeV}}\right)^4$$

Less detectable…

Fundamental theory $\xrightarrow{?}$ **PGWs**

- ✧ **Detectable amplitude**
- ✧ **Unique property**

Primordial GWs from an early Universe

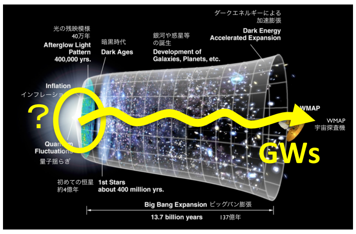

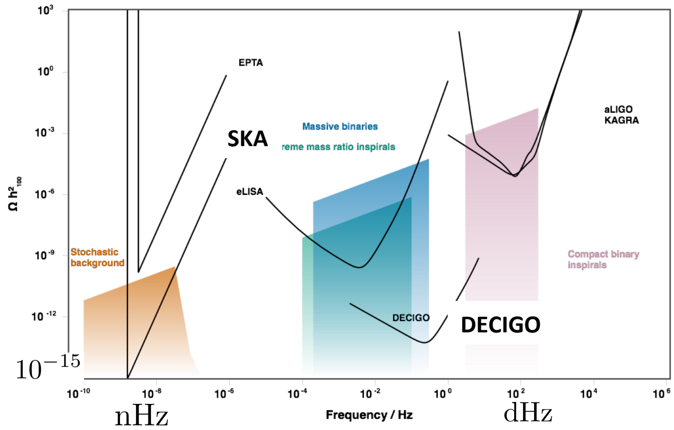

http://rhcole.com/apps/GWplotter/

Energy density of GWs (single field)

$$h_0^2\Omega_{\rm gw}(f) \simeq 10^{-17}\left(\frac{\Lambda}{10^{16}\mathrm{GeV}}\right)^4$$

Less detectable…

Axion physics
(string theory, super gravity)

→

PGWs

✧ **Detectable amplitude**
✧ **Chiral GWs spectrum**

$$\lambda\frac{\varphi}{f}\mathrm{Tr}F\tilde{F}$$

Chiral PGWs spectrum from non-Abelian gauge fields(review)

Axionic inflation with SU(2) gauge field

$$F^a_{\mu\nu} = \partial_\mu A^a_\nu - \partial_\nu A^a_\mu + g\epsilon^{abc}A^b_\mu A^c_\nu$$

$$S = S_{\rm EH} + S_{\rm axion} + S_{\rm gauge} + S_{\rm CS}$$
$$= \int d^4x\left[\frac{1}{2}R - \frac{1}{2}(\partial_\mu\varphi)^2 - V(\varphi) - \frac{1}{4}F^{a\mu\nu}F^a_{\mu\nu} - \frac{1}{4}\lambda\frac{\varphi}{f}\tilde{F}^{a\mu\nu}F^a_{\mu\nu}\right]$$

P.Adshead & M. Wyman 2012

inflaton + SU(2) gauge field

$$\varphi = \bar{\varphi}(t) + \delta\varphi \qquad A^a_i = a(t)\boxed{Q(t)}\delta^a_i + \delta A^a_i$$

If $\lambda \gg 1$ …

$$Q(t) \simeq Q_{\rm min} \equiv -\left(\frac{V_{\tilde{\varphi}}}{3\lambda g H}\right)^{1/3}$$

Inflationary dynamics (slow-roll parameters + energy density of elemag fields)

$$\tilde{\varphi} \equiv \frac{\varphi}{f}$$

If $\lambda \gg 1$ …

$$m_Q \equiv \frac{gQ}{H}$$

$$\epsilon_H = -\frac{\dot{H}}{H^2} \simeq \frac{1}{\lambda}\frac{1+m_Q^2}{m_Q}\frac{V_{\tilde{\varphi}}}{V}$$

$$\eta_H = \frac{\dot{\epsilon}_H}{\epsilon_H H} \simeq \frac{1}{\lambda}\frac{1+m_Q^2}{m_Q}\left(\frac{2V_{\tilde{\varphi}}}{V} - \frac{V_{\tilde{\varphi}\tilde{\varphi}}}{V_{\tilde{\varphi}}}\right)$$

$$\rho_E \equiv \frac{3}{2}E^2 \simeq \frac{3}{2}H^2Q^2_{\rm min}$$

$$\rho_B \equiv \frac{3}{2}B^2 \simeq \frac{3}{2}g^2Q^4_{\rm min}$$

Chiral PGWs spectrum from non-Abelian gauge fields(review)

Axionic inflation with SU(2) gauge field

$F^a_{\mu\nu} = \partial_\mu A^a_\nu - \partial_\nu A^a_\mu + g\epsilon^{abc} A^b_\mu A^c_\nu$

$$\boxed{\begin{aligned} S &= S_{\rm EH} + S_{\rm axion} + S_{\rm gauge} + S_{\rm CS} \\ &= \int d^4x \left[\frac{1}{2}R - \frac{1}{2}(\partial_\mu\varphi)^2 - V(\varphi) - \frac{1}{4}F^{a\mu\nu}F^a_{\mu\nu} - \frac{1}{4}\lambda\frac{\varphi}{f}\tilde{F}^{a\mu\nu}F^a_{\mu\nu}\right] \end{aligned}}$$

P.Adshead & M. Wyman 2012

inflaton + SU(2) gauge field

$$\varphi = \bar{\varphi}(t) + \delta\varphi \quad A^a_i = a(t)Q(t)\delta^a_i + \boxed{\delta A^a_i}$$

$$(\delta A^a_i)^{\rm TT} \leftrightarrow \delta g_{\mu\nu}$$

couples through $Q(t)$

Parity-violating interaction

$$\lambda\frac{\varphi}{f}{\rm Tr}F\tilde{F}$$

Fourier mode

$$\pm\lambda k\frac{\bar{\varphi}'}{f}\delta A^\pm_k \delta A^\pm_k$$

$$|\delta A^+_k| \neq |\delta A^-_k|$$

Generating chiral GWs spectrum

$$\boxed{\mathcal{P}^+_{\rm GW}(k) \neq \mathcal{P}^-_{\rm GW}(k)}$$

- Parity-violated spectrum!
- Detectable amplitude! $(m_Q \gtrsim 2)$

Chiral PGWs spectrum from non-Abelian gauge fields(review)

Axionic inflation with SU(2) gauge field

$F^a_{\mu\nu} = \partial_\mu A^a_\nu - \partial_\nu A^a_\mu + g\epsilon^{abc} A^b_\mu A^c_\nu$

$$\boxed{\begin{aligned} S &= S_{\rm EH} + S_{\rm axion} + S_{\rm gauge} + S_{\rm CS} \\ &= \int d^4x \left[\frac{1}{2}R - \frac{1}{2}(\partial_\mu\varphi)^2 - V(\varphi) - \frac{1}{4}F^{a\mu\nu}F^a_{\mu\nu} - \frac{1}{4}\lambda\frac{\varphi}{f}\tilde{F}^{a\mu\nu}F^a_{\mu\nu}\right] \end{aligned}}$$

P.Adshead & M. Wyman 2012

Observational constraint on CMB

Gauge field also produces scalar part.

$$\delta A + \bar{A} \longrightarrow \delta\varphi \ (\zeta)$$

affect

n_s , r (CMB observation)

In conflict with CMB observation…

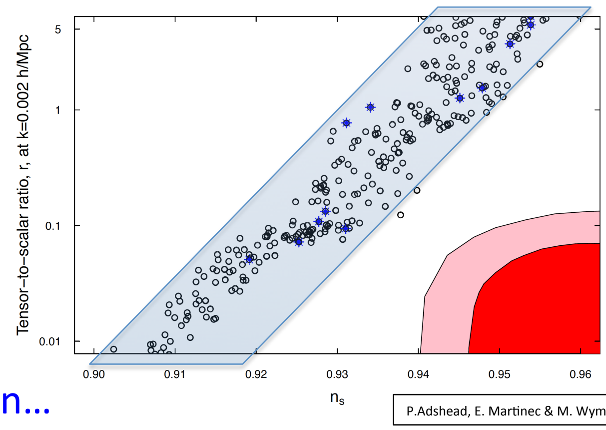

P.Adshead, E. Martinec & M. Wyman 2013

Primordial chiral GWs spectrum from non-Abelian gauge fields

Axionic inflation with SU(2) gauge field $F^a_{\mu\nu} = \partial_\mu A^a_\nu - \partial_\nu A^a_\mu + g\epsilon^{abc} A^b_\mu A^c_\nu$

$$\boxed{\begin{aligned} S &= S_{\rm EH} + S_{\rm axion} + S_{\rm gauge} + S_{\rm CS} \\ &= \int d^4x \left[\frac{1}{2}R - \frac{1}{2}(\partial_\mu \varphi)^2 - V(\varphi) - \frac{1}{4}F^{a\mu\nu}F^a_{\mu\nu} - \frac{1}{4}\lambda\frac{\varphi}{f}\tilde{F}^{a\mu\nu}F^a_{\mu\nu} \right] \end{aligned}}$$

A motivation of our study

studying the possibility to generate chiral GWs spectrum consistent with CMB observations, which are detectable in future GW experiments

A solution of this problem

$$\boxed{FF \to I^2(t)FF \qquad \left(\lambda \to \frac{\lambda}{I(t)^2} \equiv \lambda_{\rm eff}(t) : \text{dynamical} \right)}$$

Dilaton and Axion with SU(2) fields

An inflationary dynamics:

Action

$$\boxed{\begin{aligned} S &= S_{\rm EH} + S_{\rm dilaton} + S_{\rm axion} + S_{\rm gauge} + S_{\rm CS} \\ &= \int dx^4 \sqrt{-g} \left[\frac{1}{2}R - \frac{1}{2}(\partial_\mu \varphi)^2 - V(\varphi) - \frac{1}{2}(\partial_\mu \sigma)^2 - W(\sigma) - \frac{1}{4}I(\varphi)^2 F^{a\mu\nu}F^a_{\mu\nu} - \frac{1}{4}\lambda\frac{\sigma}{f}\tilde{F}^{a\mu\nu}F^a_{\mu\nu} \right] \end{aligned}}$$

The scalar fields and SU(2) gauge field

$\varphi(t)$: dilaton

$Q(t)$: VEV of the gauge fields $\qquad \boxed{A^a_i = A(t)\delta^a_i = a(t)Q(t)\delta^a_i}$

$\sigma(t)$: axion

Dilaton and Axion with SU(2) fields

An inflationary dynamics:

Action

$$S = S_{\rm EH} + S_{\rm dilaton} + S_{\rm axion} + S_{\rm gauge} + S_{\rm CS}$$
$$= \int dx^4 \sqrt{-g}\left[\frac{1}{2}R - \frac{1}{2}(\partial_\mu\varphi)^2 - V(\varphi) - \frac{1}{2}(\partial_\mu\sigma)^2 - W(\sigma) - \frac{1}{4}I(\varphi)^2 F^{a\mu\nu}F^a_{\mu\nu} - \frac{1}{4}\lambda\frac{\sigma}{f}\tilde{F}^{a\mu\nu}F^a_{\mu\nu}\right]$$

Initial conditions of the background motion

- dilaton is energy dominant (playing a role of an inflaton) :

$$3H^2 \simeq V \quad (\varphi(t) : \text{inflaton})$$ → Producing CMB fluctuations!

- weak gauge kinetic coupling function :

$$I(\varphi) \propto a(t)^n \ , \ n \lesssim -2 \quad \left(\frac{\lambda}{I(\varphi_i)^2} \ll 1\right)$$ (Suppressing axion-gauge interactions)

Dilaton and Axion with SU(2) fields

An inflationary dynamics:

The dynamics of the vev of gauge field (late time period)

$$\boxed{m_Q \equiv \frac{gQ}{H}}$$

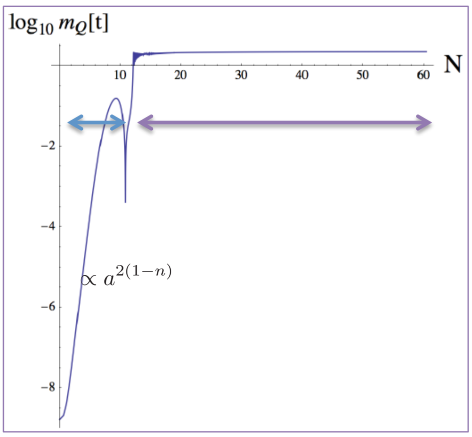

$: \dfrac{\lambda}{I(\varphi)^2} \ll 1$ Gauge field does not contribute inflationary dynamics...(CMB scale)

$: \dfrac{\lambda}{I(\varphi)^2} \gtrsim 1$ Gauge field assists inflation!

Chiral GWs are generated!

$(f \gtrsim \mathrm{nHz})$

$$V(\varphi) = \Lambda_1^4 \exp[r\varphi]$$
$$W(\sigma) = \Lambda_2^4\left(1 - \cos\left(\frac{\sigma}{f}\right)\right)$$

$(\Lambda_\varphi, \Lambda_\sigma, r, n, g, \lambda, f) = (10^{-2}, 2*10^{-3}, 1, -2, 10^{-2}, 10^7, 5,)$

Dilaton and Axion with SU(2) fields

Power spectrum of chiral GWs in late time periods :

$$\mathcal{P}_h^-(k) \simeq \frac{2H^2}{k^3}$$

$$\mathcal{P}_h^+(k) \simeq \frac{2H^2}{k^3}\left[1 + 8Q_{\rm min}^2\left|\mathcal{I}_0(m_{\bar{Q}}) - m_{\bar{Q}}\mathcal{I}_1(m_{\bar{Q}}) + (-2 + m_{\bar{Q}}^2)\mathcal{I}_2(m_{\bar{Q}})\right|^2\right]$$

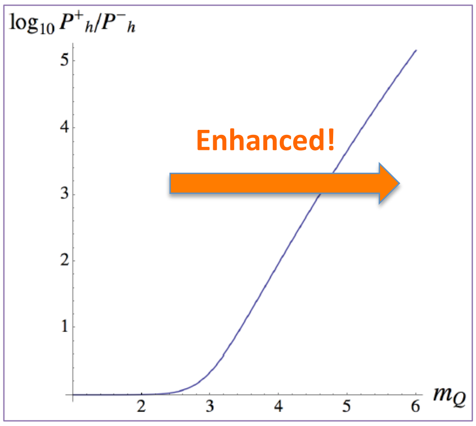

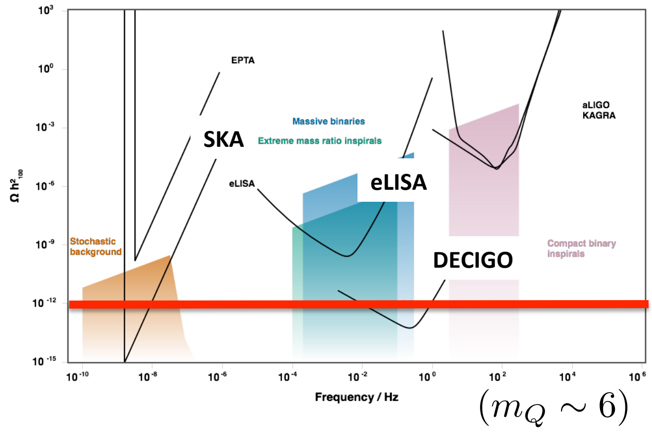

Summary & Outlook

- We study the mechanism that produces primordial chiral GWs consistent with CMB observations from a non-Abelian gauge field.

- We introduce a dilatonic field in the conventional model and make an axion-gauge interaction dynamically.

- We might discover the parameter region where chiral GWs consistent with CMB data are produced, which might be detectable in future GW experiments (DECIGO, eLISA, SKA...).

- We must check the broadness of parameter regions and reheating ages.
- We must estimate the stability condition about scalar perturbations and their spectrums quantitatively.

“The quasi-normal modes of charged scalar fields in Kerr-Newman black hole and its geometric interpretation”

by Peng Zhao

[JGRG25(2015)3b6]

The quasi-normal modes of charged scalar fields in Kerr-Newman black hole and its geometric interpretation

Peng Zhao,
Yu Tian, Xiaoning Wu, Zhaoyong Sun, JHEP11(2015)167

University of Chinese Academy of Sciences

@The 25th Workshop on General Relativity and Gravitation in Japan(JGRG25)

December 8, 2015

Catalogue

Background

1 C.V.Vishveshwara(C. V. Vishveshwara, Nature(1970).) found that there exist complex frequency modes in perturbations of Schwarzschild(Sch) black holes(BH), which is called quasi-normal modes(QNMs).

* QNMs are the characteristic modes of linear perturbations of BH that satisfy an outgoing boundary condition at infinity and an ingoing boundary condition at the horizon.

* These oscillatories and decaying modes are represented by complex characteristic frequencies:

$$\omega = \omega_R - i\omega_I \tag{1}$$

Introduction
Geometric-optics Correspondence
Charge Effects on QNMs
Background
Motivation

Background

2 Ferrari and Mashhood(V. Ferrari and B. Mashhoon, Phys. Rev. D,1984) found that the quasi-normal frequency in Sch BH in eikonal limit($l \gg 1$) can be written as:

$$\omega \approx \left(l + \frac{1}{2}\right)\Omega - i\left(n + \frac{1}{2}\right)\gamma_L, \tag{2}$$

where γ_L is the Lyapunov exponent of circular photon orbits.

3 Recently H.Yang, Y. Chen, et al (H.Yang, Y. Chen, et al, PRD(2012)) obtained the relationship between the QNMs of scalar field in Kerr BH of arbitrary spins with spherical photon orbits. They find a geometry interpretation to zero damping modes(ZDM) for Kerr holes rotating near the maximum rate and the degenerate modes in BH of any spins.

Peng Zhao, Yu Tian, Xiaoning Wu, Zhaoyong Sun, JHEP11(2015 The quasi-normal modes of charged scalar fields in Kerr-Newmar

Motivation

1. Xiangdong Zhang, et al(Helei Liu, Xiangdong Zhang, Dehua Wen, PRD(2014)) find that some super-Chandrasekhar white dwarfs and their phenomenons can be explained by the charge effect.
2. The behaviors of particle trajectories near the singularity of Sch and Reissner-Nordstrom (RN) BH are quite different.
3. When the matter fields in Kerr-Newman (KN) BH are charged, the electromagnetic field will have significant influence on the QNMs.
   So we consider the charge effects.

QNMs and Particle Motion

1. Separating the Klein-Gondon scalar field as:

$$u(t,r,\theta,\phi) = \sum_{l,m} \int e^{-i\omega t} e^{im\phi} R(r) u_\theta(\theta)\, d\omega. \tag{3}$$

   We can obtain the expression of ω_R, ω_I and the angular eigenvalue A_{lm} by WKB analysis under eikonal limit, here we use the facts that $\omega_R \sim O(l)$, $\omega_I \sim O(1)$ when $l \gg 1$.
2. Using Hamilton-Jacobi formalism:

$$g^{\mu\nu}(\partial_\mu S - qA_\mu)(\partial_\nu S - qA_\nu) + \mu_\star^2 = 0, \tag{4}$$

   we study the particle motion, especially the unstable circular orbit.

Geometric-optics Correspondence

We check the geometric-optics correspondence between the parameters of a QNMs, $(\omega, A_{lm}\ m)$, and the conserved quantities along world line, $(E, L_z$ and $\mathcal{Q})$ in KN BH, which is the same like that in Kerr hole:

Wave	Particle	Interpretation
ω_R	E	Wave frequency corresponds to energy of particle (unstable circular orbit.).
m	L_z	Azimuthal quantum number corresponds to z angular momentum (quantization of wave in ϕ direction).
A^R_{lm}	$\mathcal{Q} + L_z^2$	Real part of angular eigenvalue related to Carter constant (quantization of wave in θ direction).
ω_I	$\gamma = -E_I$	Wave decay rate corresponds to Lyapunov exponent of world lines near unstable circular orbits.
A^I_{lm}	$\mathcal{Q}_I$	Nonzero because $\omega_I \neq 0$

KN BH approach to extreme

The QNMs of uncharged massless scaler field in nearly extreme KN BH$(\mu = m/(l + \frac{1}{2}), \sigma = q/E)$:

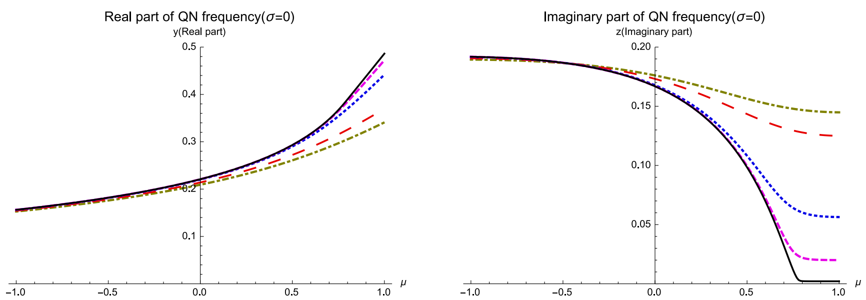

(a) The real part of QN frequency (b) The imaginary part of QN frequency

Figure: The angular momentum of BH is $\lambda = a/M = 0.8$.The dotdashed dark green line for $\rho = Q/M = 0.4$, large dashed red line for $\rho = Q/M = 0.5$, thick dotted blue line for $\rho = Q/M = 0.59$, thick dashed purple line for $\rho = Q/M = 0.599$ and black for $\rho = Q/M = 0.59999$.

ω_I approach to zero at $0.688 < \mu < 1$ when BH approach to nearly extreme, We denote $\mu_c = 0.688$ as turning point.

The apex of effective potential and The inclination angle of spherical orbit:

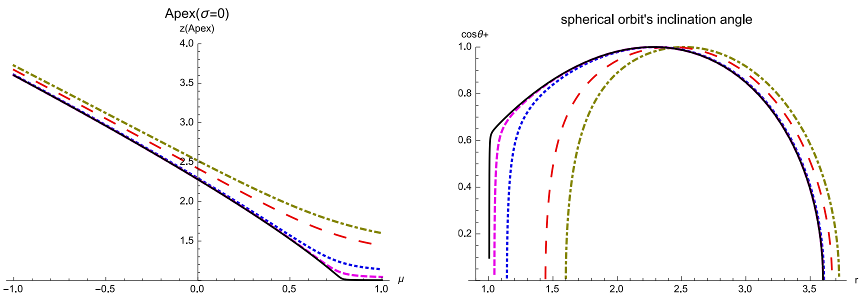

(a) The apex of effective potential (b) The inclination angle of spherical orbit

Figure: The dotdashed dark green line for $\rho = Q/M = 0.4$, large dashed red line for $\rho = Q/M = 0.5$, thick dotted blue line for $\rho = Q/M = 0.59$, thick dashed purple line for $\rho = Q/M = 0.599$ and black for $\rho = Q/M = 0.59999$.

The peak of effective potential tends to horizon in nearly extreme BH. Many spherical orbits of different maximum inclination angle have nearly the same radius, $r \approx 1$, namely the horizon.

Geometric-optics Interpretation

Under the geometric-optics correspondence between $(E, L_z, \mathcal{Q})$ and (ω, m, A_{lm}), vanishing imaginary part of quasi-normal frequency corresponds to vanishing Lyapunov exponent of radial motion of particle:

1. In the aspect of QNMs, that means the wave will exist slightly outside the horizon for a long time and do not move away very quickly when $\mu > \mu_c$;
2. In the aspect of particle, that means a lot of particle move near the horizon with different maximum inclination angle and do not fall or move away after a perturbation.

Not every nearly extreme KN BH admits this phenomenon:

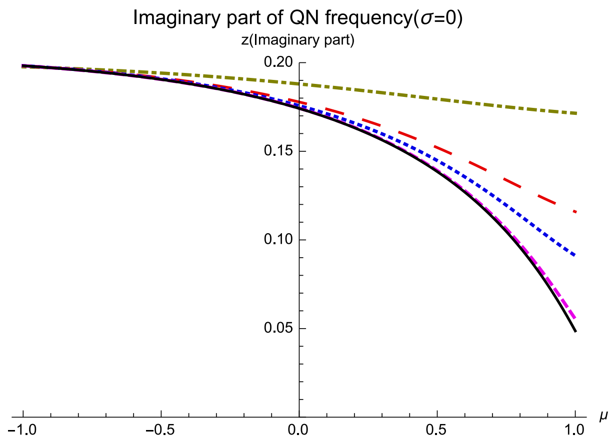

Figure: The angular momentum of BH $a/M = 0.4$. The dotdashed dark green line for $\rho = Q/M = 0.8$, large dashed red line for $\rho = Q/M = 0.9$, thick dotted blue line for $\rho = Q/M = 0.91$, thick dashed purple line for $\rho = Q/M = 0.916$ and black for $\rho = Q/M = 0.91651$.

Charged massless field

Pictures show the imaginary part of QNMs:

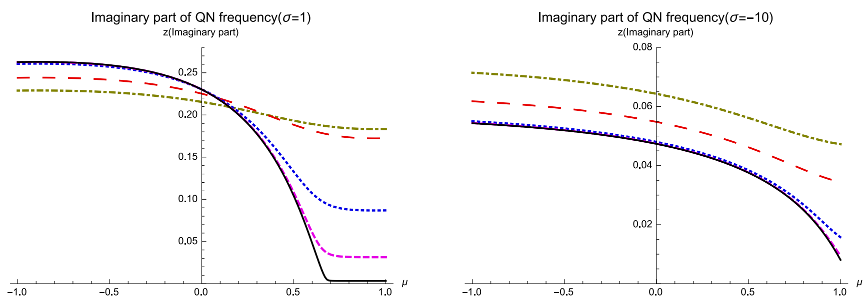

(a) The imaginary part of QN frequency (b) The imaginary part of QN frequency

Figure: The angular momentum of BH is $\lambda = a/M = 0.8$.The dotdashed dark green line for $\rho = Q/M = 0.4$, large dashed red line for $\rho = Q/M = 0.5$, thick dotted blue line for $\rho = Q/M = 0.59$, thick dashed purple line for $\rho = Q/M = 0.599$ and black for $\rho = Q/M = 0.59999$.

When the charge of field is opposite to BH and big enough, there is no zero damping modes. The electromagnetic force and the gravity are both attraction, the angular drag effect of the rotating black hole is not strong enough, resulting in no circular orbits or zero damping modes.

1. In Kerr case, the zero damping modes exist in nearly extreme BH and $\mu_c > 0.744$.
2. Unlike Kerr case, there are infinite ways for KN BH approach to nearly extreme, the field charge also affect. We obtain the expression of turning point under nearly extreme KN BH:

$$\mu_c = \frac{1}{\sqrt{2}\lambda}\sqrt{3\lambda^2 + 12 - 12\rho\sigma + 2\rho^2\sigma^2 - \sqrt{B}} \tag{5}$$

with

$$B = 136 + 56\lambda^2 + \lambda^4 - 272\rho\sigma - 56\lambda^2\rho\sigma \tag{6}$$

$$+ 184\rho^2\sigma^2 + 12\lambda^2\rho^2\sigma^2 - 48\rho^3\sigma^3 + 4\rho^4\sigma^4. \tag{7}$$

Results

1. ZDMs will exist when $\mu_c < 1$.
2. When the field is massless and uncharged, ZDMs exist in nearly extreme KN BH when the angular momentum of BH $\lambda > 0.5$.
3. In last two case when field charge are $\sigma = 1$ and -10, we obtain that $\mu_c = 0.688$ and 1.077.

Thank You!

“Status of the KAGRA detector”

by Eiichi Hirose (invited)

[JGRG25(2015)I05]

Status of the KAGRA detector

Eiichi Hirose
On behalf of KAGRA collaboration
ICRR, the University of Tokyo
Dec 8, 2015

What is KAGRA?

- KAGRA is a large-scale cryogenic gravitational wave telescope for detecting GW signals directly.
- It is a 3km-arm Fabry-Perot Michelson interferometer.
- It is being built underground Kamioka, Hida city in Gifu prefecture.
- It is one of the second-generation GW detectors (advanced LIGO, advanced Virgo, LIGO India, and KAGRA) in the world.

GW detectors in the world

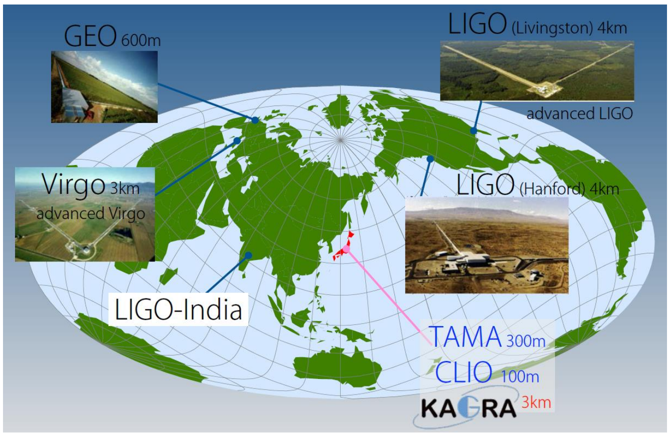

KAGRA collaboration
- ~250 members
- ~60 universities or institutes

KAGRA Collaboration

Optical configuration of KAGRA

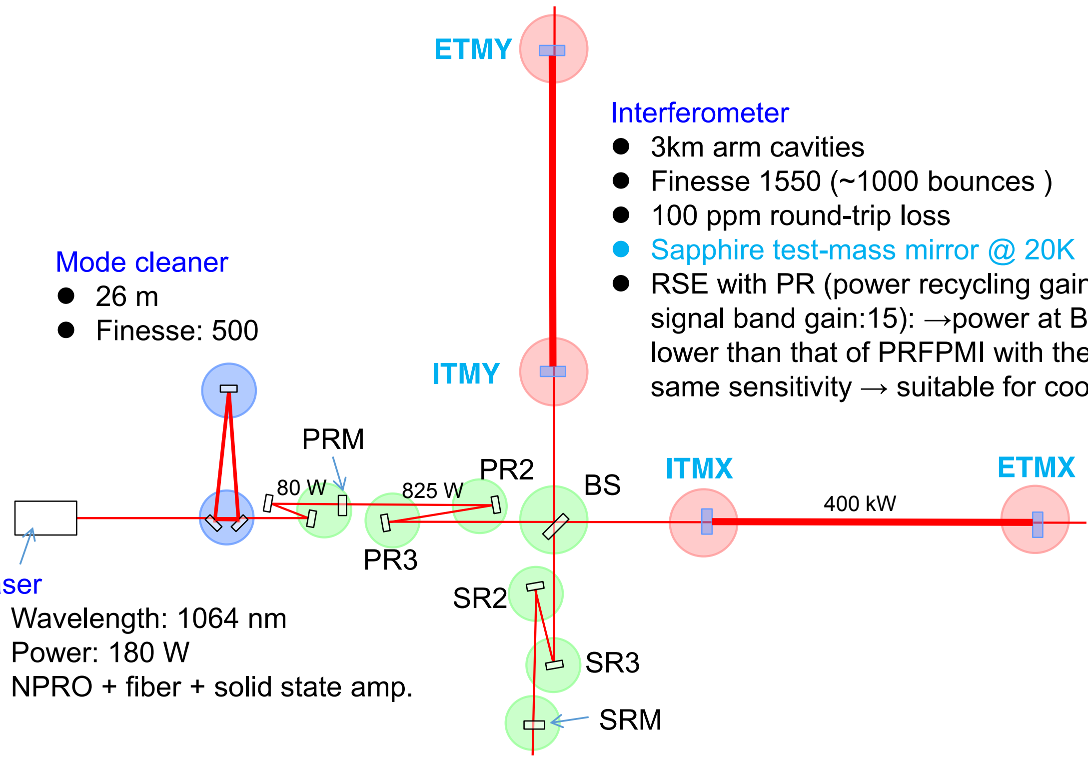

Interferometer
- 3km arm cavities
- Finesse 1550 (~1000 bounces)
- 100 ppm round-trip loss
- Sapphire test-mass mirror @ 20K
- RSE with PR (power recycling gain:11, signal band gain:15): →power at BS is lower than that of PRFPMI with the same sensitivity → suitable for cooling

Mode cleaner
- 26 m
- Finesse: 500

Laser
- Wavelength: 1064 nm
- Power: 180 W
- NPRO + fiber + solid state amp.

Key features and POC

- **Underground**
  Stable operation due to low seismic noise
- **Cryogenic mirrors and suspensions**
  Reduction of thermal noise

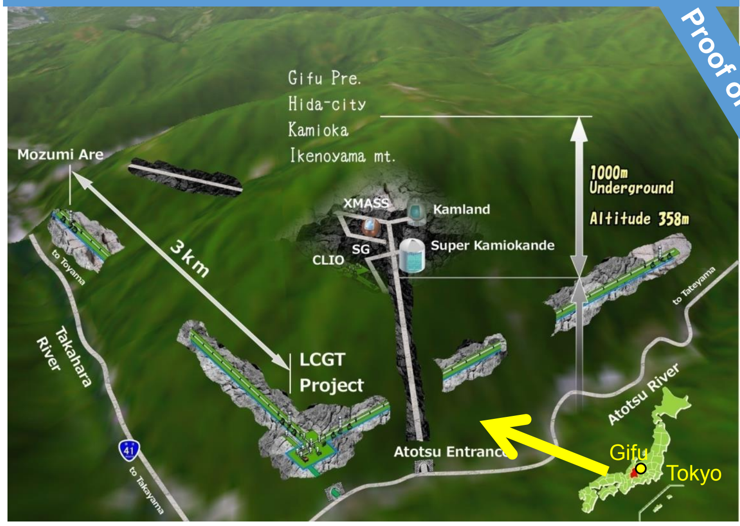

Proof of Concept

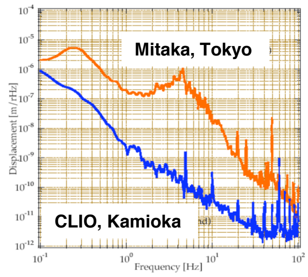

underground, cryogenic operation

Reduction of thermal noise was demonstrated by a cooled sapphire mirror (17K).
T. Uchiyama et al., PRL 108, 141101 (2011)

Goal of KAGRA

- Observe more than 1 event/year with 90% probability
- Start observation by the end of FY2017

- Most promising GW source would be NS binaries
- we need
(i) Observation range: 115Mpc (sky-average)
(ii) Duty factor: 80%
- Obs range with fundamental noise shall be 128Mpc+ with a safety factor for technical noise being 10%
(Each technical noise must be 1/10 ~ 1/100 of the goal sensitivity)

target sensitivity

http://gwcenter.icrr.u-tokyo.ac.jp/en/researcher/parameter

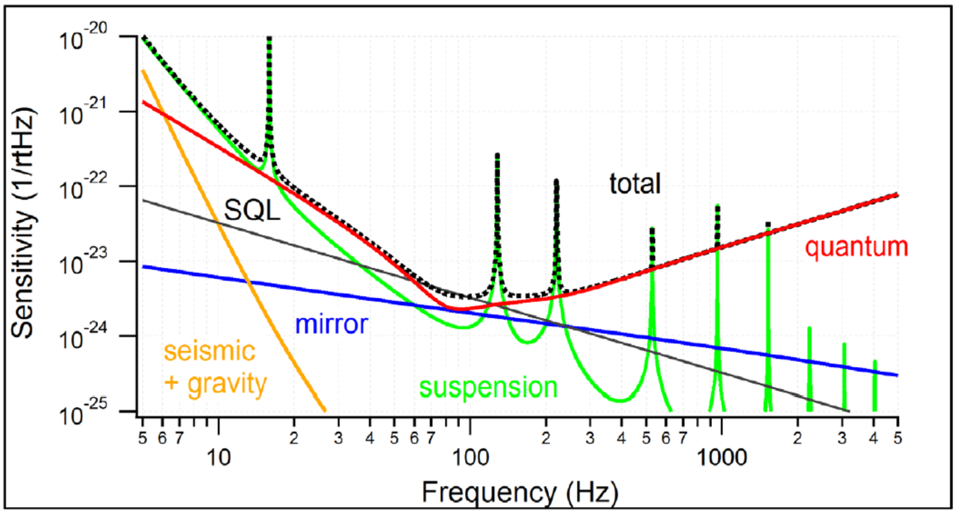

Observation range for NS binaries is 148Mpc with full power (147Mpc with 55W input)

>>> satisfies the requirement (128Mpc+)

Two-stage construction

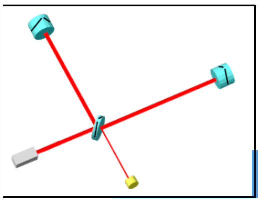

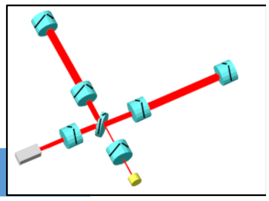

iKAGRA	bKAGRA
Tunnel/vacuum system	-
Michelson	Fabry-Perot Michelson w/ PR, RSE
Fused silica test-mass mirrors	Sapphire test-mass mirrors
Room temperature operation	Cryogenic operation
Low power input laser (2W)	Higher power input laser (180W)
Simplified vibration isolation systems	Upgraded vibration isolation systems

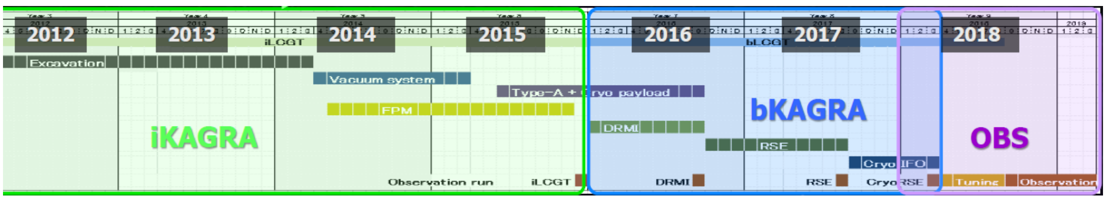

iKAGRA construction

Tunnel and vacuum system


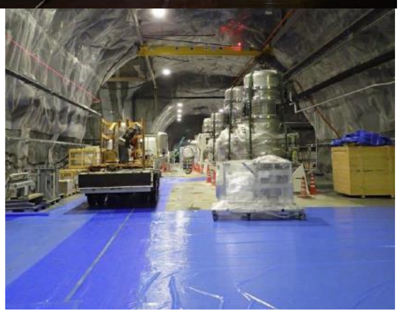

- Excavation of KAGRA tunnel was completed in Mar 2014
- Connection/leak check of 3km-arm ducts was completed
- Most vacuum tanks have been installed

Input Optics

Pre-stabilized laser

- The pre-mode cleaner was locked to the laser frequency from the control room using the digital system.
- The laser frequency was locked to the fiber ring cavity, and it was verified from the feedback signal of the pre-mode cleaner control system that the laser frequency was actually stabilized with this stabilization system.

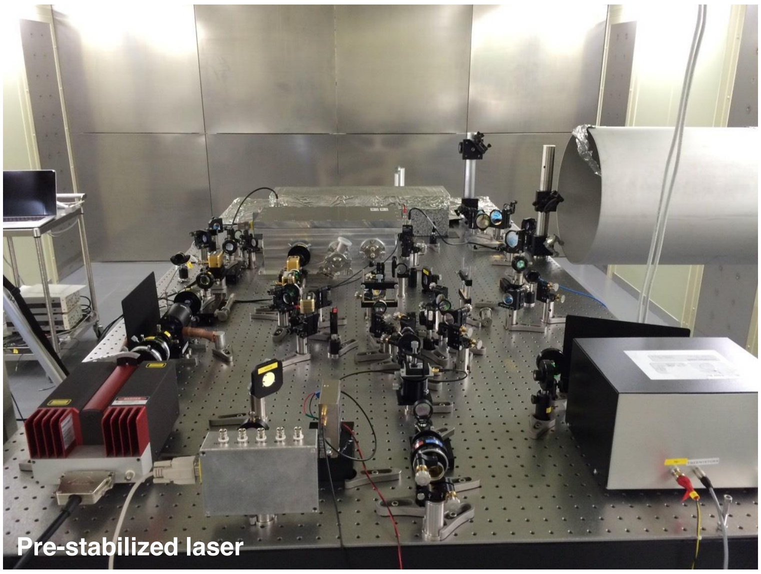

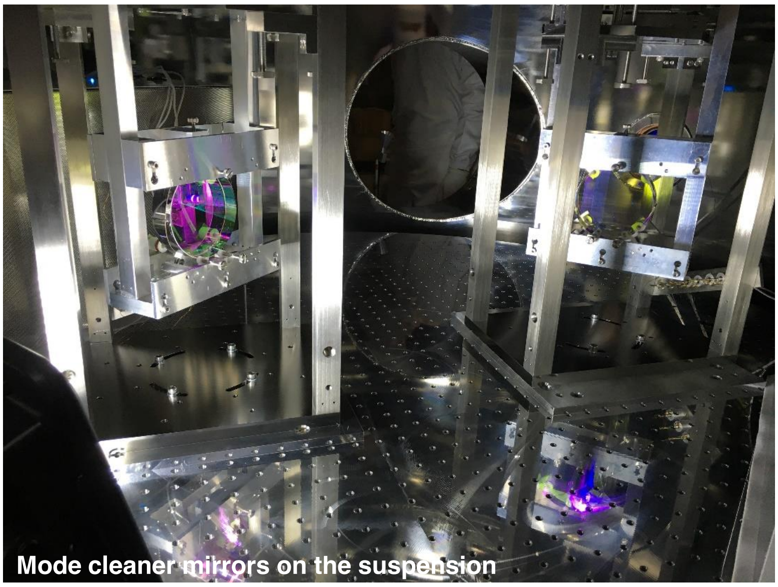

Input mode cleaner

- All the three mode cleaner mirrors/suspensions were installed in the MCF and MCF chambers.
- All the optical lever systems were installed.

Input Faraday isolator

- The input Faraday isolator and almost all the related optics were installed in the IFI chamber.

VIS (vibration isolation system)

Type B

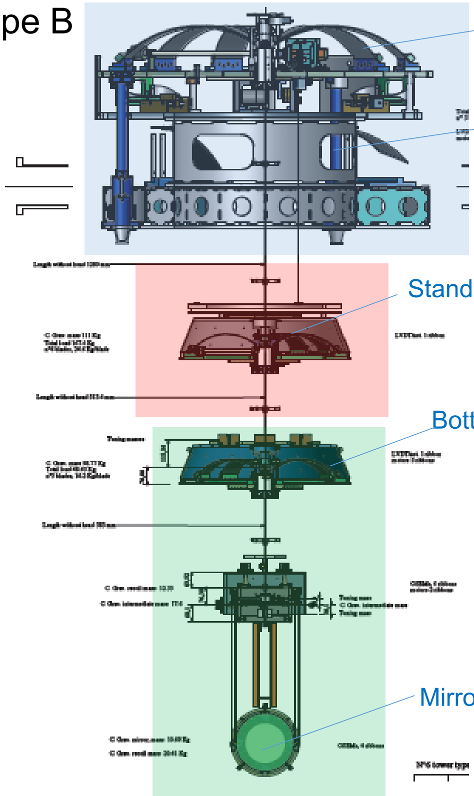

Top GAS filter

Inverted Pendulum
(not used in Type Bp)

Standard GAS filter

Bottom GAS filter

Mirror

Type A

There will be multiple Standard GAS filters

This payload part will be replaced by a cryogenic one in bKAGRA

Preparation for iKAGRA

Type-Bp' system (payload in the previous page)
is used for PR2, PR3, EXA, and EYA in iKAGRA.

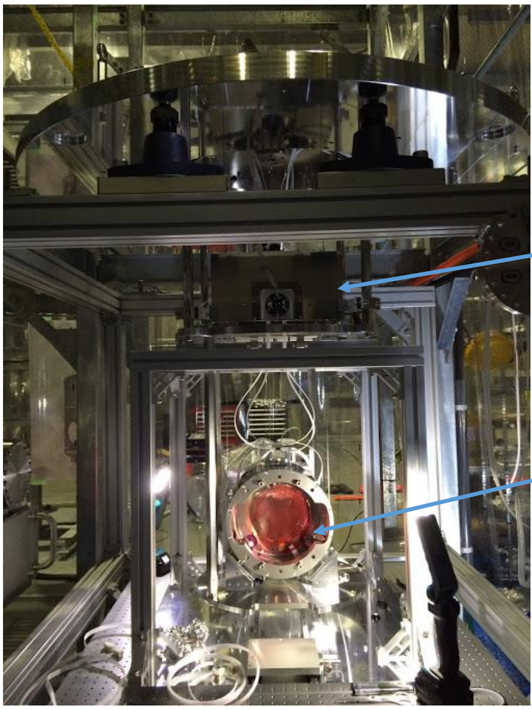

Bottom filter

Traverser

Intermediate Mass & Intermediate Recoil Mass

Test Mass & Recoil Mass

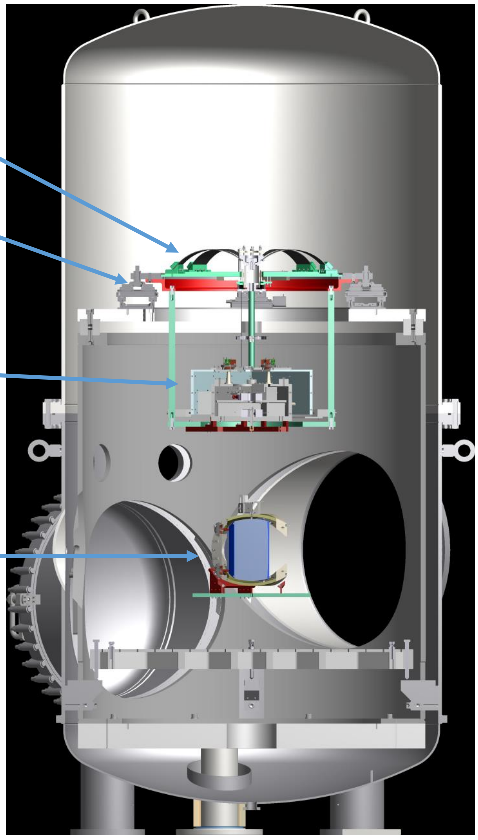

Test assembly at the site

Assembly of type-Bp' system for PR was started at the site using spare mirror.

hanging of mirror using the winch system

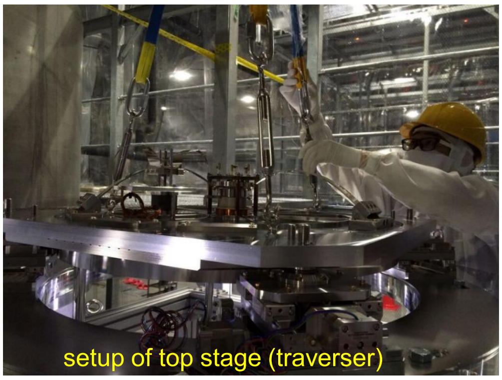

setup of top stage (traverser)

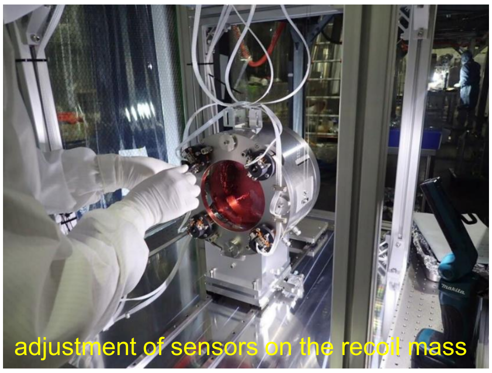

adjustment of sensors on the recoil mass

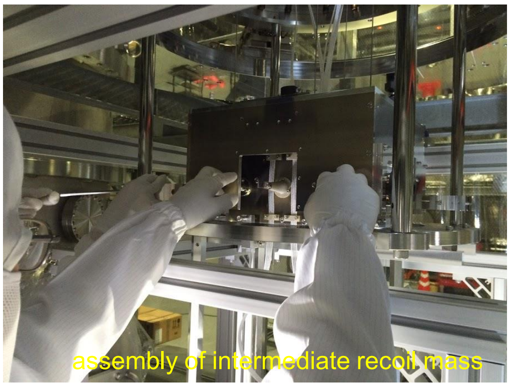

assembly of intermediate recoil mass

- all optics for iKAGRA (silica TMs, BS, PR3, PR2, MC mirrors) are completed

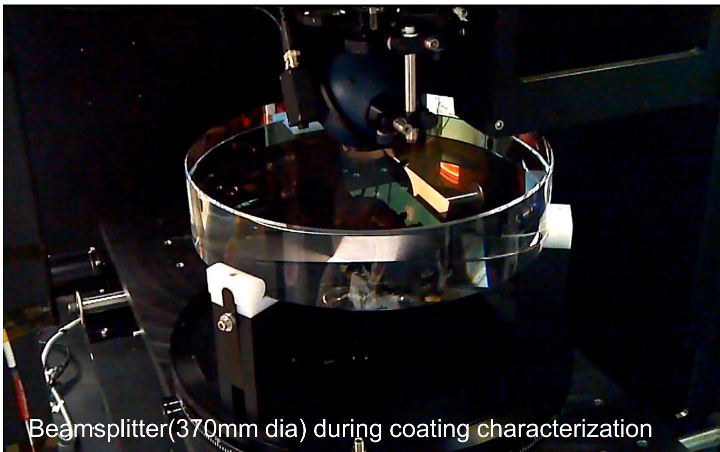

Beamsplitter(370mm dia) during coating characterization

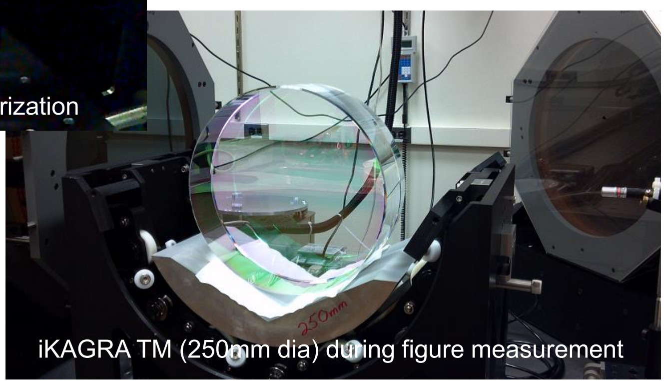

iKAGRA TM (250mm dia) during figure measurement

digital system

Installation of Digital Control system inside the tunnel, used for interferometer control and data acquisition, has been almost completed.

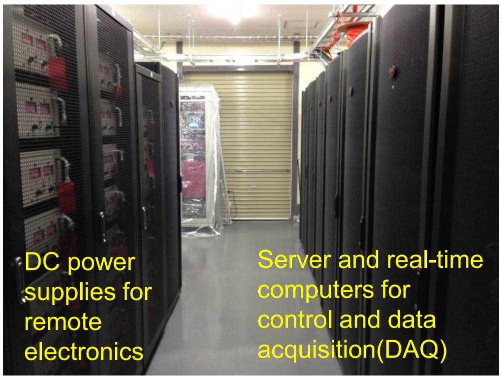

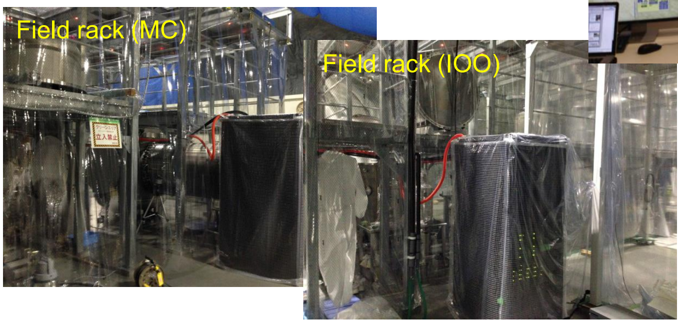

The detector can be monitored and controlled from the remote control room.

auxiliary optics

Stray light control, Optical baffles, Viewports, Optical lever, CCD monitors, Transmission monitor

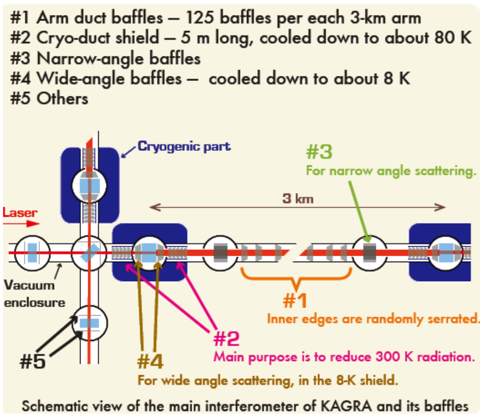

Schematic view of the main interferometer of KAGRA and its baffles

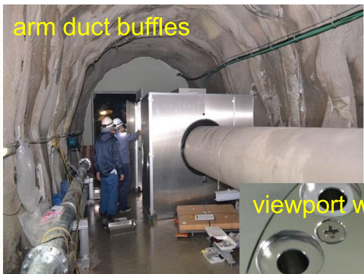

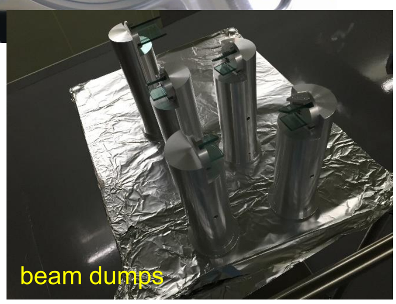

- Installation of the arm-duct baffles for both of 3km arms
- A viewport window (high quality) between the PSL room and MCF chamber
- beam dumps for MCF
- Installations of Oplevs for MCF and MCE mostly done
- Digital cameras for monitoring the light spot mostly done

Geophysics interferometer

- Construction of two fixed-mirror interferometers (1.5km x 2) along KAGRA, for both geophysical observation and KAGRA baseline monitor.
- Arrangement of environmental sensors for monitoring the tunnel, rooms, and instruments.
- Two vacuum systems have been constructed.
- Main optics and a stabilized laser have been installed into one of the vacuum systems, and their commissioning is underway

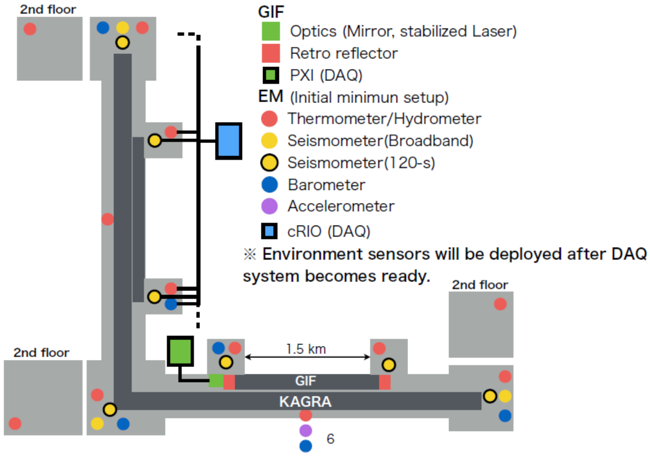

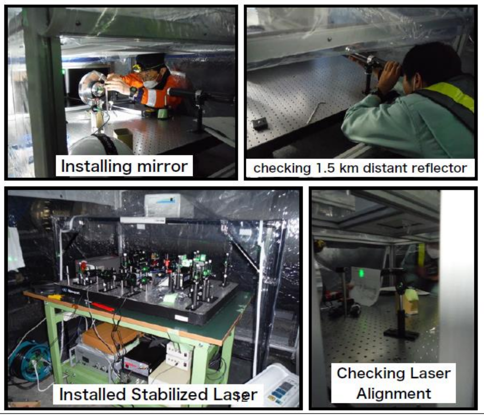

Facility

So far: wall painting, separation wall, floor, air flow, electricity, crane, network, laser clean room, clean booths, toilet, PHS, Spiral Ladder for 2ndfloor, X-end shelter, …

toward bKAGRA

R&D of full type-B system in TAMA

Everything was assembled next to a chamber. And, the full system was hung by a crane and installed into the chamber from the top. The system worked in vacuum.

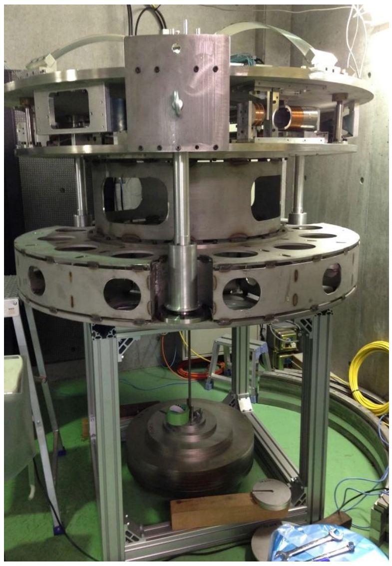

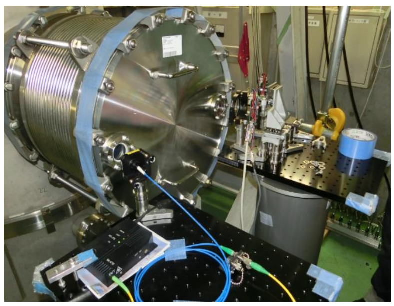

High power laser

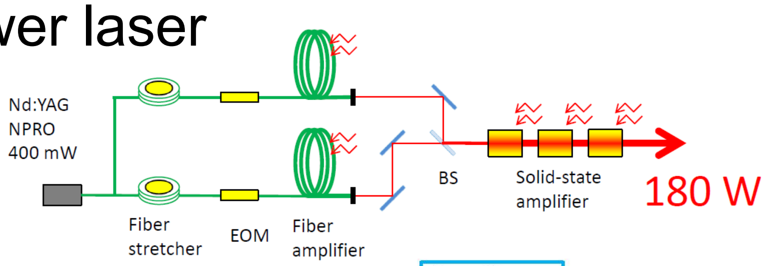

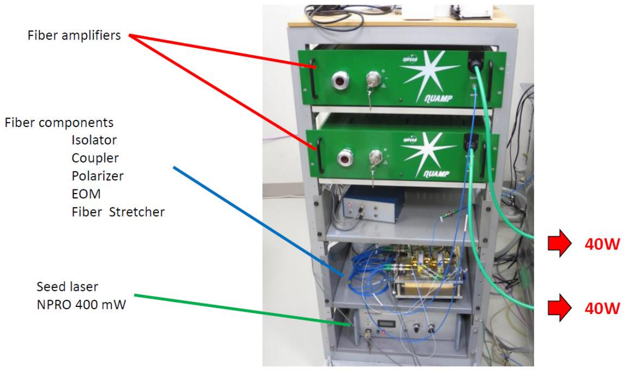

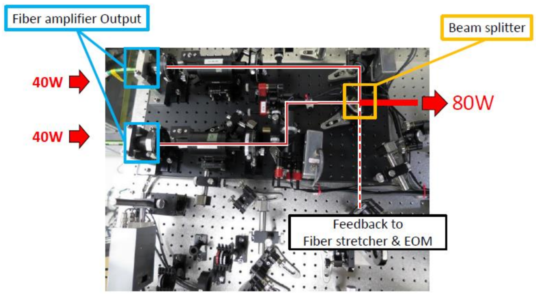

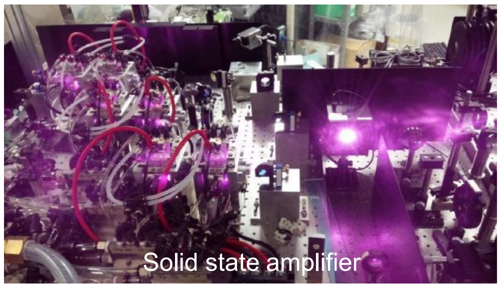

- Fiber optics and solid state amplifier system are completed
- 210W output power was obtained, but the beam profile was not good

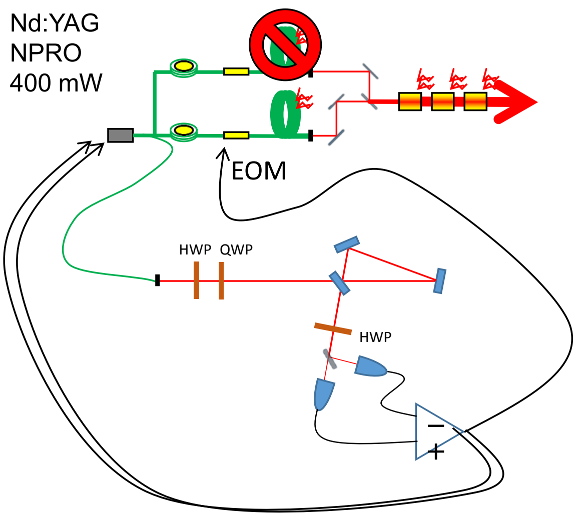

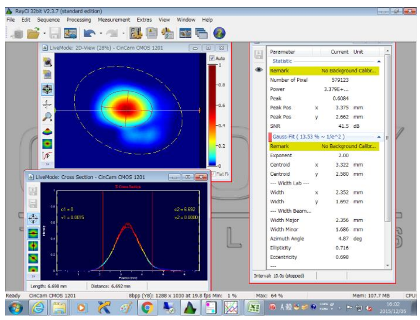

High frequency (100 kHz -)
→ feedback to EOM
Middle frequency (1 Hz -100kHz)
→ feedback to NPRO PZT
Low frequency (- 1 Hz)
→ feedback to temperature control

- Currently, output power is limited (~110W) since one of the fiber optics is broken
- Beam profile has been improved
- Frequency stabilization system is being developed

Cryostat

all cryostats have been assembled.

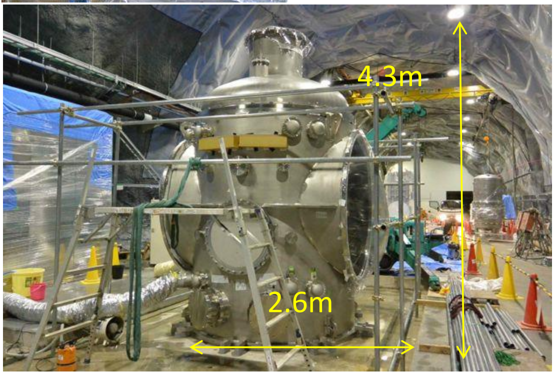

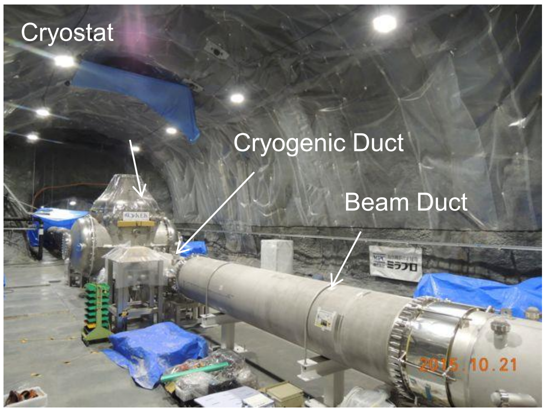

Cryogenic Payload

being developed in KEK and ICRR

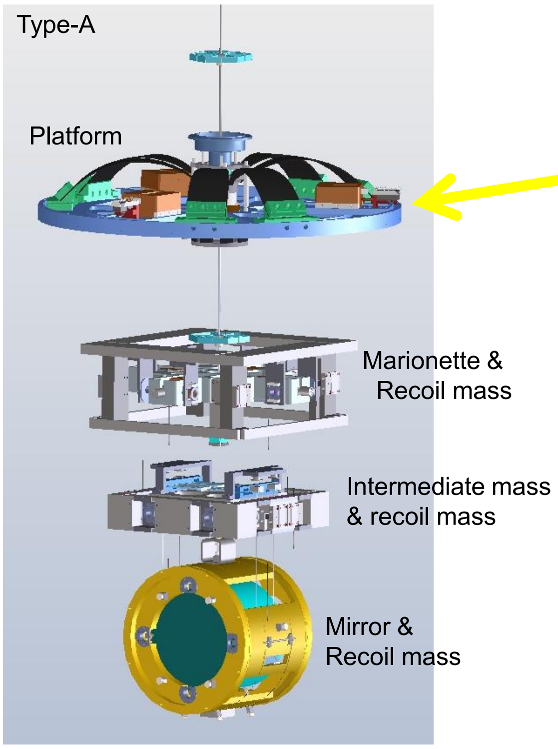

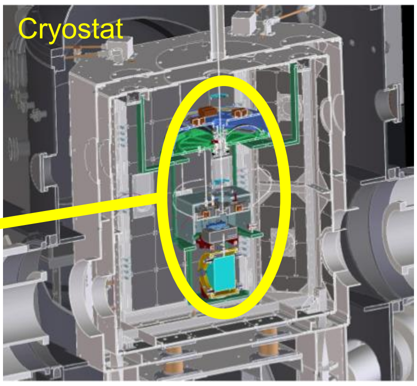

sapphire mirror

- Sapphire TMs, PRM, SRM, MMTs are to be done (ETMs, PRM, SRM are being polished and all optics will be completed in the next FY)
- Sapphire R&D (test polishing/coating with a 200mm-dia crystal) was successful
- Absorption and inhomogeneity of the ITM bulks will be very important, and we are still hoping better crystals to come
- contamination control is also a key

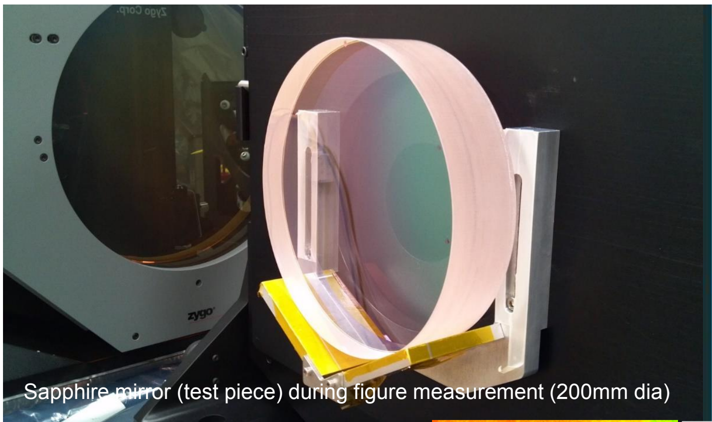
Sapphire mirror (test piece) during figure measurement (200mm dia)

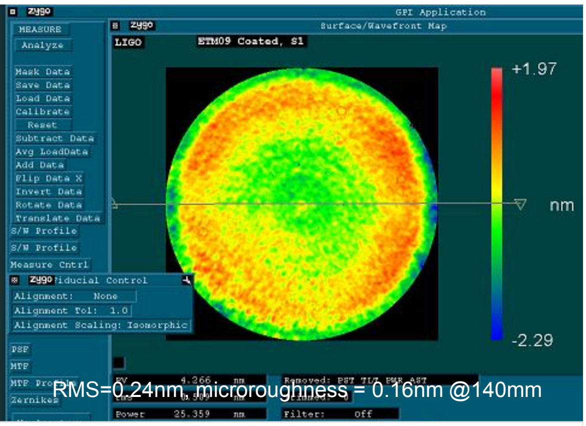

RMS=0.24nm, microroughness = 0.16nm @140mm

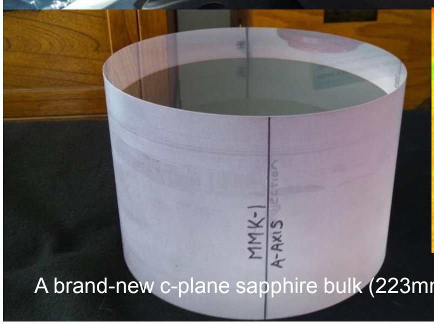
A brand-new c-plane sapphire bulk (223mm dia)

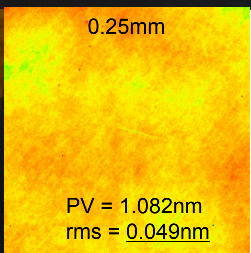

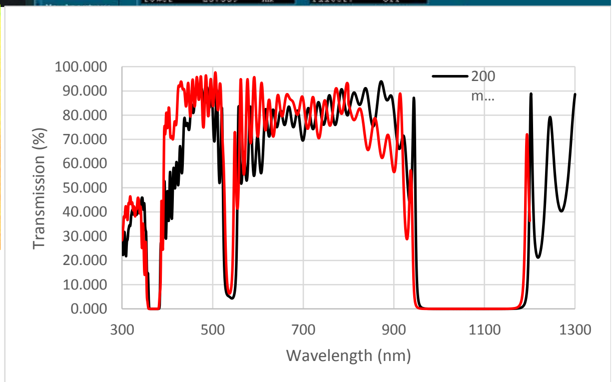

- It has been demonstrated that polish/coating will be in the specifications (PRD 89, 062003 (2014))
- crystal's absorption/homogeneity will be the keys for success

Summary

- Infrastructure for the KAGRA detector is almost completed
- Installation/commissioning of iKAGRA is in progress
- Preparation for bKAGRA is also underway

appendices

How come cryogenic sapphire?

$$\sqrt{x(\omega)^2} \propto \sqrt{\frac{T}{Q}}$$

	Fused silica (300 K)	Sapphire (300 K)	Sapphire (20 K)	
α [ppm/cm]	2 - 20	40 - 100	90	*absorption*
κ [W/m/K]	1.4	46	4.3×10^3	*thermal conductivity*
β [K^{-1}]	1.4×10^{-5}	1.3×10^{-5}	$\leq \lvert 9 \times 10^{-8} \rvert$	*dn/dt*
$\alpha\beta/\kappa$ [W^{-1}] $\times 10^{-9}$	2 - 20	1 - 3	$\leq \lvert 2 \times 10^{-4} \rvert$	

Tomaru(2002) http://arxiv.org/pdf/gr-qc/0202038.pdf

$\boxed{ds \propto \frac{\alpha\beta}{\kappa}}$ optical path difference at wavefront

Sapphire has advantages

- Thermal conductivity is high at 20K
- Thermal lensing is small at 20K
- Q is also very high

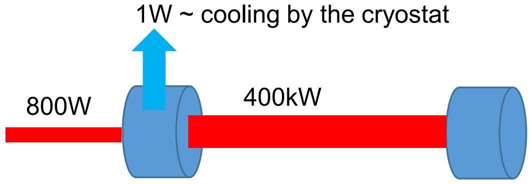

But, there are also disadvantages such as

- hardness (difficult to polish)
- absorption (<u>50ppm/cm is required</u>)
- inhomogeneity of bulk (cold lensing)

1W power input
400W***50ppm/cm***15cm*2=0.6W
400kW*1ppm=0.4W

Dec 7 - 11, 2015
JGRG25, YITP, Kyoto University

- # Excavation procedure
  - Three parties entered from two entrances.
  - One party from Mozumi entrance excavated Mozumi tunnel, Y end and, the half of Y arm.
  - One party from New Atotsu excavated New Atotsu, Center area and the rest of Y arm.
  - Another one party from New Atotsu excavated whole X arm, Sakonishi, and Xend.
  - A bypass tunnel between Xarm and New Atotsu for water drain.

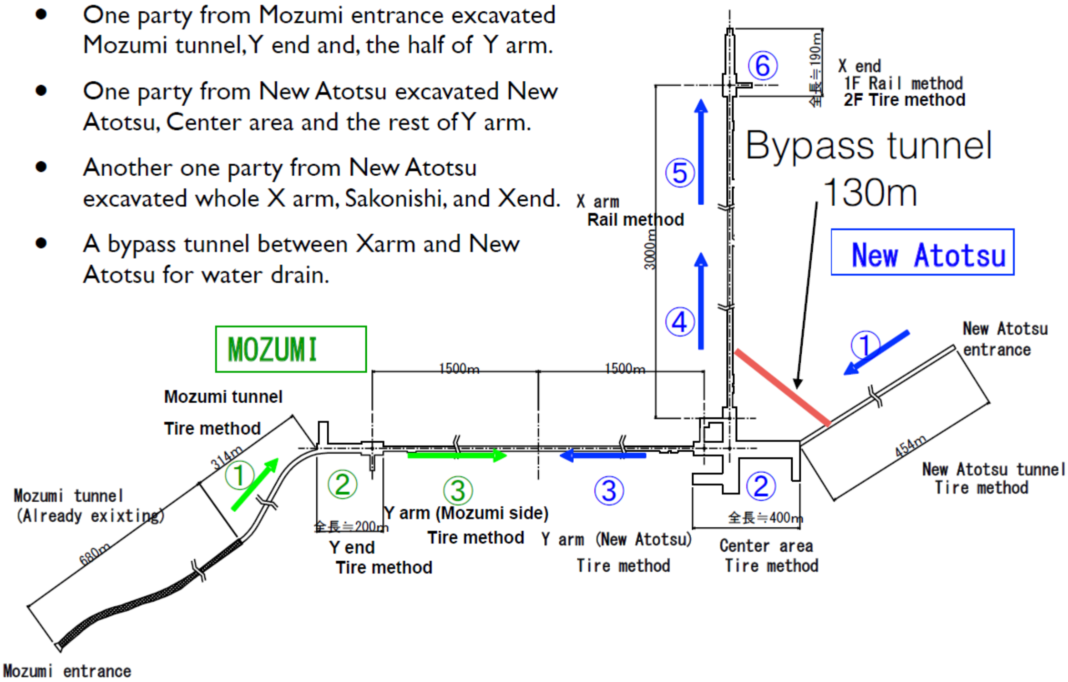

KAGRA map

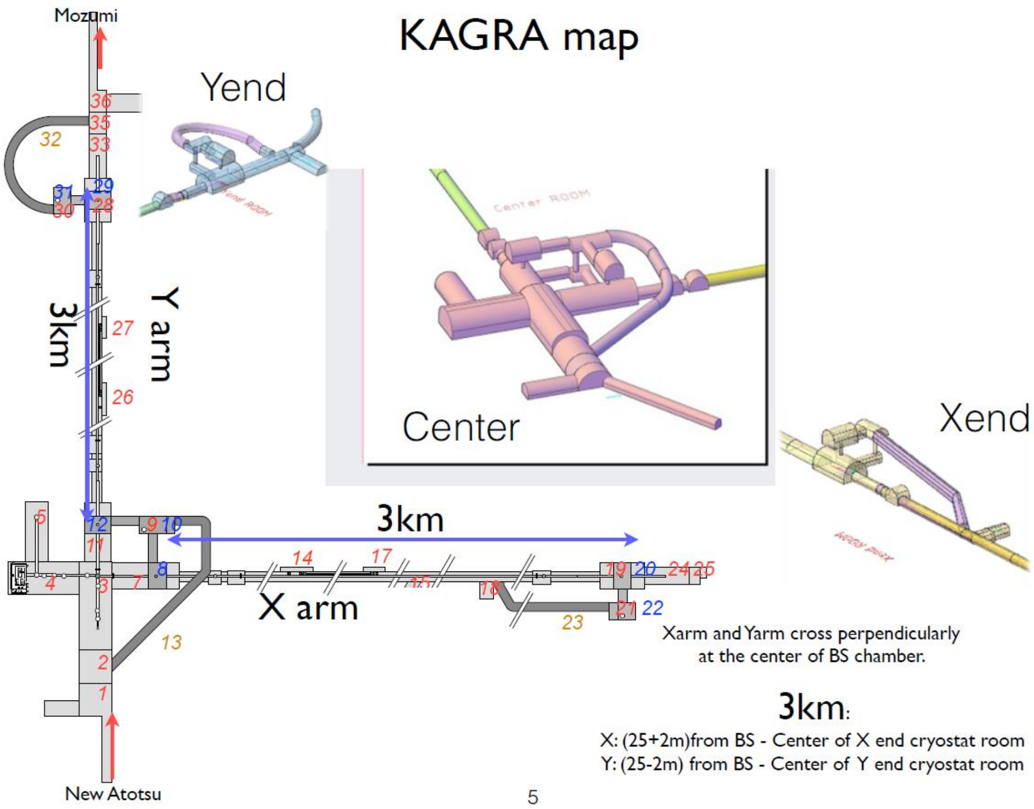

Xarm and Yarm cross perpendicularly at the center of BS chamber.

3km:
X: (25+2m)from BS - Center of X end cryostat room
Y: (25-2m) from BS - Center of Y end cryostat room

“KAGRA Data Analysis and Data Management”

by Ken-ichi Oohara (invited)

[JGRG25(2015)I06]

KAGRA Data Analysis and Data Management

Ken-ichi Oohara
Niigata University

JGRG25
2015/12/08 YITP, Kyoto University

Brief History of My Research

Brief History of My Research

- 1979/4 Nuclear Astrophysics Group (Kyoto Univ.)
- 1981 Structure of Superposed Two Kerr Metrics
  K.O. and H. Sato, Prog. Theor. Phys. 65, 1891 (1981)
- 1982 – 1984 Radiation of GW based on perturbation of a black hole metric
  with T. Nakamura, Y. Kojima
- 1984/3 Ph. D
  Excitation of the Free Oscillation of a Schwarzschild Black Hole by Gravitational Waves from a Scattered Test Particle
  Prog. Theor. Phys. 71, 738 (1984)

Brief History of My Research

- 1984 - Numerical Relativity
  with Nakamura, Miyama, Maeda, Sasaki … Shibata
- 1987/4 to Institute of High Energy Physics (KEK)
  Computer Center
  - main job: administration of the supercomputer
  - **Hitachi S-820**
    - a vector machine
    - speed: **3GFLOPS** , memory: **1GB**
    - extended memory: ~ 20GB (like SSD)
    - 32bits vector registers / 64bits scalar register

cf.
Intel Xeon v3 family
peak speed per core: 50GFLOPS

Dawn of 3D Numerical Relativity

- We started 3D (in space) simulation of coalescence of binary neutron stars using S-820 and VP-200/VP-400 (1GFLOPS, 256MB)
- post-Newtonian including back reaction of GW radiation
- a lot of technique for memory management
  - FORTRAN77: no dynamical allocation of arrays
- bugs both in the compiler and the hardware
  - too elaborate programs ?

Development of 3D Numerical Relativity

- 1993 (move to Niigata University)
  a vector-parallel computer
  Fujitsu VPP500(KEK)
  VPP300(NAOJ)
- 1.6GFLOPS/PE (VPP500), 2.2GFLOPS/PE (VPP300)
  - KEK: VPP500/80 (80PE, 256MB/PE)
    up to 64PE/job 96GFLOPS, 16GB
  - NAOJ: VPP30/16R (16PE, 2GB/PE)
    VX/4R (4PE) x 4
    up to 15PE/job(?) 33GFLOPS, 30GB
- We began fully general relativistic simulations.

Development of 3D Numerical Relativity

- A basic concept of BSSN formalism was proposed by Nakamura-san in 1987.
  (Nakamura, Oohara and Kojima, Prog. Theor. Phys. Suppl. No.90)

- Finally, Shibata succeeded in general relativistic simulation of coalescence of binary neutron stars.

Data Analysis of Gravitational Waves

- 2008 - Data analysis of GW
  with H. Takakashi, Kanda, Tagoshi, …

  - KAGRA Data Analysis Subsystem (DAS)
  - Data Management Subsystem (DMG)

Status of KAGRA Data Analysis

Common Minimum Target for iKAGRA data analysis

- Stable operation of the data transfer system and the data analysis pipeline for long period.
- To gain the experience which treats real data, and to prepare for the bKAGRA observation

Data Analysis Subgroup (DAS)

Chief: H.Tagoshi
Sub-chiefs: Y.Itoh, H.Takahashi
Core members: N.Kanda, K.Oohara, K.Hayama

Korean subgroup
Leader: Hyung Won Lee

Osaka City Univ	N.Kanda, H. Tagoshi, K.Hayama, K.Ueno, T.Narikawa, T.Yokozawa, M. Kaneyama, H.Yuzurihara, T.Yamamoto, K.Tanaka, A. Miyamoto
Univ Tokyo	Y.Itoh, K. Eda, J. Yokoyama
Nagaoka Tech	H.Takahashi, K. Sakai, Y. Sasaki, S. Ueki
Niigata Univ	K.Oohara, Y.Hiranuma, T. Wakamatsu, H. Suwabe
Toyama Univ	S. Hirobayashi, M. Nakano, K. Miyake
NAOJ	N. Ohishi, A. Shoda, Y. Fujii
ISM	S. Mano

Inje Univ	Hyung Won Lee Jeongcho Kim
Yonsei Univ	Chunglee Kim

Total: 32 (Only people with FTE>0. Undergrads. are not included)
FTE ~ 10.55

- Bi-weekly meeting: Friday 14:45-16:45
- DMG-DAS Core members' meeting : Wednesday 11:00-12:00

Data Analysis Tasks

Task	Contact person	people
CBC (Compact Binary Coalescence)	Tagoshi	Osaka C: Ueno, Yuzurihara, Narikawa, Kaneyama, Miyamoto Nagaoka: H.Takahashi Niigata: Oohara, Hiranuma, Wakamatsu
CBC-PE (Parameter Estimate)	H.W. Lee	Korea: Chunglee Kim, Jeongcho Kim Osaka CU: Narikawa, Tagoshi
Burst	Hayama	Osaka CU: Yokozawa, Kanda, Arima
Continuous	Itoh	Tokyo: Eda, Ono Osaka C: K.Tanaka, Kanda NAOJ: Tatsumi
EM follow-up	Ohishi Tagoshi Kanda	NAOJ: Ohishi, Shoda, Fujii, Osaka CU: Yokozawa
KAGALI	Oohara	Itoh, Ueno, Yuzurihara, …
New Methods & Others	------	HHT: Takahashi, Kaneyama, Oohara, Wakamatsu NHA: Nakano, Hirobayashi, Miyake, Ueno, Tagoshi ……

Data Analysis Tasks

Task	Contact person	people
CBC (Compact Binary Coalescence)	Tagoshi	Osaka C: Ueno, Yuzurihara, Narikawa, Kaneyama, Miyamoto Nagaoka: H.Takahashi Niigata: Oohara, Hiranuma, Wakamatsu
CBC-PE (Parameter Estimate)	H.W. Lee	Korea: Chunglee Kim, Jeongcho Kim Osaka CU: Narikawa, Tagoshi
Burst	Hayama	Osaka CU: Yokozawa, Kanda, Arima
Continuous	Itoh	Tokyo: Eda, Ono Osaka C: K.Tanaka, Kanda NAOJ: Tatsumi
EM follow-up	Ohishi Tagoshi Kanda	NAOJ: Ohishi, Shoda, Fujii, Osaka CU: Yokozawa
KAGALI	Oohara	Itoh, Ueno, Yuzurihara, …
New Methods & Others	------	HHT: Takahashi, Kaneyama, Oohara, Wakamatsu NHA: Nakano, Hirobayashi, Miyake, Ueno, Tagoshi ……

Compact Binary Coalescence

Burst

Continuous wave

Compact Binary Coalescence

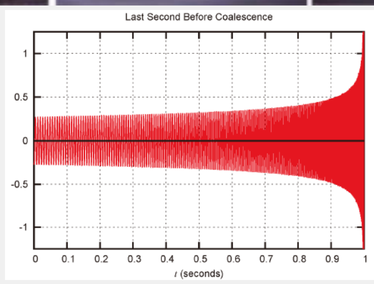

- Short duration
- Detailed theoretical waveforms are available.

- Analysis method: **matched filtering**

Matched Filtering

- Prepare the template bank of GW signals $h_k(t)$.
- Suppose the detector output $s(t)$ includes a signal of GW $h(t)$ in the noise $n(t)$:

$$s(t) = h(t) + n(t)$$

- Take correlation of $s(t)$and $h_k(t)$

$$\frac{1}{T}\int_0^T s(t)h_k(t)\,dt = \frac{1}{T}\int_0^T h(t)h_k(t)\,dt + \frac{1}{T}\int_0^T n(t)h_k(t)\,dt$$

- It will be large only if $h(t) = h_k(t)$ when T is large enough.

Matched Filtering

- Instead of $\int s(t)h_k(t)\,dt = \int \tilde{s}^*(f)\tilde{h}_k(f)\,df$ (Plancherel's theorem)

"matched filter" is defined as

$$\rho = 2\int_{-\infty}^{\infty} \frac{\tilde{s}^*(f)\tilde{h}_k(f)}{S_n(|f|)}df = 4\ \mathrm{Re}\int_0^{\infty} \frac{\tilde{s}^*(f)\tilde{h}_k(f)}{S_n(f)}df$$

- The likelihood ratio $\Lambda(h_k|s)$of presentation of signal h_k when s is observed is a monotonically increasing function of ρ.
  - $p(s|0)$: probability that s is observed when signal is absent
  - $p(s|h_k)$: probability that s is observed when signal is present

$$\Lambda(h_k\,|\,s) = \frac{p(s\,|\,h_k)}{p(s\,|\,0)}$$: likelihood ratio

$\log\Lambda(h_k\,|\,s) \propto \rho^2$ if noise is Gaussian

CBC status

- **Offline Pipeline**
  - Frequency domain matched filtering
  - Wide parameter range
  - External trigger search
- **Low Latency Pipeline**
  - Time domain matched filtering
  - Narrow parameter range
  - Alert for EM follow-ups
- **MCMC Pipeline** (with Korean group)
  - Post process
  - Detailed investigation of candidate events

MCMC: Markov Chain Monte Carlo methods

Continuous Waves

- Gravitational waves from rotating neutron stars
- Long duration signal (continuously emitted)
- Expected to be very weak in general

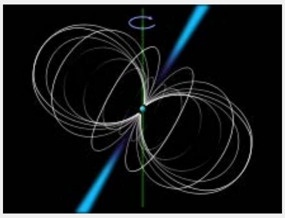

- Waveforms:
  - Sinusoidal waves (with small freq. evolution) modulated by
    - Earth motion
    - neutron stars' motion (if in binary systems)
- Analysis method: **matched filtering**

Burst Analysis

- **Target:** short duration signal
  - ➢ waveforms are not assumed
- **Possible sources:**
  - ➢ Core collapse supernovae
  - ➢ GRBs
  - ➢ Compact binary coalescence
  - ➢ … anything !

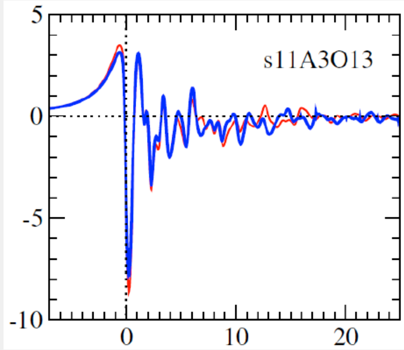

Collapse and bounce wave
Dimmelmeier et al. PRD 78, 064056

- **Analysis method:** Excess Power Method
  - ➢ search for excess of power on time-frequency plane
  - ➢ based on STFT, Q-transform and wavelet

Time-Frequency Analysis

- Traditionally for time-frequency analysis:
  - ➢ the short-time Fourier transform (STFT)
  - ➢ Q-transform
  - ➢ the wavelet analysis
- The resolution in time and frequency is restricted by "**the uncertainty principle**".

➡ **New methods**

- ➢ **NHA (Non-Harmonic Analysis)**
  - a novel technique for high-resolution signal processing proposed by Hirobayashi at Toyama Univ.
- ➢ **HHT (Hilbert-Huang Transform)**
  - a novel adaptive approach to time series analysis

High-Resolution Signal Processing

- Both NHA and HHT decompose signal $h(t)$ into a series of demodulation without Fourier transform;

$$h(t) = \sum_k a_k(t) c_k(t) = \sum_k a_k(t) \cos\theta_k(t)$$

  - **modulator** $a_k(t)$: a lower frequency signal
  - **carrier** $c_k(t)$ or $\cos\theta_k(t)$: a higher frequency signal

- $a(t)$: the time-varying amplitude
  or **the instantaneous amplitude (IA)**
- $\theta(t)$: the phase

- **the instantaneous frequency (IF)** $$f(t) = \frac{1}{2\pi}\frac{d\theta(t)}{dt}$$

Hilbert-Huang Transform

- **HHT (Hilbert-Huang Transform)**
  - a novel adaptive approach to time series analysis proposed by Nordan E. Huang (Taiwan) in 1996
  - It consists of
    - an empirical mode decomposition (EMD)
    - the Hilbert spectral analysis (HSA)

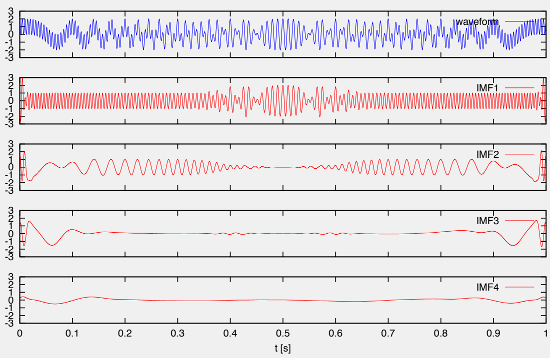

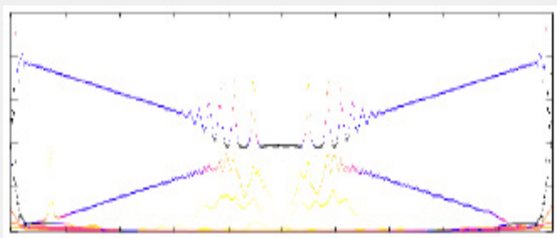

Hilbert-Huang Transform

- **The EMD: an adaptive decomposition**
  - not require an *a priori* functional basis
  - the basis functions:
    adaptively derived from the data
    by the EMD sift procedure, instead

- In can be applied to non-linear and no-stationary time series data
  - It has been applied to various fields:
    biomedical engineering, financial engineering,
    image processing, seismic studies,
    ocean engineering

Application of HHT to GW search

- I began studying application of HHT to GW search
  with H. Takahashi in 2009
  in collaboration with J. Camp (GSFC/NASA).

Applying HHT to

- Burst search
  (Sakai's talk)

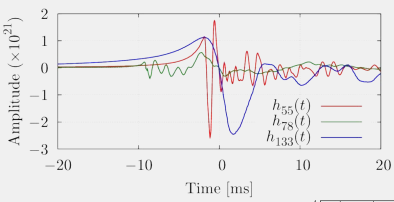

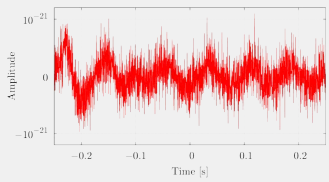

- Analysis of CBC, especially
  the post-merger phase
  (Kaneyama's PhD thesis)

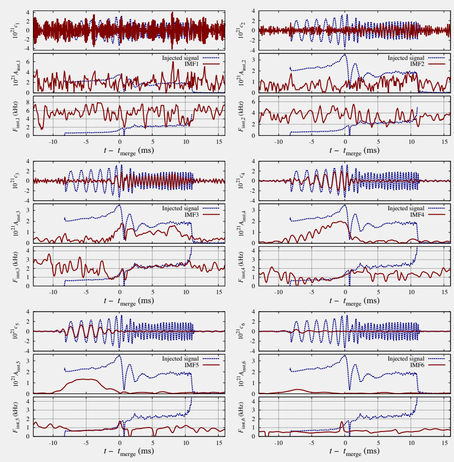

Development of KAGALI (KAGRA Algorithmic Library)

Development of KAGALI

- Software for gravitational wave data analysis:
  LSC has already opened a fine software suite,
  LALSuite, to the public.
- Nevertheless,
  we should prepare routines proper to KAGRA,
  such as for data handling tools
  and for new methods we are developing.
- KAGRA Data Analysis Subsystem (DAS) decided to develop our own software suite that will work independently to the LAL in principle.

Introduction

- KAGALI: **KAG**RA **A**lgorithmic **LI**brary
  - a data analysis library that KAGRA data analysis subsystem is developing
- KAGALI-Apps:
  - a data analysis application software packages build upon KAGALI, LALSuite and libraries developed by Virgo.
- For KAGRA data analysis,
  we will use any of available software including KAGALI, LALSuite, Virgo software, and so on.

KAGRA vs KAGALI

- **KAGURA** 神楽 in Japanese means a kind of religious music and dance based on Shinto.
- **KAGARI** 篝 or KAGARI-BI 篝火 means a bonfire or a watch fire.
- People usually build KAGARI-BI to light-up KAGUARA.
- We build **KAGALI** to light-up **KAGRA**.

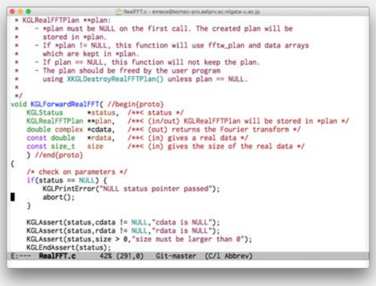

Fundamental Concepts

- KAGALI and KAGALI-Apps do not specify which language we have to use to develop them.
  But C-language is used in the major part now.

- KAGALI is assumed to be installed and work on various systems of, at least, Unix-like OS including Linux and Mac OS X.
  - We don't place first priority on portability.
    We mainly intend to achieve higher performance.
  - At present, it is confirmed for RHEL 6.x and its compatibles (SL, CentOS) as well as Mac OS X with GNU C compiler (gcc) and Intel C complier (icc).

Coding Style Guidelines

- We set coding style guidelines
  (KAGALI C-coding style guide, 2014/7/19)

  - to reduce bugs
  - to make code-debugging easy
  - to produce a common properties by which the KAGRA data analysis team can produce data analysis programs efficiently and quickly
  - to make programs easily re-usable and understandable by standardizing code appearances

Coding guidelines

- You should write a source code that is easy to understand for others and you-at-some-time-later.
- You should write a source code that is easy to understand without a comment.

Status of KAGALI

- Development of KAGALI is in progress.
- The basic framework has been determined, including error handling/bug tracing mechanism and FFTW wrappers and FrameL wrappers.
- Almost finished preparing Functions and applications for CBC analysis, HHT, etc.
  (by Ueno, Yuzurihara, Tagoshi, K.O.)
- It is still the pre-alpha version;
  we have to examine and review throughout the code.
- Some of routines in KAGALI will be applied to build the analysis pipeline for iKAGRA.
- The first released version will be open to public by bKAGRA (in 2017 ?).

Status of KAGRA Data Management

Data Management Subgroup (DMG)

Chief: N. Kanda
Sub-chiefs: K. Oohara

Osaka City Univ	N.Kanda, H. Tagoshi, K.Hayama, T.Yokozawa, H.Yuzurihara, T.Yamamoto, K.Tanaka, A. Miyamoto
Nagaoka Tech	H.Takahashi, K. Sakai, Y. Sasaki, S. Ueki
Niigata Univ	K.Oohara
Univ Tokyo	S. Miyoki, Y. Itoh

- Weekly meeting: Thursday 17:30-18:30
- DMG-DAS Core members' meeting : Wednesday 11:00-12:00

KAGRA data : flow and amount

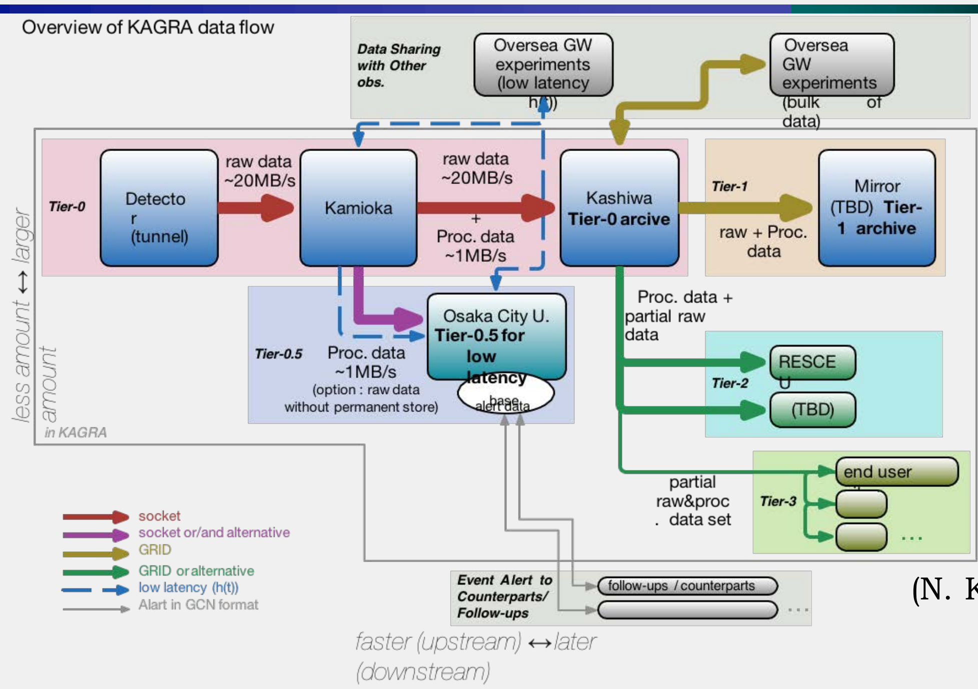

(N. Kanda)

raw data: 20 MB/s ~ 630 TB/yr ~ 50 TB/Month
proc. data for event searches: target is 1 ~ 2 MB/s
(= 5 ~ 10% size of raw data)

Current Status

- iKAGRA data system hardware are ready
  - on site (tunnel): 20TB spool × 2sets
  - at Kamioa surface: 200TB storage
  - dedicated server for the data transfer
  - calculation server: 64 cores in total
  - at ICRR Kashiwa: 100TB storage

- Low Latency Analysis server at Osaka City U. is ready
  - 392 cores in total
  - 288TB storage (144TB × 2sets)

- VPN connections between four clusters are established.
  - Kamioka – Kashiwa – OCU(orion) – OCU(gemini)
- RESEU & Niigata U. prepares additional data tree.

Software

- We are employing
  - socket transfer
  - parity check
  - log system (syslog-ng)
  - shared memory

- These are mature and solid techniques.

- Sasaki, Sakai, Ueki
  (Nagaoka Tech.)
  Kanda and K.O.
  are working hard to finish by the end of December.

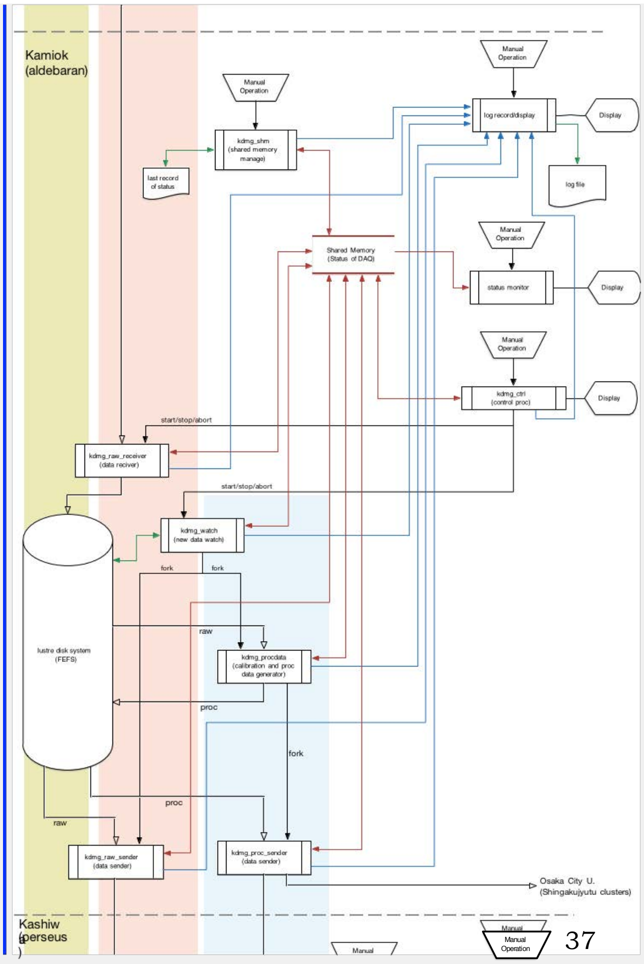

KAGRA

Thank you